Role of Serine Protease HTRA1 in the Regulation of Mouse Adipose-Derived Stromal Cell Osteogenesis

---

Dissertation

zur

Erlangung der naturwissenschaftlichen Doktorwürde
(Dr. sc. nat.)

vorgelegt der

Mathematisch-naturwissenschaftlichen Fakultät

der

Universität Zürich

von

Stephan Glanz

aus

Österreich

Promotionskomitee

Prof. Dr. Ernst Hafen (Vorsitz)
PD Dr. Peter J. Richards (Leitung der Dissertation)
Prof. Dr. Michael Hottiger
Prof. Dr. Michael Ehrmann

Zürich, 2016

"Difficult things take a long time, impossible things a little longer."

- Jure Robič

Summary

In contrast to mouse bone marrow-derived multipotent stromal cells (mBMSCs), efficient osteogenic induction of mouse adipose-derived stromal cells (mASCs) is reliant on the actions of all-*trans* retinoic acid (ATRA), the carboxylic acid form of vitamin A. However, the underlying mechanisms responsible for its mode of action remain incompletely understood. We have previously identified high temperature requirement protease A1 (HTRA1) as a novel mediator of human BMSC (hBMSC) differentiation, where it acts to enhance osteogenesis and subsequent mineralization by differentiating bone-forming cells. Furthermore, *HtrA1* expression is upregulated in mASCs in response to ATRA-containing osteogenic induction medium. We therefore asked the question whether HTRA1, in addition to its positive effects on hBMSC osteogenesis, could also influence the osteogenic differentiation of mASCs. In order to address this, we investigated the effects of small interfering RNA (siRNA)-mediated depletion of HTRA1 on the differentiation of mASCs into mineralizing osteoblasts and attempted to establish a mechanism of action for HTRA1. Investigations relied on several different techniques including qRT-PCR, protein analyses, enzyme assays and histological analyses. We could demonstrate that loss-of-function of HTRA1 was detrimental for ATRA-induced mASC osteogenesis, resulting in deficiencies in both osteogenic gene marker expression and mASC-derived osteoblast mineralization. Furthermore, we identified p70 ribosomal protein S6 kinase (p70S6k) as being a downstream target of HTRA1 and as having a pivotal role in mediating the pro-osteogenic effects of HTRA1 in mASCs in response to ATRA. In conclusion, we provide evidence to support p70S6k as an important regulator of mASC osteogenesis, being activated in response to ATRA via pathways involving HTRA1. As such, it is proposed that HTRA1 represents a newly identified positive regulator of ATRA-mediated mASC osteogenesis and mASC-derived osteoblast mineralization. Further studies are needed in order to assess the relevance of such findings in regards to the ability of mASCs to regulate bone formation and repair *in vivo*, and whether such signaling cascades are also involved in regulating the osteogenic differentiation of ASCs from other species.

Zusammenfassung

Im Gegensatz zu multipotenten Stromazellen des Knochenmarks der Maus (mBMSCs), ist die Induktion effizienter Osteogenese basierend auf Stromazellen des Fettgewebes (mASCs) abhängig vom Wirkunsmechanismus der all-trans-Retinsäure (ATRA), dem carboxylierten Metaboliten des Vitamin A. Nach wie vor sind die der Vitamin A gesteuerten, Osteogenese zu Grunde liegenden Mechanismen unklar. Die von uns bereits identifizierte hoch Temperatur anhängige Protease A1 (HTRA1) ist ein neuartiger Regulator im Differenzierungsmechanismus der menschlichen Stromazellen des Knochenmarks (hBMSC), welche durch Förderung der Zelldifferenzierung die Osteogense und die damit verbundene Mineralisierung der Knochenbildenden Zellen steuert. Des weiteren ist die Expression von *HtrA1* in mASCs als Antwort auf ATRA enthaltendes Osteogenese-Medium hochreguliert. Folglich haben wir die Frage gestellt ob HTRA1 neben seinem positiven Effekt auf die Osteogenese von hBMSCs auch die Differenzierung und Osteogenese von mASCs steuern kann. Dementsprechend haben wir den Effekt des Verlustes von HTRA1 durch kleine eingrefenden Ribonukleinsäuren (siRNA) auf das Differenzierungspotential von mASCs sich zu mineralsierenden Osteoblasten zu differenzieren untersucht und haben versucht einen der Wirkung von HTRA1 zu Grunden liegenden Mechanismus zu etablieren. Dabei kamen verschiedenste Techniken wie quantitative Echtzeit Polymerase Kettenreaktion (qRT-PCR), Protein Analyse, enzymatische Untersuchungen sowie histologische Analysen zum Einsatz. Dadurch konnten wir zeigen, dass der Verlust von HTRA1 auf die von ATRA induzierte Osteogenese von mASCs schwerwiegende Folgen hat und nicht nur die Expression genetischer Marker der Osteogenese sondern darüber hinaus auch das Mineralisierungspotential der mASCs stark beeinträchtigt. Des weiteren haben wir nicht nur die p70 Ribosomale Protein S6 Kinase (p70S6K) als ein untergeordnetes Ziel von HTRA1 identifiziert sondern konnten auch zeigen, dass dieser eine entscheidende Funktion in der Vermittlung des pro-Osteogenese Effekts von HTRA1 in mASCs unter dem Einfluss von ATRA zukommt. Zusammenfassend lässt sich sagen, dass wir starke Indizien haben, welche das Modell von p70S6K als einen fundamentalen Regulator der Osteogenese von mASCs untermauern, welche durch ein Netzwerk über die Aktivierung von HTRA1 durch ATRA aktiviert wird. Folglich sehen wir HTRA1 als einen neuartig identifizierten positiven Regulator der ATRA induzierten Osteogenese und einherghender Mineralisierung der Osteoblasten von

mASCs. Dennoch, weitere Studien sind notwendig um die Relevanz der Ergebnisse in Hinblick auf die Fähigkeit von mASCs die Formation sowie Reparatur von Knochen *in vivo* zu regulieren, sowie ob die zu Grunde liegenden Signalnetzwerke ebenso in der Regulation der Osteogenese von anderen Spezies beteiligt sind.

Table of contents

Abbreviations

4E-BP1	eukaryotic initiation factor 4E binding protein 1
ALP	alkaline phosphatase
ASC	adipose derived stromal cell
ATRA	all-trans retinoic acid
BMD	bone mineral density
BMP	bone morphogenetic protein
BMPR	BMP receptor
BMSC	bone marrow stromal cell
DAPI	4`,6-diamidino-2-phenylindiole
DMEM	Dulbecco's modified eagle medium
ECM	extracellular matrix
ESC	embryonic stem cell
FBS	fetal bovine serum
FHL2	four and a half LIM domains 2
HtrA1	high temperature requirement protease A1
MAPK	mitogen-activated protein kinase
MSC	multipotent stromal cell
mTOR	mammalian target of rapamycin
mTORC	mTOR complex
p70S6K	p70 ribosomal protein S6 kinase
PCR	polymerase chain reaction
pNPP	p-nitrophenylphosphate
qRT-PCR	quantitative real-time PCR
RAR	retinoic acid receptor
SAM	senescence accelerated mice
siRNA	small interfering RNA
TSC2	tuberous sclerosis complex 2

1. Introduction

1.1. Stem cells

In multicellular organisms, an ovum and a sperm cell fuse to give rise to the earliest developmental stage, the zygote. This single cellular zygote is composed of a haploid chromosome set from the maternal as well as the paternal side, resulting in the diploid chromosome set of the final organism. This cell is totipotent, which means it has the greatest differentiation potential and can differentiate into all of the three germ layers, endoderm, mesoderm and ectoderm and form all cells of an organism. This in in contrast to multipotent stromal cells (MSCs), where the differentiation potential is limited to certain cell types only.

1.1.1. Stem cells in the historical context

In the historical context, evidence for the existence of stem cells comes from experiments with mouse teratocarcinomas, transplantable, progressively growing tumours that maintain a wide variety of diversely differentiated tissues within the tumour [1]. In 1954, LeRoy Stevens et al. [2] found that in their mouse model of spontaneous testicular teratocarcinomas, cells within the tumours were originating from primordial germ cells in foetal testes. Further teratocarcinomas could be experimentally induced by the ectopic transplantation of germinal ridges containing these primordial germ cells [3] as well as cells of early embryos [1, 4]. By demonstrating that teratocarcinomas containing multiple cell types can form upon transplantation of a single tumour stem cell, the embryonal carcinoma (EC) cells, Stevens and Little [2] noted that “Pluripotent embryonic cells appear to give rise to both rapidly differentiating cells and others which like themselves, remain undifferentiated”, the foundation for the field of stem cell research was set [1, 5]. At that early time point, the test for the maintenance of pluripotency was to show that a clonal population can give rise to a teratocacrinoma with multiple and largely well-differentiated tissues when re-injected into a mouse [1, 5]. As observed by Martin and Evans in 1974 [6], under *in vitro* conditions, single clones of stem cells even

differentiated into spontaneously beating cardiac myocytes and nerve cells [7]. Further investigations of the embryoid bodies formed by EC cells revealed that the first step of differentiation is into primary extra-embryonic endoderm, exactly as formed by cells isolated from the inner cell mass from a mouse blastocyst [1]. This was the beginning of the realization that the teratoma forming EC cells might not be malignant and abnormal cancer cells but rather possibly early embryonic cells [1, 8]. Indeed, EC cells when incorporated into a normal mouse blastocyst did not form any malignant tissue but instead contributed to the development of a chimeric animal of which most tissues were proven to be derived from the injected tissue-cultured EC cells [1, 9]. Furthermore EC cells did not only contribute to the soma [10] but most importantly of all, to the germ-line [11], therefore providing a route for retroviral genetic manipulation from culture to creature [1, 12, 13].

1.1.2.Stem cell mechanisms of differentiation

Based on the given potential of these historical findings, stem cell research quickly gained broad attention amongst the scientific community as well as the public and as a consequence, has developed significantly during the past 40 years. From successful identification and utilization of stem cells to form and genetically modify chimeric organisms as mentioned above, the focus has quickly shifted towards a more applied approach to address relevant health issues. The initial realization of one cell being able to commit and contribute to all tissues within an organism soon led to efforts to direct this potential to specifically regenerate and restore damaged tissues or ideally, replace whole organs on demand to circumvent limitations of the body's regenerative capacity. Despite the seemingly limitless potential of stem cell research, major drawbacks and limitations were quickly realized when those regenerative approaches were transferred into the human system. The assumption that one stem cell if exposed to the injured environment would automatically take over regeneration, quickly proved to be wrong and was much more complex than expected. Nonetheless, the initial findings were still valid, fascinating and firing the idea of regenerative applications. Consequently, the focus has since shifted towards

understanding the mechanisms controlling the initial events of stem cell commitment during embryonic development, as well as tissue maintenance throughout adult life.

1.1.3.Differentiation of adult stem cells

In contrast to the initial idea that the number of stem cells declines with the progression of differentiation during adult development, stem cells were found to be located in niches of multiple tissues throughout adulthood maintaining tissue repair and homeostasis. These so-called adult stem cells are found in various tissues of the body, such as, but not limited to the blood, skin, intestines and bone. Due to ethical concerns intertwined with the use of pluripotent embryonic stem cells (ESCs) for regenerative purposes, the discovery of MSCs in the adult was of particular interest. Hence, efforts in stem cell research are now concentrated on elucidating and utilizing the differentiation dynamics of MSCs, and to even re-program them back to pluripotency for subsequent regenerative applications.

There are basically three hierarchical mechanisms in cell differentiation to be distinguished: dedifferentiation, transdifferentiation and reprogramming. In dedifferentiation, a cell reverts back to a stage less differentiated from within its own lineage, allowing proliferation before redifferentiating and replacing damaged tissues. Transdifferentiation is extending dedifferentiation even further to a point where a switch in lineage commitment is possible with subsequent differentiation into a different cell type. Reprogramming even aims to revert cells to pluripotency, thus allowing them to commit to any desired cell type [14].

1.1.4.Dedifferentiation

For example, in Zebrafish, when resecting major parts of the heart ventricle [15], residing differentiated cardiomyocytes dedifferentiate [16] and proliferate [17] to regenerate the missing tissue [14, 18]. In urodele amphibians, dedifferentiation is taken to the next level as they are able to regenerate whole limbs. Cells adjacent to the wound dedifferentiate to form a blastema consisting of undifferentiated cells, which then proliferate and redifferentiate to regenerate the missing part of the limb

[14, 19]. The key player throughout the process of dedifferentiation is the retinoblastoma protein RB, which under normal conditions acts as a tumour suppressor by inhibiting E2F activating transcription factors, thereby stabilizing the cell cycle inhibitor p27 and recruiting chromatin remodelling factors [19]. Upon regenerative cues, RB becomes inactivated by hyper-phosphorylation allowing differentiated cells to re-enter the cell cycle and dedifferentiate [20]. However, in mammalian heart muscle cells, hyper-phosphorylation of RB alone is insufficient to promote re-entry into the cell cycle [21], as the tumour suppressor ARF up-regulates p53, which then compensates for RB inactivation [22, 23]. Consequently, inactivation of RB and ARF is needed to render mammalian myocytes capable of dedifferentiating and re-entering the cell cycle again. As such, the most rigorous regenerative potential seen in vertebrates is in those lacking ARF, indicating that in the context of mammalian evolution, ARF may aroused at the expense of impaired regenerative potential [24]. In mammalian cardiomyocytes a combined approach of inhibiting p38 mitogen-activated protein kinase (MAPK), which blocks cell cycle progression associated with myogenic differentiation, and activation of fibroblast growth factor 1 (FGF1) [25], which induces fetal gene expression in mature cardiomycytes, allows mature cells to dedifferentiate and proliferate again [26, 27]. The same dedifferentiating effect could be achieved in an approach where cells were treated with the cardiomyogenesis promoting ligand Neuregulin [28], which binds to and activates the tyrosine kinase receptor Erb, thereby showing that there might be multiple routes of dedifferentiation [29, 30].

1.1.5.Transdifferentiation

In transdifferentiation, cells first dedifferentiate, but in contrast to the mechanisms mentioned above, they then have the potential to commit to a new lineage. By expressing the three factors *Ascl1*, *Brn2* and *Myt1l*, mouse embryonic and postnatal fibroblasts could be efficiently reprogrammed to a pluripotent state and subsequently transdifferentiated into functional neurons, along with the expression of neuron-specific proteins, and the ability to generate action potentials and form functional synapses [31]. To date, several reports exist showing successful transdifferentiation

of mouse fibroblasts into cardiomyocytes either by expression of the specific factors *Gata4*, *Mef2c* and *Tbx5* [32] or even by transient transfection with microRNAs 1, 133a, 208a and 499-5p in combination with a JAK inhibitor [33]. Another example which highlights the plasticity of differentiation are adipose-derived stromal cells (ASCs) [34]. ASCs have the potential of multi-lineage commitment and can be differentiated into various cell types such as adipocytes, chondrocytes, myocytes and osteoblasts in the presence of lineage specific induction factors [35].

1.1.6. Reprogramming / iPS

In addition to transdifferentiation from one cell type to another, reprogramming is the ultimate form of transdifferentiation where cells can be dedifferentiated all the way back to their pluripotent state, and are therefore termed induced pluripotent stem (iPS) cells. However, there is still some discrepancy regarding the pluripotent identity of iPS cells in which major global transcriptional differences have been identified [36-38]. Generation of iPS cells was initially achieved by expression of the three pluripotency key factors, termed Yamanaka cocktail after its inventor, OCT4, SOX2 and NANOG [39, 40]. In addition to these factors acting as transcriptional repressors [41-46] for genes associated with differentiation [47, 48], they're also responsible for the regulation of various processes at the epigenetic level. These include early globally organizational changes in the euchromatin histone modification H3K4me2 in pluripotency-related gene promoters, in combination with repressive H3K27me3 chromatin modifications. Given the contribution of chromatin remodelling [49, 50] to pluripotency [51], this led to the discovery that the use of transcriptionally activating epigenetic regulators can partly replace Yamanaka factors, such as Rcor2 [52], Tet1 [53], TH2A and TH2B [54]. Alternatively, this can also be induced by suppression of certain chromatin modifiers such as DOT1L [55], which methylates H3K79 and promotes expression of epithelial-to-mesenchymal transition associated genes. By using a combination of microRNAs (miRNA) mir-200c, mir-302s, mir-369s [56] or mir-302, mir-367 [57], complete reversion of mouse and human somatic cells to pluripotency could be achieved without expression of any factors and at a considerably higher efficiency.

1.1.7. Chemical reprogramming / iPS cells

With the continuing insight and understanding of the underlying dedifferentiation mechanisms triggered by the Yamanaka cocktail, it soon became apparent that these factors could be partly or even completely substituted by chemical compounds (termed chemical reprogramming). Due to the reported improvement in efficiency and safety, this transgene-free approach is of particular importance when aiming for therapeutic applications in humans. The chemicals used in these transgene-free approaches target chromatin-modifying enzymes resulting in the restoration of the cell's pluripotent state. The most prominent approach reported so far utilizes a combination of two small-molecule kinase inhibitors, the so called "2i" components of which the PD0325901 inhibitor targets the FGF/ERK signaling pathway and CHIR99021 which specifically inhibits the kinase GSK3, known to promote self-renewal of ESCs. These factors render the cells in a pluripotent state by global DNA hypo-methylation [58] and by the upregulation of key pluripotency factors [59, 60] such as Nanog and Prdm14 [61]. Similar to 2i, the DNA methyltransferase inhibitor 5-aza-cytidine has been reported to induce pluripotency by blocking transcriptional repressive methylation of DNA [62]. By inhibiting the transcriptionally repressive deacetylation of histones using histone deacetylase (HDAC) inhibitors [63], pluripotency in mouse and human fibroblasts could be induced along with a reduction in the expression of pluripotency factors [64]. Other reports have described the pluripotency-inductive potential of Vitamin C [65] in human and mouse fibroblasts through epigenetic regulation, specifically a reduction in di- and trimethylation of H3K36 through regulation of the Jhdm1a/1b demethylases [66]. Small molecule induced pluripotency [67], by specifically targeting signaling pathways and epigenetic modifications, could be achieved entirely trans-gene free by exchanging the Yamanaka factors with FSK, GSK3 inhibitor CHIR99021, TGF-β inhibitor 616462 and the SAH inhibitor DZNep [68]. However, this approach is limited to rodents, as in humans indispensable activation of OCT4 by small molecules has so far not been achieved [69]. Reprogramming of adult stromal cells therefore represents a robust alternative to ESCs, thereby not only circumventing ethical concerns but also utilizing cells from autologous adult donor material.

1.2. The stem cell niche

In the context of transdifferentiation and reprogramming, the understanding of the stem cell's microenvironment within physiological conditions, the so-called niche, is of major importance [70]. Stem cells are localized to a broad range of tissues throughout the body, from relatively dormant tissues such as muscle and brain [71-74], to the rapidly self-renewing ones [75-77], such as intestinal epithelium, with a complete turn over in as little as 3-5 days. Even in relatively dormant tissues with low or almost no turnover [78], cells can be quickly activated to maintain homeostasis. Examples include cognitive-induced activation of neurons of the subgranular zone of the hippocampus [79], injury-induced proliferation and differentiation of muscle stem cells [80].

1.2.1. The stem cell niche in the historical context

Already back in 1977 it was shown by Dexter et al. through the use of *in vitro* co-cultures, that hematopoietic stem cells (HSCs) are dependent on other bone marrow residing cells such as epithelial cells and adipocytes [81]. Lord et al. showed through the use of colony forming assays (CFU), the spatial organisation of stem and progenitor cells within the bone marrow [82]. Based on these findings, Schofield concluded in 1978 that stem cells were located in and regulated by particular sites: "…a hypothesis is proposed in which the stem cell is seen in association with other cells which determine its behaviour. It becomes essentially a fixed tissue cell. Its maturation is prevented and, as a result, its continued proliferation as a stem cell is assured. Its progeny, unless they can occupy a similar stem cell 'niche', are first generation colony-forming cells, which proliferate and mature to acquire a high probability of differentiation, i.e., they have an age-structure."[83]. Subsequently, the interaction between stem cells and their niche environment was further elucidated in mutagenesis experiments by modifying the niche, and thereby inducing changes in the residing stem cells.

1.2.2. Bone marrow MSC niche

MSCs are present in a variety of adult tissues [84] residing in specific environments termed niches. And it is through the influence of tissue specific matrix, nearby differentiated cells and key soluble molecules within these niches that determines when stem cells should differentiate [83].

In addition to HSCs, MSCs are also present within the bone marrow [85, 86] and have the capability of differentiating into multiple lineages such as chondrocytes, osteoblasts, fibroblasts, adipocytes, endothelial cells and myocytes [87]. Osteoblasts are derived from MSCs through the process of osteogenesis, and are responsible for producing the osteoid matrix at the interface between bone marrow and calcified collagen, being mediated through the actions of secreted enzymes which crosslink fibrillary collagen, non-collagenous proteins and proteoglycans. Subsequently, this matrix thickens and deposition of calcium phosphate leads to mineralization [88]. The bone marrow is mainly composed of hematopoietic cells of which a fraction are found in close proximity to bone-lining osteoblasts therefore underlining a reciprocal communication between these two cell types [89]. Indeed, there is evidence to suggest that a close relationship exists between osteogenesis and haematopoiesis within the bone marrow niche [89, 90]. The most prominent example of this is the ability of osteoblasts to produce a broad range of hematopoietic growth factors [91], including NF-κB ligand (RANKL) which mediates differentiation of osteoclasts from HSCs [92]. Furthermore, an increase in osteoblast activity triggers a reciprocal expansion in HSC numbers [93-96], although depletion of bone resorbing osteoclasts does not affect HSC numbers [97]. Ablation of miRNA processing of pre-osteoblasts leads to HSC hyper-proliferation and aberrant haematopoiesis [98]. HSCs themselves, when in a quiescent state, are preferentially found in close proximity to small arterioles of the endosteal bone marrow, which are encapsulated by CSPG4+ pericytes. HSCs upon pharmacological or genetic activation of their cell cycle, re-locate from the CSPG4+ periarteriolar niche to the LEPR+ niches. Therefore it is assumed that the location of the HSCs is affecting their cycling behaviour most likely due to a difference in micro environmental stimuli [99].

1.2.3.Niche inductivity of the bone

It has been shown that the fate of stem cells within the bone marrow is influenced by its surrounding mechanical properties such as stiffness, geometry and adhesion which primes adaptions in cytoskeletal tension [100]. On matrices with osteoid-like stiffness, MSCs undergo osteogenic differentiation, whereas on a softer matrix, MSCs become more myogenic [101], independent of soluble factors [102]. When MSCs were cultured in bi-potential osteogenic-adipogenic media, high stiffness substrates favoured osteogenic and low stiffness primed adipogenic differentiation [103]. Under physiological conditions within the bone marrow, MSCs are exposed to a broad range of stiffnesses, from very soft tissues such as white marrow to very stiff environment such as osteoid. Hence, osteoblasts localize to the stiff osteoid interface, but are also in close proximity to the soft matrix surrounding pre-osteoblasts. However, it still remains to be determined as to how undifferentiated MSCs residing in the soft compartment of the bone marrow migrate to tissues of greater stiffness upon lineage commitment to osteoblasts [104]. Although it has been suggested that differentiation occurs gradually, being dependent on extracellular matrix (ECM) elasticity cues during migration [105, 106].

Considering the influence of the niche on the differentiation fate of the niche residents, a deeper understanding of how the stem cell fate can be ultimately directed towards osteogenesis is of major importance for developing effective strategies for bone regeneration and repair.

1.3. Mesenchymal stromal cells (MSCs)

MSCs have the potential to differentiate into at least four different cell lineages: osteoblasts, adipocytes, chondrocytes and myocytes [107, 108] and are therefore promising candidates for use in tissue regeneration. Subsequently, it was discovered that MSC populations are not only limited to the bone marrow, but are also found in other tissues [109] such as adipose [110], placenta [111], skin [112], umbilical cord [113-115], dental pulp [116], amniotic fluid [117], synovial membrane [118] and even breast milk [119]. In addition to their ability for multipotent differentiation, MSCs are also characterised by the expression of a set of surface markers, such as CD73, CD90 and CD105, together with the absence of endothelial and hematopoietic markers, including CD31, CD34 and CD45 [108]. Nonetheless, MSCs isolated from different tissues [120] have shown significant differences in colony morphology, differentiation potential and gene expression [121-123], thus bringing into question their biological comparability despite fulfilment of minimal marker criteria.

1.3.1. Therapeutic applications of MSCs

In addition to their stem cell based multi-lineage differentiation capacity, MSCs have gained increasing attention due to their immunomodulatory and paracrine effects [124-126] which are promising features for therapeutic applications [127, 128]. MSCs have been shown to act on the innate as well as the adaptive immune system by affecting the expression of cytokines and by supressing T cell activity [129] through down-regulation of NF-κB signaling [130] and the induction of cell cycle arrest [131]. Although the underlying mechanisms controlling these events are poorly understood, systemic infusions of MSCs to treat models of lung injury, myocardial infarction, diabetes, multiple sclerosis, renal and hepatic failure have shown promising outcomes [128, 132]. Despite the poor homing of MSCs, considerable therapeutic benefits were observed even in the absence of MSCs at the place of injury. The underlying mechanism still remains elusive although it is assumed to be based on paracrine factors secreted by MSCs. These factors can act systemically to activate tissue-resident stem cells and thus promote regeneration within the affected niche

through stimulation of proliferation, inhibition of apoptosis, and remodelling of the extracellular matrix [133]. The clinical use of MSCs has proven particularly promising in the treatment of bone related diseases such as, but not limited to, osteogenesis imperfecta in children [134, 135]. An alternative approach is to promote differentiation of MSCs into bone generating osteoblasts through stimulation with bone morphogenetic protein (BMP). BMP acts as a chemoattractant for MSCs and enhances their migration to the site of repair [136]. Upon binding to their cognate receptors on MSCs, the BMPRs, intracellular signal transduction through SMAD signaling is activated [137] which can be enhanced through cross-talk with the Notch signaling pathway [138]. In particular, the SMAD complex translocates to the nucleus where it interacts with and activates multiple osteogenesis related transcription factors such as Runx2, Osx, Dlx5 and Msx2 [139]. In the same manner, it can also influence the actions of transcriptional repressors such as Hoxc8 by removing it from the osteopontin (OPN) promoter, thereby allowing for transcription of *OPN* and the induction of osteoblasts differentiation [140].

1.4. Osteogenesis

Osteogenesis, also frequently referred to as ossification, is the process of newly formed bone material being produced on the surface of existing bone as depicted in figure 1. Since this process is highly dependent on fully functional stem cells [141], the detailed pathology of bone biology and its key players are highlighted in the following chapter.

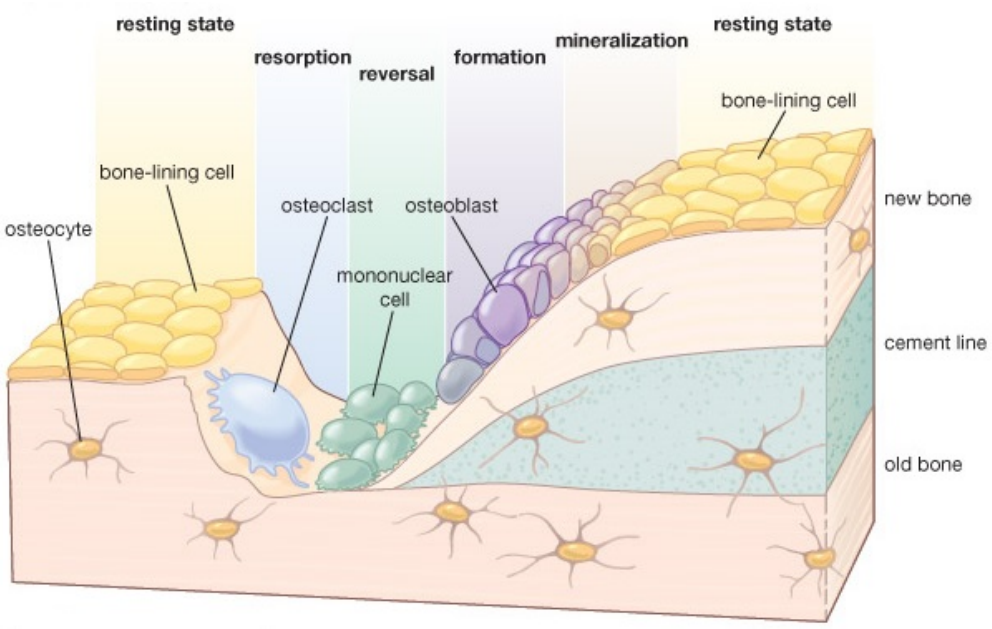

Fig. 1: Schematic model of the human bone remodelling cycle. (Encyclopaedia Britannica, Inc. 2010)

1.4.1. Bone development

Contrary to public conceptions, the bone of a living organism is not only a stiff inorganic scaffold to provide stability to the body, but also a highly biologically active endocrine organ that is undergoing constant remodeling and homeostasis. In order to do so, many different factors and cell types are required to perform specific functions in a tightly controlled and balanced manner to keep the bone in a healthy state.
Generally, two types of naturally occurring ossification are distinguished:

1. Intramembranous ossification is the process of new bone formation during fetal development and bone fracture repair, and is the typical means by which rudimentary bone develops. It is taking place in the development of the flat bones of the skull, in the maxilla, mandible and clavicles, as well as during bone fracture healing. In intramembranous ossification, fibrous membranes are replaced by bone tissue. A stepwise creation of the final bone tissue can be described as follows: Firstly, the ossification center is created by MSCs. For this, the MSCs cluster together, typically around blood vessels to ensure sufficient nutrients, and start differentiating towards osteoblasts. They now begin the active process of mineralizing their surrounding matrix (later called osteoid). These small islands of mineralized connective tissue (or osteoid) are then called spicules. These spicules can further be increased in size by surrounding osteoblasts that now start the calcification of the outer layer of the spicules. An osteoblast that becomes incorporated into mineralized bone tissue differentiates towards the very final step in the life of an osteoblast, the so-called osteocyte. The growing spicules will start to merge over time, resulting in trabeculae bone tissue, which further increases in size, at which point it is called woven bone. Now for the first time, an outer membrane is formed around the bone tissue by the MSCs, termed the periosteum. This defines the primary ossification center, and the region between mature bone tissue and the periosteum, i.e. the region of active ossification by osteoblasts. Finally, the bone collar is formed, thereby defining the end point of intramembranous ossification of this type of bone tissue [142, 143].

2. Endochondral ossification on the other hand, is the bone generating step of the long bones, and consequently of most bones of the body. While this bone formation step also occurs during fetal development and bone repair, unlike intramembranous ossification, hyaline cartilage is present during this type of bone formation. In the beginning, chondrocytes that evolve from chondroblasts form a cartilage ECM around themselves, thereby creating a cartilage template of the future bone development. Through continuous cell division, interstitial growth, or by increasing the volume of their ECM and hence increasing the thickness of the cartilage model, the template size is augmented. Once the cartilage model is formed, the primary center of

ossification is built at the center of the cartilage, followed by secondary ossification centers at the distal tips of the structure. Similar to intramembranous ossification, the ECM now becomes gradually calcified, thereby creating bone tissue, the spongy bone, which replaces the cartilage tissue. This is achieved by a process called chondrocyte hypertrophy, where the secretion of collagens and other proteoglycans is stopped, and instead the secretion of a protein called alkaline phosphatase (ALP) is initiated. After osteoclasts break down this newly formed bone tissue, the medullary cavity is created, giving rise to the bone marrow, which continues to expand towards the end of the bone. In the meantime, structures like the periosteum and the bone collar are also developed, resulting in the mature bone tissue [144].

In addition to the bone tissue itself, bone is also comprised of the bone marrow tissue as shown in figure 2. This “loose” tissue within the bone fills up the medullary cavity of the bone and can be distinguished into two different kinds of bone marrow: the red bone marrow consists mainly of the hematopoietic stem cell pool which give rise to platelet, red and white blood cells, and the yellow bone marrow which consists mainly of adipocytes, but also of precursor cells for osteoblasts, osteoclasts, fibroblasts and macrophages. The function of the yellow bone marrow goes beyond the storage of energy for the organism, but involves nutrient and energy supply for haematopoiesis, as well as an indirect involvement in haematopoiesis by secreting growth factors like colony stimulating factors, that initiate the maturation of blood precursor cells [145]. Both bone marrow types are highly vascularized, as their central metabolic roles require a significant supply of oxygen and nutrients and enabling the release of mature blood cells into the circulation [146].

The bone marrow is therefore central to the process of haematopoiesis, which provides vital blood cells of all types, as well as supplying cells to the lymphatic system. Growing evidence furthermore supports the theory of the bone marrow as having major endocrine functions important for many processes of the whole body [147, 148].

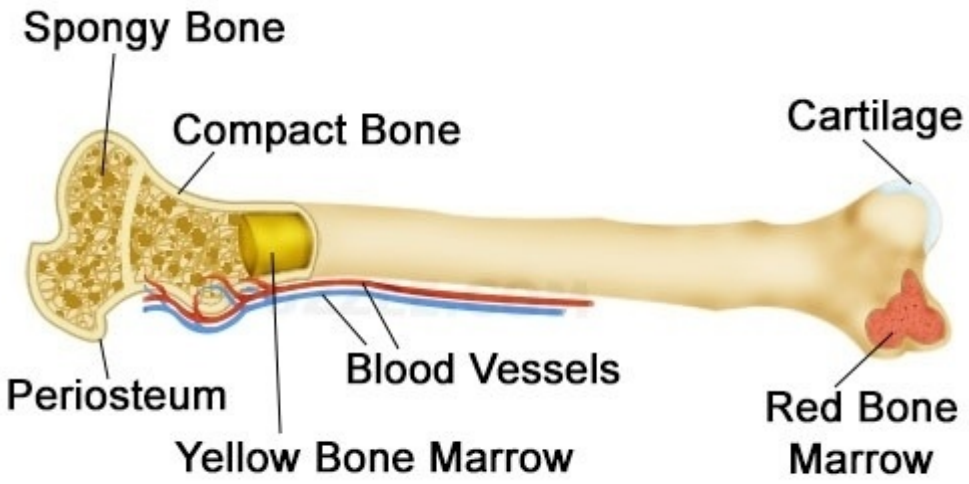

Figure 2: Schematic overview of a human long bone and its components. (www.buzzle.com)

1.4.2.Bone turnover and remodelling

Importantly, healthy bone tissue is not only undergoing ossification, as this would make the bone very fragile over a lifelong period, but also resorption. This tightly controlled balance of bone production and resorption termed bone turnover, ensures the integrity of the inorganic components of the bone. A dynamic balanced state where the production and resorption of the bone material results in a stable bone mass is an obvious prerequisite for intact bone tissue, where dysregulation of the bone production/ -resorption rate can result in bone diseases such as osteopetrosis and osteoporosis [149]. Many factors are involved in the regulation of bone turnover and an overview of the cells involved in this process are introduced in more detail in the following chapter.

1.4.3.Bone cells and their function

The biologically highly active bone tissue is kept alive by a number of cells, each of which is important to maintain intact bone. The following list highlights the most important cells types and their main function in bone remodelling:

1. Osteoblasts are, in mature bone, found mostly on the surface of the bone ossification center between periosteum and bone tissue, and are the cells responsible for bone synthesis. Although they can actively calcify their surrounding ECM, calcification or mineralization, *in vivo* only occurs at the so-called osteon, which is a site of interconnected osteoblasts. This calcification and mineralization of the ECM occurs in a highly specific manner, starting with the secretion of very dense and cross-linked collagen. Organic phosphate and calcium is then actively precipitated on this collagen scaffold, resulting in the final hydroxyapatite. This is facilitated with the help of the secreted protein ALP, which precipitates the calcium-phosphate-hydroxide salt. Notably, the combination of collagen and hydroxyapatite results in a tissue that fulfils both tensile and compressive strength, resulting in excellent stability characteristics of the bone. The osteoblasts are found in large numbers on the surface of the bone either in an active or silent state, termed lining cells. Once the osteoblast is buried in the extracellular inorganic region of the bone, it is called an osteocyte, where it still exhibits important functions for maintaining bone integrity [150]. Besides ALP, osteoblasts also secret other proteins like osteopontin and osteocalcin, which are important for bone production but will not be discussed further here.

2. Osteoclasts are, contrary to osteoblasts, responsible for the resorption of bone material. Typically found in pits on the surface of the bone, the resorptive bays or Howship´s lacunae, they actively resorb the hydroxyapatite and collagen of the bone by acidifying the environment in and secreting a number of collagenases. The acidity is reached by the secretion of an acid phosphatase, which is stored in large amounts in lysosomes in the cytoplasm of the cell. When needed, the osteoclasts are able to release high levels of these lysosomes. In order to optimize the resorption efficiency, osteoclasts contrary to osteoblasts, are organized in a polar manner, where one side of the cell is characterized by having a ruffled border. These can be described as villi which dramatically increase the surface area of the osteoclasts, thereby facilitating molecule exchange over the cell membrane [151].

3. Osteoprogenitor cells that are found primarily in the cavity of the bone marrow, build one half of the stem cell pool found in the bone. Also called pre-osteoblasts, these cells are the progenitor cells of the osteoblasts that are responsible for bone synthesis [152].

4. HSCs are also found in the cavity of the bone marrow and represent the pool of cells which can, upon stimulus, differentiate towards the myelopoietic and erythropoietic cell type and enter the blood circulatory system.

5. MSCs are found in large numbers in the bone marrow of all bones and thereby constitute the second class of stem cells found in the bone.

6. White adipose tissue (WAT) of the bone marrow is, contrary to public perception, the most common tissue found in the bone marrow. Produced by adipocytes, it fulfils very important endocrine functions, some of which have only recently been discovered [147]. Its secretion of, for instance, adiponectin and leptin has global applications in the body and is likely to be an important key player in fat homeostasis of the whole body. The WAT is believed to be an energy reservoir for the cells of the hematopoietic stem cell line to terminally differentiate, when needed.

1.4.4. Bone function

Next to its function to provide stability, bone exhibits functions in the body that may be somewhat unexpected. The following list of major functions of the bone exemplifies why bone is classified as an organ:

1. Calcium homeostasis is a central function of bone tissue, as the calcium released by osteoclast activity would otherwise be harmful to the organism at certain concentrations. Furthermore, a calcium reservoir for bone formation is thereby always guaranteed on site, and the calcium concentrations for other parts of the organism, e.g. the blood plasma, are easily controlled as this can have a major impact on various processes, such as blood pressure regulation [153]. Furthermore, a relatively low concentration of calcium needs to be

guaranteed, as the calcium ion represents an important second messenger molecule. An overview of the calcium homeostasis in the human body can be seen in figure 3.

2. pH buffering properties are another important feature as the bone is able to rebalance occurring pH changes of the bone and the blood by releasing or absorbing alkaline salts.

3. A certain amount of detoxification of several harmful compounds was described. These can later on be gradually released so that a controlled breakdown or excretion is guaranteed (e.g. lead poisoning [154]).

4. Fat storage is one of the most important features of the bone. In fact, the role of WAT in the marrow of the bone is not completely understood and probably holds important but, as yet, unknown functions. However, the fat tissue in the bone is also an energy source for the HSCs, enabling them to differentiate towards fully functional blood cells, as mentioned earlier [145].

5. As an endocrine organ, bone can store and release many hormones and growth-factors that are essential to the human body. Insulin regulation is for instance realized partially by osteocalcin, as well as the phosphate homeostasis which is directly controlled via FGF-23 [155].

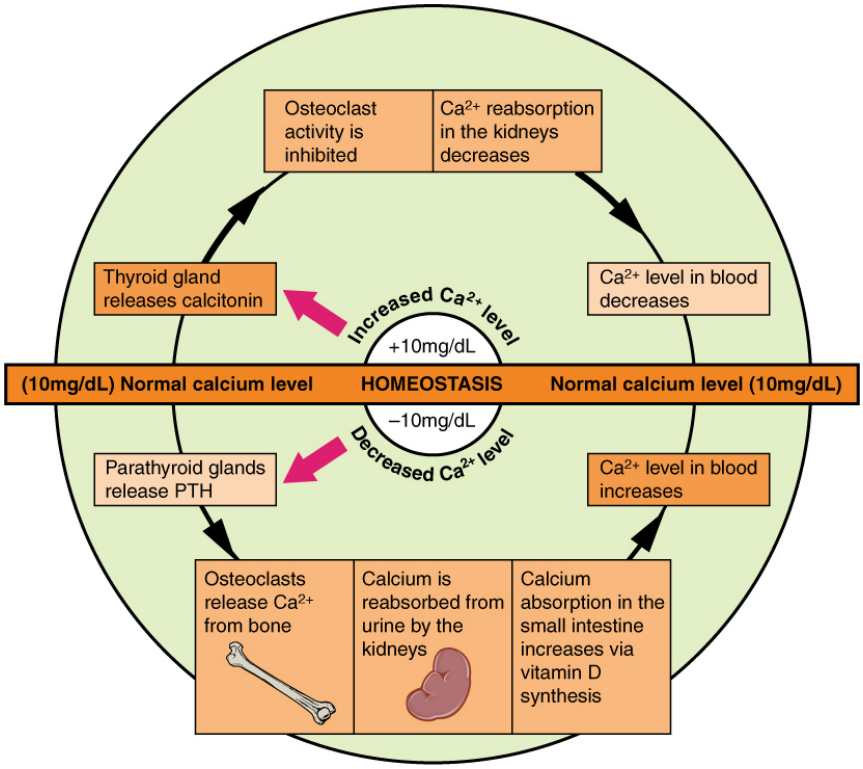

Fig. 3: Schematic overview of the calcium homeostasis in the human body (www.philschatz.com).

1.4.5.Pathophysiology of bone remodelling

Bone turnover is a balanced state of bone production and resorption A large number of steroid and protein hormones, as well as other multiple factors and cells, control the regulation of bone remodelling. Alterations in these processes can result in severe disease or pathophysiological conditions that affect bone integrity. This chapter therefore highlights well-known factors and their contribution to pathological conditions of the bone.

Cytokines play a major role in bone resorption. They can stimulate osteoclast maturation and development. Pathologically upregulated levels of, for instance IL-6, are known to be involved in osteopenia-like diseases [156]. Many cell types are under a constant control by cytokines, which are released by cells all over the body.

Hormones such as parathyroid hormone (PTH), along with Vitamin D are responsible for calcium and phosphate release into the circulation of the body. PTH is able to indirectly stimulate osteoclast activity and thereby induce the release of calcium from

the bone into the blood. It is directly sensed by osteoblasts, which in turn increase the expression of the receptor activator of nuclear factor kappa-B ligand (RANKL), a cytokine belonging to the tumor necrosis factor family (TNF), which can inhibit the expression of its antagonist osteoprotegerin (OPG). Under these conditions, osteoclastogenesis is induced, and bone resorption enhanced [157-159].

Other hormones like testosterone and estrogen play important roles especially in the development and maintenance of bone. While some functions of these hormones on a cellular level are understood, others remain unclear [160]. As an example, in healthy bone, estrogens are known to be inhibitory towards bone resorption, resulting in a drastic increase in bone resorption upon estrogen deficiency [161].

Intact stem cell differentiation machinery is the bottleneck underlying the availability of osteoblasts and osteoclasts in the bone. An imbalance in the activity of either of these two cell types results in a disturbed bone formation/ -resorption rate, which can ultimately lead to osteoporotic bone. The exact cause for such a loss in bone homeostasis and its full influence on bone turnover is poorly understood, but currently under investigation [162] and thus highlights the complexities of maintaining healthy bone.

1.4.6.Bone diseases

Since bone is a metabolically active and tightly regulated tissue, malfunctions in any of the involved parameters can result in medical conditions of the bone and even other tissues. The most common ones are further discussed in the following section:

1.4.6.1. Effects of age on bone quality

The bone tissue undergoes global changes during aging. It is generally accepted that bone density declines with age. The reasons for this are as diverse as the cells involved in bone maintenance [160, 163]. While bone mineral density (BMD) is gradually declining in men and women from the age of 30 on, the menopause induces another rapid decline in BMD in women. Moreover, a key player in the ageing bone appears to be PTH. The integrated PTH secretory response is increased with age, independent of the gender. However, the exact mechanism as to how this increase results in decreased BMD is not understood [164].

Another likely scenario to contribute to bone loss with aging is a deficiency in stem

cell differentiation. As stem cells continuously contribute to the pool of osteoblasts and osteoclasts, a decline in either of those cell types would also result in bone deficiency. For instance, an impaired capacity of the BMSCs to differentiate towards the osteoblastic lineage, could lead to decreased bone synthesis and a subsequent increase in bone resorption rate [165].

1.4.6.2. Osteoporosis

Osteoporosis is a worldwide health issue affecting millions of people. It is a slowly progressing disease characterized by a decrease in bone mass and density. The resulting loss in bone strength results in an increased fragility of the bone, which makes it especially dangerous for elderly people due to high a high incidence of fractures. Next to the BMD being affected, the microarchitecture as well as the amount and variety of cells and proteins in the bone is altered. Finally, peak bone mass is pathologically lowered, when compared to healthy bone tissue [166]. One potential cause of osteoporosis is an imbalance in bone turnover:

1. Insufficient bone synthesis (e.g. due to dysfunctional osteoblasts or reduced osteoblast activity/ numbers)
2. Increased bone resorption (e.g. due to hyper-active osteoclasts).

In human medicine, osteoporosis is categorized as being either; postmenopausal osteoporosis, also referred to as primary type 1 osteoporosis, and is prevalent in women after menopause due to decreased levels of estrogen or senile osteoporosis, or primary type 2 osteoporosis, which occurs in both men and women starting around 75 years of age. An additional form of osteoporosis termed secondary osteoporosis can also occur at any age in both genders and is caused by multiple factors, such as chronic medical abuse and excessive glucocorticoid use (steroid-induced osteoporosis)

The treatments available for osteoporosis attempt to prevent either the progression of osteoporosis itself, or the fracture risk associated with osteoporosis. They extend from calcium and vitamin D supplementation, although controversially discussed [167], to bisphosphonates. While calcium and vitamin D supplementation stabilizes the bone directly, the bisphosphonates on the other hand are believed to inhibit osteoclasts and thereby compensate for the reduced bone synthesis or increased

bone resorption. The mode of action of bisphosphonates is surprisingly simple, yet very effective: the bisphosphonates themselves bind to calcium, which is only found at high concentrations in the bone. An osteoclast resorbing the calcium that is now bound to bisphosphonates induces apoptosis. While non-amino bisphosphonates bind to ATP and make it unavailable for the cell, thereby creating a huge lack of energy for the cell, amino-containing bisphosphonates bind to and block the enzyme “farnesyl diphosphate synthase” (FFPS), which ultimately leads to an induction of apoptosis of the osteoclast [162, 166-168].

1.5. Molecular regulation of osteogenesis

Bone mineralization is a precisely orchestrated multi-step process in which MSCs migrate and divide, followed by a differentiation cascade from cartilage forming chondroblasts to osteoblasts, and ultimately mineral deposition and bone formation [139]. Bone marrow residing MSCs are first differentiating into pre-osteoblasts at the expense of proliferation capacity [169], and subsequently develop into mature osteoblasts which then foster deposition of mineral leading to matrix mineralization and bone formation [170]. A certain fraction of bone forming osteoblasts may differentiate further into bone residing osteocytes. Besides bone generation, the absorption of bone through osteoclasts is crucial to maintain a balanced homeostasis within the bone. Osteoclast activity, in particular osteoclast maturation, is regulated by osteoblasts through RANK signaling [171]. Osteoclast precursors are expressing the RANK receptor on their cell surface and binding of osteoblast-secreted RANKL triggers differentiation into the osteoclast lineage. Osteoclasts then exert their activity through the matrix degrading protease Cathepsin K [172]. In order to limit the bone resorption, osteoblasts are further expressing the RANKL competitor OPG, which binds to RANK with equal affinity and therefore inhibits promotion of osteoclastogenesis [173]. Hence, a delicate orchestration of RANKL and OPG expression is crucial to ensure proper maturation of BMSCs to osteoblast and maintain a balanced bone homeostasis.

1.5.1. Signaling events governing osteogenesis

As major players in osteoblast differentiation [174], alterations in the expression levels of BMPs have been shown to results in strong bone-related abnormalities during development [175, 176]. BMPs themselves are extracellular acting multifunctional signaling cytokines that belong to the large transforming growth factor-beta (TGF-β) super family, consisting of about 60 isoforms [177]. In todays clinical applications, recombinant forms of human BMP-2 and BMP-7 are widely used in therapeutic interventions to treat bone related conditions, such as non-union, delayed union, spinal fusions, root canal surgery and osteoporosis [174]. In the

canonical signaling pathway, the two surface receptors BMPRI/BMPRII upon binding of the ligands TGF-β and BMP, phosphorylate and activate SMADs [178], which then in turn interact and activate various downstream proteins such as Runx2, leading to up-regulation of bone related genes [179]. Similarly, non-canonical SMAD-independent signaling results in the same Runx2 activation, although through the p38 MAPK pathway [169]. The spatiotemporal tightly regulated activity of Runx2 and BMP-activated SMADs is crucial for bone formation and maintenance, as is the delicate interaction and cross-talk with other major signaling pathways such as Wnt [180-182], Hedgehog (Hh) [183, 184], Notch, MAPK and mammalian target of rapamycin (mTOR) [185].

The intracellular transducers of BMP signaling are the Smad proteins which are divided into three classes, the receptor regulated Smad (R-Smad), the common mediator Smad (C-Smad) and the inhibitory Smads (I-Smad) [186], each consisting of an N-terminal nuclear localization signal and DNA-binding domain, a middle linker domain and a BMPRI binding C-terminal domain [187, 188].

Upon ligand binding, BMPRII initiates the kinase activity of BMPRI resulting in the phosphorylation of the R-Smad 1 and 5 [169]. These in turn disassociate from the BMPRs to form a complex with the cytosolic C-Smad 4 and undergo translocation to the nucleus [139] where they regulate transcriptional activity either directly [189, 190] or through interaction with DNA-binding proteins [174, 191].

BMP signaling facilitates expression of Dlx5 on osteoblasts, which in turn induces expression of Runx2 in osteoprogenitor cells. Subsequently Runx2 and Smad interact and co-operatively regulate transcription of osteogenic target genes [192].

The previously mentioned threonine and proline rich linker domain of the Smad proteins is the anchor point for cross-talk between BMP and MAPK signaling [193], as it can be phosphorylated by Erk and GSK3-β and subsequently ubiquitinated and degraded, thereby preventing its nuclear translocation and propagation of the BMP ligand induced signal [194]. Recently, mTORC2, a major effector of mTOR signaling, has been identified as a mediator of BMP signaling [195] and TGF-β induced phosphorylation of Akt [196]. Akt can block phosphorylation and activation of downstream Smad3 through mTOR, thereby blocking TGF-β signals downstream and finally expression of osteogenic genes [196].

mTOR is a well conserved checkpoint protein kinase that has recently emerged as a major player in osteogenesis by integrating signals received from growth factors,

nutrients and cellular energy metabolism [197, 198] and by regulating cell-cycle progression and MSC differentiation [185].

mTOR exerts its kinase function through the C-terminal catalytic domain [199, 200] and through binding and multimer formation with other regulatory components [201, 202]. Depending on its association with various adaptor proteins, mTOR can form two distinct multi-protein complexes, subsequently termed either mTORC1, which regulates adipogenesis, osteogenesis and myogenesis or mTORC2, which exclusively regulates myogenesis (see Figure 4), whereas the adaptor proteins Raptor and Rictor determine the substrate specificity.

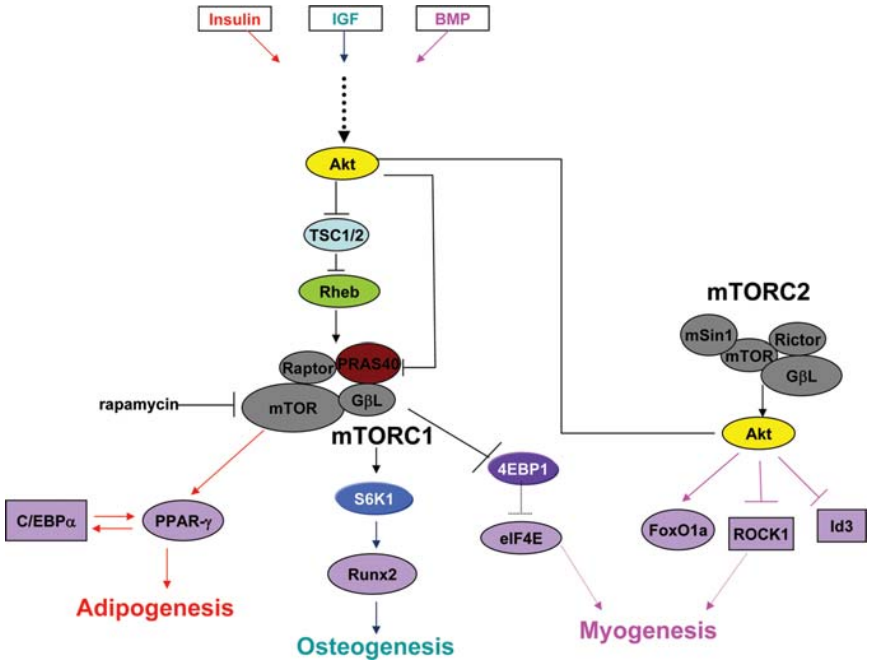

Fig. 4: The mTOR signaling pathway in MSC differentiation [185]

mTORC1 contains mTOR associated with regulator-associated protein of mTOR (Raptor), as well as G protein β subunit-like protein (GβL), and this complex specifically phosphorylates ribosomal protein S6 kinase 1 (S6K1) and eukaryotic initiation factor 4E-binding protein 1 (4E-BP1). By contrast, mTORC2 consists of mTOR, rapamycin-insensitive companion of mTOR (Rictor), mammalian stress-activated protein kinase-interacting protein 1 (mSin1) and GβL. As a complex it acts to phosphorylate and activate Akt. However, located upstream in the signaling cascade there is the tuberous sclerosis complex (TSC) [203, 204] and its immediate downstream target Ras homolog enriched in brain (Rheb), which then activates mTOR kinase [205, 206]. In addition, mTOR can undergo autophosphorylation [207]

and its activity can be inhibited by rapamycin, resulting in alterations in 4E-BP1 and S6K1 activity [199].

For MSCs undergoing osteogenesis, the mTOR/S6K1 signaling pathway plays a central role [208, 209]. S6K1 has been shown to regulate osteogenesis indirectly, acting on multiple levels such as TNF-α-induced interleukin-6 synthesis [210], fibroblast growth factor (FGF) 2-stimulated interleukin-6 synthesis [211], platelet-derived growth factor-BB-induced interleukin-6 synthesis [212], BMP-4-stimulated vascular endothelial growth factor (VEGF) synthesis [213] and FGF-2-stimulated VEGF release [214]. It is widely accepted that mTOR signaling affects osteoblast proliferation and differentiation [209, 215, 216] as well as proliferation of MSCs [215, 216]. However the effects of rapamycin on osteogenesis remain controversial, with both inhibitory [217, 218] and stimulatory [208, 219] actions having being reported. Nonetheless, in mouse BMSCs, rapamycin has been shown to inhibit osteoblast differentiation [209] by blocking osteoblast-specific gene expression, ALP activity and mineralization of extracellular matrix [217]. Given its possible detrimental role in osteogenesis, further insights into mTOR signaling are required in order to reveal the detailed contributions and mechanisms involved in osteoblast lineage commitment of MSCs.

1.5.2.Cross-talk in osteogenic signaling

Cross-talk between signaling pathways involved in MSC differentiation might occur to synergistically regulate key components of osteoblast maturation. For example, Hedgehog signaling, where Sonic Hedgehog (Shh) together with Gli2 induces BMP2 expression thereby stimulating osteogenic differentiation [220], or where Shh alone up-regulates TGF-βII and therefore inhibits differentiation into the chondrocyte lineage during bone development [192].

Moreover, Wnt signaling is involved in the formation and maintenance of bone through multiple mechanisms such as stem cell renewal, osteoblastogenesis and inhibition of osteoblast apoptosis [221]. Upon binding of the Wnt ligand to its cognate receptor frizzled and the co-receptor LRP5/6 [222], cytoplasmic β-catenin degradation stops and it translocates to the nucleus where it activates gene

expression [223]. Signaling cross-talk during osteoblast differentiation occurs through modulation of Wnt signaling by BMP2, as it stimulates expression of Wnt, LRP and Fz receptors [224]. In differentiating osteoblasts, the canonical Wnt signaling interacts with Runx2 thereby mediating BMP9 driven osteogenic signaling [225] by recruiting β-catenin and Runx2 to the osteocalcin promoter [169]. Furthermore, an increase in complex formation between TCF4 and Runx2 has been reported, which in turn increase expression of TGF-βRI and therefore osteogenesis [226]. Taken together, cross-talk between BMP and Wnt signaling occurs on multiple levels in tissue maintenance during fracture repair as well as differentiation of MSCs into the osteoblast lineage [139, 227]. This is most evident in the case of protein Wnt10b, which up-regulates expression of the core binding factor alpha 1 (Cbfa1/Runx2), Distal-less homeobox 5 (Dlx5) and osterix, thereby committing the cell towards the osteoblast lineage. Simultaneously, it inhibits adipogenesis by down-regulating C/EBP-α and PPAR-γ [228]. C/EBP-β in turn has been found to be regulated through Spry1 which is critical for adipocyte differentiation and acts as a transcriptional coactivator also on PSD-95, DLG, ZO-1 and PDZ-binding motif TAZ [229]. Members of the MAPK family of proteins such as extracellular signal-regulated proteins kinase (ERK), c-Jun N-terminal kinase (JNK) and p38 are equally involved in regulating the lineage commitment of MSCs [230]. Interference of the MAPK pathway favours adipogenesis by affecting the downstream osteogenic effectors ERK and JNK. Over-expression of the Twist-1 and Dermo-1, members of the TWIST family of helix-loop-helix transcription factors, results in decreased osteo-/ chondrogenic differentiation potential and a shift towards adipogenesis [231]. Additionally, the basic leucine-zipper transcription factor Maf and the Zinc-finger protein 467 (Zfp467) [232] have also been identified as having equal importance in the process of osteogenic differentiation. By directly acting on the cell-cycle, the tumor suppressor pRb can promote osteogenesis in two ways, either by interacting with Runx2 to enhance osteogenic differentiation or by acting together with E2F to suppress PPAR-γ and subsequent adipocyte differentiation [233].

Recently it has been shown that besides cross-talk of multiple signaling pathways, miRNAs are involved in the regulation of osteoblastogenesis as well [179, 234]. For example, the miRNA miR-218 has been found to facilitate osteoblast differentiation by inhibiting sclerostin or the miR-2861, which represses histone deacetylase 5 (HDAC5) expression and thereby promotes osteoblast differentiation. More

specifically, *RUNX2* gene expression and osteoblast differentiation can be inhibited by miR-204, miR-211 [235] and directly targeted by miR-355 [236], or osteoblastogenesis can be inhibited indirectly by interfering with translation of Smad1 through miR125b and miR26a [237].

Another signaling network affecting *RUNX2* gene expression and therefore osteoblast maturation is the Notch pathway where the Notch intracellular domain directly interacts with transcription factors and/or co-activator to modulate gene expression [238]. Furthermore, Notch signaling has been found to potentially mediate crosstalk and balance between osteoblast and osteoclast formation through its expression enhancing effect on RANKL and OPG [238]. Nevertheless, Notch signaling is clearly involved in osteoblast maturation and osteogenesis, as demonstrated by impaired bone formation and quality in mice deficient in Notch, along with defects in chondrogenesis [239]. Additionally NF-κB indirectly acts on downstream regulators such as HIF-2α, β-catenin and last but not least, Runx2 [240], although the majority of findings point out the inhibitory action of NF-κB on osteoblast differentiation by interfering with Smad signaling [241].

The sheer endless points of cross-talk between signaling networks and transcription factors underline the complexity of osteoblastogenesis and bone development. Consequently, a better understanding of the regulatory networks will undoubtedly help to provide new starting points for the development of alternative strategies to treat bone disorders.

1.6. BMSCs in age-related bone loss

As BMSCs can give rise to both osteoblasts and adipocytes [107], an imbalance between these differentiation processes may generate increases in adipocytes at the expense of osteoblasts, leading to an increase in fat marrow and potentially bone loss [242, 243]. Adipocyte differentiation is a two-phase process, mediated through transcription factors peroxisome proliferators activated receptor-γ (PPARγ) and C/CAAT/enhancer binding proteins (C/EBPs), in which pre-adipocytes mature into adipocytes. The large degree of plasticity allows transdifferentiation from pre-adipocytes to osteoblasts mediated through the osteogenic transcription factors Runt-related transcription factor 2 (Runx2) and Osterix (Osx) [170, 243, 244]. Overexpression of the BMP-2 downstream target Runx2 has been shown to be sufficient to effectively transdifferentiate pre-adipocytes into mineral forming osteoblasts [245]. Maintenance of a stable bone mass throughout life requires a precise balance in signaling events for BMSC differentiation into osteoblast and HSC differentiation into osteoclasts [246, 247]. In general, bone loss gradually occurs with aging as a result of hormonal changes, and is dependent on gender and various risk factors [248, 249]. Risk factors may be non-heritable, such as age-related changes, oxidative stress, apoptosis, sex-steroid deficiency and life style, or heritable due to epigenetic alterations [248]. The main contributor of cellular aging is senescence due to shortening of telomeres, deficiencies in repair mechanisms as well as epigenetic alterations, thereby restricting cellular proliferation and regeneration potential [250]. The well known co-occurrence of aging and deficits in bone quality have been investigated in numerous animal models, the results of which have allowed for new insights into a broad spectrum of underlying molecular mechanisms controlling bone quality. Some examples of these are discussed below.

1.6.1. SAMP6 mouse model

The senescence-accelerated mouse (SAMP6) model is not only characterized by the occurrence of spontaneous fractures but moreover, by a phenotype closely

resembling human osteoporosis such as a decrease in bone strength, mineral density and trabecular volume [251]. Recent studies investigating the underlying molecular mechanisms of this animal model are contradictory. On the one hand, impaired interleukin 4 (IL-4) signaling was suggested to cause the osteoporotic phenotype due to the promotion of osteoclast differentiation [252]. However, an oppositional overproduction of IL-4 also results in an impaired bone phenotype as characterized by a reduction in bone formation and quality [253]. Furthermore, BMSCs of SAMP6 mice show an impaired osteogenic potential whilst favouring adipogenesis [254, 255]. Therefore an investigation into alterations in osteogenic and adipogenic genes may provide more insight into the molecular mechanisms underlying the osteoporotic phenotype of SAMP6 mice [254].

1.6.2.Klotho mouse model

Another model of premature aging with the prevalence of impaired bone quality is the Klotho mouse model where the disruption of a type-I membrane protein, namely klotho gene [256], primarily leads to elevated serum phosphate levels [257]. This is suggested to cause secondary cytotoxic levels along with deficits in organ function and subsequent acceleration of the aging process. As with the SAMP6 model, bone turnover parameters in the klotho model are reduced, along with an increase in BMSC adipogenesis and a decrease in osteoblastogenesis [258]. Additionally, it has been suggested that the Klotho protein exerts its action on bone quality through its ability to regulate the stimulatory actions of fibroblast growth factor 23 (FGF23) on BMSC osteogenesis [259], whereas FGF23 in turn has been postulated to be the main underlying cause of accelerated aging due its inhibitory actions on the hormonally active vitamin D metabolite $1,25(OH)_2D_3$ therefore impairing bone formation [260].

1.6.3. Telomerase deficiencies

As previously mentioned, the contribution of telomere shortening to the aging process is thought to be significant, and therefore of particular interest. Telomere length stability through cell division is mediated by telomerase. Mutation of the RNA component (TERC) of the reverse transcription subunit (TERT) of telomerase inhibits telomere maintenance and displays an accelerated aging phenotype along with early reductions in bone mineral density [261, 262]. The inability to maintain telomere length seems to contribute majorly to bone loss with progressing age [263]. Similarly, disruption of the Werner helicase (Wrn) shows a premature aging phenotype and in *Wrn*$^{-/-}$ mice, as well as the *Terc-/- Wrn*$^{-/-}$ mice, BMSCs are impaired in their mineralization potential *in vitro,* along with an increase in bone marrow fat content *in vivo* [262, 264]. Although a decreased efficiency in osteogenic potential of BMSCs is considered the main cause of this model, the contribution of BMSCs committing to adipogenesis remains elusive, as knocking out *Terc* has been shown to actually have a negative impact on BMSC adipogenesis [262].

1.6.4. Deficiencies in DNA repair

As with the disruption of helicase and telomerase function as described above, mutation of the xeroderma pigmentosum factor D (XPD) helicase gives similar premature aging phenotypes [265] along with impaired bone quality [266]. Partial or full disruption of an endonuclease involved in DNA repair, the excision repair cross complementary group 1-xeroderma pigmentosum group F (ERCC1-XPF), not only shows a reduction in osteogenic potential of BMSC, but further also is characterised by a senile osteoporotic phenotype [267]. Similarly, deficiencies in the Cdc42-specific negative regulator Cdc42GAP, which is involved in DNA damage repair and therefore essential for regulating genome stability, results in a phenotype displaying impaired bone quality [268]. In a model of Hutchinson-Gilford progeria syndrome (HGPS), established through disruption of the Lamin A gene by insertion [269], significant upregulation of p53 is prevalent in association with bone abnormalities. Comparably, knock-out of the lamin A processing metalloproteinase Zmpste24, shows similar

bone characteristics as the HGPS model, notably the hyperactivation of the p53 pathway, whereas a decline in BMSCs has been identified as the major underlying cause of the age-related bone loss [270]. Directly enhancing p53 results in similar reductions of life span along with the onset of a senile osteoporotic phenotype [271], possibly being due to a p53 mediated increase in mitochondrial sensitivity to high oxidative stress, therefore promoting aging [272].

1.6.5.Oxidative Stress

Oxidative stress occurs when reactive oxygen species (ROS), such as superoxide anions, hydrogen peroxide and hydroxyl radicals, accumulate due to an age-related decrease in ROS scavenging enzymes such as superoxide dismutase (SOD), glutathione peroxidase (GPx), glutathione (GSH) and catalase (CAT). This accumulation leads to non-physiological levels of ROS inducing damage on the genomic and protein level, subsequently impairing differentiation and maintenance of BMSCs, and finally leading to osteoporosis [248, 273, 274]. This has been confirmed on various levels in animal models such as *Sod*$^{-/-}$ mice, which show the expected increase in ROS, and more importantly, have a lower bone mineral density and reduced number of osteoblasts and osteoclast than their wild-type litter mates [275, 276]. On the level of transcription factors, β-catenin and FOXO play a central role in the defence of ROS induced damage. High levels of ROS lead to increased concentrations of FOXO in the nucleus and transcriptional activation of target genes involved in DNA repair (Gadd45), ROS detoxification (Sod2 and Cat), cell cycle arrest (CyclinG2, Cdkn1a and Cdkn1b) and apoptosis (Faslg and Bin1) [273]. Hence, mice with deficiencies in FOXOs show an increase in ROS levels, which in turn leads to an impaired BMSC differentiation and consequently lower osteoblast numbers [277]. Furthermore, FOXO retains β-catenin in the nucleus [278, 279], thereby antagonizing Wnt signaling which is an essential stimulus for BMSC differentiation into osteoblast [280].

1.6.6.Non-genomic factors in aging of BMSCs

Besides the widely accepted genomic contribution to bone formation and maintenance, the involvement of epigenetic factors has gained significant interest. The well-known contribution of decreasing methylation to the mechanism of senescence [281, 282] has been investigated in a model, where the SNF2-like gene (PASG), associated with regulation of genome methylation, has been knocked-out. The resulting phenotype shows significant hypomethylation along with an increase of senescence markers such as p16, p21 and p53, but most notably of all, severe impairment in bone development [283]. Furthermore, the loss of a glycosyl phosphatidylinositol-anchored cell surface protein, a stem cell antigen (Sca-1/Ly-6A) [284], has been investigated in a Sca-1 knock-out model, which shows an increased susceptibility to fractures due to a senile osteoporotic phenotype [285]. The underlying cause is suggested to be progressive depletion of osteoprogenitor cells as a consequence of deficiencies in stem cell self-renewal. Additionally, the reduction in osteoblast numbers lead to decreases in RANKL mediated regulation of osteoclasts and consequently an increase in bone resorption.

1.6.7.Non-modifiable risk factors

Apoptosis of cells within the bone microenvironment, in particular the age related dysfunction and decay of osteocytes, leads to an increase of locally released RANKL, thereby stimulating osteoclastogenesis and accelerating the resorption of bone [286]. In the mouse model, inhibition of apoptosis in osteocytes leads to an increase in trabecular bone mass due to reduced extracellular RANKL [287]. As levels of sex steroids, such as oestrogens in women and androgens in men, are naturally declining with age, their anti-apoptotic effect on osteocytes is lost and thus contributes to age-related bone loss [288-290].

Gender specific differences in bone structure are not only restricted to the later stages of life. Already during puberty, differences in bone composition and size become evident. Female oestrogens can act to restrict periosteal bone formation, whereas male androgens act to induce bigger and stronger bones [248, 291]. These

initial differences in peak bone mass and size are considered a major reason for the higher prevalence of osteoporosis amongst females [248]. On the other hand, at later stages in life, in particular the early postmenopausal period, the decreasing physiological levels of sex-steroids accelerate the decline in BMD through alterations in osteoclast, osteoblasts and osteocytes function, resulting in an imbalance between bone formation and bone resorption [274, 292]. In particular, the rate of bone turnover is accelerated within the cortical compartment, and delayed within the trabecular compartment, ultimately leading to an increase in cortical porosity [293-295]. Nonetheless, after the initially accelerated decline in BMD in women, the rates of bone loss are equal amongst both genders [296].

1.6.8.Modifiable Risk Factors

Besides the aforementioned non inheritable and non modifiable risk factors, there are a few modifiable factors with considerable potential to influence BMSC differentiation and the occurrence of osteoporosis, such as dietary composition, physical activity, smoking and alcohol consumption [248]. For example, and inadequate intake of phosphate, calcium and vitamin D, not only impairs mineralization and bone formation, but also enhances the resorption of bone [297, 298], and can even influence neuromuscular function and balance [299]. Therefore, the availability of calcium and a high-protein diet is associated with a higher BMD and reduced susceptibility to fractures [300, 301]. Moreover, regarding the previously mentioned role of ROS on bone homeostasis, dietary implementation of antioxidants such as fruits and phytochemicals, also helps to relieve cellular ROS stresses [302, 303]. Besides targeted dietary intake, a reduction in cellular ROS levels could also be achieved through implementation of regular physical activity [248, 304]. In the recent past, the dramatic benefits of physical activity in prevention of, but not limited to, cardiovascular disease became widely accepted. In the context of bone formation, the mechanical stimulus induced by exercise is registered by osteocytes [305] and triggers a decrease in their secretion of the Wnt-signaling inhibitor sclerostin [247, 306-309], which in turn leads to a subsequent activation of Wnt-signaling mediated osteogenesis [310-312]. Contrary to the beneficial effects of exercise, frequent and

excessive intake of alcohol [313-316] as well as smoking [317-319] have been shown to decrease BMD due to inhibition of osteogenesis and accelerated bone resorption.

1.7. MSC-targeted therapies to treat age-related bone disease

The very first steps taken in the development of stem cell based therapies go back to the year 1951, when donor bone marrow aspirates where used to improve healing of bone defects by percutaneous application at the defective site [320, 321]. Despite great interest and efforts in stem cell based therapies for bone regeneration during the last 30 years, their implementation in today's clinical routine still lags far behind the initial expectations [322]. The gold standard for repair of bone defects is still autologous bone grafting, where the patients own bone, mostly removed from the iliac crest, is transplanted to the defective site. The side effects of this including donor site morbidity, donor material limitation and quality with a particular emphasis on osteoporotic cases, has led to alternatives being sought where various combinations of cells from different origins, bioactive carriers and growth factors are now used to repair small to big sized defects [322-324]. In this regard, the use of BMSCs or ASCs has gained increasing support as a suitable cell-based alternative to enhance bone regeneration and quality. Indeed, ASCs have shown robust osteogenic potential [35, 322, 325, 326] in several animal models [327, 328] as well as in various clinical trials [329-332]. Already, adipose tissue has advanced to the preferred source of adult stem cells as they have a higher abundance combined with easier accessibility and reduced donor site morbidity [35, 333, 334]. Hence, allogeneic as well as autologous BMSCs and ASCs have been widely applied in the clinical environment to a variety of conditions, such as acute trauma, non-union of bone upon trauma, osteonecrosis of femur head, spinal fusion and osteoarthritis [322].

1.7.1. ASCs in bone regeneration and repair

ASCs are particularly well suited for applications in bone repair as they are, in contrast to BMSCs, more tolerant to low oxygen conditions as found in low vascularized, newly formed bone [330]. Furthermore, ASCs are well known for their paracrine action, secreting angiogenic cytokines such as hepatocyte growth factor and vascular endothelial growth factor and thereby promoting homing signals for

resident stem cells [335]. Non-genetically modified, autologous ASCs have been used successfully to repair large craniofacial defects through ectopic vascularized bone formation. This involved the dissection of bone from the patient's iliac crest, fibula or ribs and the generation of ground bone chips. Further, this material was then mixed with osteoinductive recombinant human growth factors such as BMP-2 or BMP-7, and combined with *ex vivo* expanded ASCs into a pre-shaped titanium mesh [322]. As restoration of blood supply is critical for integration and survival of ASC containing bone grafts, as an intermediate step, this mesh was implanted for several months into a large and highly vascularized muscle such as latissimus dorsi or rectus abdominis to stimulate vascular ingrowth, before being inserted for integration into the defective area. By four months post surgery, sufficient bone had formed to support dental implants [322, 330, 336]. In order to prevent ectopic bone formation, a mixture of ASCs and BMP-2 soaked β-tricaclium phosphate granules, again in an individually shaped titanium mesh, is directly applied at the target site. In this case, dental implants were successfully supported by the newly formed bone ten months post surgery [337]. Also in difficult larger fractures with multiple pieces, ASCs combined with fibrin glue and autologous bone chips, have been shown to restore bone function [338].

1.7.2.*In vitro* studies

One of the limiting factors in bone tissue engineering, is the availability of autologous material. As such, artificial resorbable materials are being developed which serve as both a carrier for donor MSCs and an osteoconductive platform for use in repairing bone defects. In particular, hydroxyapatite and calcium phosphate exert osteoconductive properties and consequently are considered the ideal substrate to be used as a matrix. The use of porous hydroxyapatite as a carrier for MSCs has successfully been applied to non-union fractures and diaphyseal defects, to a level where osseous integration of implants was observed after months and even years [339-341]. Successful spinal fusion through the use of a β-tricalcium phosphate scaffold carrier supplemented with MSCs has been applied to a wide range of patients with a successful healing rate as high as 95% [342].

Numerous combinations of animal models, defect sizes and carriers even in combination with transient gene expression have also been investigated, and thereby highlight the robust osteogenic potential of ASCs to repair various kinds of bone defects across species. ASCs combined with nano-biphasic calcium phosphate (NanoBCP) and alginate gel or with apatite-coated PLGA scaffolds were found to be effective in repairing critical size cranial defects in a rats [343, 344]. Furthermore, ASCs seeded on either PLA scaffolds [339] , gelatine foam [340] or coral [241] have successfully been used to repair bone defects in rats, rabbits and dogs respectively. In a further study, ASCs were combined with either BMP-2 coated PLGA scaffolds or transfected to overexpress BMP-2 and Runx2, which in both cases resulted in successful ectopic bone formation [345], suggesting that once transplanted, osteogenic induced ASCs are able to remain viable, maintain their osteogenic properties and even stimulate resident stem cells of the injured environment [346].

1.7.3.Clinical studies

In the clinical environment, ASCs have been applied to repair large bone defects of the calvaria following injury. Autologous ASCs applied as a mixture with milled autologous bone from the iliac crest and fibrin glue, has successfully been used to repair such defects within 3 months [338]. Similarly, ASCs in a mixture with BMP-2 on a β-tricalcium phosphate scaffold could successfully restore oral function in a hemimaxillectomy-induced defect within 12 months [330].Despite the promising clinical outcomes following the use of ASCs, further safety evaluations are still needed, especially considering their immunosuppressive capacity which could facilitate and favour tumour growth under certain conditions [346]. Nonetheless, their easy accessibility in combination with low donor site morbidity and the ability to undergo robust osteogenesis, makes them ideal candidates for future clinical studies.

1.7.4. Bone and fat: the osteogenic potential of ASCs

As previously discussed, ASCs display self-renewal, are multipotent [110, 347] and undergo multilineage differentiation into adipocytes, chondrocytes, myoblasts and osteoblasts [346, 348]. As compared to BMSCs, the accessibility of ASCs is much easier and can be acquired through lipoaspiration from the fat tissue at a much higher abundance and with less donor site morbidity [349, 350]. Furthermore, autologous ASC sources within the human body are widespread, allowing for much higher volumes of aspirate in comparison to BMSCs harvested from the bone marrow [351]. Bone marrow aspirates are limited to a 100ml, which will yield roughly 6x10^6 cells/ml of which 0,001% - 0,01% are BMSCs. By contrast, aspirates from liposuction procedures which will easily yield aspirates of 1000ml – 2000ml with 2x10^6 cells/ml of which 10% are thought to be stem cells [34, 352], which is already enough to repair small bone defects without the need of extensive *ex vivo* cultivation [107, 353]. Consequently, ASCs have become a very attractive and competitive alternative to the limiting autologous bone graft in bone tissue replacement therapies, which still represents the gold standard for the treatment of bone defects [34]. ASCs in humans can be isolated from fat tissue at various locations, although the preferred source in mice is the inguinal fat pad. ASCS are usually liberated from the fat tissue through collagenase digestion, yielding a heterogeneous cell population of erythrocytes, fibroblasts, endothelial cells, smooth muscle cells, pericytes and ASCs which then have to be sub-cultured on a plastic surface in order to obtain a homogeneous population of ASCs [34, 35]. Besides the minimal criteria of multi-lineage differentiation and plastic adherence, ASCs have to express the stromal surface markers CD73, CD90, and CD105 but must not express markers of the hematopoietic lineage c-kit, CD14, CD11b, CD34, CD45, CD19, CD79-α and human leukocyte antigen-DR [108]. Interestingly, ASCs have a higher proliferative capacity with stable population doublings and a lower level of senescence as compared to BMSCs [34, 354, 355]. Furthermore, the impact of aging seems to be more prevalent on the differentiation potential of BMSCs than in ASCs [34, 356-358].

1.7.5.Osteogenic differentiation of ASCs

In order to better understand the intricacies governing ASC osteogenesis, studies have primarily focused on establishing *in vitro* differentiation assays. The osteogenic differentiation of ASCs is primarily performed through the use of osteogenic medium with the functional components being β-glycerophosphate, ascorbic acid and dexamethasone. Alternative approaches include BMP-2 treatment [343, 359], NF-κB activation [360], use of histone deacetylases [361], mechanical stimulation[362], and application of pulsed direct current fields [363, 364]. In some cases, the replacement of dexamethasone with all-*trans* retinoic acid (ATRA) is considered to be an essential requirement for efficient ASC osteogenesis [365]. Besides its osteogenic promoting effect, ATRA has been found to simultaneously inhibit adipogenic differentiation by inhibiting C/EBPbeta-mediated transcription through down-regulation of the pro-adipogenic transcription factor CCAAT/enhancer-binding protein α and β [366-368]. The pro-osteogenic effect of ATRA could be further enhanced by co-addition of BMP-2, most likely due to the fact that ATRA promotes expression of the BMP-2 receptor BMPR-IB [369]. In contrast to BMP-2, ATRA alone has the ability to induce osteogenic differentiation of mouse ASCs. In fact, BMP-2 has been observed to actually enhance adipogenesis [368, 369], which is most likely dependent on the expression of its receptors [370].

The same synergistic effect of ATRA and BMP-2 applies as well to the expression and activity of ALP, which is stimulated by ATRA alone, and further enhanced when treated together with BMP-2. ATRA's ability to influence ALP expression is mediated through its binding to the nuclear RARs(RAR/RXR) and subsequent activation of retinoic acid response elements (RARE) located within the ALP promoter [371]. By contrast, activation of RAREs in response to ATRA results in the reduced expression of pro-adipogenic genes PPARγ, C/EBPα and C/EBPδ thereby supressing adipocyte differentiation and promoting osteoblast differentiation. In contrast to the findings of Yang et al [391], Hisada et al [392] reported that ATRA mediated upregulation of pro-osteogenic genes was limited to ALP only, as no changes were observed in the expression levels of osterix, bone sialoprotein or osteocalcin. However, work from our own laboratory has revealed that ATRA-mediated osteogenesis of ASCs is

associated with increases in numerous osteogenic genes, and includes amongst others, high temperature requirement serine protease A1 (HTRA1) [372].

1.8. HTRA1

HTRA1 combines the crucial dual function of chaperone and protease in an ATP-independent manner [373]. The HTRA family of proteins were initially identified in *E. coli*, where HTRA1 mutants failed to grow at elevated temperatures [374] or failed to digest periplasm located misfolded proteins (DegP) [375]. Consequently, the HTRA family of proteins has been shown to promote tolerance against protein folding stresses of various origins. Besides fulfilling basic maintenance task on a cellular level such as degradation of misfolded or damaged proteins, HTRAs are further involved in the regulation of various signaling pathways by inactivating corresponding signaling molecules [373]. HTRA1 and HTRA2 are considered to be key regulators of tumour development [372, 373, 376-381]. Whereas HTRA1 is a secreted protease, HTRA2 acts exclusively at the intracellular level [377]. HTRA1 is predominantly secreted into the extracellular space and only about one fifth remains in the cytoplasm, preferentially attached to microtubules and the plasma membrane [376]. In bacteria, the HTRA homologue DegP, protects cells from misfolded proteins through a combination of chaperone and proteolytic activity [373, 382]. DegP recognizes misfolded proteins via its PDZ domain 1 (postsynaptic density of 95 kDa, Discs large and zonula occludens 1), which assists in bringing the substrate into the vicinity of the proteolytic site for subsequent degradation.

1.8.1. Structural properties

The HTRA family of proteins share the same well conserved architectural properties such as an N-terminal signal sequence in the mammalian HtrA1, -3 and -4 which is crucial for the directed secretion, a trypsin-like protease domain, one or two carboxy-terminal PDZ domains, an Insulin-like growth factor-binding protein (IGFBP) /Mac25 domain and a Kazal-type serine protease inhibitor domain [373]. One common feature amongst the HTRA family of proteases is their assembly in a homo-oligomeric state, ranging from trimers to dodecamers. However, the functional unit of HTRA1 seems to be a trimer with a switch from lower to higher oligomeric states

upon substrate binding [383-386]. The oligomer is stabilized by residues of the protease domains, and has a funnel-like shape with the functional protease domains located at the top and the PDZ domains ranging to the outside (see Figure 5). The PDZ domain is mediating specific protein-protein interactions by preferentially binding to 3-4 amino acid residues at the C-terminus of target proteins [387]. Due to their high mobility, the PDZ domains are thought to move around till they capture a substrate molecule, which upon binding, is then delivered to the proteolytic active interior of the funnel-shaped trimer [373].

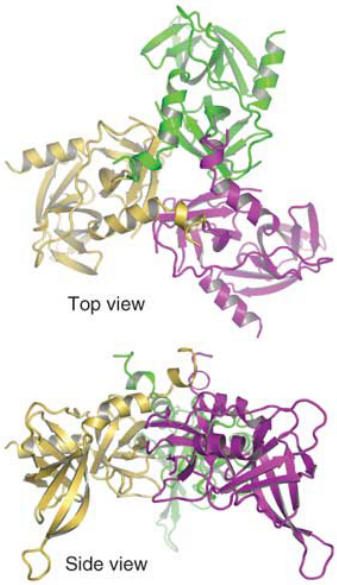

Fig. 5: Ribbon structure of inactive HtrA1 [386]

The function of the IGFBP/Mac25 domain remains to be elucidated, although it is predicted that it contributes to the substrate specificity of the PDZ domain as it is known that IGFBP/Mac25 regulates IGF signaling by assisting binding and cleavage of IGFBP-5 [388]. Another common feature amongst the HTRA family of proteins is the Kazal-type serine protease inhibitor domain which is located upstream of the protease domain and it is suggested that it inhibits the proteolytic activity in the absence of a substrate by specifically binding to the proteolytic active domain, although this remains to be fully elucidated [389-391].

1.8.2.Proteolytic activity

The PDZ domain is connected to the protease domain via a flexible linker allowing mobility upon substrate binding, which then triggers activation of the protease activity along with its homo-oligomerization. In contrast to its bacterial homologues, the proteolytic activation of mammalian HTRA1 is unique by means of the fact that the PDZ domain is not required for its activation as constructs without the PDZ domain show no reduction in activity [386]. The specificity of HtrA1 lies on the one hand within the amino acid composition of the catalytic triad which in turn specifies the secondary structure of the proteolytic site [373] and on the other hand within the before mentioned substrate specificity of the PDZ domain. In the native protein, the signal of a misfolded protein bound to the PDZ domain is transmitted to the protease of HTRA1 via the L3 sensor loop. Activity of HTRA1 is precisely regulated by induced-fit substrate binding and reversibly switched on and off upon peptide binding to the proteolytic site, in contrast to the activation of classical serine proteases [376]. Consequently, another regulatory mechanism has to exist to regulate its proteolytic activity, most likely mediated through local restriction to certain subcellular compartments [376]. Besides its capacity for protein-protein interactions, the PDZ domain is further capable of interacting with phospholipids in biological membranes via its positively charged patches to a negatively charged counterpart [376].

1.8.3.Chaperone and signaling functions

Besides their protease activity, bacterial HTRAs are involved in protein quality control and exhibit various chaperone functions for protein stabilization [373]. DegP as found in Gram-negative bacteria, protects cells from folding stresses through a combined proteolytic and chaperone activity [373, 382]. Similar to its eukaryotic counterpart HTRA1, DegP utilizes its PDZ domain 1 to recognize misfolded polypetides and subsequently upon binding, presents the substrate to the proteolytic site. Additionally, DegP exerts its chaperone function in multiple ways such as protecting folded proteins during the periplasmic shuttling by encapsulation [383] or by promoting folding of the periplasmic α-amylase MalS through facilitation of crucial disulphide

bond formation [382, 392]. DegP has also been reported to assist in refolding of denatured citrate synthase [382] and through this “holding” action preventing aggregation of non functional proteins [393, 394].

Furthermore, HTRAs have been suggested to exert signaling tasks in eukaryotic systems, as in the case of HTRA1 where loss of function has been correlated with decreased sensitivity to anti-cancer drugs along with an increase in cell migration [395-397]. This is in contrast to its over-expression, which acts to inhibit proliferation *in vitro* and tumour growth *in vivo* [380]. Consequently, HTRA1 may act as a tumour suppressor [376]. HTRA1 has been shown to stimulate cell proliferation through IGF1 release upon IGFBP5 cleavage [388]. It also has been reported to be involved in neuronal maturation by proteolytic inactivation of TGF-β [398] and further act to inhibit cell proliferation by binding to multiple TGFβ family members, such as BMP4, growth differentiation factor 5 (GDF5) and activin [399]. As previously mentioned, HTRA1 is known to regulate mTOR signaling through cleavage of TSC2 and thereby affect downstream 4E-BP2 and S6K [400]. The extracellular activity of HTRA1 involves degradation of proteins within the extracellular matrix, such as fibromodulin, decorin, fibromodulin, clusterin, a disintegrin and metalloproteinase domain-containing 9 (ADAM9), vitronectin, α2-macroglobulin [401] aggrecan, type II collagen, biglycan, clusterin [399, 402], and amyloid precursor protein fragment Aβ [403], thereby triggering various signaling cascades.

1.8.4.HTRA1 in musculoskeletal diseases (MSDs)

Evidence now exists that HTRA1 also plays a critical role in the development and progression of MSD [372] affecting bone, cartilage and muscle, by its ability to modify the ECM through degradation of components such as fibronectin, type-II collagen, decorin, aggrecan, elastin, bone sialoprotein and matrix Gla protein, leading to subsequent fragment related malignancies [372, 403-409]. Some of the MSDs in which HTRA1 has been linked with are described below.

1.8.5.Arthritis

Increased production of HTRA1 has been associated with osteoarthritis, a disease characterised by degeneration of the articular cartilage [404, 406]. Similarly, in rheumatoid arthritis, synovial fibroblasts are suggested to play a key role in the process of degradation [403, 406, 410] by secretion of matrix-degrading enzymes, such as matrix metalloproteinases (MMPs), whose production has been shown to be upregulated in response to HTRA1 [409, 411]. Furthermore, it has been suggested that this effect may be indirectly mediated through the proteolytic generation of fibronectin and proteoglycan fragments by HTRA1 [403, 409, 412, 413].

1.8.6. Intervertebral disc (IVD) degeneration

Similarly, changes in turnover of extracellular matrix and cell activity due to an excess of matrix degrading enzymes are thought to be the main underlying cause for the degeneration of IVDs [406, 414-416]. Furthermore, HTRA1 was shown to be upregulated in tissue samples taken from degenerated human IVDs, along with increases in reactive fibronectin fragment species [393]. Furthermore, both HTRA1 and fibronectin fragments were capable of inducing MMP production by isolated IVD cells, thereby providing further support for HTRA1's detrimental role in IVD degeneration [407].

1.8.7. Muscle dystrophy

IGFBP5 represents another potential HTRA1 substrate, acting as a positive regulator of muscle regeneration, and is thought to be of central importance in influencing the development of Duchenne muscular dystrophy (DMD) [388, 406, 417]. DMD is characterized by progressive muscle degeneration, where muscle fibres are degenerated and replaced by adipose and fibrous tissue [418, 419], ultimately leading to premature death. Based on the observation that HTRA1 levels are

elevated in DMD patients and IGFBP5 decreased, it has been hypothesized that HTRA1 acts to impair IGFBP-mediated muscle regeneration resulting in increased adipose and fibrous tissue within the muscle, and thus paving the way for muscular dystrophy [406]. In contrast to its degenerative actions, HTRA1 has also been identified as a positive regulator of human MSC osteogenesis, being expressed in osteocytes and osteoblasts within the bone matrix [399, 402].

1.8.8. HTRA1 in bone formation

The contribution of HTRA1 to osteogenic differentiation and bone formation has been shown in developing mouse embryos, as well as in an adult mouse fracture model [399, 402]. In differentiating osteogenic human BMSCs in vitro, an increase in HTRA1 production in the early phase of osteogenic induction has been observed in association with increases in the well-known osteogenic markers Runx2, ALP, IBSP and COL1A1 [372]. Furthermore, the knock-down of *HTRA1* impaired hBMSC osteogenesis and additionally enhanced adipogenesis [372]. By contrast, earlier studies have shown that HTRA1 overexpression in differentiating mouse 2T3 osteoblasts, prevented BMP-2 induced mineralization. It was suggested that these effects were mediated through both the protease and PDZ domain possibly influencing BMP-2 signaling or via the degradation of specific matrix proteins [408].

1.9. A blend of vitamin A and HTRA1 for robust osteogenesis?

1.9.1. Vitamin A in the historical context

The Nobel prize awarded for the discovery of vitamin A goes back to the year 1906, when Hopkins discovered that no animal can survive only on a mixture of protein, fat, carbohydrates, water and salt [420], but an “accessory fat soluble food factor” [421], later termed “fat soluble A” [422] and finally vitamin A, was essential for survival [423]. Soon afterwards, physiological hypervitaminosis A was found to cause thinning of the long bone cortex with subsequent spontaneous fractures [424-426]. Vitamin A’s dual effects on bone formation are most likely due to dose dependent physiological responses. At concentrations in the nanomolar range, vitamin A has been reported to act as an inhibitor of bone formation [427-431], whereas at the micromolar range, it takes on an enhancing role [432].

1.9.2. Vitamin A uptake and metabolism

Vitamin A is taken up with the regular diet in the form of either retinyl esters as found in eggs, liver, milk, cereals or as carotenoids from vegetables such as spinach and carrots [433]. Enterocytes take up retinyl esters and carotenoids to incorporate them into the chylomicrons and subsequently release them into the circulatory system via the lymphatic system. Vitamin A can be converted to an active form, termed retinol, or can be stored as retinyl esters [432, 433]. Within the target cells, retinol is oxidised to retinal by alcohol dehydrogenase and bound to cellular retinol-binding protein (CRBP) for the next oxidation step, in which retinal dehydrogenase (RALDH) oxidises it to the biological active form, ATRA [432]. Within the cell, a physiological level of ATRA is maintained through its active synthesis by RALDH, and its oxidative metabolism through cytochrome P450s such as CYP26A1 and CYP26B1 [434-437]. ATRA can be further metabolized to more polar, biological inactive products such as

4-hydroxy-retinoic acid (4-OH-RA), 18-hydroxy-retinoic acid (18-OH-RA), 4-oxo-RA and 5,6-epoxy-retinoic acid (5,6-epoxy-RA) [438, 439].

1.9.3.ATRA mediated signaling

There are three isotypes of retinoic acid receptors (RARs) α,β and γ, with at least two different isoforms each, which upon binding of ATRA, heterodimerize with the co-receptor retinoid X receptor (RXRA) and act as transcriptional activators by binding to the RARE within promoters of target genes [440-443]. After ATRA is bound, the RXR/RAR heterodimer undergoes a conformational change within the ligand binding domain, which in turn facilitates the recruitment of co-activators, such as of steroid receptors (SRC)/p160 and p300/CREB-binding protein [440, 441].

1.9.4.ATRA as inducer and inhibitor of transcription

The primary ATRA response can occur within minutes and promote transcription of RARE harbouring immediate early genes, which are mainly coding for transcription factors such as the homeobox gene (HoxaI) [444, 445]. These primary effects of ATRA on transcription factor activation can also result in a secondary response, leading to the transcription of genes which do not harbour an active RARE [446]. In the absence of ATRA, co-repressors, such as nuclear receptor co-repressor (NCoR), silencing mediator of RAR and thyroid hormone receptor (SMRT) [447], histone deacetylases (HDACs) and mSin3A bind and actively repress binding to RARE elements and subsequent transcriptional activation [440, 448]. By contrast, ATRA can also repress transcription by increasing expression of genes such as orphan nuclear receptor germ cell nuclear factor (GCNF) which then acts as a repressor for genes necessary for maintenance of pluripotency such as Sox2, Nanog and Oct4, and thereby induce differentiation [449, 450]. Translocation of the activated RXR/RAR complex to the nucleus is facilitated either by cellular retinoic acid-binding protein II (CRABPII) or fatty acid-binding protein (FABP) 5 [441]. Contrary to CRABPII, FABP5 fosters binding of ATRA to peroxisome proliferator-activated

receptors (PPARs) α, β, γ and δ, which can also heterodimerize with RXR and activate PPAR response elements (PPRE) in promoter regions of target genes [451-454].

1.9.5.Receptor cross-talk

Last but not least, besides RARs, RXRs and PPARs, retinoids can also bind retinoid-related orphan receptors (ROR) β and γ [455, 456], which regulate gene transcription by binding to their cognate ROR response element (RORE) within target genes as monomers [457, 458]. In addition to their effects at the genomic level, retinoids have also been shown to possess non-genomic regulatory potential such as the phosphorylation of proteins and binding to RNA. ATRA can trigger phosphorylation of ERK [459], which can then induce phosphorylation and activation of other downstream kinases [432, 441]. Another non-genomic action of cytosolic RARA is RNA related, as it has been reported to bind to mRNAs and specifically inhibit their translation [460-462].

1.10. Hypothesis and aims of the thesis

It has been shown that HTRA1 is up-regulated in mASCs undergoing osteogenic differentiation [372] and it is well reported that ATRA, used as active component in osteogenic induction media, regulates development [463], differentiation and proliferation of stem cells [446]. Knock-down of *HTRA1* in hBMSCs impairs their osteogenic differentiation potential, therefore not only highlighting the importance of HTRA1 in human MSC osteogenesis, but also raising the question as to whether HTRA1 regulates osteogenesis in MSCs from other sources and species, and through what mechanism does it mediate its pro-osteogenic effects.
Therefore, it is hypothesized that HTRA1 also plays an important role in regulating ATRA-mediated mASC osteogenesis and that it influences the activation of specific osteoinductive signaling pathways. This hypothesis will be tested by fulfilling the following aims:

- Aim 1: Identify the regulatory pathways governing ATRA-induced *HtrA1* expression in mASCs.

- Aim 2: Examine the effects of ATRA on signal transduction pathways in osteogenic mASCs.

- Aim 3: Evaluate the contribution of HTRA1 to ATRA-mediated mASCs osteogenesis.

- Aim 4: Determine a mechanism of action for HTRA1 in regulating ATRA-mediated mASC osteogenesis.

The results generated from this study will enhance our understanding of the role played by HTRA1 in the osteogenic differentiation of mASCs and subsequently allow further insight into the intricacies governing this process. Furthermore, the identification of new and novel signaling events controlling osteogenesis will further reveal new targets, which could be manipulated for the purpose of enhancing, or even inhibiting, osteogenic mineralisation.

2. Results

2.1. Overview of published and submitted manuscripts

2.1.1 Loss-of-function of HtrA1 abrogates all-*trans* retinoic acid-induced osteogenic differentiation of mouse adipose-derived stromal cells through deficiencies in p70S6k activation.

Authors : **Glanz S,** Mirsaidi A, Cristina López-Fagundo, Tiaden AN, Richards PJ.

Journal : Under review *Stem Cells and Development (January 2016) IF:3.727*

Contribution: Designed, performed and analyzed the majority of experiments.

2.1.2 Novel function of serine protease HTRA1 in inhibiting adipogenic differentiation of human mesenchymal stem cells via MAP kinase-mediated MMP upregulation

Authors : Tiaden AN*, Bahrenberg G*, Mirsaidi A, **Glanz S**, Blüher M, Richards PJ. *authors contributed equally

Journal : In Press, Accepted Manuscript in *Stem Cells (August 2015) IF:6.523*

Contribution: Assistance in generation of qPCR data and data analysis.

2.1.3 Use of biomimetic microtissue spheroids and specific growth factor supplementation to improve tenocyte differentiation and adaptation to a collagen-based scaffold *in vitro.*

Authors: Theiss F, Mirsaidi A, Mhanna R, **Glanz S**, Bahrenberg G, Tiaden AN, Richards PJ.

Journal: In Press, Accepted Manuscript in *Biomaterials (August 2015) IF:8.557*

Contribution: Assistance in generation of qPCR data and immunoblotting.

2.1.4 Human serine protease HTRA1 positively regulates osteogenesis of human bone marrow-derived mesenchymal stem cells and mineralization of differentiating bone-forming cells through the modulation of extracellular matrix protein.

Authors: Tiaden AN, Breiden M, Mirsaidi A, Weber FA, Bahrenberg G, **Glanz S**, Cinelli P, Ehrmann M, Richards PJ.
Journal: *Stem Cells. 2012;30(10):2271-82. IF:6.523*
Contribution: Assistance in generation of qPCR data and immunoblotting.

2.1.5 Detrimental role for human high temperature requirement serine protease A1 (HTRA1) in the pathogenesis of intervertebral disc (IVD) degeneration.

Authors: Tiaden AN, Klawitter M, Lux V, Mirsaidi A, Bahrenberg G, **Glanz S**, Quero L, Liebscher T, Wuertz K, Ehrmann M, Richards PJ.
Journal: *J Biol Chem. 2012;287(25):21335-45. IF:4.573*
Contribution: Assistance in generation of qPCR data and immunoblotting.

2.1.1. Loss-of-function of HtrA1 abrogates all-*trans* retinoic acid-induced osteogenic differentiation of mouse adipose-derived stromal cells through deficiencies in p70S6k activation.

Authors : **Glanz S,** Mirsaidi A, Cristina López-Fagundo, Tiaden AN, Richards PJ.

Journal : Under review *Stem Cells and Development (January 2016) IF 3.727*

Contribution: Designed, performed and analyzed the majority of experiments.

Stem Cells and Development

Stem Cells and Development: http://mc.manuscriptcentral.com/scd

Loss-of-Function of HtrA1 Abrogates All-Trans Retinoic Acid-Induced Osteogenic Differentiation of Mouse Adipose-Derived Stromal Cells Through Deficiencies in p70S6K Activation

Journal:	*Stem Cells and Development*
Manuscript ID	Draft
Manuscript Type:	Original Research Report
Date Submitted by the Author:	n/a
Complete List of Authors:	Glanz, Stephan; University of Zurich, CABMM; University of Zurich, Zurich Center for Integrative Human Physiology Mirsaidi, Ali; University of Zurich, CABMM López-Fagundo, Cristina; University of Zurich, CABMM Tiaden, André; University of Zurich, CABMM Richards, Peter; University of Zurich, CABMM; University of Zurich, Zurich Center for Integrative Human Physiology
Keyword:	Osteogenesis, Cell Signaling, Differentiation, MSC, Tissue specific stem cells
Abstract:	All-*trans* retinoic acid (ATRA) is a potent inducer of osteogenic differentiation in mouse adipose-derived stromal cells (mASCs), although the underlying mechanisms responsible for its mode of action have yet to be completely elucidated. High temperature requirement protease A1 (HtrA1) is a newly recognized modulator of human multipotent stromal cell (MSC) osteogenesis and as such, may play a role in regulating ATRA-dependent osteogenic differentiation of mASCs. In the current study, we assessed the influence of small interfering RNA (siRNA)-induced repression of HtrA1 production on mASC osteogenesis and examined its effects on ATRA-mediated mammalian target of rapamycin (mTOR) signaling. Inhibition of HtrA1 production in osteogenic mASCs resulted in a significant reduction of alkaline phosphatase (ALP) activity and mineralized matrix formation. Western blot analyses revealed the rapid activation of Akt (Ser473) and p70S6K (Thr389) in ATRA-treated mASCs, and that levels of phosphorylated p70S6K were noticeably reduced in HtrA1-deficient mASCs. Further studies using mTOR inhibitor rapamycin and siRNA specific for the p70S6K gene *Rps6kb1* confirmed ATRA-mediated mASC osteogenesis as being dependent on p70S6K activation. Finally, transfection of cells with a constitutively active rapamycin-resistant p70S6K mutant could restore the mineralizing capacity of HtrA1-deficient mASCs. These findings therefore lend further support for HtrA1 as a positive mediator of MSC osteogenesis and provide new insights into the molecular mode of action of ATRA in regulating mASC lineage commitment.

Mary Ann Liebert Inc., 140 Huguenot Street, New Rochelle, NY 10801

Mary Ann Liebert Inc., 140 Huguenot Street, New Rochelle, NY 10801

Loss-of-Function of HtrA1 Abrogates All-*Trans* Retinoic Acid-Induced Osteogenic Differentiation of Mouse Adipose-Derived Stromal Cells Through Deficiencies in p70S6K Activation

Stephan Glanz[1,2*], Ali Mirsaid[1,*], Cristina López-Fagundo[1], André N. Tiaden[1], Peter J. Richards[1,2]

From the [1]Bone and Stem Cell Research Group, CABMM, University of Zurich, 8057 Zurich, Switzerland, [2]Zurich Center for Integrative Human Physiology (ZIHP), University of Zurich, 8057 Zurich, Switzerland. *Authors contributed equally.

Author Email addresses: Stephan.glanz@cabmm.uzh.ch, ali.mirsaidi@cabmm.uzh.ch, clopezfagundo@gmail.com, nicki.tiaden@cabmm.uzh.ch, peter.richards@cabmm.uzh.ch

Running title: Regulation of mASC Osteogenesis by HtrA1

To whom correspondence should be addressed: Dr. Peter J. Richards, Center for Applied Biotechnology and Molecular Medicine, University of Zürich, Winterthurerstrasse 190, Zürich 8057, Switzerland, Tel:+41-44-635-3800, Email: peter.richards@cabmm.uzh.ch

Footnotes and Abbreviations

The abbreviations used are: ALP, alkaline phosphatase; ATRA, all-*trans* retinoic acid; BMP, bone morphogenetic protein; BMPR, BMP receptor; GAPDH, glyceraldehyde-3-phosphate dehydrogenase; 4E-BP1, eukaryotic initiation factor 4E binding protein 1; hBMSC, human bone marrow stromal cells; HtrA1, high temperature requirement protease A1; mASC, mouse adipose-derived stromal cells; mBMSC, mouse bone marrow stromal cells; mTOR, mammalian target of rapamycin; p70S6K, p70 ribosomal protein S6 kinase; SAM, senescence-accelerated mouse; TSC2, Tuberous sclerosis complex 2.

Mary Ann Liebert Inc., 140 Huguenot Street, New Rochelle, NY 10801

Abstract

All-*trans* retinoic acid (ATRA) is a potent inducer of osteogenic differentiation in mouse adipose-derived stromal cells (mASCs), although the underlying mechanisms responsible for its mode of action have yet to be completely elucidated. High temperature requirement protease A1 (HtrA1) is a newly recognized modulator of human multipotent stromal cell (MSC) osteogenesis and as such, may play a role in regulating ATRA-dependent osteogenic differentiation of mASCs. In the current study, we assessed the influence of small interfering RNA (siRNA)-induced repression of HtrA1 production on mASC osteogenesis and examined its effects on ATRA-mediated mammalian target of rapamycin (mTOR) signaling. Inhibition of HtrA1 production in osteogenic mASCs resulted in a significant reduction of alkaline phosphatase (ALP) activity and mineralized matrix formation. Western blot analyses revealed the rapid activation of Akt (Ser473) and p70S6K (Thr389) in ATRA-treated mASCs, and that levels of phosphorylated p70S6K were noticeably reduced in HtrA1-deficient mASCs. Further studies using mTOR inhibitor rapamycin and siRNA specific for the p70S6K gene *Rps6kb1* confirmed ATRA-mediated mASC osteogenesis as being dependent on p70S6K activation. Finally, transfection of cells with a constitutively active rapamycin-resistant p70S6K mutant could restore the mineralizing capacity of HtrA1-deficient mASCs. These findings therefore lend further support for HtrA1 as a positive mediator of MSC osteogenesis and provide new insights into the molecular mode of action of ATRA in regulating mASC lineage commitment.

Mary Ann Liebert Inc., 140 Huguenot Street, New Rochelle, NY 10801

Introduction

Efficient osteogenic induction of mouse adipose-derived stromal cells (mASCs) is reliant on the actions of all-*trans* retinoic acid (ATRA), the carboxylic acid form of vitamin A [1-7]. This is in contrast to mouse and human bone marrow stromal cells (BMSCs), where dexamethasone is primarily used to instigate osteogenesis through upregulation of four and a half LIM domains 2 (FHL2) and activation of Wnt/β catenin signaling [8]. ATRA's ability to influence osteoblast differentiation has been observed in several different cell systems and is considered to be largely dependent on the concentration of ATRA used. Whilst ATRA acts to enhance osteogenesis at micromolar concentrations [1-7, 9, 10], at nanomolar concentrations, it has been shown to inhibit both osteoblast gene expression and mineralization [11-13]. The concentration of ATRA used to stimulate mASC osteogenesis *in vitro* is generally within the range of 1 to 5 μM, where it acts to enhance the expression of several osteogenic markers including alkaline phosphatase (*Alpl*) and osteopontin (*Spp1*), and to induce mineralization of mASC-derived osteoblasts [3, 4]. In addition, ATRA's ability to direct mASCs along the osteoblast lineage *in vitro* has also been exploited for the purpose of enhancing mASC-induced new bone formation *in vivo*. Priming of mASCs with ATRA prior to their implantation into mouse calvarial defects resulted in accelerated bone regeneration as compared to mice treated with unstimulated mASCs [14]. However, the mechanisms through which ATRA instigates its osteogenic effects in these cells remain unclear. Findings from studies investigating the combined effects of ATRA and bone morphogenetic protein (BMP)-2 on mASC osteogenesis suggested that ATRA's primary function was to regulate BMP signaling through enhanced BMP receptor (BMPR) expression [1]. However, ATRA also has the ability to induce osteogenic differentiation of mASCs in the

Mary Ann Liebert Inc., 140 Huguenot Street, New Rochelle, NY 10801

absence of exogenous BMP-2 [2-7]. Therefore, it's likely that in addition to BMP signaling, ATRA targets other pathways critically involved in regulating mASC osteogenesis.

We have previously identified high temperature requirement protease A1 (HtrA1) as a novel mediator of human BMSC (hBMSC) differentiation, where it acts to enhance osteogenesis and subsequent mineralization by differentiating bone-forming cells [7]. Furthermore, *HtrA1* expression is upregulated in mASCs in response to ATRA-containing osteogenic induction medium [7]. HtrA1 is a member of the HtrA family of serine proteases and has been linked to various biological processes by virtue of its ability to interact with numerous intracellular and extracellular substrates [15]. Tuberous sclerosis complex 2 (TSC2) was the first cytoplasmic HtrA1 substrate to be identified, and its degradation by HtrA1 was shown to result in activation of the mammalian target of rapamycin (mTOR) pathway as confirmed by alterations in the phosphorylation of downstream targets eukaryotic initiation factor 4E binding protein 1 (4E-BP1) and p70 ribosomal protein S6 kinase (p70S6K) [16]. This bears particular significance with regards to mASC osteogenesis, based on the fact that mTOR signaling plays a positive role in the osteogenic induction of several cell types including BMSCs [17-19]. However, no studies have yet sort to investigate its involvement in mediating the osteoinductive effects of ATRA on mASCs, or whether HtrA1's ability to influence mTOR signaling plays a role in determining mASC osteogenic potential. In the present study, we investigated the role of HtrA1 in the ATRA-dependent differentiation of mASCs into mineral-forming bone cells and assessed its influence over mTOR signaling events during the course of mASC osteogenesis.

Mary Ann Liebert Inc., 140 Huguenot Street, New Rochelle, NY 10801

Materials and Methods

Materials

Antibodies specific for non-phosphorylated Akt, mTOR, p70S6K, 4E-BP1 and phosphorylated Akt (Ser473), mTOR (Ser2448), p70S6K (Thr389) and (Thr421/Ser424), 4E-BP1 (Thr37/46) and S6 ribosomal protein (Ser235/236) were all purchased from Cell Signaling, BioConcept (Allschwil, Switzerland). Mouse monoclonal anti-tubulin was from Sigma-Aldrich (Buchs, Switzerland). Mouse HA-probe antibody and anti-GAPDH were from Santa Cruz Biotechnology, LabForce AG (Muttenz, Switzerland). A polyclonal anti-HtrA1 antibody was generated as previously described [20]. HRP-labeled secondary antibodies specific for mouse or rabbit IgG were purchased from Jackson ImmunoResearch (Suffolk, UK). Rapamycin was purchased from Enzo Life Science (Lausen, Switzerland). The expression plasmids pRK7-HA-S6K1-F5A-E389-R3A (Addgene plasmid # 8991) and pRK7-HA-S6K1-KR (Addgene plasmid # 8985), were kind gifts from John Blenis [21].

Isolation and Culture of mASCs

Primary mASCs were isolated from SAM mice as previously described [4, 5]. All animal research procedures were approved by the Animal Experimentation Committee of the Veterinary Office of the Canton of Zurich, Switzerland and followed the guidelines of the Swiss Federal Veterinary Office for the use and care of laboratory animals. Briefly, subcutaneous inguinal fat pads were removed and digested in Hepes buffer containing 0.1% collagenase A (Roche Diagnostics, Rotkreuz, Switzerland) and 0.2% bovine serum albumin for 40 min at 37°C. Adherent stromal cells were maintained in complete medium consisting of Dulbecco's modified eagle medium (DMEM-low glucose, with GlutaMAX) (Life Technologies, Zug, Switzerland),

supplemented with 10% fetal bovine serum (FBS) (Bioswisstec, Schaffhausen, Switzerland) and antibiotics. Supernatant was replaced after 1 day with fresh complete medium and cells were used between passage 1 and 4 following initial analysis for mesenchymal and hematopoietic cell markers by flow cytometry as previously described [4].

Osteogenic Differentiation of mASCs

mASCs were plated at 5000 cells/cm^2 and incubated in alpha-minimum essential medium (α-MEM) (Life Technologies), supplemented with 10% FBS (Bioswisstec), 50 µM L-ascorbic acid 2-phosphate sesquimagnesium salt hydrate, 10 mM β-glycerophosphate and 5 µM retinoic acid (all from Sigma-Aldrich) for up to 21 days with regular changes of medium as previously described [4]. Alkaline phosphatase (ALP) activity was quantified in cell lysates using p-nitrophenylphosphate (pNPP) liquid substrate (Sigma-Aldrich) and values normalized to total protein content and reaction time as previously described [4]. Mineralization was visualized using Alizarin red and the amount of staining determined by measuring optical densities at 570 nm following extraction using 10% cetylpyridinium chloride (Sigma-Aldrich). Optical densities were then converted to micromoles (µM) of Alizarin red using a standard curve and normalized to cell number. The mean cell number was determined by automated counting of 4′,6-diamidino-2-phenylindole (DAPI) stained nuclei in at least 6 random fields of view. Images were captured on a Leica DMI 6000 inverted fluorescence microscope (Leica Microsystems, Heerbrugg, Switzerland). Image processing and nuclear counts were performed using NIH Image J software.

Mary Ann Liebert Inc., 140 Huguenot Street, New Rochelle, NY 10801

Quantitative Reverse Transcription PCR (RT-qPCR)

Total RNA was isolated from mASCs and purified using TRIzol reagent (Invitrogen AG, Basel, Switzerland) according to the manufacturer's instructions. RNA (0.5 µg) was reverse transcribed to cDNA using Superscript II (Invitrogen AG) and random hexanucleotide primers (Promega AG, Dübendorf, Switzerland). Quantification of mRNA expression was performed with TaqMan Gene Expression Assays (Applied Biosystems, Rotkreuz, Switzerland) specific for *HtrA1* (Mm00479887), *Rps6kb1* (Mm01310033), *Alpl* (Mm01187117) and *Spp1* (Mm01611440) using the StepOnePlus Real-Time PCR System (Applied Biosystems) and values normalized to *Mrps12* (Mm00488728) mRNA levels and presented as fold change according to the $2^{-\Delta\Delta CT}$ method. Each 10 µl reaction consisted of 1x TaqMan Fast Universal PCR Master Mix (Applied Biosystems), 1x TaqMan Gene Expression Assay and 10 ng cDNA (based upon initial RNA concentrations). All reactions were performed in triplicate in fast optical 96-well reaction plates (Applied Biosystems) at 95°C for 20 seconds and 40 cycles of 95°C for 1 second and 60°C for 20 seconds.

Western Blot Analysis

Total cellular protein was extracted from mASCs using CelLytic M (Sigma-Aldrich) containing protease and phosphatase inhibitor cocktails (Sigma-Aldrich). For the analysis of HtrA1 in mASC supernatants, cells were treated for 3 days with osteogenic induction medium and then for a further 24 h in fresh FCS-free osteogenic induction medium before harvesting and concentrating supernatants 30-fold using Amicon Ultra-15, 10 kDa mwco filter units (Millipore). In each case, protein amounts were quantified using BioRad Protein Assay (BioRad, Reinach, Switzerland). Protein samples were boiled for 5 min in loading buffer (50 mM Tris-HCl, pH 6.8,

2% SDS, 10% glycerol, 100 mM DTT, 0.002% Bromophenol blue) and equal amounts of protein loaded onto 12% SDS-PAGE gels. Protein was then electroblotted onto PVDF membranes using the Trans-Blot Turbo blotting system (BioRad) and incubated in 5% skimmed milk, 50 mM Tris-HCl, pH 7.6, 150 mM NaCl, 0.1% Tween 20 (TBST) for 1 h at room temperature. Membranes were then incubated overnight at 4°C with primary antibodies specific for HtrA1 or phosphorylated or non-phosphorylated Akt, mTOR, p70S6K, S6 ribosomal protein and 4E-BP1. Monoclonal mouse anti-tubulin or anti-GAPDH were used to control for equal protein loading of cell lysates. Coomassie blue staining was used to control for equal protein loading of cell supernatants. After washing in TBST three times for 5 min each, membranes were incubated with a HRP-conjugated anti-mouse or anti-rabbit IgG (1:10'000) for 1 h at room temperature. Following a further washing step, peroxidase activity was detected using SuperSignal West Pico Chemiluminescent Substrate (Thermo Scientific, Lausanne, Switzerland).

Small Interfering RNA (siRNA) Studies

Specific knock down of gene expression was performed with Silencer Select siRNA (Ambion, Life Technologies) specific for *HtrA1* (s80180) or *Rps6kb1* (s91055) using previously described methods [7]. Briefly, mASCs ($1x10^5$ cells) were transfected with 20 nM of targeted siRNA or negative control siRNA (Negative Control-1) using the NEON Transfection System (Life Technologies). Following transfection, cells were seeded in cell culture plates with fresh growth medium (without antibiotics) and incubated for 24 h at 37°C, 5% CO_2. Medium was then replaced with either fresh growth medium or osteogenic differentiation medium and total RNA or protein harvested at selected time points for further analysis. The effects of siRNA mediated

Mary Ann Liebert Inc., 140 Huguenot Street, New Rochelle, NY 10801

gene knockdown on osteogenic-induced mASC ALP activity and mineralization was determined using the ALP activity assay and Alizarin Red staining respectively.

siRNA and Plasmid Co-Transfection

mASCs were transfected with Silencer Select siRNA specific for *HtrA1* or Negative Control-1 and 1 μg of mammalian expression plasmid pRK7-HA-S6K1-F5A-E389-R3A (constitutively active p70S6K), pRK7-HA-S6K1-KR (kinase dead p70S6K) or empty control plasmid pcDNA3 using the NEON Transfection System as described above. After 24 h, cells were induced to undergo osteogenesis and mineralization quantified after 21 days using Alizarin red staining as described above.

Statistical Analysis

One-way analysis of variance (ANOVA) followed by Tukey's post-hoc test was performed for multiple group comparisons using SPSS19.0 (SPSS Inc., Chicago, IL). In all cases, a *p*-value of < 0.05 was considered statistically significant.

Results

We have previously demonstrated that HtrA1 plays a vital role in the regulation of osteogenesis in hBMSCs [7]. In the current report, we further investigated this property of HtrA1 in ATRA-stimulated mASCs and aimed to establish its role in regulating mASC osteogenesis and mASC-derived osteoblast mineralization.

Mary Ann Liebert Inc., 140 Huguenot Street, New Rochelle, NY 10801

HtrA1 Deficiency Impairs ATRA-Mediated mASC Osteogenic Differentiation

In order to examine the influence of loss-of-function of *HtrA1* on the osteogenic capacity of mASCs in response to treatment with osteogenic medium containing ATRA, we analyzed mineral production by mASC-derived osteoblasts, as well as ALP expression and enzyme activity. Analysis of HtrA1 in mASC supernatants by Western blot confirmed HtrA1 protein production to be effectively reduced in osteogenic mASCs treated with siRNAs specific for *HtrA1* (Fig. 1A). We next assessed the influence of loss-of-function of HtrA1 on the osteogenic potential of mASCs. mASCs treated with control siRNA underwent efficient osteoblastogenesis and mineralization following stimulation with osteogenic medium for 10 days, as determined by Alizarin red staining (Fig. 1B). However, Alizarin red staining of osteogenic-induced mASCs in which HtrA1 had previously been depleted was noticeably reduced (Fig. 1B). Further quantitative analysis of extracted Alizarin red stain revealed the mineralizing capabilities of HtrA1-deficient mASC-derived osteoblasts to be significantly impaired ($p < 0.001$) as compared to siControl (Fig. 1C). In accordance with our previous findings [7], ATRA-mediated osteogenic induction of mASCs resulted in significant increases in both *HtrA1* (Fig. 1D) and *Alpl* (Fig. 1E) expression levels in a time dependent manner. Similarly, ALP enzyme activity was also significantly enhanced in response to osteogenic induction at all time points tested (Fig. 1F). As expected, *HtrA1* knockdown of mASCs significantly suppressed *HtrA1* expression in osteogenic mASCs over the course of the study (Fig. 1D). ATRA-mediated increases in *Alpl* expression levels were also significantly impaired in HtrA1-deficient mASCs (Fig. 1E) and were accompanied by significant decreases in ALP enzymatic activity at all time points tested (Fig. 1F). These findings therefore demonstrate a functional role for HtrA1 in regulating ATRA-

mediated mASC osteogenesis and in the generation of a mineralized matrix by mASC-derived osteoblasts.

HtrA1 Deficiency Impairs ATRA-Mediated p70S6K Activation in mASCs

Having demonstrated HtrA1 to be a necessary component for efficient mASC osteogenesis, we next considered its potential mode of action. Based on HtrA1's previously reported role in the activation of mTOR targets p70S6K and 4E-BP1 in tumor cell lines [16], we assessed the possible influence of HtrA1 deficiency on mTOR signaling in ATRA-stimulated mASCs. As no studies have yet sought to determine the effects of ATRA-mediated osteogenic induction on mTOR signaling in mASCs, we initially performed a series of Western blot analyses to ascertain the activation status of kinases located both upstream and downstream of mTOR. Phosphorylation levels of Akt (Ser473), mTOR (Ser2448), p70S6K (Thr389) and 4E-BP1 (Thr37/46) were assessed in mASCs over the course of 2 h following ATRA-mediated osteogenic induction. A noticeable increase in Akt and p70S6K phosphorylation was already evident in osteogenic-induced mASCs after only 10 min and had reduced to basal levels by 1 h (Fig. 2A). However, basal levels of phosphorylated mTOR were only minimally affected after 10 min, and 4E-BP1 remained relatively unchanged at all time points tested. We next proceeded to investigate the influence of *HtrA1* silencing on Akt/mTOR/p70S6K/4E-BP1 phosphorylation in differentiating mASCs. Western blot analysis of cell lysates from HtrA1-deficient mASCs revealed no differences in phospho-Akt levels, and only minor reductions in phospho-mTOR and –4EBP1 levels as compared to siControl (Fig. 2B). By comparison however, HtrA1-deficient mASCs demonstrated marked reductions in the levels of p70S6K phosphorylated at either Thr389 or Thr421/Ser424, as well phospho-S6 ribosomal protein levels. These results are

Mary Ann Liebert Inc., 140 Huguenot Street, New Rochelle, NY 10801

therefore suggestive of ATRA-mediated p70S6K activation as being a potential HtrA1 target and a means by which it could influence ATRA-dependent mASC osteogenesis.

Loss-of-Function of p70S6K Impairs mASC Osteogenesis

In order to address the functional relevance of p70S6K activation in the context of mASC osteogenesis, we next assessed the effects of p70S6K inhibition on ALP expression and matrix mineralization in mASCs undergoing ATRA-mediated osteogenic differentiation. Short-term treatment of mASCs with the mTOR inhibitor rapamycin prior to osteogenic induction markedly reduced mTOR phosphorylation and completely abolished p70S6K phosphorylation, whilst Akt phosphorylation levels remained unaffected (Fig. 3A). Next, we evaluated the effects of long-term exposure of mASCs to rapamycin with regards to their ability to differentiate into mineralizing osteoblasts. Alizarin red staining of osteogenic mASCs was significantly reduced by rapamycin treatment in a concentration dependent manner (Fig. 3B and C), thus confirming that mTOR signaling was required for mASC-derived osteoblastogenesis.

Further investigations employing siRNA mediated knockdown of the p70S6K gene *Rps6kb1* were also performed in order to assess the effects of specifically inhibiting p70S6K activity on mASC osteogenesis. p70S6K protein and activity levels were noticeably reduced in *Rps6kb1*-deficient mASCs after short-term osteogenic induction (Fig. 4A). We next investigated the effects of *Rps6kb1* knockdown on mASC-derived osteoblast mineralization using Alizarin red staining. A marked reduction in Alizarin red staining was observed in *Rps6kb1*-deficient mASCs after 14 days of culture in osteogenic medium (Fig. 4B). Further quantitative analysis of extracted Alizarin red stain revealed the mineralizing capabilities of p70S6K-deficient mASC-derived osteoblasts to be significantly impaired as compared to siControl ($p < 0.001$) (Fig. 4C).

Mary Ann Liebert Inc., 140 Huguenot Street, New Rochelle, NY 10801

Gene expression analyses of mASCs undergoing osteogenesis confirmed efficient *Rps6kb1* knockdown throughout the course of the study and revealed a significant reduction in *Rps6kb1* gene expression at day 14 in siControl in response to osteogenic induction (Fig. 4D). Furthermore, the expression levels of osteogenic markers *Alpl* (Fig. 4E) and osteopontin (*Spp1*) (Fig. 4F) in mASCs undergoing osteogenesis were significantly reduced in p70S6K-deficient cells. These results clearly identify p70S6K activation as being a necessary requirement for efficient osteogenic differentiation of mASCs and provide a potential means through which HtrA1 may regulate ATRA-mediated mASC osteogenesis.

Restoration of HtrA1-Deficient mASC Osteogenesis Using a Constitutively Active p70S6K Mutant

In view of the fact that mASC osteogenesis is dependent on both HtrA1 and p70S6K, and that loss-of-function of HtrA1 impairs p70S6K activation, we sought to determine whether transfection of mASCs with a constitutively active p70S6K mutant could relieve the detrimental effects of HtrA1 deficiencies on mASC osteogenesis. mASCs were transfected with either an empty plasmid, or plasmids encoding a rapamycin-resistant constitutively active (p70S6KCA) or kinase inactive (p70S6KKI) HA-tagged p70S6K [21]. The expression of p70S6KCA and p70S6KKI in transfected mASCs was confirmed by Western blot analysis using an HA-probe antibody (Fig. 5A). Furthermore, the increased activation status of p70S6K in cells transfected with plasmid encoding p70S6KCA was confirmed by Western blot analysis of phosphorylated S6 ribosomal protein levels in mASCs induced to undergo osteogenesis in the presence of rapamycin (Fig. 5A). RT-qPCR confirmed that siRNA mediated reduction of *HtrA1* mRNA expression was unaffected in cells co-transfected with plasmid DNA (Fig. 5B). Next, we

Mary Ann Liebert Inc., 140 Huguenot Street, New Rochelle, NY 10801

transfected HtrA1-deficient mASCs with empty plasmid, p70S6KCA or p70S6KKI and assessed their ability to influence mASC-derived osteoblast formation through quantification of Alizarin red staining after 21 days. HtrA1-deficient mASCs transfected with p70S6KKI demonstrated comparable reductions in Alizarin red staining as observed in HtrA1-deficient mASCs treated with the empty control plasmid (Fig. 5C and D). In both cases, Alizarin red staining was significantly reduced as compared to siControl/ empty plasmid-transfected cells. By contrast, Alizarin red staining was significantly enhanced in HtrA1-deficient mASCs transfected with p70S6KCA as compared to cells transfected with either empty plasmid ($p < 0.001$) or p70S6KKI ($p < 0.01$). Moreover, when compared to siControl/ empty plasmid-transfected cells, HtrA1-deficient mASCs transfected with the p70S6KCA failed to demonstrate any significant reductions in Alizarin red staining ($p = 0.925$). Taken together, these findings identify p70S6K as being of critical importance in ATRA-mediated mASC osteogenesis and that activation of p70S6K is reliant, at least in part, on the actions of HtrA1.

Discussion

mASCs represent a readily available source of osteoprogenitor cells, which unlike mBMSCs, have the advantage of being able to sustain a high level of osteogenic differentiation potential with age and under conditions of low bone quality [4, 22-25]. Subsequently, mASCs are fast becoming the preferred choice for stem cell-based approaches in bone tissue engineering [26, 27]. Certainly, results from our previous studies have confirmed that mASCs harvested from SAMP6 mice, a model for senile osteoporosis, have the capability of increasing bone quality when re-injected back into SAMP6 tibia [5]. However, despite their widespread usage, the underlying mechanisms through which mASC osteogenic differentiation is controlled remains

Mary Ann Liebert Inc., 140 Huguenot Street, New Rochelle, NY 10801

incompletely understood. In the current report, we identify the serine protease HtrA1 as being a positive regulator of ATRA-induced mASC osteogenesis and mASC-derived osteoblast mineralization. Furthermore, we provide evidence, which supports p70S6K as playing a role in mediating the pro-osteogenic effects of HtrA1 in mASCs in response to ATRA.

Mammalian HtrA1 was originally identified by Zumbrunn and Trueb [28] and has since been implicated in numerous biological processes and diseases [15, 29]. Findings from our own studies have revealed HtrA1 to be a potent modulator of hBMSC multipotency as evidenced by its ability to inhibit adipogenesis and stimulate osteogenesis [7]. However, several studies also exist in which HtrA1 has been classified as a negative regulator of osteogenesis both *in vitro* and *in vivo* [30, 31]. Clearly therefore, further investigations are required in order to clarify HtrA1's function in osteogenesis and to ascertain its potential mechanism of action. Here we provide further evidence in support of HtrA1's role as a positive regulator of MSC osteogenesis.

HtrA1 is classified as a secreted serine protease and as such, its influence over cellular processes is largely thought to be due to its extracellular actions [7, 20, 32]. However, it is also equally likely that HtrA1 instigates many of its effects intracellularly. Indeed, HtrA1 has been shown to interact with and functionally regulate several intracellular substrates including tubulin [33], proTGFβ1 [34], tau [35], X-linked inhibitor of apoptosis protein (XIAP) [36] and TSC2 [16]. In the context of the present study, HtrA1's regulatory influence over TSC2 activity holds particular relevance given the importance of mTOR signaling in stem cell multipotency [17-19].

The mTOR protein makes up the catalytic subunit of two separate complexes, namely mTOR complex 1 (mTORC1) and mTOR complex 2 (mTORC2) [37]. mTORC1 functions to control cell growth and protein synthesis through phosphorylation of 4E-BP1 and p70S6K, and has been implicated in osteoblast differentiation [17, 38-40]. mTORC1 is negatively regulated by

the GTPase-activating protein TSC1/2 complex and as such, relies on the actions of Akt for its activation through phosphorylation of TSC2 [41]. Although several studies have demonstrated activation of the Akt/mTOR signaling pathway in response to ATRA [42-44], no investigations have yet been undertaken to examine Akt/mTOR activation in ATRA-stimulated mASCs or to evaluate its consequences for their commitment towards osteoblasts. Our findings have demonstrated that the Akt/mTOR/p70S6K pathway is rapidly activated in mASCs in response to ATRA. Similar rapid increases in several other kinase cascades have previously been demonstrated in various cell systems in response to ATRA [45-48]. Such effects are considered to be independent of the classical genomic effects of ATRA, and are instead regulated through atypical, non-genomic events possibly through interactions with membrane-associated retinoic acid receptors (RARs) [49]. The ability of the mTOR inhibitor rapamycin to completely suppress ATRA-mediated p70S6K activation in these cells suggests that despite the minimal increases in phospho-mTOR (Ser2448), ATRA-mediated p70S6K activation in mASCs is rapamycin sensitive and as such, reliant on mTOR signaling. It is important to note that although p70S6K is well recognized as a downstream target of mTOR, phosphorylation of mTOR at Ser2448 is also considered to represent a feedback signal from p70S6K [50]. If indeed the case, then ATRA-mediated p70S6K activation in mASCs may possibly be reliant on increases in mTOR activity through the phosphorylation of sites other than Ser2448. Certainly, mTOR has been reported to have several potential phosphorylation sites whose functions remain largely undefined [51]. As with rapamycin treatment, loss-of-function of HtrA1 also resulted in reductions in mTOR and p70S6K phosphorylation in the absence of any changes in phospho-Akt. However, in contrast to rapamycin, the removal of HtrA1 was unable to completely abolish mTOR or p70S6K phosphorylation.

Mary Ann Liebert Inc., 140 Huguenot Street, New Rochelle, NY 10801

Although p70S6K activity is considered to be of paramount importance in determining mASC adipocyte lineage commitment [52], its functional role in mASC osteogenesis has not yet been established. Our findings from studies using the mTOR inhibitor rapamycin, along with siRNA-dependent inhibition of *Rps6kb1* gene expression, confirmed that the mTOR/p70S6K signaling pathway was indeed an essential requirement for efficient mASC osteogenesis and mASC-derived osteoblast mineralization. As far as we are aware, this is the first report to demonstrate such a role for mTOR/p70S6K in ATRA-mediated mASC osteogenesis. Therefore, these studies identified both HtrA1 and mTOR/p70S6K as being important regulators of ATRA-mediated mASC osteogenesis. However, it was still unclear as to whether HtrA1's ability to regulate p70S6K phosphorylation in response to ATRA was directly related to its pro-osteogenic effects. We therefore performed a study in which we introduced plasmids encoding DNA for either constitutively active or kinase inactive mutants of p70S6K into HtrA1-deficient mASCs in an attempt to rescue osteoblastogenesis. Indeed, our results revealed that the mineralizing capacity of HtrA1-deficient mASC-derived osteoblasts could be fully restored when cells were engineered to express the constitutively active p70S6K mutant.

These findings therefore identify p70S6K activation as a regulatory target of HtrA1 and an important event in mediating HtrA1's pro-osteogenic effects in ATRA-stimulated mASCs. However, based on the fact that mTOR phosphorylation at Ser2448 may be the result of feedback regulation by p70S6K, it still remains to be determined as to the involvement of mTOR in mediating HtrA1's effects. Certainly, we would anticipate that if HtrA1 were acting to regulate p70S6K activity through its interaction with TSC2 [16], then reductions in mTOR activity would be apparent [53]. However, the suggestion that the TSC-complex may in fact regulate p70S6K independently of mTOR [54], may offer an additional means by which HtrA1

Mary Ann Liebert Inc., 140 Huguenot Street, New Rochelle, NY 10801

could activate p70S6K without the need for alterations in mTOR activity. Alternatively, HtrA1 may act to regulate p70S6K phosphorylation through mTOR, but in a TSC2-independent manner. Certainly, mTOR is not solely reliant on TSC2 inhibition for its activation as confirmed by studies in which Akt was shown to activate mTOR by relieving the inhibitory effects of proline-rich Akt/PKB substrate 40 kDa (PRAS40) on mTORC1 [55], and more recently, through its ability to promote mTORC1 phosphorylation at Ser1415 via the actions of IkB kinase alpha (IKKα) [56]. Further studies are therefore required in order to ascertain the involvement of TSC2 and mTOR in mediating the effects of HtrA1 on p70S6K phosphorylation in osteogenic mASCs.

In summary, we have identified p70S6K as an important regulator of mASC osteogenesis, being activated in response to ATRA via pathways involving mTOR and HtrA1 (Fig. 6). As such, it is proposed that HtrA1 represents a newly identified positive regulator of ATRA-mediated mASC osteogenesis and mASC-derived osteoblast mineralization.

Acknowledgements

SG was supported by SNSF grants 31003A_134935 and 31003A_156313. AM and ANT were supported by the Uniscientia Foundation and Forschungskredit University of Zurich. CLF was supported by the Whitaker International Program.

Disclosure Statement

The authors declare that they have no competing financial interests.

References

1. Wan DC, YY Shi, RP Nacamuli, N Quarto, KM Lyons, and MT Longaker. (2006). Osteogenic differentiation of mouse adipose-derived adult stromal cells requires retinoic acid and bone morphogenetic protein receptor type IB signaling. Proc Natl Acad Sci U S A 103:12335-12340.
2. Wan DC, MT Siedhoff, MD Kwan, RP Nacamuli, BM Wu, and MT Longaker. (2007). Refining retinoic acid stimulation for osteogenic differentiation of murine adipose-derived adult stromal cells. Tissue Eng 13:1623-631.
3. Malladi P, Y Xu, GP Yang, and MT Longaker. (2006) Functions of vitamin D, retinoic acid, and dexamethasone in mouse adipose-derived mesenchymal cells. Tissue Eng 12:2031-2040.
4. Mirsaidi A, KN Kleinhans, M Rimann, AN Tiaden, M Stauber, KL Rudolph, and PJ Richards. (2012). Telomere length, telomerase activity and osteogenic differentiation are maintained in adipose-derived stromal cells from senile osteoporotic SAMP6 mice. J Tissue Eng Regen Med 6:378-390.
5. Mirsaidi A, K Genelin, JR Vetsch, S Stanger, F Theiss, RA Lindtner, B von Rechenberg, M Blauth, R Müller, GA Kuhn, S Hofmann Boss, HL Ebner, and PJ Richards. (2014). Therapeutic potential of adipose-derived stromal cells in age-related osteoporosis. Biomaterials 35:7326-7335.
6. Mirsaidi A, AN Tiaden, and PJ Richards. (2013). Preparation and osteogenic differentiation of scaffold-free mouse adipose-derived stromal cell microtissue spheroids (ASC-MT). Curr Protoc Stem Cell Biol 27: Unit 2B.5.

Mary Ann Liebert Inc., 140 Huguenot Street, New Rochelle, NY 10801

7. Tiaden AN, M Breiden, A Mirsaidi, FA Weber, G Bahrenberg, S Glanz, P Cinelli, M Ehrmann, and PJ Richards. (2012). Human serine protease HTRA1 positively regulates osteogenesis of human bone marrow-derived mesenchymal stem cells and mineralization of differentiating bone-forming cells through the modulation of extracellular matrix protein. Stem Cells 30:2271-2282.

8. Hamidouche Z, E Haÿ, P Vaudin, P Charbord, R Schüle, PJ Marie, and O Fromigué. (2008) FHL2 mediates dexamethasone-induced mesenchymal cell differentiation into osteoblasts by activating Wnt/beta-catenin signaling-dependent Runx2 expression. FASEB J 22:3813-3822.

9. Hisada K, K Hata, F Ichida, T Matsubara, H Orimo, T Nakano, H Yatani, R Nishimura, and T Yoneda. (2013). Retinoic acid regulates commitment of undifferentiated mesenchymal stem cells into osteoblasts and adipocytes. J Bone Miner Metab 31:53-63.

10. Song HM, RP Nacamuli, W Xia, AS Bari, YY Shi, TD Fang, and MT Longaker. (2005). High-dose retinoic acid modulates rat calvarial osteoblast biology. J Cell Physiol 202:255-262.

11. Ohishi K, S Nishikawa, T Nagata, N Yamauchi, H Shinohara, J Kido, and H Ishida. (1995). Physiological concentrations of retinoic acid suppress the osteoblastic differentiation of fetal rat calvaria cells in vitro. Eur J Endocrinol 133:335-341.

12. Iba K, H Chiba, T Yamashita, S Ishii, and N Sawada. (2001). Phase-independent inhibition by retinoic acid of mineralization correlated with loss of tetranectin expression in a human osteoblastic cell line. Cell Struct Funct 26:227-233.

13. Lind T, A Sundqvist, L Hu, G Pejler, G Andersson, A Jacobson, and H Melhus. (2013). Vitamin a is a negative regulator of osteoblast mineralization. PLoS One 8:e82388.

Mary Ann Liebert Inc., 140 Huguenot Street, New Rochelle, NY 10801

14. Cowan CM, OO Aalami, YY Shi, YF Chou, C Mari, R Thomas, N Quarto, RP Nacamuli, CH Contag, B Wu, and MT Longaker. (2005). Bone morphogenetic protein 2 and retinoic acid accelerate in vivo bone formation, osteoclast recruitment, and bone turnover. Tissue Eng 11, 645-58.

15. Clausen T, M Kaiser, R Huber, and M Ehrmann. (2011). HTRA proteases: regulated proteolysis in protein quality control. Nat Rev Mol Cell Biol 12:152-162.

16. Campioni M, A Severino, L Manente, IL Tuduce, S Toldo, M Caraglia, S Crispi, M Ehrmann, X He, J Maguire, M De Falco, A De Luca, V Shridhar, and A Baldi. (2010). The serine protease HtrA1 specifically interacts and degrades the tuberous sclerosis complex 2 protein. Mol Cancer Res 8:1248-1260.

17. Singha UK, Y Jiang, S Yu, M Luo, Y Lu, J Zhang, and G Xiao. (2008). Rapamycin inhibits osteoblast proliferation and differentiation in MC3T3-E1 cells and primary mouse bone marrow stromal cells. J Cell Biochem 103:434–446.

18. Isomoto S, K Hattori, H Ohgushi, H Nakajima, Y Tanaka, and Y Takakura. (2007). Rapamycin as an inhibitor of osteogenic differentiation in bone marrow-derived mesenchymal stem cells. J Orthop Sci 12:83–88.

19. Shoba LN, and JC Lee. (2003). Inhibition of phosphatidylinositol 3-kinase and p70S6 kinase blocks osteogenic protein-1 induction of alkaline phosphatase activity in fetal rat calvaria cells. J Cell Biochem 88:1247–1255.

20. Grau S, PJ Richards, B Kerr, C Hughes, B Caterson, AS Williams, U Junker, SA Jones, T Clausen, and M Ehrmann. (2006). The role of human HtrA1 in arthritic disease J Biol Chem 281:6124-6129.

Mary Ann Liebert Inc., 140 Huguenot Street, New Rochelle, NY 10801

21. Schalm SS, and J Blenis. (2002). Identification of a conserved motif required for mTOR signaling. Curr Biol 12:632-639.

22. Schipper BM, KG Marra, W Zhang, AD Donnenberg, and JP Rubin. (2008). Regional anatomic and age effects on cell function of human adipose-derived stem cells. Ann Plast Surg 60:538-544.

23. Zhu M, E Kohan, J Bradley, M Hedrick, P Benhaim, and P Zuk. (2009). The effect of age on osteogenic, adipogenic and proliferative potential of female adipose-derived stem cells. J Tissue Eng Regen Med 3:290-301.

24. Khan WS, AB Adesida, SR Tew, JG Andrew, and TE Hardingham. (2009). The epitope characterization and the osteogenic differentiation potential of human fat pad-derived stem cells is maintained with ageing in later life. Injury 40:150-157.

25. Shi YY, RP Nacamuli, A Salim, and MT Longaker. (2005). The osteogenic potential of adipose-derived mesenchymal cells is maintained with aging. Plast Reconstr Surg 116:1686-1696.

26. Liu HY, JF Chiou, AT Wu, CY Tsai, JD Leu, LL Ting, MF Wang, HY Chen, CT Lin, DF Williams, and WP Deng. (2012). The effect of diminished osteogenic signals on reduced osteoporosis recovery in aged mice and the potential therapeutic use of adipose-derived stem cells. Biomaterials 33:6105-6112.

27. You L, L Pan, L Chen, JY Chen, X Zhang, Z Lv, and D Fu. (2012). Suppression of zinc finger protein 467 alleviates osteoporosis through promoting differentiation of adipose derived stem cells to osteoblasts. J Transl Med 10:11.

28. Zumbrunn J, and B Trueb. (1996). Primary structure of a putative serine protease specific for IGF-binding proteins. FEBS Lett 398:187-92.

Mary Ann Liebert Inc., 140 Huguenot Street, New Rochelle, NY 10801

29. Tiaden AN, and PJ Richards. (2013). The emerging roles of HTRA1 in musculoskeletal disease. Am J Pathol 182:1482-488.

30. Graham JR, A Chamberland, Q Lin, XJ Li, D Dai, W Zeng, MS Ryan, MA Rivera-Bermúdez, CR Flannery, and Z Yang. (2013). Serine protease HTRA1 antagonizes transforming growth factor-β signaling by cleaving its receptors and loss of HTRA1 in vivo enhances bone formation. PLoS One. 8:e74094.

31. Wu X, SM Chim, V Kuek, BS Lim, ST Chow, J Zhao, S Yang, V Rosen, J Tickner, and J Xu. (2014). HtrA1 is upregulated during RANKL-induced osteoclastogenesis, and negatively regulates osteoblast differentiation and BMP2-induced Smad1/5/8, ERK and p38 phosphorylation. FEBS Lett 588:143-50.

32. Tiaden AN, M Klawitter, V Lux, A Mirsaidi, G Bahrenberg, S Glanz, L Quero, T Liebscher, K Wuertz, M Ehrmann, and PJ Richards. (2012). Detrimental role for human high temperature requirement serine protease A1 (HTRA1) in the pathogenesis of intervertebral disc (IVD) degeneration. J Biol Chem 287:21335-21345.

33. Chien J, T Ota, G Aletti, R Shridhar, M Boccellino, L Quagliuolo, A Baldi, and V Shridhar. (2009). Serine protease HtrA1 associates with microtubules and inhibits cell migration. Mol Cell Biol 29:4177-4187.

34. Shiga A, H Nozaki, A Yokoseki, M Nihonmatsu, H Kawata, T Kato, A Koyama, K Arima, M Ikeda, S Katada, Y Toyoshima, H Takahashi, A Tanaka, I Nakano, T Ikeuchi, M Nishizawa, and O Onodera. (2011). Cerebral small-vessel disease protein HTRA1 controls the amount of TGF-β1 via cleavage of proTGF-β1. Hum Mol Genet 20:1800-1810.

35. Tennstaedt A, S Pöpsel, L Truebestein, P Hauske, A Brockmann, N Schmidt, I Irle, B Sacca, CM Niemeyer, R Brandt, H Ksiezak-Reding, AL Tirniceriu, R Egensperger, A Baldi, L

Dehmelt, M Kaiser, R Huber, T Clausen, and M Ehrmann. (2012). Human high temperature requirement serine protease A1 (HTRA1) degrades tau protein aggregates. J Biol Chem 287:20931-20941.

36. He X, A Khurana, JL Maguire, J Chien, and V Shridhar. (2012). HtrA1 sensitizes ovarian cancer cells to cisplatin-induced cytotoxicity by targeting XIAP for degradation. Int J Cancer 130:1029-1035.
37. Zoncu R, A Efeyan, and DM Sabatini. (2011). mTOR: from growth signal integration to cancer, diabetes and ageing. Nat Rev Mol Cell Biol 12:21–35.
38. Kim J, Y Jung, H Sun, J Joseph, A Mishra, Y Shiozawa, J Wang, PH Krebsbach, and RS Taichman. (2012). Erythropoietin mediated bone formation is regulated by mTOR signaling. J Cell Biochem 113:220–228.
39. Kim JK, J Baker, JE Nor, and EE Hill. (2011). mTor Plays an Important Role in Odontoblast Differentiation. J Endod 37:1081–1085.
40. Tang C-H, DY Lu, TW Tan, WM Fu, and RS Yang. (2007). Ultrasound Induces Hypoxia-inducible Factor-1 Activation and Inducible Nitricoxide Synthase Expression through the Integrin/Integrin-linked Kinase/Akt/Mammalian Target of Rapamycin Pathway in Osteoblasts. J Biol Chem 282:25406–25415.
41. Tee AR, BD Manning, PP Roux, LC Cantley, and J Blenis. (2003). Tuberous sclerosis complex gene products, Tuberin and Hamartin, control mTOR signaling by acting as a GTPase-activating protein complex toward Rheb. Curr Biol 13:1259-1268.
42. La L, Y Li, J Smith, A Sassano, S Uddin, S Parmar, MS Tallman, S Minucci, N Hay, and LC Platanias. (2005). Activation of the p70 S6 kinase by all-trans-retinoic acid in acute promyelocytic leukemia cells. Blood 105:1669-1677.

Mary Ann Liebert Inc., 140 Huguenot Street, New Rochelle, NY 10801

43. Busada JT, VA Chappell, BA Niedenberger, EP Kaye, BD Keiper, CA Hogarth, and CB Geyer. (2015). Retinoic acid regulates Kit translation during spermatogonial differentiation in the mouse. Dev Biol 397:140-149.

44. Chen N, and JL Napoli. (2008). All-trans-retinoic acid stimulates translation and induces spine formation in hippocampal neurons through a membrane-associated RARalpha. FASEB J 22:236-245.

45. Masiá S, S Alvarez, AR de Lera, and D Barettino. (2007). Rapid, nongenomic actions of retinoic acid on phosphatidylinositol-3-kinase signaling pathway mediated by the retinoic acid receptor. Mol Endocrinol 21:2391-2402.

46. Gianni M, A Bauer, E Garattini, P Chambon, and C Rochette-Egly. (2002). Phosphorylation by p38MAPK and recruitment of SUG-1 are required for RA-induced RAR gamma degradation and transactivation. EMBO J 21:3760-3769.

47. Alsayed Y, S Uddin, N Mahmud, F Lekmine, DV Kalvakolanu, S Minucci, G Bokoch, and LC Platanias. (2001). Activation of Rac1 and the p38 mitogen-activated protein kinase pathway in response to all-trans-retinoic acid. J Biol Chem 276:4012-4019.

48. Bost F, L Caron, I Marchetti, C Dani, Y Le Marchand-Brustel, and B Binétruy. (2002). Retinoic acid activation of the ERK pathway is required for embryonic stem cell commitment into the adipocyte lineage. Biochem J 361:621-627.

49. AI Tanoury Z, A Piskunov, and C Rochette-Egly. (2013). Vitamin A and retinoid signaling: genomic and nongenomic effects. J Lipid Res 54:1761-1775.

50. Chiang GG, and RT Abraham. (2005). Phosphorylation of mammalian target of rapamycin (mTOR) at Ser-2448 is mediated by p70S6 kinase. J Biol Chem 280:25485-25490.

51. Ekim B, B Magnuson, HA Acosta-Jaquez, JA Keller, EP Feener, and DC Fingar. (2011). mTOR kinase domain phosphorylation promotes mTORC1 signaling, cell growth, and cell cycle progression. Mol Cell Biol 31:2787-27801.

52. Carnevalli LS, K Masuda, F Frigerio, O Le Bacquer, SH Um, V Gandin, I Topisirovic, N Sonenberg, G Thomas, and SC Kozma. (2010). S6K1 plays a critical role in early adipocyte differentiation. Dev Cell 18:763-774.

53. Inoki K, Y Li, T Xu, and KL Guan. (2003). Rheb GTPase is a direct target of TSC2 GAP activity and regulates mTOR signaling. Genes Dev 17:1829-1834.

54. Jaeschke A, J Hartkamp, M Saitoh, W Roworth, T Nobukuni, A Hodges, J Sampson, G Thomas, and R Lamb. (2002). Tuberous sclerosis complex tumor suppressor-mediated S6 kinase inhibition by phosphatidylinositide-3-OH kinase is mTOR independent. J Cell Biol 159:217-224.

55. Vander Haar E, SI Lee, S Bandhakavi, TJ Griffin, and DH Kim. (2007). Insulin signalling to mTOR mediated by the Akt/PKB substrate PRAS40. Nat Cell Biol 9:316-323.

56. Dan HC, A Ebbs, M Pasparakis, T Van Dyke, DS Basseres, and AS Baldwin. (2014) Akt-dependent activation of mTORC1 complex involves phosphorylation of mTOR (mammalian target of rapamycin) by IκB kinase α (IKKα). J Biol Chem 289:25227-25240.

FIG. 1. Effect of *HtrA1* knockdown on osteogenic induction of mASCs. mASCs were pre-treated with control siRNA (siControl) or 2 selected siRNAs targeting *HtrA1* (siHtrA1-A and siHtrA1-B) for 24 h and induced to undergo osteogenesis for up to 10 days. **(A)** Western blot analysis of HtrA1 protein in FCS-free concentrated supernatants from siRNA-treated mASCs after 4 days of osteogenic induction using an antibody specific for HtrA1. Gels were stained with Coomassie Blue to confirm equal protein loading. **(B)** Alizarin red staining of siRNA-treated mASCs 10 days post osteogenic induction. **(C)** Extracted Alizarin red stain was quantified and normalized to cell number. * $p < 0.001$ as compared to siControl using one-way ANOVA. Gene expression levels of *HtrA1* **(D)** and *Alpl* **(E)** were determined in osteogenic mASCs at selected time points using RT-qPCR and the fold change as compared to uninduced mASCs (day 0) determined using the $2^{-\Delta\Delta CT}$ method. **(F)** ALP enzymatic activity levels were measured in siRNA-treated mASCs over the course of 10 days of osteogenic differentiation using a colorimetric-based ALP activity assay. All values are expressed as mean ± S.D (triplicates). * $p < 0.05$, ** $p < 0.001$ as compared to uninduced mASCs at day 0; # $p < 0.05$, ## $p < 0.001$ comparison between siControl and siHtrA1 using one-way ANOVA.

FIG. 2. Western blot analysis of kinase activity in mASCs in response to ATRA-mediated osteogenic induction. **(A)** mASCs were stimulated with osteogenic medium (OM) for up to 2 h and cell lysates analysed by immunoblotting at selected time points using antibodies specific for phosphorylated or non-phosphorylated Akt, mTOR, p70S6K and 4E-BP1. A mouse anti-tubulin antibody was used to confirm equal protein loading. The influence of osteogenic induction on mASC protein phosphorylation was compared to undifferentiated mASCs (time point 0 min). **(B)** mASCs were pre-treated with control siRNA (siControl) or siRNA targeting *HtrA1* (siHtrA1) for

Mary Ann Liebert Inc., 140 Huguenot Street, New Rochelle, NY 10801

24 h and stimulated with osteogenic medium (OM) for 10 min. Untreated mASCs incubated in growth medium (GM) alone served as non-differentiated controls. Cell lysates were extracted and analysed by immunoblotting using antibodies specific for phosphorylated or non-phosphorylated Akt, mTOR, p70S6K, S6 ribosomal protein or 4E-BP1. A mouse anti-tubulin antibody was used to confirm equal protein loading. Results are representative of at least two separate experiments.

FIG. 3. Effect of rapamycin on osteogenic induction of mASCs. **(A)** mASCs were incubated with growth medium (GM) or osteogenic medium (OM) for 10 min and cell lysates analysed by immunoblotting using antibodies specific for phosphorylated or non-phosphorylated Akt, mTOR, or p70S6K. In order to assess the effects of mTOR inhibition on protein activation, cells were also pre-treated for 2 h with 20 nM rapamycin (Rap) or vehicle (0.1% DMSO) prior to osteogenic induction. A mouse anti-tubulin antibody was used to confirm equal protein loading. Results are representative of at least two separate experiments. **(B)** The influence of different concentrations of rapamycin on mASC-derived osteoblast mineralization was determined by Alizarin red staining at day 14. **(C)** Extracted Alizarin red stain was quantified and normalized to cell number and comparisons made between vehicle-treated and rapamycin-treated osteogenic mASCs. All values are expressed as mean ± S.D (triplicates). * $p < 0.001$ as compared to mASCs treated without rapamycin using one-way ANOVA.

FIG. 4. Effect of *Rps6kb1* knockdown on osteogenic induction of mASCs. mASCs were pre-treated with control siRNA (siControl) or 2 selected siRNAs targeting *Rps6kb1* (siRps6kb1-A and siRps6kb1-B) for 24 h and induced to undergo osteogenesis for up to 14 days. **(A)** Western

blot analysis of p70S6K and phospho-S6 ribosomal protein (p-S6) in siRNA-treated mASCs using antibodies specific for p70S6K and p-S6 respectively. A mouse anti-tubulin antibody was used to confirm equal protein loading. **(B)** Alizarin red staining of siRNA-treated mASCs 14 days post osteogenic induction. **(C)** Extracted Alizarin red stain was quantified and normalized to cell number. * $p < 0.001$ as compared to siControl using one-way ANOVA. **(D-F)** Gene expression levels of *Rps6kb1* **(D)**, *Alpl* **(E)** and *Spp1* **(F)** were determined in osteogenic mASCs at selected time points using RT-qPCR and the fold change as compared to uninduced mASCs determined using the $2^{-\Delta\Delta CT}$ method. All values are expressed as mean ± S.D (triplicates). * $p < 0.05$, ** $p < 0.01$, *** $p < 0.001$ as compared to uninduced mASCs at day 0; # $p < 0.01$, ## $p < 0.001$ comparison between siControl and siRps6kb1 using one-way ANOVA.

FIG. 5. Influence of p70S6K activity on siHtrA1-mediated suppression of mASC osteogenesis. **(A)** mASCs were transfected with empty plasmid, or plasmids encoding influenza hemagglutinin (HA)-tagged constitutively active (p70S6KCA) or kinase inactive (p70S6KKI) p70S6K mutants and immunoblotting performed after 24 h using an HA-probe antibody (HA-p70S6K) or anti-phospho-S6 ribosomal protein antibody (p-S6). A mouse anti-GAPDH antibody was used to confirm equal protein loading. **(B)** The effect of plasmid DNA transfection on siRNA-mediated *HtrA1* gene silencing in mASCs was determined after 24 h using RT-qPCR. **(C)** The influence of plasmid DNA transfection on mASC-derived osteoblast formation in in HtrA1-deficient mASCs was determined by Alizarin red staining at day 21 post osteogenic induction. **(D)** Extracted Alizarin red stain was quantified and normalized to cell number. All values are expressed as mean ± S.D (triplicates). * $p < 0.01$, ** $p < 0.001$ as compared to siControl/ empty plasmid

Mary Ann Liebert Inc., 140 Huguenot Street, New Rochelle, NY 10801

treated cells; ; # $p < 0.01$, ## $p < 0.001$ comparisons between siHtrA1/p70S6KCA and siHtrA1/p70S6KKI or siHtrA1/p70S6KCA and siHtrA1/empty plasmid using one-way ANOVA.

FIG. 6. Model of ATRA-induced mASC osteogenesis. Based on our findings, we propose that ATRA drives osteoblast commitment of mASCs through activation of p70S6K in a non-canonical and non-genomic manner. This appears not only to be dependent on rapamycin-sensitive signaling pathways, but also on the actions of HtrA1. However, the mechanism through which HtrA1 mediates its effects on p70S6K phosphorylation, and its influence over mTOR signaling, still remain to be determined.

Mary Ann Liebert Inc., 140 Huguenot Street, New Rochelle, NY 10801

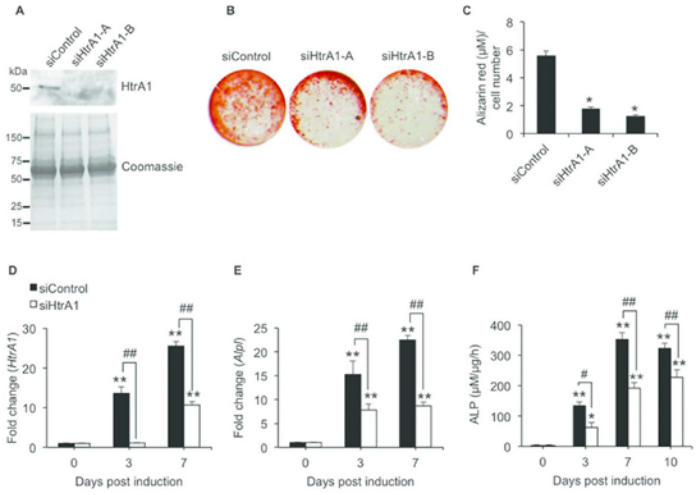

FIG. 1. Effect of *HtrA1* knockdown on osteogenic induction of mASCs. mASCs were pre-treated with control siRNA (siControl) or 2 selected siRNAs targeting *HtrA1* (siHtrA1-A and siHtrA1-B) for 24 h and induced to undergo osteogenesis for up to 10 days. **(A)** Western blot analysis of HtrA1 protein in FCS-free concentrated supernatants from siRNA-treated mASCs after 4 days of osteogenic induction using an antibody specific for HtrA1. Gels were stained with Coomassie Blue to confirm equal protein loading. **(B)** Alizarin red staining of siRNA-treated mASCs 10 days post osteogenic induction. **(C)** Extracted Alizarin red stain was quantified and normalized to cell number. * $p < 0.001$ as compared to siControl using one-way ANOVA. Gene expression levels of *HtrA1* **(D)** and *Alpl* **(E)** were determined in osteogenic mASCs at selected time points using RT-qPCR and the fold change as compared to uninduced mASCs (day 0) determined using the $2^{-\Delta\Delta CT}$ method. **(F)** ALP enzymatic activity levels were measured in siRNA-treated mASCs over the course of 10 days of osteogenic differentiation using a colorimetric-based ALP activity assay. All values are expressed as mean ± S.D (triplicates). * $p < 0.05$, ** $p < 0.001$ as compared to uninduced mASCs at day 0; $^{\#}$ $p < 0.05$, $^{\#\#}$ $p < 0.001$ comparison between siControl and siHtrA1 using one-way ANOVA.
75x56mm (300 x 300 DPI)

Mary Ann Liebert Inc., 140 Huguenot Street, New Rochelle, NY 10801

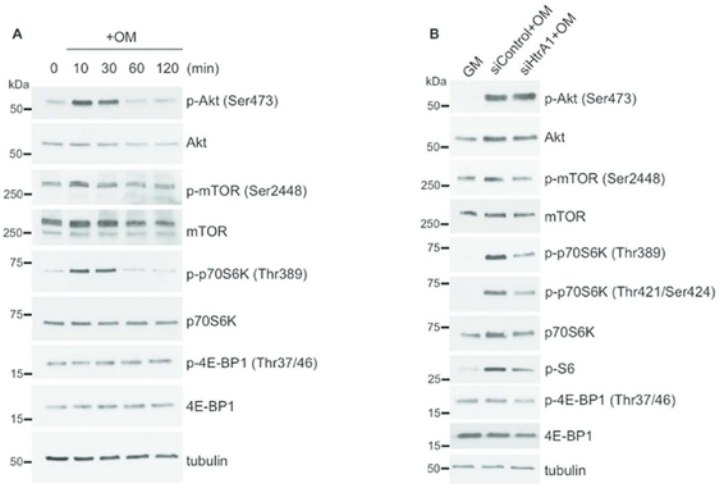

FIG. 2. Western blot analysis of kinase activity in mASCs in response to ATRA-mediated osteogenic induction. **(A)** mASCs were stimulated with osteogenic medium (OM) for up to 2 h and cell lysates analysed by immunoblotting at selected time points using antibodies specific for phosphorylated or non-phosphorylated Akt, mTOR, p70S6K and 4E-BP1. A mouse anti-tubulin antibody was used to confirm equal protein loading. The influence of osteogenic induction on mASC protein phosphorylation was compared to undifferentiated mASCs (time point 0 min). **(B)** mASCs were pre-treated with control siRNA (siControl) or siRNA targeting HtrA1 (siHtrA1) for 24 h and stimulated with osteogenic medium (OM) for 10 min. Untreated mASCs incubated in growth medium (GM) alone served as non-differentiated controls. Cell lysates were extracted and analysed by immunoblotting using antibodies specific for phosphorylated or non-phosphorylated Akt, mTOR, p70S6K, S6 ribosomal protein or 4E-BP1. A mouse anti-tubulin antibody was used to confirm equal protein loading. Results are representative of at least two separate experiments.
71x50mm (300 x 300 DPI)

Mary Ann Liebert Inc., 140 Huguenot Street, New Rochelle, NY 10801

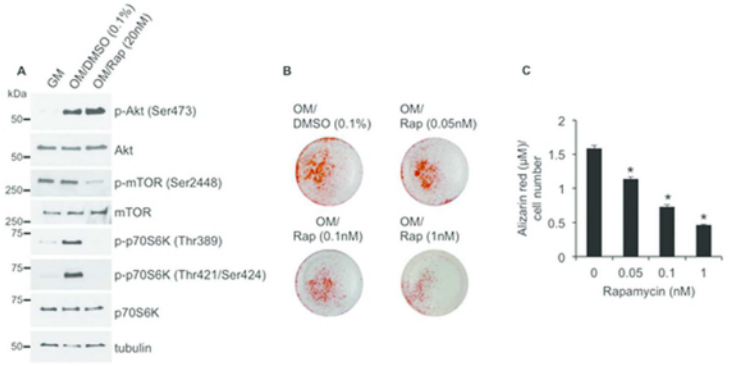

FIG. 3. Effect of rapamycin on osteogenic induction of mASCs. **(A)** mASCs were incubated with growth medium (GM) or osteogenic medium (OM) for 10 min and cell lysates analysed by immunoblotting using antibodies specific for phosphorylated or non-phosphorylated Akt, mTOR, or p70S6K. In order to assess the effects of mTOR inhibition on protein activation, cells were also pre-treated for 2 h with 20 nM rapamycin (Rap) or vehicle (0.1% DMSO) prior to osteogenic induction. A mouse anti-tubulin antibody was used to confirm equal protein loading. Results are representative of at least two separate experiments. **(B)** The influence of different concentrations of rapamycin on mASC-derived osteoblast mineralization was determined by Alizarin red staining at day 14. **(C)** Extracted Alizarin red stain was quantified and normalized to cell number and comparisons made between vehicle-treated and rapamycin-treated osteogenic mASCs. All values are expressed as mean ± S.D (triplicates). * $p < 0.001$ as compared to mASCs treated without rapamycin using one-way ANOVA.
52x27mm (300 x 300 DPI)

Mary Ann Liebert Inc., 140 Huguenot Street, New Rochelle, NY 10801

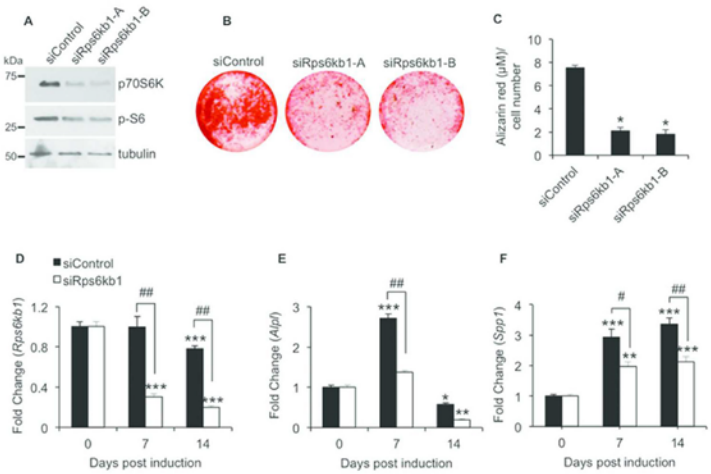

FIG. 4. Effect of *Rps6kb1* knockdown on osteogenic induction of mASCs. mASCs were pre-treated with control siRNA (siControl) or 2 selected siRNAs targeting *Rps6kb1* (siRps6kb1-A and siRps6kb1-B) for 24 h and induced to undergo osteogenesis for up to 14 days. **(A)** Western blot analysis of p70S6K and phospho-S6 ribosomal protein (p-S6) in siRNA-treated mASCs using antibodies specific for p70S6K and p-S6 respectively. A mouse anti-tubulin antibody was used to confirm equal protein loading. **(B)** Alizarin red staining of siRNA-treated mASCs 14 days post osteogenic induction. **(C)** Extracted Alizarin red stain was quantified and normalized to cell number. * $p < 0.001$ as compared to siControl using one-way ANOVA. **(D-F)** Gene expression levels of *Rps6kb1* **(D)**, *Alpl* **(E)** and *Spp1* **(F)** were determined in osteogenic mASCs at selected time points using RT-qPCR and the fold change as compared to uninduced mASCs determined using the $2^{-\Delta\Delta CT}$ method. All values are expressed as mean ± S.D (triplicates). * $p < 0.05$, ** $p < 0.01$, *** $p < 0.001$ as compared to uninduced mASCs at day 0; $^{\#}$ $p < 0.01$, $^{\#\#}$ $p < 0.001$ comparison between siControl and siRps6kb1 using one-way ANOVA.
65x43mm (300 x 300 DPI)

Mary Ann Liebert Inc., 140 Huguenot Street, New Rochelle, NY 10801

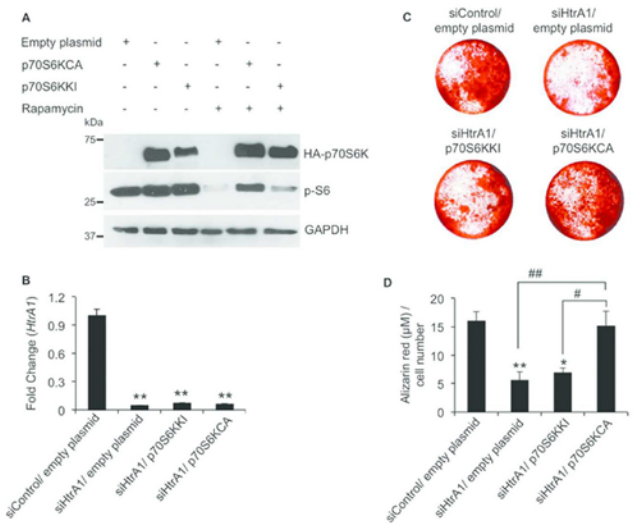

FIG. 5. Influence of p70S6K activity on siHtrA1-mediated suppression of mASC osteogenesis. **(A)** mASCs were transfected with empty plasmid, or plasmids encoding influenza hemagglutinin (HA)-tagged constitutively active (p70S6KCA) or kinase inactive (p70S6KKI) p70S6K mutants and immunoblotting performed after 24 h using an HA-probe antibody (HA-p70S6K) or anti-phospho-S6 ribosomal protein antibody (p-S6). A mouse anti-GAPDH antibody was used to confirm equal protein loading. **(B)** The effect of plasmid DNA transfection on siRNA-mediated *HtrA1* gene silencing in mASCs was determined after 24 h using RT-qPCR. **(C)** The influence of plasmid DNA transfection on mASC-derived osteoblast formation in in HtrA1-deficient mASCs was determined by Alizarin red staining at day 21 post osteogenic induction. **(D)** Extracted Alizarin red stain was quantified and normalized to cell number. All values are expressed as mean ± S.D (triplicates). * $p < 0.01$, ** $p < 0.001$ as compared to siControl/ empty plasmid treated cells; ; $^{\#}$ $p < 0.01$, $^{\#\#}$ $p < 0.001$ comparisons between siHtrA1/p70S6KCA and siHtrA1/p70S6KKI or siHtrA1/p70S6KCA and siHtrA1/empty plasmid using one-way ANOVA.
75x56mm (300 x 300 DPI)

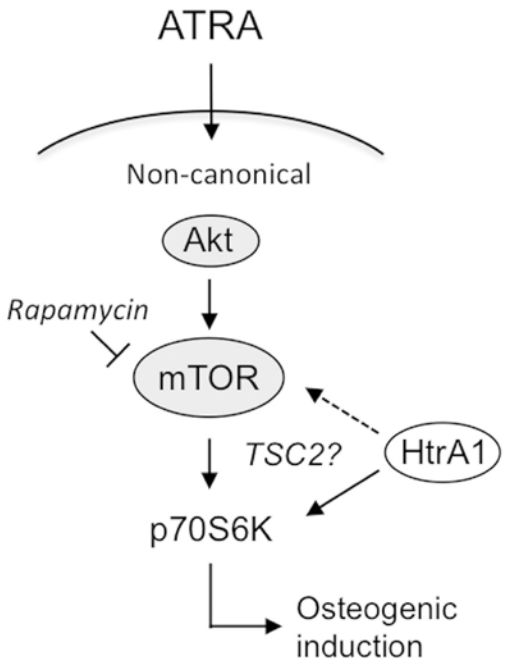

FIG. 6. Model of ATRA-induced mASC osteogenesis. Based on our findings, we propose that ATRA drives osteoblast commitment of mASCs through activation of p70S6K in a non-canonical and non-genomic manner. This appears not only to be dependent on rapamycin-sensitive signaling pathways, but also on the actions of HtrA1. However, the mechanism through which HtrA1 mediates its effects on p70S6K phosphorylation, and its influence over mTOR signaling, still remain to be determined.
119x143mm (300 x 300 DPI)

Mary Ann Liebert Inc., 140 Huguenot Street, New Rochelle, NY 10801

2.1.2. Novel function of serine protease HTRA1 in inhibiting adipogenic differentiation of human mesenchymal stem cells via MAP kinase-mediated MMP upregulation

Authors : Tiaden AN*, Bahrenberg G*, Mirsaidi A, **Glanz S**, Blüher M, Richards PJ.
*authors contributed equally

Journal : Under review *Stem Cells (August 2015) IF:6.523*

Contribution: Assistance in generation of qPCR data and data analysis.

Novel function of serine protease HTRA1 in inhibiting adipogenic differentiation of human mesenchymal stem cells via MAP kinase-mediated MMP upregulation

André N. Tiaden[1*], Gregor Bahrenberg[1,2*], Ali Mirsaidi[1,2], Stephan Glanz[1,2], Matthias Blüher[3], Peter J. Richards[1,2*]

[1]Bone and Stem Cell Research Group, CABMM, University of Zurich, 8057 Zurich, Switzerland. [2]Zurich Center for Integrative Human Physiology (ZIHP), University of Zurich, 8057 Zurich Switzerland. [3]Department of Medicine, Dermatology und Neurology, Department of Endocrinology und Nephrology, University of Leipzig, Leipzig, Germany.

*authors contributed equally

Author contributions

André N Tiaden: Collection and/or assembly of data, Data analysis and interpretation

Gregor Bahrenberg: Collection and/or assembly of data, Data analysis and interpretation

Ali Mirsaidi: Collection and/or assembly of data, Data analysis and interpretation

Stephan Glanz: Collection and/or assembly of data

Matthias Blüher: Provision of study material or patients, Collection and/or assembly of data, Data analysis and interpretation

Peter J Richards: Conception and design, Financial support, Collection and/or assembly of data, Data analysis and interpretation, Manuscript writing, Final approval of manuscript

***Correspondence:** Dr. Peter J. Richards, Bone and Stem Cell Research Group, Competence Center for Applied Biotechnology and Molecular Medicine, Room 13-L-86, University of

Zurich, Winterthurerstrasse 190, CH-8057 Zurich, Switzerland, Telephone: +41-44-635-3800; E-mail: peter.richards@cabmm.uzh.ch

SG and GB were supported by SNSF grants 31003A_134935 and 31003A_156313. AM and NAT were supported by the Uniscientia Foundation and the Forschungskredit University of Zurich.

Running Head: HTRA1 inhibits mesenchymal stem cell adipogenesis

Keywords: Adipogenesis; adult stem cells; cell signaling; diabetes; differentiation

ABSTRACT

Adipogenesis is the process by which mesenchymal stem cells (MSCs) develop into lipid-laden adipocytes. Due to their high prevalence within adipose tissue, adipocytes play a central role in regulating circulating fatty acid levels, which is considered to be of critical importance in maintaining insulin sensitivity. High temperature requirement protease A1 (HTRA1) is a newly recognized regulator of MSC differentiation, although its role as a mediator of adipogenesis has not yet been defined. The aim of this work was therefore to evaluate HTRA1's influence on hMSC adipogenesis and to establish a potential mode of action. We report that the addition of exogenous HTRA1 to adipogenic human MSCs suppressed their ability to develop into lipid laden adipocytes. These effects were demonstrated as being reliant on both its protease and PDZ domain, and were mediated through the actions of c-Jun N-terminal kinase (JNK) and matrix metalloproteinases (MMPs). The relevance of such findings with regards to HTRA1's potential influence on adipocyte function *in vivo*, is made evident by the fact that HTRA1 and MMP-13 were readily identifiable within inflammatory infiltrate present in visceral adipose tissue samples from insulin resistant obese human subjects. These data therefore implicate HTRA1 as a negative regulator of MSC adipogenesis and are suggestive of its potential involvement in adipose tissue remodeling under pathological conditions.

INTRODUCTION

Adipogenesis is a complex developmental process in which mesenchymal stem cells (MSCs) first become committed adipo-precursor cells and then undergo a tightly regulated differentiation program to generate mature adipocytes [1, 2]. Of critical importance in the body's ability to adapt to energy requirements, is the capacity for pre-adipocytes to develop into adipocytes and for them to be able to acquire more fat. Both these conditions require alterations in cell shape and volume, and are heavily reliant on the versatility and integrity of the adipocyte extracellular matrix (ECM), termed basal lamina [3]. The basal lamina is composed of numerous core proteins, including type IV collagen [4, 5], various laminin isoforms [5], and heparan sulfate proteoglycan (HSPG) [6] to name but a few, and is subject to continual turnover mediated by a wide variety of matrix metalloproteinases (MMPs) [7, 8]. Interference with basal lamina dynamics may therefore have significant consequences to adipogenesis and subsequent adipocyte stability.

Dysregulation of adipogenesis and adipose tissue remodeling has been linked to several human disorders, most notably of which is obesity-induced insulin resistance [9, 10]. A characteristic feature of obese adipose tissue is the presence of an inflammatory infiltrate consisting mainly of macrophages, thought to be instigated by elevated levels of adipocyte-derived cytokines as well as an increased incidence of adipocyte cell death [11]. Exposure to such an environment not only impairs adipocyte responsiveness to insulin, but can also lead to deviations in the differentiation status of pre-adipocytes [9]. As such, there is currently a strong focus on the identification of key factors involved in the regulation of adipogenic commitment.

HTRA1 has been newly identified as a modulator of human MSC (hMSC) differentiation, whereby it acts to enhance osteoblast formation most likely through proteolytic modification of the ECM, and its expression levels in bone tissue coincide with

the appearance of new bone formation during fracture repair in mice [12]. Furthermore, preliminary findings from loss of function studies have suggested that HTRA1's ability to influence hMSC lineage commitment may extend to adipogenic differentiation [12]. However, the extent to which these effects are mediated by secreted HTRA1 and the possible mechanisms underlining its mode of action remain to be determined. Certainly, the growing number of reports pertaining to HTRA1's ability to modulate the ECM both under normal physiological conditions and in disease, may provide some basis for how it could potentially interact with and regulate adipocyte formation [13-15].

To define HTRA1's role in adipogenesis and its potential physiological relevance, we investigated the effects of exogenously added recombinant HTRA1 on the development of hMSCs into mature adipocytes and further analysed its expression levels in visceral adipose tissue from obese patients. We demonstrate that HTRA1 acts to significantly suppress adipocyte development, primarily through upregulation of JNK activity and MMP production. We further localized HTRA1 and MMP-13 to sites of immune cell infiltrate within the adipose tissue of an insulin resistant obese patient. This work thus identifies HTRA1 as being a potentially novel mediator of adipose tissue homeostasis.

MATERIALS AND METHODS

Materials

Anti-ERK1/2, anti-phospho-ERK1/2 (Thr202/Tyr204), anti-SAPK/JNK, anti-phospho-SAPK/JNK (Thr183/Tyr185), anti-p38, anti-phospho-p38 (Thr180/Tyr182) were all purchased from Cell signaling Technology (Leiden, The Netherlands). Anti-tubulin was from Sigma-Aldrich. Anti-type IV collagen (M3F7) and anti-laminin γ-1 (2E8) were from the Developmental Studies Hybridoma Bank (University of Iowa). Anti-fibronectin (MAB1936) was from Merck Millipore (Schaffhausen, Switzerland). Monoclonal anti-human HTRA1 was generously supplied by Prof. Michael Ehrmann (University Duisburg-Essen, Germany) and generated as previously described [16]. Rabbit anti-MMP-13 was purchased from Abcam (Cambridge, UK). Mouse IgG, HRP- or Cy3-labeled secondary antibodies specific for mouse or rabbit IgG were purchased from Jackson ImmunoResearch (Suffolk, UK), and biotin-labeled goat anti-mouse IgG and Vectastain ABC system used in immunohistochemical staining studies was from Reactolab SA (Servion, Switzerland). Biotinylated swine anti-rabbit IgG was from Dako (Baar, Switzerland). Histidine-labeled HTRA1 proteins were overexpressed in *E. coli* and purified using previously described methodologies [16].

hMSC Culture

The hMSCs employed in this work were provided by the Texas A&M Health Science Center College of Medicine Institute for Regenerative Medicine at Scott & White through a grant from NCRR of the NIH, Grant # P40RR017447. hMSCs were isolated from bone marrow aspirates and multipotency fully defined in accordance with the minimal criteria outlined by International Society for Cellular Therapy [17]. hMSCs were maintained at 37°C, in 5% CO_2 and 98% humidity in normal growth medium consisting of Dulbecco's modified eagle

medium (DMEM-low glucose, with GlutaMAX) (Life Technologies, Zug, Switzerland), supplemented with 10% fetal bovine serum (FBS, BioWest), penicillin/streptomycin (50 units/ml; 50 μg/ml), and used between passage 5 and 8 unless otherwise stated.

Adipogenic differentiation of hMSCs

The adipogenic differentiation of hMSCs was performed using a protocol previously established in our laboratory [12]. Briefly, hMSCs seeded in cell culture plates at 10'000 cells/cm^2 were incubated for 3 days with adipogenic induction medium consisting of normal growth medium (DMEM-high glucose, GlutaMAX) supplemented with 1 μM dexamethasone, 10 μg/ml insulin, 0.1 mM Indomethacin, and 0.5 mM isobutylmethylxanthine (IBMX) (all from Sigma-Aldrich). Cells were subsequently cultured in adipogenic maintenance medium consisting of IBMX-free adipogenic medium, and replenished with fresh medium every 72 h for up to 14-24 days unless otherwise stated. Adipocyte formation was confirmed by positive staining of lipid droplets by Oil Red O (Sigma-Aldrich). Oil Red O staining was quantified by extraction with isopropanol absorption measured at 510 nm using a Multiplate reader (Infinite M200, Tecan). Values were normalized to cell number assessed by DAPI staining as described below. For recombinant HTRA1 addition studies, hMSCs undergoing adipogenic differentiation were treated with recombinant HTRA1 starting at day 3 after adipogenic induction. For inhibition studies, cells were treated with recombinant HTRA1 in the presence of MMP-3 inhibitor NNGH, MMP-13 inhibitor CL-82198, or MAP Kinase inhibitors PD98059, SP600125 and SB239063 (all from Enzo Life Science, Lausen, Switzerland). DMSO (0.05%) was added as vehicle control and was equivalent to highest concentration of inhibitor used.

RT-qPCR

Gene expression levels were quantified by reverse-transcription quantitative PCR (RT-qPCR) using TaqMan Gene Expression Assays (Life Technologies) (Supporting Information Table S1) as previously described [12]. Total RNA was harvested from cells at selected time points during differentiation and 0.5µg of total RNA reverse-transcribed using Superscript II (Life Technologies). An equivalent of 10ng total RNA was applied as cDNA template in the successive qRT-PCR reaction using the StepOnePlus (Life Technologies). Values were normalized to *GUSB* mRNA levels and presented as fold change as compared to control cells or cells treated with vehicle alone (value = 1) according to the $2^{-\Delta\Delta CT}$ method.

siRNA Assays

Silencing of *HTRA1* and *MMP13* gene expression was performed with Silencer Select siRNA oligos (Life Technologies) according to the manufacturer's protocol as previously described [12]. For *HTRA1* knockdown, hMSCs (1 x10^5) were transfected with 40 nM *HTRA1*-specific (s11279, s11280) or negative control siRNA (Negative Control-1) using the NEON Transfection System (Life Technologies). Transfected cells were immediately seeded in cell culture plates with fresh growth medium (without antibiotics) and incubated for 24 h at 37°C, 5% CO2. Medium was then replaced with either fresh growth medium or adipogenic differentiation and total RNA and supernatants harvested at selected time points for further analysis. For *MMP13* knockdown, adherent hMSCs were initially seeded in cell culture plates and cultured in induction medium for 3 days. Thereafter, hMSCs were transfected for 24 h with 40 nM *MMP13*-specific (11496, 104024) or negative control siRNA (Negative Control-1) using Lipofectamine RNAiMAX (Life Technologies). Supernatants were subsequently replaced with adipogenic maintenance medium and total RNA and supernatants harvested at selected time points for further analysis. The effect of *HTRA1* and *MMP13* gene silencing on lipid droplet formation was evaluated by Oil Red O staining as described above.

Proteolysis Assays

HTRA1 mediated digestion of BODIPY-FL-labeled DQ-elastin or DQ-type IV collagen was performed using EnzChek assay kits (Life Technologies) as previously described [18].

ELISAs

Extracellular protein levels of HTRA1, MMP-3, MMP-13, syndecan-1 and -4 were measured in the supernatants of hMSCs at selected time points by ELISA. The HTRA1 ELISA was performed as previously described [19]. The MMP-3, MMP-13, Syndecan-1 and -4 specific ELISAs were performed using Duo-Set ELISA Development Systems according to the manufacturer's instructions (R & D Systems, Abingdon, UK).

FACS Analysis

Subconfluent adherent hMSCs were detached using Accutase (Life Technologies) and resuspended in ice cold FACS buffer (PBS/BSA 0.1%) in round bottom 96-well plates to 2 $x10^6$/ml. Cells were incubated on ice for 1 h with equimolar concentrations of his-labeled recombinant HTRA1 either alone, or in combination with heparin, heparanase, chondroitinase (all from Sigma-Aldrich), collagenase (Roche), or peptide competitors of integrin binding CS1 and GRGDSP (from ANAWA Trading SA, Zurich, Switzerland). Cells were then washed in cold FACS buffer and incubated with a FITC conjugated rabbit anti-6xHis tag antibody (Lucerna-Chem, Luzern, Switzerland) on ice for 1 h. Bound HTRA1 was detected by FACS analysis using a FACS-Canto II (BD Biosciences) and quantified using FlowJo 10 software.

Protein Electrophoresis and Immunoblotting

Whole cell extracts from untreated or HTRA1 treated hMSCs were harvested using CelLytic M (Sigma Aldrich) supplemented with protease and phosphatase inhibitor cocktails (Sigma Aldrich) and 1mM PMSF at 2 weeks post adipogenic induction. Protein concentrations were determined by Bradford-based protein assay (Bio-Rad). Protein samples were boiled for 5 min in loading buffer (50 mM Tris-HCl, pH 6.8, 2% (v/v) SDS, 10% (v/v) glycerol, 100 mM DTT, 0.002% (w/v) bromophenol blue) and equal amounts of protein analyzed by SDS-PAGE using or 10% or 4-15% precast Tris-HCl gels (BioRad) under reducing conditions and electroblotted onto PVDF membranes using the Trans-Blot Turbo blotting system (BioRad). Membranes were then blocked with 5% (w/v) skim milk in TBST (50mM Tris-HCl, pH 7.6, 150mM NaCl, 0.05% (v/v) Tween 20) for 1 h at room temperature and then incubated with specific antibodies overnight at 4°C at recommended dilutions in blocking buffer. Antibody binding was detected using HRP-conjugated secondary antibodies followed by incubation in Super Signal West Pico or West Dura Chemiluminescent Substrate (Life Technologies) and exposed to x-ray film.

Preparation and identification of Fnfs

For the identification of native Fnfs in supernatants, hMSCs undergoing adipogenic differentiation for 14 days were treated for a further 24 h with HTRA1 (45 nM) in fresh growth medium without FCS. Where indicated, HTRA1 was also added in combination with CL-82198 (20 nM). Supernatants were then harvested and immediately placed on ice. Cellular debris was removed by centrifugation and the remaining supernatant concentrated 40-fold by centrifugation at 3000G for 30 min in Amicon Ultra columns (10 kDa size exclusion, Millipore). Concentrated protein solutions were then supplemented with protease inhibitor cocktail (1:100, Sigma Aldrich) and 1mM PMSF and separated on a 4-12% SDS-PAGE pre-cast gel (BioRad). Methods for preparing purified Fnfs generated from HTRA1-digested plasma fibronectin were carried out as previously described [18]. Fnfs were visualized by

immunoblotting using a specific antibody against the N-terminus of fibronectin and detected using an HRP-conjugated secondary antibody as described above.

VLDL uptake

Lipid uptake by adipogenic hMSCs was performed using DiI-labeled human VLDL (KALEN Biomedical) at late time points of adipogenesis between days 18-24. Cultured hMSCs were rinsed once with PBS and then incubated for 3 h under standard culture conditions in assay buffer supplemented with DiI-labeled VLDL (4 μg/ml) and carrier protein ApoE2 (3 μg/ml, PeproTech, UK). Following incubation, cells were washed 3 times with PBS and fixed with PBS-buffered formaldehyde (4%) for 30 min. Nuclei were stained with DAPI (1:10'000) in PBS for 10 min and mounted in Mowiol containing 2.5% (w/v) DABCO. Images were captured using a Leica DMI6000B automated inverted research microscope system (Leica Microsystems). Relative linear median fluorescence intensity (RMFI) was quantified using NIH ImageJ software as described previously with some modifications [20]. Briefly, images were processed using identical image acquisition settings and exposure times. TIFF files were converted to 8-bit gray-scale mode and inverted onto a white background. Negative and positive staining controls were used to set measurable limits and threshold levels, and were then applied to all samples. Finally, RMFI was calculated as mean grey value per area and normalized to the number of cells per image as assessed by automated counting of DAPI-positive nuclei staining using the ImageJ software.

Immunofluorescence staining

hMSCs undergoing adipogenesis were fixed with PBS-buffered formaldehyde (4%) for 30 min, washed 3 times with PBS and then blocked for 30 min in 2% BSA and 5% normal goat serum in PBS. Cells were incubated overnight at 4^{o}C with a monoclonal mouse anti-type IV collagen or monoclonal mouse anti-Laminin γ-1 antibodies, or an isotype control at an

equivalent concentration. Antibody binding was detected using a Cy3-conjugated secondary antibody and nuclei stained with DAPI. Cells were mounted with Mowiol containing 2.5% DABCO and images captured using a Leica DMI6000B automated inverted research microscope system (Leica Microsystems). Positive staining was quantified as described above. Relative mean fluorescence intensity (RMIF) was quantified using NIH ImageJ software as described above.

Immunohistochemical staining

Dewaxed paraffin sections of adipose tissue were rehydrated and blocked in normal serum (Jackson ImmunoResearch) for 30 min. Sections were then incubated for 1 h at 37^{o}C with monoclonal mouse anti-HTRA1 (2.5 μg/ml) or rabbit anti-MMP-13 (5 μg/ml), and staining specificity controlled for using either mouse or rabbit IgG at equivalent concentrations. Sections were then washed in PBS and incubated with biotinylated goat anti-mouse IgG (1:200) or swine anti-rabbit IgG (1:400) for 1 h at 37^{o}C followed by washing and a further incubation for 30 min with Vectastain. Sections were then developed using 3,3' diaminobenzidine tetrahydrochloride (DAB), counterstained with Harris' Hematoxylin and mounted in Mowiol.

Human Patients

Visceral tissue was obtained during bariatric surgery from morbidly obese, non-diabetic patients (Supporting Information Table S2). All adipose tissue donors gave written informed consent before the study, which had been approved by the Ethics Committee of the Medical Faculty, University of Leipzig. Insulin sensitivity was defined by the glucose infusion rate (GIR) during the steady state of an euglycemic hyperinsulinemic clamp as previously described [21].

Statistical Analysis

Two-tailed unpaired Student's *t*-test for comparison of two groups or one-way analysis of variance (ANOVA) with Tukey's post hoc test for multiple group comparisons were used. In all cases, a *P*-value of < 0.05 was considered statistically significant, and all data were expressed as mean ± standard deviation (S.D).

RESULTS

HTRA1 suppresses lipid uptake and droplet formation in adipogenic hMSCs

Preliminary studies utilizing an HTRA1-specific ELISA were conducted to investigate HTRA1 production by hMSCs. In undifferentiated control hMSCs, secreted HTRA1 levels increased over culture time, reaching a maximum level of 9.6 ± 0.5 ng/ml after 10 days of culture (Fig. 1A). HTRA1 production also increased over time in hMSC cultures undergoing adipogenesis, although levels were significantly reduced as compared to the undifferentiated control hMSCs throughout the 2 week culture period. Interestingly, these observations are in direct contrast to the stimulatory effects of osteogenic induction on HTRA1 production by hMSCs [12]. These data therefore suggest that reductions in HTRA1 might be a necessary requirement for hMSC adipogenesis. To address this model, we effectively eliminated endogenous HTRA1 from the culture system through the use of small interfering RNA (siRNA) (Supporting Information Fig. S1A) and assessed the ability of hMSCs to undergo adipogenesis using Oil Red O staining. Indeed, hMSCs deficient in HTRA1 produced significantly more lipid droplets than those treated with control siRNA, thereby indicating that loss of HTRA1 had an overall positive influence on adipocyte formation (Fig. 1B). Furthermore, stimulation of HTRA1 deficient hMSCs with functional HTRA1 could reduce Oil Red O staining to a level comparable to that observed in control cultures (Fig. 1C). These

studies also provided the first evidence that the addition of exogenous HTRA1 acts to suppress lipid droplet formation in developing adipocytes. Note that an HTRA1 variant (ΔMac) was used that is lacking its N-terminal Mac domain, for which no function is known to date [22] (Supporting Information Fig. S1B). Furthermore, N-terminal truncation does not affect HTRA1 function (Supporting Information Fig. S1C) and therefore this variant is termed HTRA1 throughout.

As HTRA1 contains both a C-terminal PDZ domain and a functional serine protease domain, we asked whether either domain was required for determining HTRA1's inhibitory influence over hMSC adipogenesis. Therefore, we generated several different proteolytically active and inactive recombinant HTRA1 proteins (Supporting Information Fig. S1B and S1C) and assessed their ability to influence oil droplet formation in adipogenic hMSCs. Indeed, inactivation of HTRA1's proteolytic activity through replacement of residue Ser328 with Ala (HTRA1 S328A), significantly impaired it's ability to inhibit lipid droplet formation in adipogenic hMSCs (Fig. 1D). Similarly, deletion of the PDZ domain in proteolytically active HTRA1 (HTRA1ΔPDZ) also abolished its inhibitory action on hMSC adipogenesis. These findings led us to conclude that HTRA1's inhibitory influence over hMSC adipogenesis most likely involves its binding to one or more substrates essentially involved in the development of lipid laden adipocytes, possibly via its PDZ domain. When considering potential substrate candidates, we became aware of a previous study in which HTRA1 was shown to cleave Xenopus syndecan-4 [23]. Syndecans are cell surface HSPGs and represent a predominant feature of developing adipocytes, in which they play a central role in mediating lipid uptake [6]. In order to investigate this, we assessed the potential for various recombinant HTRA1 proteins to bind to hMSCs using fluorescence activated cell sorting (FACS) analysis. We could demonstrate that intact, but proteolytically inactive HTRA1 S328A was able to bind to hMSCs in a PDZ-dependent manner (Fig. 2A). The involvement of the PDZ domain in

cellular binding of HTRA1 was further substantiated through the use of a recombinant HTRA1 containing the PDZ domain only (HTRA1Δprotease) (Fig. 2B). We next investigated whether removal of heparan sulfate (HS) using heparanase or competition with heparin could reduce cellular binding of HTRA1, and thereby provide support for an HTRA1-HSPG interaction. Indeed, the ability of HTRA1 S328A (Fig. 2C) and HTRA1Δprotease (Fig. 2D) to bind to hMSCs was markedly reduced by pre-treatment with heparanase. Similarly, pre-treatment of cells with heparin could also dramatically reduce cellular binding of both HTRA1 S328A (Fig. 2E) and HTRA1Δprotease (Fig. 2F). By contrast, replacement of heparanase with collagenase (Supporting Information Fig. S2A) or chondroitinase (Supporting Information Fig. S2B), and heparin with integrin-binding competitor peptides CS-1 (Supporting Information Fig. S2C) or GRGDSP (Supporting Information Fig. S2D), had little or no effect on the cellular binding capacity of HTRA1's PDZ domain.

Although these data demonstrated HTRA1's ability to bind to HSPG, they fell short of confirming whether HSPG was a proteolytic substrate of HTRA1. To address this question, we used an ELISA to determine levels of cleaved soluble syndecan-4 in supernatants from hMSCs at various stages of adipogenesis. Low levels of soluble syndecan-4 were observed at day 10 (4.2 pg/ml ± 1.5) and day 21 (16.4 pg/ml ± 1.9) in normally differentiating adipogenic hMSCs (Fig. 2G). By contrast, significantly higher soluble syndecan-4 levels were measured in hMSCs treated with HTRA1 at day 10 (44.8 pg/ml ± 3.5; $P < 0.001$) and day 21 (84 pg/ml ± 7.7; $P < 0.001$). Again, these effects were determined as being dependent on HTRA1 possessing an intact PDZ domain, and were therefore in accordance with the findings from our binding studies. Studies were also undertaken to examine soluble syndecan-1. However, protein levels remained below detection limits in all treatment groups (data not shown). Based on syndecan-4 being a prominent regulator of lipid uptake by differentiating adipocytes [6], we surmised that HTRA1-induced syndecan-4 shedding would result in significant

impairment of this process. Studies to investigate activate lipid uptake in adipogenic hMSCs were therefore undertaken using fluorescently labeled VLDL (VLDL-DiI). The uptake and accrual of high levels of VLDL-DiI in normally differentiating cells was apparent after a 3 h incubation period (Fig. 2H). However, VLDL-DiI levels were significantly diminished in hMSCs that had previously been treated with HTRA1. Furthermore, the inability of HTRA1 to exert a significant influence over VLDL-DiI uptake in the absence of either a protease or PDZ domain, convincingly supports a causal relationship between HTRA1's ability to impair lipid accrual in adipogenic hMSCs and its propensity to interact with and cleave HSPG from the cell surface.

Induction of MMPs by HTRA1

Although HTRA1 has the potential to directly interact with and cleave HSPG, it is also possible that the observed effects are indirect e.g. via other proteases. Our previous studies utilizing synovial fibroblasts and intervertebral disc cells have identified MMPs to be strongly upregulated in response to HTRA1 stimulation, being mediated through the production of reactive fibronectin species [18, 19]. In addition to their ability to induce HSPG cleavage and shedding [24], MMPs are also potent regulators of adipogenesis, having both inhibitory and stimulatory effects [7, 8, 25]. This led us to investigate the possibility that MMP production by adipogenic hMSCs might be regulated by HTRA1. Indeed, treatment of adipogenic hMSCs with HTRA1 resulted in significant increases in the mRNA expression levels of *MMP1* (Fig. 3A), *MMP3* (Fig. 3B), *MMP9* (Fig. 3C), and *MMP13* (Fig. 3D). Additionally, ELISA measurements of supernatants revealed significant increases in MMP-3 (Fig. 3E) and MMP-13 (Fig. 3F) protein levels. Small, but significant increases in *MMP9* and *MMP13* mRNA expression, along with MMP-3 and -13 protein production, were also observed in hMSCs treated with HTRA1 S328A, although to a significantly lesser degree as compared to

HTRA1. In order to ascertain whether the observed increases in MMP production were associated with increases in MMP activity, we undertook immunofluorescence studies to assess the levels of major MMP substrates present within cultures of differentiating hMSCs. The basal lamina of adipogenic hMSCs stained positive for both laminin (Fig. 4A) and type IV collagen (Fig. 4B) at day 22 after adipogenic induction. Based on HTRA1's ability to upregulate MMP production, we additionally examined whether it could also induce alterations in type IV collagen and laminin in adipogenic hMSC cultures. Indeed, treatment with HTRA1 resulted in a significant reduction in the levels of both laminin (Fig. 4A) and type IV collagen (Fig. 4B). Furthermore, the effects of HTRA1 were significantly more pronounced than either HTRA1 S328A or HTRA1ΔPDZ, and were therefore in accordance with HTRA1's ability to regulate MMP production. Although it's possible that changes in the basal lamina were additionally due to factors other than MMPs, we are confident that they were not the direct result of HTRA1's actions based on the findings from previous studies in which HTRA1 failed to degrade either type IV collagen or laminin [13]. Indeed, we were only able to observe partial degradation of type IV collagen by HTRA1 at concentrations starting from 0.86 μM, 20-fold higher than that used in our culture system (Supporting Information Fig. S3).

As HTRA1-generated fibronectin fragments (Fnfs) are known to be potent stimulators of MMP production [18, 19], we additionally investigated whether such fragments could be identified within adipogenic hMSC cultures. Protein analysis of supernatants from hMSCs identified several Fnf species, including the well described 29 kDa Fnf (Supporting Information Fig. S4A) [18, 19]. Interestingly, levels of this particular fragment decreased upon adipogenic induction of control cultures, but was still present in the supernatants of adipogenic hMSCs treated with HTRA1. Furthermore, proteolytic inactive HTRA1 S328A failed to generate such Fnfs, thereby confirming it to be dependent on HTRA1's protease

activity. In order to investigate whether the 29 kDa Fnf had the same capabilities as HTRA1 in terms of stimulating MMP production by adipogenic hMSCs, we purified HTRA1-generated Fnfs (Supporting Information Fig. S4B) and assessed their ability to influence MMP expression in comparison to HTRA1. Although Fnfs at a final concentration of up to 40 μg/ml were able to stimulate *MMP1* (Supporting Information Fig. S4C), *MMP3* (Supporting Information Fig. S4D) and *MMP13* (Supporting Information Fig. S4E) expression in adipogenic hMSCs, levels were significantly reduced as compared to HTRA1 treatment. Moreover, the addition of Fnfs failed to have any significant impact on the level of oil droplet formation in adipogenic hMSCs (Supporting Information Fig. S4F). It therefore seems unlikely than Fnfs are the major instigators of MMP production and adipogenic suppression in hMSCs in response to HTRA1 addition.

The inhibitory effects of HTRA1 are dependent on MMP and MAP kinase activation

Having established MMP overproduction as being a predominant feature in HTRA1 stimulated hMSCs, we sought to determine whether they had any significant relevance in defining HTRA1's influence over hMSC adipogenesis. In order to investigate this, we utilized MMP inhibitors NNGH and CL-82198 at concentrations deemed to be selective for the inhibition of MMP-3 and MMP-13 respectively [26, 27], as well as siRNA targeted knockdown of *MMP13* gene expression. Initial immunofluorescence studies confirmed that type IV collagen levels were significantly elevated in HTRA1-treated cultures when exposed to NNGH (Fig. 5A) or CL-82198 (Fig. 5B) as compared to hMSCs treated with HTRA1 alone. Similarly, both NNGH (Fig. 5C) and CL-82198 (Fig. 5D) significantly reduced HTRA1's ability to generate cleaved soluble syndecan-4 in adipogenic hMSC cultures in a concentration dependent manner. Based on our assumption that alterations in basal lamina composition are the predominant driving force behind HTRA1's anti-adipogenic effects, we anticipated that the inhibition of either MMP-3 or MMP-13 in HTRA1-treated cultures should

preserve adipocyte development as compared to hMSCs treated with HTRA1 alone. In order to investigate this, we quantified Oil Red O staining in adipogenic HTRA1-treated hMSCs cultured in the presence or absence of either MMP inhibitor. Our findings confirmed that inhibition of either MMP-3 (Fig. 5E) or MMP-13 (Fig. 5F) could significantly restore oil droplet formation in HTRA1-treated adipogenic hMSCs to levels similar to those observed in adipogenic hMSCs cultured in the absence of HTRA1. These observations were additionally supported when *MMP13* gene expression was silenced in adipogenic hMSCs. *MMP13* expression could be effectively suppressed in both HTRA1-treated and untreated adipogenic hMSCs (Supporting Information Fig. S5A), and was shown to significantly impair HTRA1's ability to inhibit oil droplet formation as determined by quantitative analysis of Oil Red O staining (Supporting Information Fig. S5B). Furthermore, when analyzing the supernatants of HTRA1-treated adipogenic hMSCs in which the MMP-13 inhibitor had been added, we observed a clear decrease in the amount of the HTRA1-generated 29 kDa Fnf (Supporting Information Fig. S5C and S5D). This finding therefore lends additional support to the theory that in this culture system at least, HTRA1's capacity to induce MMP expression and impair adipogenesis in hMSCs is primarily mediated through mechanisms unrelated to Fnfs, and that at least in the case of MMP-13, Fnf generation in cultured hMSCs is actually dependent on the actions of MMPs rather than HTRA1 proteolysis directly.

Having therefore confirmed the central importance of MMPs in mediating HTRA1's effects on adipogenic hMSCs, we explored potential mechanisms through which HTRA1 could induce MMP production. Our previous findings from studies utilizing primary cultures of IVD cells have hinted towards the MAP kinase signaling pathway as playing a significant role in mediating the upregulation of MMPs in response to HTRA1 [18]. Moreover, alterations in MAP kinase activation are known to have a profound influence on both adipogenesis and adipose tissue function [28]. Based on this, we investigated the role of MAP kinase signaling in adipogenesis and evaluated its involvement in mediating HTRA1's effects

on adipogenic hMSCs. Initial Western blot analysis of adipogenic hMSCs revealed minimal levels of activated ERK, JNK and p38 at day 14 post induction (Fig. 6A). By contrast, phosphorylated levels of both ERK, JNK and p38 were noticeably increased in HTRA1-treated hMSCs in both a protease and PDZ dependent manner. In order to further investigate the involvement of MAP kinase signaling in MMP expression in adipogenic hMSCs, we utilized MAP kinase inhibitors PD98059, SP600125 and SB239063 at concentrations deemed to be selective for the inhibition of ERK, JNK and p38 respectively [29, 30]. Treatment of adipogenic hMSCs with MAP kinase inhibitors significantly reduced the basal expression of *MMP3* at day 17 post induction (Fig. 6B). The enhanced *MMP3* expression observed in HTRA1-treated adipogenic hMSCs was similarly reduced following the addition of MAP kinase inhibitors. By contrast, no significant changes in *MMP13* expression levels were observed in adipogenic hMSCs treated with PD98059, and HTRA1's ability to upregulate *MMP13* expression was not significantly affected (Fig. 6C). However, inhibition of JNK or p38 activity had a profound effect on both basal *MMP13* levels, as well as on HTRA1 - mediated upregulation of *MMP13* expression. In order to assess the possible consequence of such changes in MMP expression on hMSC adipogenesis, we investigated the effects of MAP kinase inhibitors on oil droplet formation in hMSCs undergoing adipogenesis. Neither PD98059 or SP600125 had any significant effect on oil droplet formation in normally differentiating hMSCs (Fig. 6D). By contrast, basal levels of oil droplet formation were dramatically reduced in control cultures treated with SB239063. The addition of either PD98059 or SP600125 to HTRA1-treated adipogenic hMSCs resulted in significant increases in Oil Red O staining, and in the case of SP600125, fully restored oil droplet formation to levels comparable to those observed in cultures undergoing adipogenesis in the absence of HTRA1. However, the addition of SB239063 failed to alleviate the inhibitory effects of HTRA1, and instead led to a significant reduction in Oil Red O staining as compared to hMSCs treated with HTRA1 alone.

Detection of HTRA1 in visceral fat from obese patients

In order to validate the relevance of these findings with regards to HTRA1's potential role in mediating adipogenesis *in vivo*, immunohistochemical analysis was performed on visceral adipose tissue taken from obese patients (Supporting Information Table S2) that were diagnosed as being either insulin sensitive (IS) or insulin resistant (IR) as described previously in detail [21]. Analysis of visceral fat from either IS (Supporting Information Fig. S6A) or IR (Supporting Information Fig. S6B) obese patients revealed HTRA1 primarily localized to large blood vessels found throughout the tissue. HTRA1 was also identified in areas of macrophage infiltrate detected as crown-like structures in both IS (Fig. 7A) and IR (Fig. 7B) obese patients, although the level of staining at these sites was markedly enhanced in IR adipose tissue in accordance with increases in infiltrate. Furthermore, immune cell infiltrate expressing HTRA1 also showed positive staining for MMP-13 (Fig. 7C), thus re-enforcing the concept of there being a close working relationship between these two proteases. In all cases, specificity of immunostaining was confirmed using relevant IgG isotype controls (Fig. 7D-F).

DISCUSSION

In the current study, we have identified HTRA1 as a potent inducer of MAP kinase-dependent MMP production in adipogenic hMSC cultures, the result of which leads to modulation of ECM components and impaired lipid droplet accrual in differentiating cells. Furthermore, the observation that HTRA1 is present at high levels in visceral adipose tissue at sites of increased inflammatory cell infiltration is suggestive of its active involvement in mediating adipose tissue function under pathological conditions.

HTRA1 is now well established as a key regulator of ECM turnover, having been linked to various diseases in which the breakdown of normal ECM is a prominent

pathological feature [13-16, 18]. Findings from our own studies into the role of HTRA1 in joint and IVD degeneration have led to the suggestion that HTRA1 may instigate tissue breakdown through an upregulation in MMP production, most likely via the action of reactive Fnf species [18, 19]. In the context of adipose tissue, MMP-mediated ECM remodelling and reorganization forms an integral part of normal tissue homeostasis, being required for adipocyte differentiation and function [7, 8]. Abnormal fluctuations in MMP levels within adipose tissue may therefore represent an important factor in determining adipocyte health and subsequent risk of disease. This is supported by our current findings where increased production of MMPs by adipogenic hMSCs in response to HTRA1 led to a loss of vital ECM components and impaired lipid accrual. Such observations are therefore suggestive of HTRA1 as having a detrimental role in hMSC adipogenesis and that these effects are related to the actions of MMPs. However, in contrast to previous studies [18, 19], these effects do not appear to be reliant on the generation of Fnfs. In fact, we provide evidence to suggest that MMP-13 itself may be responsible for the appearance of such fragments in response to HTRA1. As such, alternative mechanisms must exist through which HTRA1 can instigate changes in hMSC MMP production and adipogenic potential.

Some insights into HTRA1's mode of action could be gleaned through manipulation of its trypsin-like serine protease domain and its protein-binding PDZ domain. Certainly, both domains were of critical importance in determining HTRA1's inhibitory influence over hMSC adipogenesis, being required for both efficient MMP production as well as for the observed decreases in type IV collagen, laminin and lipid uptake in adipogenic hMSCs. Of particular interest was the novel finding that HTRA1 could interact with surface bound HS in a PDZ-dependent manner. It is possible therefore that sequestration of HTRA1 to the cell surface by HS would allow for close interactions to form between HTRA1 and HS-containing glycoproteins. This concept is supported by the finding that increased levels of soluble

syndecan-4 could be detected in adipogenic hMSC cultures treated with structurally intact HTRA1. Syndecans are important regulators of lipid uptake in differentiating adipocytes [6, 31] and their liberation from the cell surface by proteolytic cleavage may constitute a potential cause of diminished lipid accrual in adipogenic hMSCs following HTRA1 treatment. In addition to syndecans, numerous other glycoproteins also exist within the adipocyte ECM, including the previously identified HTRA1 substrate nidogen [13]. Nidogen represents an important stabilizing component of the adipocyte basal lamina through its binding to type IV collagen and laminin [32]. The possible targeting of nidogen by HTRA1 may therefore represent an alternative means through which the ECM could be affected by HTRA1, and adipogenesis inhibited. Interestingly, nidogen cleavage by HTRA1 also has the potential to generate various fragment species *in vitro*, although their influence on MMP production and adipogenesis remains to be determined.

HTRA1's ability to both induce MMP production and inhibit hMSC adipogenesis was additionally identified as being dependent on the activities of JNK, and to a lesser extent, ERK. Interpretation of the data concerning the involvement of p38 were hampered by the fact that inhibition of p38 activation resulted in a significant reduction in oil droplet formation in adipogenic hMSCs regardless of treatment conditions. The regulation of MMP expression by MAP kinases is well documented [reviewed in 33], and several studies have now identified ERK and JNK as potent negative regulators of MSC adipogenesis [34-36]. Despite having demonstrated the importance of MAP kinase activation in mediating the effects of HTRA1 during hMSC adipogenesis, we were unable to ascertain the cause for such signaling events. Certainly, both the proteolytic activity and PDZ domain of HTRA1 were essential requirements for efficient MAP kinase activation, thereby inferring substrate binding and degradation were necessary. One potential means by which HTRA1 could invoke MAP kinase activation in the context of the current study, is through syndecan-4 shedding, whereby

disruption of the syndecan-4 to MAP kinase signaling cascade may have contributed to increases in JNK activity levels [37].

The relevance of such findings is made apparent by the fact that both MAP kinases and MMPs are centrally linked to the pathophysiology of adipose tissue, being implicated in the development of insulin resistance in obese mice and humans [28, 38, 39]. Adipocyte dysfunction clearly plays a major role in determining the severity of insulin resistance among obese patients and as such, factors which negatively influence adipocyte development are likely to contribute to and potentially exacerbate the disease state [9]. In this regard, inappropriately high levels of HTRA1 in the adipose tissue of obese individuals may be viewed as being potentially harmful and an indication of deficiencies in adipocyte development and function. The significance of this is made evident by the fact that HTRA1 could be detected in the visceral fat from obese patients, and that levels were greatest at sites where cellular infiltration was most apparent, encompassing adipocytes in typical crown like structures. This, together with the fact that MMP-13 was also localized to these same regions, lends further support to the concept of HTRA1 representing a novel mediator of adipogenesis and fat turnover. Furthermore, based on the fact that macrophages are considered to represent the predominant cell type within crown-like structures [11, 40], and are potent inducers of MMPs in adipocytes [41], these findings may also offer a potential source from which HTRA1 may be introduced into adipose tissue.

CONCLUSIONS

In conclusion, our findings identify HTRA1 as a negative regulator of hMSC adipogenesis, which may be of relevance when considering its potential role in the underlying processes governing adipose tissue and adipocyte dysregulation. Moreover, the differential effects imparted by HTRA1 on hMSC adipogenic and osteogenic differentiation may also offer novel

insights into its potential impact on other pathological conditions such as age-related bone loss, where its capacity to inhibit adipogenesis and stimulate osteogenesis would be deemed beneficial to the preservation of bone quality [42].

ACKNOWLEDGEMENTS

SG and GB were supported by SNSF grants 31003A_134935 and 31003A_156313. AM and NAT were supported by the Uniscientia Foundation. The authors would like to express their gratitude to Daniela Kern for preparing the patient tissue sections.

DISCLOSURE OF POTENTIAL CONFLICTS OF INTEREST

The authors indicate no potential conflicts of interest.

REFERENCES

1. Rosen ED, MacDougald OA.Adipocyte differentiation from the inside out. Nat Rev Mol Cell Biol 2006;7:885–896.
2. Christodoulides C, Lagathu C, Sethi JK et al. Adipogenesis and WNT signaling. Trends Endocrinol Metab 2009;20:16-24.
3. Mariman EC, Wang P. Adipocyte extracellular matrix composition, dynamics and role in obesity. Cell Mol Life Sci 2010;67:1277-92.
4. Sillat T, Saat R, Pöllänen R et al. Basement membrane collagen type IV expression by human mesenchymal stem cells during adipogenic differentiation. J Cell Mol Med 2012;16:1485-95.
5. Noro A, Sillat T, Virtanen I et al. Laminin production and basement membrane deposition by mesenchymal stem cells upon adipogenic differentiation. J Histochem Cytochem 2013;61:719-30.

6. Wilsie LC, Chanchani S, Navaratna D et al. Cell surface heparan sulfate proteoglycans contribute to intracellular lipid accumulation in adipocytes. Lipids Health Dis 2005;4:2.
7. Maquoi E, Munaut C, Colige A et al. Modulation of adipose tissue expression of murine matrix metalloproteinases and their tissue inhibitors with obesity. Diabetes 2002;51:1093-101.
8. Chavey C, Mari B, Monthouel MN et al. Matrix metalloproteinases are differentially expressed in adipose tissue during obesity and modulate adipocyte differentiation. J Biol Chem 2003;278:11888-96.
9. Guilherme A, Virbasius JV, Puri V et al. Adipocyte dysfunctions linking obesity to insulin resistance and type 2 diabetes. Nat Rev Mol Cell Biol 2008;9:367-77.
10. Lee MJ, Wu Y, Fried SK. Adipose tissue remodeling in pathophysiology of obesity. Curr Opin Clin Nutr Metab Care 2010;13:371-6.
11. Cinti S, Mitchell G, Barbatelli G et al. Adipocyte death defines macrophage localization and function in adipose tissue of obese mice and humans. J Lipid Res 2005;46:2347-55.
12. Tiaden AN, Breiden M, Mirsaidi A et al. Human serine protease HTRA1 positively regulates osteogenesis of human bone marrow-derived mesenchymal stem cells and mineralization of differentiating bone-forming cells through the modulation of extracellular matrix protein. Stem Cells 2013;30:2271-2282.
13. Vierkotten S, Muether PS, Fauser S. Overexpression of HTRA1 leads to ultrastructural changes in the elastic layer of Bruch's membrane via cleavage of extracellular matrix components. PLoS One 2011;6:e22959.
14. Tiaden AN, Richards PJ. The emerging roles of HTRA1 in musculoskeletal disease. Am J Pathol 2013;182:1482–1488.
15. Beaufort N, Scharrer E, Kremmer E et al. Cerebral small vessel disease-related protease HtrA1 processes latent TGF-β binding protein 1 and facilitates TGF-β signaling. Proc Natl Acad Sci U S A 2014;111:16496-501.

16. Grau S, Baldi A, Bussani R et al. Implications of the serine protease HtrA1 in amyloid precursor protein processing. Proc Natl Acad Sci U S A 2005;102:6021-6.
17. Dominici M, Le Blanc K, Mueller I, et al. Minimal criteria for defining multipotent mesenchymal stromal cells. The International Society for Cellular Therapy position statement. Cytotherapy 2006;8:315-7.
18. Tiaden AN, Klawitter M, Lux V et al. Detrimental role for human high temperature requirement serine protease A1 (HTRA1) in the pathogenesis of intervertebral disc (IVD) degeneration. J Biol Chem 2012;287:21335-45.
19. Grau S, Richards PJ, Kerr B et al. The role of human HtrA1 in arthritic disease. J Biol Chem 2006;281:6124-9.
20. Burgess A, Vigneron S, Brioudes E et al. A Loss of human Greatwall results in G2 arrest and multiple mitotic defects due to deregulation of the cyclin B-Cdc2/PP2A balance. Proc Natl Acad Sci U S A 2010;107:12564-9.
21. Klöting N, Fasshauer M, Dietrich A et al. Insulin-sensitive obesity. Am J Physiol Endocrinol Metab 2010;299:E506-15.
22. Eigenbrot C, Ultsch M, Lipari MT et al. Structural and functional analysis of HtrA1 and its subdomains. Structure 2012;20:1040-50.
23. Hou S, Maccarana M, Min TH et al.The secreted serine protease xHtrA1 stimulates long-range FGF signaling in the early Xenopus embryo. Dev Cell 2007;13:226-41.
24. Manon-Jensen T, Multhaupt HA, Couchman JR. Mapping of matrix metalloproteinase cleavage sites on syndecan-1 and syndecan-4 ectodomains. FEBS J 2013;280:2320-31.
25. Shih CL, Ajuwon KM. Inhibition of MMP-13 prevents diet-induced obesity in mice and suppresses adipogenesis in 3T3-L1 preadipocytes. Mol Biol Rep 2015;42:1225-32.
26. Kim EM, Shin EJ, Choi JH et al. Matrix metalloproteinase-3 is increased and participates in neuronal apoptotic signaling downstream of caspase-12 during endoplasmic reticulum stress. J Biol Chem 2010;285:16444-52.

27. Rath T, Stöckle J, Roderfeld M et al. Matrix metalloproteinase-13 is regulated by toll-like receptor-9 in colorectal cancer cells and mediates cellular migration. Oncol Lett 2011:2:483-488.
28. Bost F, Aouadi M, Caron L et al. The role of MAPKs in adipocyte differentiation and obesity. Biochimie 2005;87:51-6.
29. Ando C, Takahashi N, Hirai S et al. Luteolin, a food-derived flavonoid, suppresses adipocyte-dependent activation of macrophages by inhibiting JNK activation. FEBS Lett 2009:583:3649-54.
30. Vallet S, Mukherjee S, Vaghela N et al. Activin A promotes multiple myeloma-induced osteolysis and is a promising target for myeloma bone disease. Proc Natl Acad Sci U S A 2010;107:5124-9.
31. Kasza I, Suh Y, Wollny D et al. Syndecan-1 is required to maintain intradermal fat and prevent cold stress. PLoS Genet 2014;10:e1004514.
32. Yurchenco PD. Basement membranes: cell scaffoldings and signaling platforms. Cold Spring Harb Perspect Biol 2011;3:a004911.
33. Reuben PM, Cheung HS. Regulation of matrix metalloproteinase (MMP) gene expression by protein kinases. Front Biosci 2006;11:1199-215.
34. Tominaga S, Yamaguchi T, Takahashi S et al. Negative regulation of adipogenesis from human mesenchymal stem cells by Jun N-terminal kinase. Biochem Biophys Res Commun 2005;326:499-504.
35. Chiu LH, Yeh TS, Huang HM et al. Diverse effects of type II collagen on osteogenic and adipogenic differentiation of mesenchymal stem cells. J Cell Physiol 2012;227:2412-20.
36. Fu L, Tang T, Miao Y et al. Stimulation of osteogenic differentiation and inhibition of adipogenic differentiation in bone marrow stromal cells by alendronate via ERK and JNK activation. Bone 2008;43:40-7.

37. Saoncella S, Calautti E, Neveu W et al. Syndecan-4 regulates ATF-2 transcriptional activity in a Rac1-dependent manner. J Biol Chem 2004;279:47172-6.
38. Unoki H, Bujo H, Shibasaki M et al. Increased matrix metalloproteinase-3 mRNA expression in visceral fat in mice implanted with cultured preadipocytes. Biochem Biophys Res Commun 2006;350:392-8.
39. Meissburger B, Ukropec J, Roeder E et al. Adipogenesis and insulin sensitivity in obesity are regulated by retinoid-related orphan receptor gamma. EMBO Mol Med 2011;3:637-51.
40. Murano I, Barbatelli G, Parisani V et al. Dead adipocytes, detected as crown-like structures, are prevalent in visceral fat depots of genetically obese mice. J Lipid Res 2008;49:1562-8.
41. Gao D, Bing C. Macrophage-induced expression and release of matrix metalloproteinase 1 and 3 by human preadipocytes is mediated by IL-1β via activation of MAPK signaling. J Cell Physiol 2011;226:2869-80.
42. Rosen CJ, Bouxsein ML. Mechanisms of disease: is osteoporosis the obesity of bone? Nat Clin Pract Rheumatol 2006;2:35-43.

Figure 1. HTRA1 suppresses lipid uptake and droplet formation in adipogenic hMSCs. **(A):** ELISA measurement of HTRA1 secretion in supernatants from undifferentiated (control) and differentiated (adipogenic) hMSCs. *p < 0.001 as compared to adipogenic hMSCs. **(B):** Quantification of Oil Red O staining in adipogenic hMSCs treated with scrambled siRNA (scr) or siRNAs specific for HTRA1 (H1 and H2) at day 14 post induction. Scale bar = 1 mm. **(C):** Quantification of Oil Red O staining in hMSCs treated with siRNA specific for HTRA1 (H2), HTRA1 (45 nM) or a combination of both H2 and HTRA1. *p < 0.01 as compared to siRNA (scr) treated cells. **(D):** Quantification of Oil Red O staining in hMSCs at day 14 post adipogenic induction cultured in the absence (untreated) or presence of recombinant HTRA1 (45 nM). *p < 0.001 as compared to untreated. Scale bar = 1 mm. Data are representative of at least 2 separate experiments performed in triplicate. Abbreviations: hMSC, human mesenchymal stem cells; ELISA, enzyme-linked immunosorbent assay; HTRA1, high temperature requirement protease A1; siRNA, small interfering RNA.

Figure 2. HTRA1 interacts with surface bound HSPG. **(A-F):** hMSC binding of PDZ domain-containing HTRA1 S328A (0.45 μM) **(A)** or HTRA1Δprotease (0.45 μM) **(B)** as compared to HTRA1ΔPDZ (0.45 μM) was determined by FACS analysis using a FITC labeled anti-histidine antibody. The involvement of HSPG in the binding of HTRA1 S328A **(C, E)** and HTRA1Δprotease **(D, F)** was assessed using either heparanase (10 U/ml) **(C, D)** or heparin (10 μg/ml) **(E, F)**. **(G):** ELISA measurement of soluble syndecan-4 levels in the supernatants of untreated or HTRA1 (45 nM) treated hMSCs at day 10 and 21 post adipogenic induction. **(H):** Quantification of VLDL-DiI (red) uptake in untreated or HTRA1 (45 nM) treated hMSCs at day 24 post adipogenic induction. Nuclei were stained with DAPI (blue). Scale bar = 75 μm. *p < 0.001 as compared to untreated hMSCs. Data are representative of at least 2 separate experiments performed in triplicate. Abbreviations:

hMSC, human mesenchymal stem cells; HTRA1, high temperature requirement protease A1; HSPG, heparan sulfate proteoglycan; ELISA, enzyme-linked immunosorbent assay; FITC, Fluorescein isothiocyanate; VLDL-DiI, very low density lipoprotein- dialkylcarbocyanine.

Figure 3. HTRA1 upregulates MMP production by adipogenic hMSCs. RT-qPCR analysis of *MMP1* **(A)**, *MMP3* **(B)**, *MMP9* **(C)** and *MMP13* **(D)** gene expression in untreated or HTRA1 (45 nM) treated hMSCs at day 21 post adipogenic induction. Data was normalized to *GUSB* and expressed as fold change as compared to untreated hMSCs (value = 1) using the comparative C_T method. **(E, F):** ELISA measurements of MMP-3 **(E)** and -13 **(F)** protein in supernatants from untreated or HTRA1 (45 nM) treated hMSCs at day 21 post adipogenic induction. *$p < 0.05$, **$p < 0.001$ as compared to untreated hMSCs. Data are representative of at least 2 separate experiments performed in triplicate. Abbreviations: hMSC, human mesenchymal stem cells; HTRA1, high temperature requirement protease A1; MMP, matrix metalloproteinase; RT-qPCR, reverse transcription-quantitative polymerase chain reaction; ELISA, enzyme-linked immunosorbent assay.

Figure 4. (A, B): Immunofluorescence staining of laminin (red) **(A)** and type IV collagen (red) **(B)** in untreated or HTRA1 (45 nM) treated hMSCs at day 24 post adipogenic induction. Nuclei were stained with DAPI (blue). Scale bar = 100 μm. *$p < 0.01$ as compared to untreated hMSCs. Data is representative of at least 2 separate experiments performed in triplicate. Abbreviations: hMSC, human mesenchymal stem cells; HTRA1, high temperature requirement protease A1.

Figure 5. HTRA1's effects are mediated through MMP activities. **(A, B):** Quantification of type IV collagen staining in untreated or HTRA1 (45 nM) treated hMSCs at day 22 post adipogenic induction following pre-treatment with either vehicle control or with 10 μM of

NNGH **(A)** or 20 μM of CL-82198 **(B)**. **(C, D):** ELISA measurement of soluble syndecan-4 levels in the supernatants of untreated or HTRA1 (45 nM) treated hMSCs at day 17 post adipogenic induction following pre-treatment with either vehicle control or with varying concentrations of NNGH **(C)** or CL-82198 **(D)**. **(E, F)**: Quantification of Oil Red O staining in untreated or HTRA1 (45 nM) treated hMSCs at day 18 post adipogenic induction following pre-treatment with either vehicle control or with varying concentrations of NNGH **(E)** or CL-82198 **(F)**. *$p < 0.05$, **$p < 0.01$, ***$p < 0.001$ as compared to controls from untreated or HTRA1-treated groups respectively. Data are representative of at least 2 separate experiments performed in triplicate. Abbreviations: hMSC, human mesenchymal stem cells; HTRA1, high temperature requirement protease A1; MMP, matrix metalloproteinase; ELISA, enzyme-linked immunosorbent assay.

Figure 6. HTRA1's effects are mediated through MAP kinase activities. **(A):** Effect of recombinant HTRA1 on MAP kinase activation in adipogenic hMSCs at day 14 as determined by Western blot analysis of protein lysates using specific antibodies against JNK, p38 and ERK. An anti-tubulin monoclonal was used to confirm equal loading. **(B-D):** Quantitative analysis of *MMP3* expression **(B)**, *MMP13* expression **(C)** and Oil Red O staining **(D)** in untreated or HTRA1 (45 nM) treated hMSCs at day 17 post adipogenic induction following pre-treatment with either vehicle control or with PD98059 (10 μM), SP600125 (20 μM) or SB239063 (10 μM). RT-qPCR data was normalized to *GUSB* and expressed as fold change relative to untreated, control hMSCs (value = 1) using the comparative C_T method. *$p < 0.05$, **$p < 0.01$, ***$p < 0.001$ as compared to controls from untreated or HTRA1-treated groups respectively. Data are representative of at least 2 separate experiments performed in triplicate. Abbreviations: hMSC, human mesenchymal stem cells; HTRA1, high temperature requirement protease A1; MMP, matrix metalloproteinase; MAP,

mitogen-activated protein; RT-qPCR, reverse transcription-quantitative polymerase chain reaction; GUSB, Glucuronidase, beta.

Figure 7. Identification of HTRA1 in adipose tissue. Paraffin wax sections of human visceral (omental) adipose tissue from insulin sensitive (IS) or insulin resistant (IR) obese patients were incubated with an anti-HTRA1 antibody **(A, B)**, anti-MMP-13 antibody **(C)** or relevant IgG controls **(D-F)**, and positive staining identified using an appropriate HRP-labeled polyclonal antibody with subsequent development using 3,3'-diaminobenzidine (brown). *Arrow heads,* HTRA1 or MMP-13 present in immune cell infiltrate in crown-like structures. Scale bar = 200 μm. Abbreviations: HTRA1, high temperature requirement protease A1; MMP, matrix metalloproteinase; HRP, horseradish peroxidase.

Supplementary Fig. 1. (A): ELISA measurement of HTRA1 in supernatants from adipogenic hMSCs (Adipo) treated with scrambled siRNA (scr) or siRNA specific for HTRA1 (H1 and H2). *$p < 0.001$ as compared to siRNA (scr) treated cells. **(B):** Schematic of recombinant human HTRA1 proteins; active HTRA1 (ΔMac), inactive HTRA1 (HTRA1 S328A), active HTRA1 without PDZ domain (HTRA1ΔPDZ), inactive HTRA1 without PDZ domain (HTRA1 S328AΔPDZ), HTRA1 without protease domain (HTRA1ΔProtease). The purified recombinant histidine-labeled human HTRA1 proteins were also visualized on a Coomassie blue-stained SDS-PAGE gel. *M*, protein marker; *lane 1*, HTRA1; *lane 2*, HTRA1 S328A; *lane 3*, HTRA1ΔPDZ; *lane 4*, HTRA1 S328AΔPDZ; *lane 5*, HTRA1ΔProtease. **(C):** Proteolytic activity of recombinant HTRA1 proteins (45 nM) towards BODIPY-FL-labeled DQ elastin (25 μg/ml) at 37^{o}C as determined using a Multiplate reader. Abbreviations: hMSC, human mesenchymal stem cells; HTRA1, high temperature requirement protease A1; ELISA, enzyme-linked immunosorbent assay; siRNA, small interfering RNA; SDS-PAGE, sodium dodecyl sulfate polyacrylamide gel electrophoresis.

Supplementary Fig. 2. Fluorescence activated cell sorting (FACS) analysis of recombinant HTRA1 binding to non-differentiated hMSCs. HTRA1Δprotease (0.45 μM) was incubated with hMSCs for 1 h at 4^{o}C and cell-bound HTRA1 protein detected using a FITC labeled anti-his antibody. The influence of pre-incubating cells with collagenase (1 mg/ml) **(A)**, chondroitinase (10 U/ml) **(B)**, CS1 (50 μM) (**C**) or GRGDSP (50 μM) **(D)** on the percentage of cell-bound HTRA1Δprotease was calculated using FlowJo 10 software. Data are representative of least two individual experiments performed in duplicate. Abbreviations: hMSC, human mesenchymal stem cells; HTRA1, high temperature requirement protease A1; FACS, fluorescence activated cells sorting.

Supplementary Fig. 3. Capacity for HTRA1 to degrade type IV collagen. Varying concentrations of HTRA1 or HTRA1 S328A were incubated with DQ-type IV collagen (25 μg/ml) at 37^{o}C and the relative fluorescence units (RFU) generated after 24 h determined using a Multiplate reader. Abbreviations: HTRA1, high temperature requirement protease A1.

Supplementary Fig. 4. (A): Western blot analysis of native Fnfs in concentrated supernatants harvested from 14 day old undifferentiated hMSCs (control), untreated adipogenic hMSCs, or adipogenic hMSCs treated with HTRA1 (45 nM) for a further 24 h. Protein was subjected to immunoblotting using antibody Mab 1936 specific for the fibronectin amino-terminal fibrin- and heparin-binding domain. *Arrow head* indicates the HTRA1-cleaved 29 kDa Fnf. **(B):** An equimolar ratio of human plasma-derived Fn and HTRA1 were incubated in TBS, pH 8.5, for 16 h at 37^{o}C and Fnfs purified by affinity chromatography and analysed on a Coomassie Blue stained 4-15% gradient SDS-PAGE gel. Fn and HTRA1 alone were also loaded and served as controls. *Arrow head* indicates the purified 29 kDa Fnf due to HTRA1-mediated cleavage.

(C-E): RT-qPCR analysis of *MMP1* **(C)**, *MMP3* **(D)** and *MMP13* **(E)** in adipogenic hMSCs at day 11 following treatment with HTRA1 (45 nM), purified HTRA1-digested Fn (40 μg/ml) (Fn+HTRA1) or TBS, pH 7.6, eluate from the affinity purification reaction using HTRA1 alone (TBS+HTRA1). Data was normalized to *GUSB* and expressed as fold change as compared to untreated hMSCs (value = 1) using the comparative C_T method. **(F):** Oil Red O staining of adipogenic hMSCs at day 14 following treatment with HTRA1 (45 nM), Fn+HTRA1 or TBS+HTRA1. *$p < 0.05$, **$p < 0.01$, ***$p < 0.001$ as compared to untreated cells. Scale bar = 2 mm. Data are representative of least two individual experiments performed in triplicate. Abbreviations: hMSC, human mesenchymal stem cells; HTRA1, high temperature requirement protease A1; Fnf, fibronectin fragments; SDS-PAGE, sodium dodecyl sulfate polyacrylamide gel electrophoresis; RT-qPCR, reverse transcription-quantitative polymerase chain reaction; GUSB, Glucuronidase, beta; MMP, matrix metalloproteinase; TBS, Tris-buffered saline.

Supplementary Fig. 5. (A): RT-qPCR analysis of *MMP13* gene expression in untreated or HTRA1 (45 nM) treated adipogenic hMSCs at day 3 following pre-treatment with scrambled control siRNA (scr) or siRNAs specific for *MMP13* (M1 and M2). Data was normalized to *GUSB* and expressed as fold change relative to untreated siRNA (scr) hMSCs (value = 1) using the comparative C_T method. **(B):** Quantification of Oil Red O staining in adipogenic hMSCs at day 22 following treatment with either a scrambled control siRNA (scr), siRNAs specific for *MMP13* (M1 and M2), or a combination of both siRNAs and HTRA1 (45 nM). *$p < 0.05$, **$p < 0.01$, ***$p < 0.001$ as compared to siRNA (scr) controls from untreated or HTRA1 -treated groups respectively. Data are representative of least two individual experiments performed in triplicate. **(C):** Western blot analysis of native Fnfs in concentrated supernatants harvested from 14-day-old adipogenic hMSCs treated for 24 h without (untreated) or with CL-82198 (20 μM), HTRA1 (45 nM) or HTRA1 and CL-82198. Protein

was subjected to immunoblotting using Mab 1936 specific for the Fn amino-terminal fibrin- and heparin-binding domain. *Arrow heads* indicate the 29 kDa Fnf due to HTRA1 treatment. **(D):** Coomassie stained gel of total protein from supernatant to control for equal loading. Data are representative of least two individual experiments. Abbreviations: hMSC, human mesenchymal stem cells; HTRA1, high temperature requirement protease A1; RT-qPCR, reverse transcription-quantitative polymerase chain reaction; GUSB, Glucuronidase, beta; MMP, matrix metalloproteinase; siRNA, small interfering RNA; Fnf, fibronectin fragments.

Supplementary Fig. 6. Identification of HTRA1 in adipose tissue. Paraffin wax sections of human visceral (omental) adipose tissue from IS or IR obese patients were incubated with an anti-HTRA1 antibody **(A, B)** or relevant IgG controls **(C, D)**, and positive staining identified using an appropriate HRP-labeled polyclonal antibody with subsequent development using 3,3'-diaminobenzidine (*brown*). *Asterisks*, HTRA1-positive blood vessels; Scale bar = 200 μm. Insulin sensitivity was defined as glucose infusion rate (GIR) during the steady state of an euglycemic-hyperinsulinemic clamp > 70 μmol/kg/min, insulin resistance as GIR < 50 μmol/kg/min. Abbreviations: HTRA1, high temperature requirement protease A1; IS, insulin sensitive; IR, insulin resistant; HRP, horseradish peroxidase.

Fig. 1.

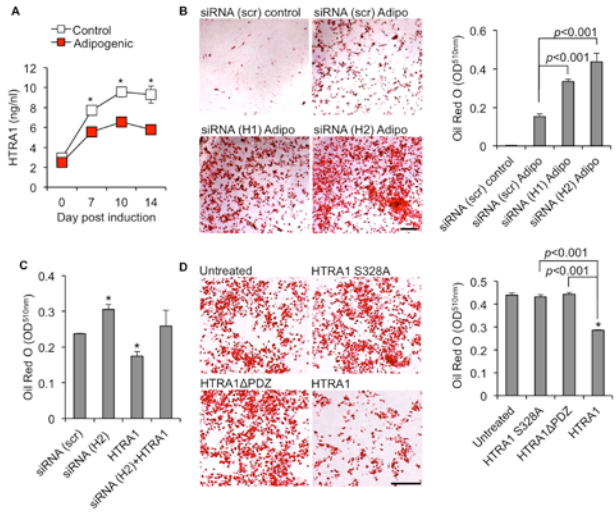

Fig. 2.

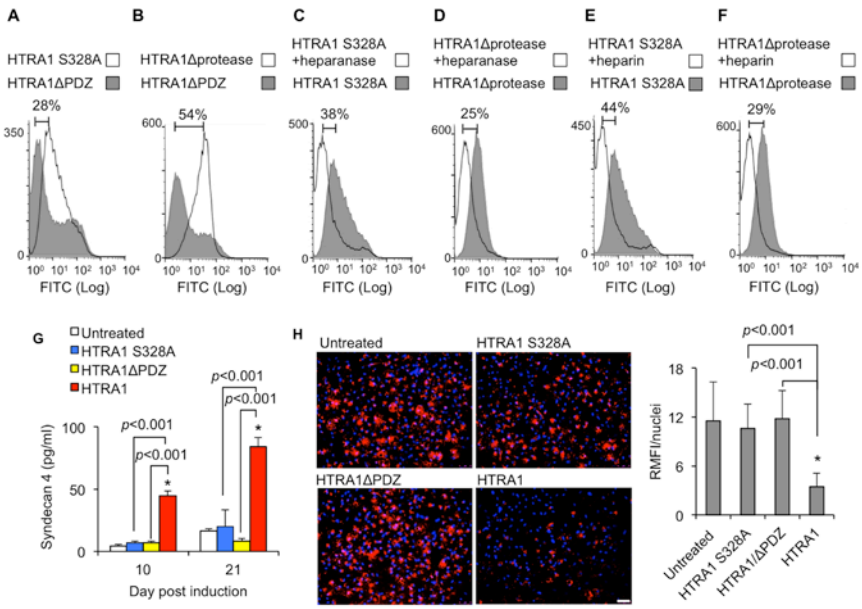

Fig. 3.

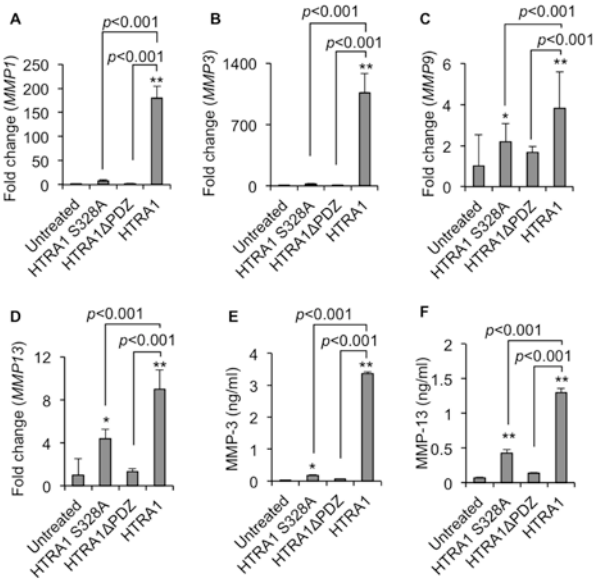

Fig. 4.

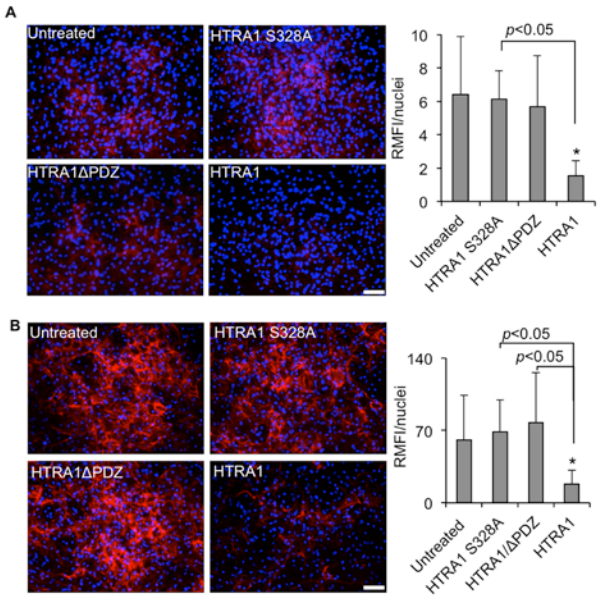

Fig. 5.

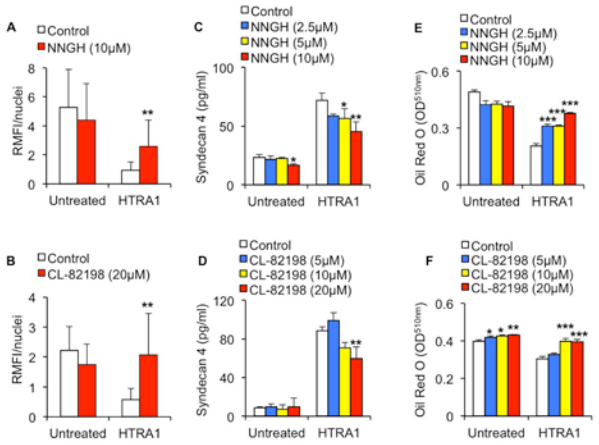

Fig. 6.

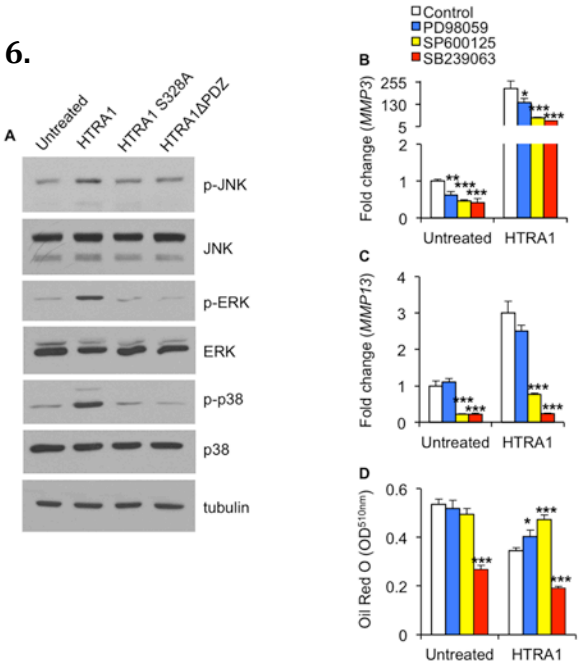

Fig. 7.

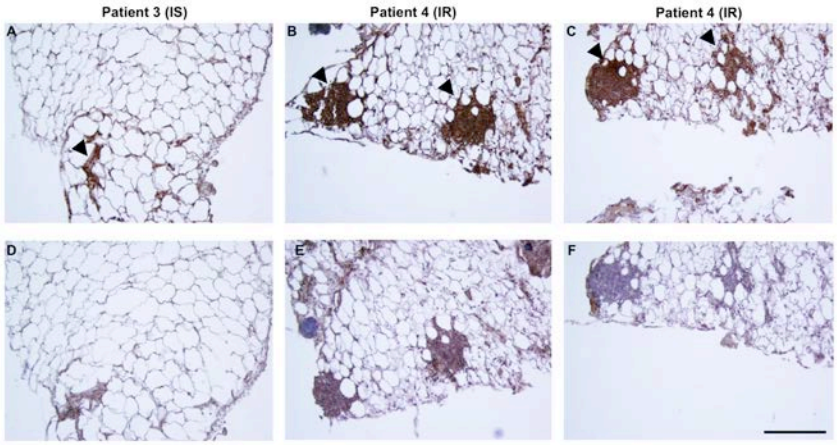

Fig. S1.

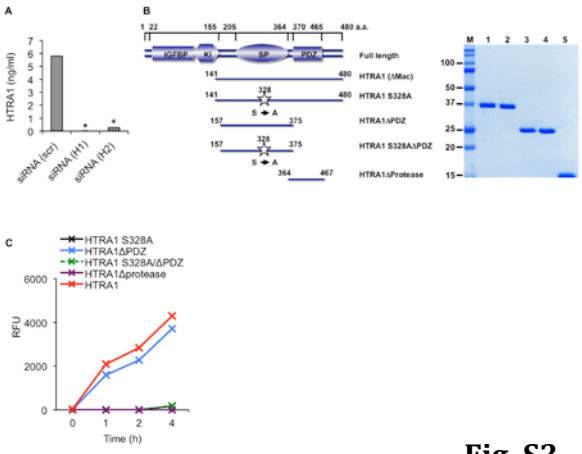

Fig. S2.

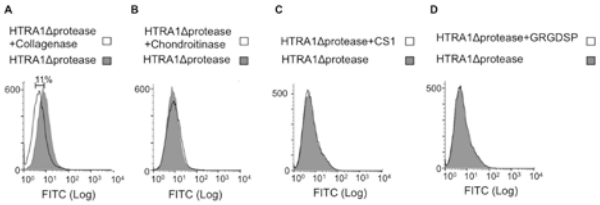

Fig. S3.

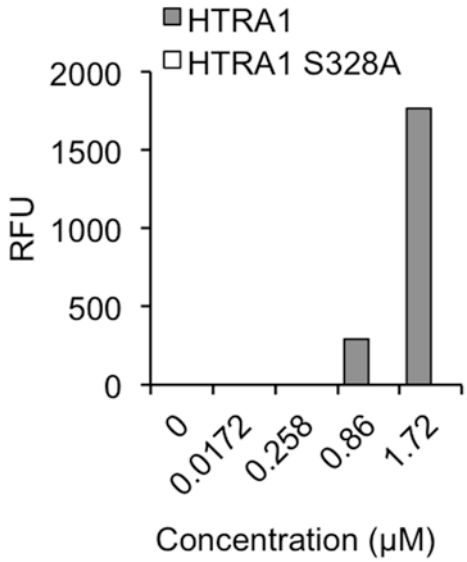

Fig. S4.

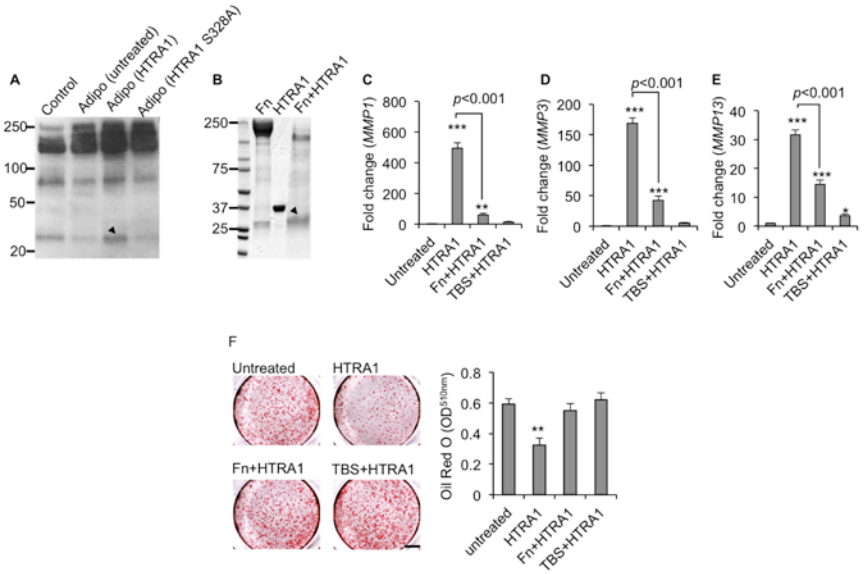

Fig. S5.

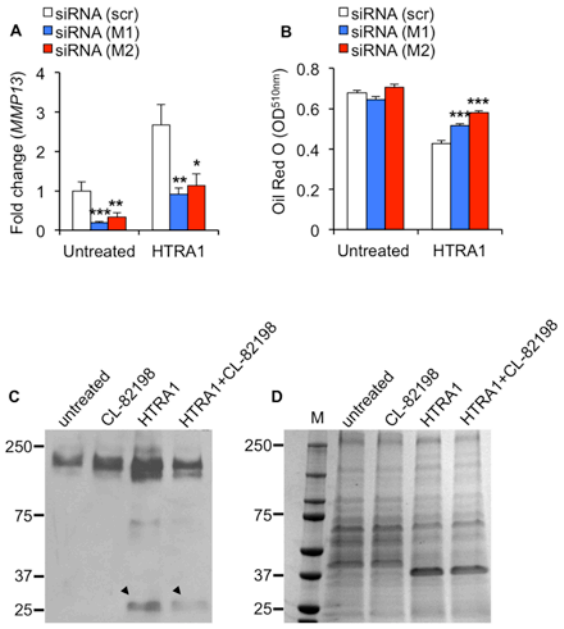
A
siRNA (scr)
siRNA (M1)
siRNA (M2)
Fold change (MMP13)
Untreated
HTRA1
B
Oil Red O (OD510nm)
C
untreated
CL-82198
HTRA1
HTRA1+CL-82198
250
75
37
25
D
M

Fig. S6.

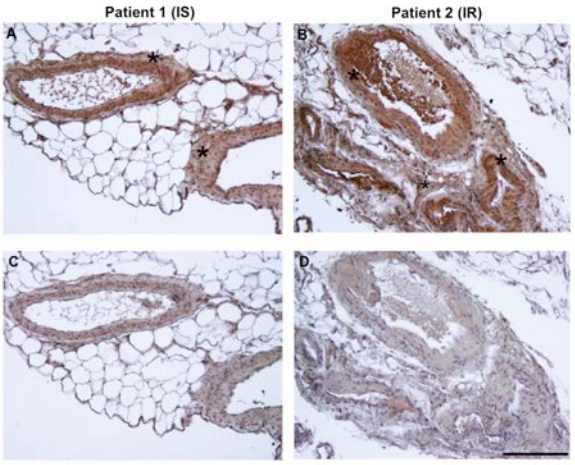
Patient 1 (IS)
Patient 2 (IR)
A
B
C
D

2.1.3. Use of biomimetic microtissue spheroids and specific growth factor supplementation to improve tenocyte differentiation and adaptation to a collagen-based scaffold *in vitro.*

Authors: Theiss F, Mirsaidi A, Mhanna R, Kümmerle J, **Glanz S**, Bahrenberg G, Tiaden AN, Richards PJ.

Journal: In Press, Accepted Manuscript in *Biomaterials (August 2015) IF:8.557*

Contribution: Assistance in generation of qPCR data and immunoblotting.

Biomaterials 69 (2015) 99–109

Contents lists available at ScienceDirect

Biomaterials

journal homepage: www.elsevier.com/locate/biomaterials

Use of biomimetic microtissue spheroids and specific growth factor supplementation to improve tenocyte differentiation and adaptation to a collagen-based scaffold *in vitro*

Felix Theiss [a, b, c], Ali Mirsaidi [a, d], Rami Mhanna [e, f], Jan Kümmerle [a, b, c], Stephan Glanz [a, d], Gregor Bahrenberg [a, d], André N. Tiaden [a], Peter J. Richards [a, d, *]

[a] Center for Applied Biotechnology and Molecular Medicine (CABMM), University of Zurich, Winterthurerstrasse 190, 8057 Zurich, Switzerland
[b] Equine Department, Vetsuisse-Faculty, University of Zurich, Winterthurerstrasse 260, 8057 Zurich, Switzerland
[c] Graduate School for Cellular and Biomedical Sciences, University of Bern, 3012 Bern, Switzerland
[d] Zurich Center for Integrative Human Physiology (ZIHP), University of Zurich, 8057 Zurich, Switzerland
[e] Cartilage Engineering and Regeneration, ETH Zurich, 8093 Zurich, Switzerland
[f] American University of Beirut, Faculty of Engineering and Architecture, Riad El Solh, 1107 2020 Beirut, Lebanon

ARTICLE INFO

Article history:
Received 16 April 2015
Received in revised form
6 August 2015
Accepted 7 August 2015
Available online 10 August 2015

Keywords:
Tendon
Growth factors
TGF (transforming growth factor)
Microsphere
In vitro test

ABSTRACT

Tenocytes represent a valuable source of cells for the purposes of tendon tissue engineering and regenerative medicine and as such, should possess a high degree of tenogenic differentiation prior to their use *in vivo* in order to achieve maximal efficacy. In the current report, we identify an efficient means by which to maintain differentiated tenocytes *in vitro* by employing the hanging drop technique in combination with defined growth media supplements. Equine tenocytes retained a more differentiated state when cultured as scaffold-free microtissue spheroids in low serum-containing medium supplemented with L-ascorbic acid 2-phosphate, insulin and transforming growth factor (TGF)-β1. This was made evident by significant increases in the expression levels of pro-tenogenic markers collagen type I (*COL1A2*), collagen type III (*COL3A1*), scleraxis (*SCX*) and tenomodulin (*TNMD*), as well as by enhanced levels of collagen type I and tenomodulin protein. Furthermore, tenocytes cultured under these conditions demonstrated a typical spindle-like morphology and when embedded in collagen gels, became highly aligned with respect to the orientation of the collagen structure following their migration out from the microtissue spheroids. Our findings therefore provide evidence to support the use of a biomimetic microtissue approach to culturing tenocytes and that in combination with the defined growth media described, can improve their differentiation status and functional repopulation of collagen matrix.

1. Introduction

Tendon lesions in equine and human athletes are mainly the result of overstrain injury rather than percutaneous trauma, where the athletic discipline generally predisposes specific tendons to injuries. In the racehorse and event horses, injuries occur most frequently in the suspensory ligament and the superficial digital flexor tendon (SDFT) [1]. In humans, tendinopathy is most commonly diagnosed in the Achilles, patellar, rotator cuff and medial/lateral elbow tendons and accounts for 30–50% of all sports-related injuries [2]. As such, there is an ever growing need for more effective therapies with which to combat tendon injuries and the ensuing degeneration associated with such trauma. The use of cell-based tissue engineering approaches are fast emerging as alternative therapeutic strategies for the management of tendon injury both in humans and animals [3]. Indeed, a growing number of reports now exist in which multipotent stromal cells (MSCs) isolated from various sources have been successfully implemented in the treatment of both experimentally induced tendon defects [4–7], as well as in clinical cases of tendinopathy [8,9]. The use of MSCs primarily relies on their ability to differentiate into fully functional tendon cells, termed tenocytes. As such, investigators have also sought to utilize mature tenocytes directly as an

* Corresponding author. Bone and Stem Cell Research Group, Competence Center for Applied Biotechnology and Molecular Medicine, Room 13-L-86, University of Zürich, Winterthurerstrasse 190, CH-8057 Zürich, Switzerland.
E-mail address: peter.richards@cabmm.uzh.ch (P.J. Richards).

http://dx.doi.org/10.1016/j.biomaterials.2015.08.013
0142-9612/

additional means by which to regenerate tendon tissue as evidenced by the initiation of human clinical trials [source: ClinicalTrials.gov, Trial Number: NCT01343836 and source: ClinicalTrialsRegister.eu, Trial Number: 2010-021869-73] with the aim to evaluate the efficacy of autologous tenocytes in treating chronic tendinopathy.

Tenocytes are fibroblast-like cells derived from embryonic mesenchyme and form a three dimensional network of cell processes throughout the extracellular matrix linked by gap junctions [10]. These cell processes not only connect tenocytes with each other, but also enclose the collagen bundles. It is thought that this close relationship between tenocytes and collagen fibril bundles enables cellular load sensing and coordination of response to load. Characterization of tenocyte gene expression has revealed several markers considered to be essential for their development into fully functional tendon-forming cells, of which tenomodulin (TNMD) may be considered one of the most important and well studied [11–13]. TNMD is a type II transmembrane protein that is mainly expressed in dense connective tissues, and is generally regarded as being a late marker of tendon development [14]. *TNMD* gene expression is positively regulated during tendon development by scleraxis (SCX) [14,15], a transcription factor considered essential for efficient tendon differentiation [16]. However, both TNMD and SCX have also been detected in tissues from sources other than tendon, thereby bringing into question their reliability as specific markers of tendon [17]. Despite this fact, both TNMD and SCX still serve as a means by which to gauge the differentiation status of tenocytes isolated from tendon tissue.

It has previously been reported that *in vitro*, mature tenocytes have a reduced tendency to express *TNMD*, as well as collagen type 1 (*COL1*), and lose their elongated morphology when cultured for extended periods [18–20]. This so called dedifferentiation of cultured tenocytes is not only considered to be potentially detrimental to their efficiency as a cell-based therapy in tendon repair, but also to their usefulness as an *in vitro* cell system for developing and testing alternative treatments. In this regard, various studies have been undertaken with an aim to improving the genotype and phenotype of isolated tenocytes. Of critical importance in this regard, is the growth medium and its components used to maintain tenocytes in culture. Several investigators have identified transforming growth factor (TGF)-β and insulin-like growth factor (IGF)-1 as being potent inducers of tenogenic differentiation in both MSCs and tenocytes [21–26], allowing cells to maintain a tenogenic genotype and phenotype *in vitro*. Furthermore, the transfer of cultured tenocytes to high density, three-dimensional (3D) growth environments also appears to stimulate differentiation and prevent cellular dedifferentiation to some degree [21,25–27].

The primary focus of the present study was to determine whether equine tenocytes could generate self-assembled gravity-enforced 3D microtissue spheroids *in vitro*, and if so, could this improve their tenogenic differentiation status over that of tenocytes cultured under standard 2D conditions. Furthermore, various combinations of growth factor supplementation were evaluated in terms of their ability to influence the genotype and/or phenotype of equine tenocytes maintained as 2D or 3D cultures. Equine tenocytes cultured as hanging drops formed microtissue spheroids, and after 2 and 6 days of culture, displayed significantly greater levels of several recognized tendon cell markers as compared to monolayer cultures as determined by RT-qPCR. Moreover, the use of low serum growth media supplemented with TGF-β1 in combination with insulin and ascorbic acid enhanced these effects, and when used to stimulate microtissue-derived tenocytes embedded in collagen scaffolds, induced phenotypic features typical of differentiated tenocytes. Our findings therefore suggest that scaffold-free biomimetic microtissue spheroids, in combination with specific chemical compositions of growth media, may represent an efficient means by which to maintain equine tenocyte differentiation *in vitro*. Such a system may therefore allow for tendon cell and tissue biology to be studied *in vitro* using conditions that more closely simulate the *in vivo* situation and could potentially offer an alternative strategy for stimulating tendon tissue formation *in vivo*.

2. Materials and methods

2.1. Animals

Tenocytes were isolated from the superficial digital flexor tendon of Warm blood horses, aged between 2 and 4 years, which were naturally destroyed for clinical reasons other than orthopaedic disease and where owner consent was obtained.

2.2. Isolation and culture of equine tenocytes

Tenocytes were isolated in accordance with previously established methodologies [17,20]. The mid-metacarpal region of the superficial digital flexor tendon was harvested under sterile conditions. All tendons were free of pathology on clinical and post mortem examination. After removal of the peritendineum, tendon sections of approximately 1 cm in length were cut into 2 mm^3 pieces and subjected to 0.2% collagenase NB4 (Roche Diagnostics, Rotkreuz, Switzerland) and 0.3% dispase II (Roche Diagnostics) digestion overnight in phosphate-buffered saline (Life Technologies, Zug, Switzerland) containing 5% penicillin/streptomycin (Life Technologies) on an orbital shaker at 37 °C. Digested tissue was filtered through a 70 μm cell strainer, centrifuged and cells resuspended in normal growth medium (GM) consisting of Dulbecco's modified eagle medium (DMEM-high glucose) supplemented with 10% fetal bovine serum (FBS) and penicillin/streptomycin (all from Life Technologies). Supernatant was replaced after 1 day and thereafter every 3–4 days with fresh GM and cells were used between passage 4 and 7 unless otherwise stated. The potential contamination of tenocyte cultures with MSCs was assessed through the use of osteogenic and adipogenic induction assays according to previously described methodologies [28]. Briefly, monolayer cultures of equine tenocytes were incubated for 14 days with either osteogenic or adipogenic induction medium and stained with Alizarin red or Oil Red O in order to assess osteogenic and adipogenic differentiation respectively. Additionally, MSCs isolated from equine adipose tissue were also incubated with either osteogenic or adipogenic induction medium and served as a positive multipotent cell control.

2.3. Stimulation of equine tenocytes

For 2D monolayer cultures, equine tenocytes seeded at 6×10^4 cells/cm^2 and stimulated with GM, or DMEM-high glucose supplemented with either; (i) 1% FBS and TGFβ1 (10 ng/ml; Peprotech, London, UK); (ii) 1% FBS, TGFβ-1 (10 ng/ml) and IGF-1 (50 ng/ml; Peprotech, London, UK) (termed tenogenic differentiation medium-I; TDM-I) or with; (iii) 1% FBS, 50 μM L-ascorbic acid 2-phosphate sesquimagnesium salt hydrate, 0.5 μg/ml insulin (all from Sigma–Aldrich, Buchs, Switzerland) and 10 ng/ml human TGF-β1 (termed tenogenic differentiation medium-II; TDM-II). In order to generate tenocyte (TC)-microtissue spheroids, cells were seeded as hanging drops in Terasaki plates (VWR International, Dietikon, Switzerland) in GM, TDM-I or TDM-II according to previously published methodologies [29]. Briefly, equine tenocytes were adjusted to 4×10^4 to 2×10^5 cells/ml in culture medium and a 25 μl cell suspension transferred to individual wells of a Terasaki plate. The plate was then sealed with a lid and inverted in order to

generate hanging drops and enable gravity-enforced TC-microtissue spheroid formation. Cells grown as either monolayers or as microtissue spheroids were then harvested at selected time points for further analysis.

2.4. Tenocyte outgrowth studies

The potential for tenocytes to grow out from microtissue spheroids structures was examined using both 2D and 3D culture systems. TC-microtissues were initially cultured for 6 days in hanging drops using either GM or TDM-II. In the case of 2D outgrowth studies, TC-microtissues were transferred to 48-well plates at 60 spheroids/well for up to 3 days, and cell outgrowth visualized at selected time points by phase contrast microscopy. For analysis of cell outgrowth under 3D culture conditions, TC-microtissues consisting of 5×10^3 cells were mixed with 0.8% bovine collagen (Koken Co., Tokyo, Japan) at 800 microtissues/ml and transferred to silicon molds containing support ridges in order to allow for effective anchoring of the collagen gel [30]. Collagen gels cultured with either GM or TDM-II were harvested at selected time points, fixed in 4% paraformaldehyde for 12 h and then embedded in paraffin wax and sections stained using hematoxylin and eosin.

2.5. Quantitative reverse-transcription polymerase chain reaction (qRT-PCR)

Total RNA was isolated and purified using TRIzol reagent (Life Technologies) according to the manufacturer's instructions. RNA (0.5 μg) was reverse transcribed to cDNA using superscript II (Life Technologies) and random hexanucleotide primers (Promega AG, Dübendorf, Switzerland). Quantification of mRNA expression was performed with TaqMan Gene Expression Assays (Life Technologies) specific for *COL1A2* (Ec03469522_m1), *COL2A1* (Ec03467390_m1), *COL3A1* (Ec03469743_m1), *SCX* (Ec03818452_s1), *TNMD* (Ec03467883_m1) and *SOX9* (Ec03469763_s1) using the StepOnePlus Real-Time PCR System (Life Technologies) and values normalized to *GAPDH* (Ec03210916_gH) and presented as $2^{-\Delta CT}$. Each 10 μl reaction consisted of 1× TaqMan Fast Universal PCR Master Mix (Life Technologies), 1× TaqMan Gene Expression Assay and 10 ng cDNA. All reactions were performed in fast optical 96-well reaction plates (Life Technologies) at 95 °C for 20 s and 40 cycles of 95 °C for 1 s and 60 °C for 20 s.

2.6. Histology

For hematoxylin and eosin staining, dewaxed paraffin sections (5 μm) were rehydrated and stained with Harris' hematoxylin (Sigma–Aldrich, Buchs, Switzerland) for 2 min, rinsed in tap water, and treated with Scott's tap water for a further 2 min. Following washing in tap water, sections were stained with eosin Y (Sigma–Aldrich) for 3 min, rinsed quickly in tap water, dehydrated and mounted in DPX (Sigma–Aldrich). For immunohistochemical analysis, rehydrated tissue sections were blocked with normal 10% rabbit serum for 30 min and then incubated with polyclonal goat anti-collagen type I (1:100; LabForce, Muttenz, Switzerland) for 1 h at 37 °C. Sections were then washed in PBS and incubated with biotinylated rabbit anti-goat IgG (1:200; Reactolab SA, Servion, Switzerland) for 1 h at 37 °C followed by washing and a further incubation for 30 min with Vectastain (Reactolab SA). Sections were then developed using 3,3′ diaminobenzidine tetrahydrochloride (DAB), counterstained with Harris' Hematoxylin and mounted in DPX.

For active caspase-3 staining of TC-microtissue spheroids, paraffin wax tissue sections were initially microwaved in Target Retrieval Solution (Dako, Zug, Switzerland) for a total of 20 min at 750 W and then counterstained with Hemalaun for 2 min. Endogenous peroxidase activity was quenched using 3% H_2O_2 and sections blocked for 10 min using Protein Block Serum-Free (Dako). Slides were then incubated with rabbit anti-human/mouse active caspase-3 (1:50; R&D Systems, Abingdon, UK) overnight at 4 °C. Staining was detected using the Envision System (Dako) and developed using 3-amino-9-ethylcarbazole (AEC) (Life Technologies). Sections were subsequently mounted in Kaiser's gelatin glycerin (Fluka, Buchs, Switzerland) and visualized by light microscopy. Fetal equine TC-microtissue spheroids were included as a positive control for use in the active caspase-3 staining assay based on the consistently high numbers of apoptotic fetal equine tenocytes observed in microtissues after 6 days of culture. Equine fetal tendon cells were obtained from the Laboratory of Cellular Therapy, Department of Musculoskeletal Medicine, University Hospital of Lausanne.

2.7. Immunoblotting

Protein was analyzed by SDS-PAGE using 4–15% precast Tris–HCl gels (Bio-Rad Laboratories AG, Cressier, Switzerland) under reducing conditions, and electroblotted onto PVDF membranes using the Trans-Blot Turbo blotting system (Bio-Rad Laboratories AG). After blocking in 5% fat-free milk, 50 mM Tris–HCl, pH 7.6, 150 mM NaCl, 0.1% Tween 20 (TBS-T) for 1 h at room temperature, membranes were incubated overnight at 4 °C with rabbit anti-tenomodulin (1:1000; Abcam, Cambridge, UK) or mouse anti-tubulin (1:10′000; Sigma–Aldrich). After washing in TBS-T, membranes were incubated for 1 h at room temperature with HRP-conjugated goat anti-rabbit (1:10′000; LabForce) followed by incubation in SuperSignal West Pico Chemiluminescent Substrate (Thermo Fisher Scientific, Reinach, Switzerland) and exposure to X-ray film.

2.8. Statistical analysis

All statistical analyses were carried out using SPSS19.0 (SPSS Inc., Chicago, IL). Parametric analysis of normally distributed data was performed using one-way analysis of variance (ANOVA) with Tukey's post hoc test for multiple group comparisons. In all cases, a p-value of <0.05 was considered statistically significant, and all data were expressed as mean ± standard deviation (S.D.).

3. Results

3.1. Equine tenocytes form microtissue spheroids in hanging drop cultures

Equine tenocyte cultures were deemed to be free of contaminating MSCs based on the lack of any discernable levels of mineralization or oil droplet formation when subjected to culture conditions conducive to either osteogenesis or adipogenesis respectively (Supp. Fig. 1). The equine tenocytes utilized in the current study typically demonstrated a fibroblast-like morphology when cultured in 2D monolayers as determined by phase contrast microscopy (Fig. 1a and b). The randomness of their orientation became apparent as cells approached confluency (Fig. 1b). Following their incorporation into hanging drop cultures, equine tenocytes readily self-assembled into microtissue spheroids after 60 h of incubation (Fig. 1c–h). The capacity for equine tenocytes to form microtissue spheroids was largely dependent on the initial cell seeding density, where 2500 (Fig. 1e and f) to 5000 (Fig. 1g and h) cells was considered to be the optimal cell number for efficient

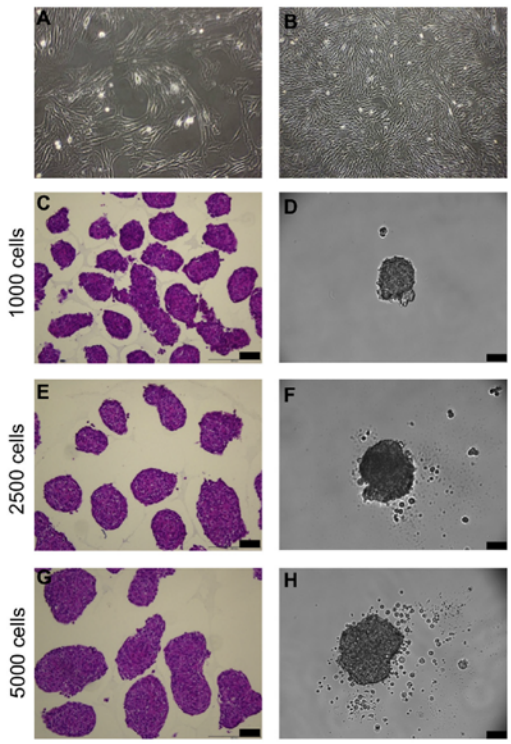

Fig. 1. Representative phase contrast images of sub-confluent (A) (magnification 20×) and confluent (B) (magnification 10×) equine tenocytes grown as 2D monolayer cultures. Representative images of hematoxylin and eosin stained paraffin wax sections of equine TC-microtissue spheroids after 60 h of culture using 1000 (C), 2500 (E) or 5000 (G) equine tenocytes. Phase contrast images of single hanging drops 60 h following seeding with 1000 (D), 2500 (F) or 5000 (H) equine tenocytes. Scale bar = 75 μm.

microtissue formation in the given time frame. During the first 4 days of hanging drop culture, cells were found randomly dispersed throughout the microtissue spheroids and lacked the characteristic fibroblast-like appearance of cells grown in 2D cultures (Fig. 2a and b) (Supp. Fig. 2a). However, by day 6, the majority of cells within the microtissue spheroids displayed an elongated phenotype and had become more ordered in appearance (Fig. 2c) (Supp. Fig. 2b). The capacity for equine tenocytes to tolerate the hanging drop 3D culture environment was made evident by the lack of caspase-3 activity in the microtissue spheroids at any of the time points tested (Fig. 2e–g). By contrast, high levels of caspase-3 activity were found to be a predominant feature of fetal equine TC-microtissues (Fig. 2d and h).

3.2. Variations in culture media composition significantly influence TC-microtissue phenotype and genotype

We next evaluated the effects of different growth media on the capacity of equine tenocytes to form microtissue spheroids over a 6 day period. In comparison to equine tenocytes cultured as hanging drops in the presence of GM alone (Fig. 3a *top panel*), there was a clear delay in the formation of single microtissue spheroids by cells grown in TDM-I (Fig. 3a *middle panel*) or TDM-II (Fig. 3a *lower panel*). In contrast to GM-treated cells, both TDM-I- and TDM-II-treated cells initially formed numerous smaller spheroids during the first 4 days of culture, but had generally coalesced by day 6 to form a single microtissue spheroid (Fig. 3b). Furthermore, in the case of cells cultured in TDM-II, there was also an appreciable accumulation of extracellular material surrounding the spheroid culture at days 4 and 6. In order to ascertain the influence of culture conditions on the tenocyte genotype, we analysed the expression levels of several tenogenic markers including *COL1A2*, *COL3A1*, *SCX*, and *TNMD*, as well as the chondrogenic markers *COL2A1* and *SOX9*. Comparisons were made between equine tenocytes that had been grown under 2D- or 3D-culture conditions with GM, TDM-I or TDM-II.

3.2.1. 2D cultures

Cells cultured for 2 days in either TDM-I or TDM-II showed significant increases in *COL1A2*, *COL3A1*, *SCX* and *SOX9* expression levels as compared to cells in GM alone (Fig. 4a). However, expression levels of *TNMD* remained undetectable in all treatment groups. By day 6, cells cultured in TDM-II showed the greatest increases in gene expression for all makers tested, and represented the only culture condition in which *TNMD* expression could be detected. These results were therefore already suggestive of TDM-II as being a potential alternative to conventional growth medium for the maintenance of equine tenocytes in a more tenogenic-like state.

3.2.2. 3D cultures

Treatment of TC-microtissue spheroids for 2 days with either TDM-I or TDM-II induced significant increases in *SCX* expression as compared to cultures receiving GM alone (Fig. 4b). TDM-II additionally induced significant increases in *COL3A1* and *SOX9* at this early time point. Expression levels of *COL1A2*, *COL3A1*, *SCX* and *TNMD* remained significantly elevated at day 6 in cultures treated with either TDM-I or TDM-II, with the greatest effects being observed in TDM-II-treated microtissues. In the case of *SOX9* expression, although TDM-I and TDM-II treatments resulted in significantly more gene expression in comparison to GM alone, *SOX9* mRNA levels were significantly reduced in all treatment groups at day 6 as compared to day 2 measurements ($p < 0.001$). Furthermore, incubation of TC-microtissues in low serum GM supplemented with TGFβ-1 alone for 6 days had no stimulatory effects on tenogenic marker expression, although *SOX9* expression was significantly upregulated (Supp. Fig. 3). Therefore, in addition to its beneficial effects on tenogenic gene expression in tenocyte monolayers, TDM-II also appeared to have a pro-tenogenic effect when used to culture tenocytes in 3D microtissue spheroids.

3.2.3. 2D vs. 3D cultures

Comparisons in gene expression were also made between tenocytes grown in 2D or 3D culture systems. Microtissues cultured in GM alone for 2 days showed significant increases in *COL1A2*, *COL3A1*, *SCX* and *SOX9* expression levels when compared to tenocytes grown in monolayers (Fig. 5a). Similarly, microtissues stimulated with TDM-I or TDM-II demonstrated significant increases in *COL3A1*, *SCX* and *SOX9* expression as compared to their 2D counter parts. However, incorporation of tenocytes into 3D microtissues did not significantly enhance their capacity to express *COL1A2* in response to TDM-I or TDM-II. By contrast, *TNMD* mRNA was only detected in TC-microtissues, with the greatest levels being observed following TDM-II treatment. At day 6, overall gene expression was either unchanged or significantly reduced in GM-treated TC-microtissues as compared to tenocyte monolayers (Fig. 5b). Conversely, TC-microtissues cultured in TDM-I expressed greater levels of *COL1A2*, *COL3A1* and *TNMD* as compared to

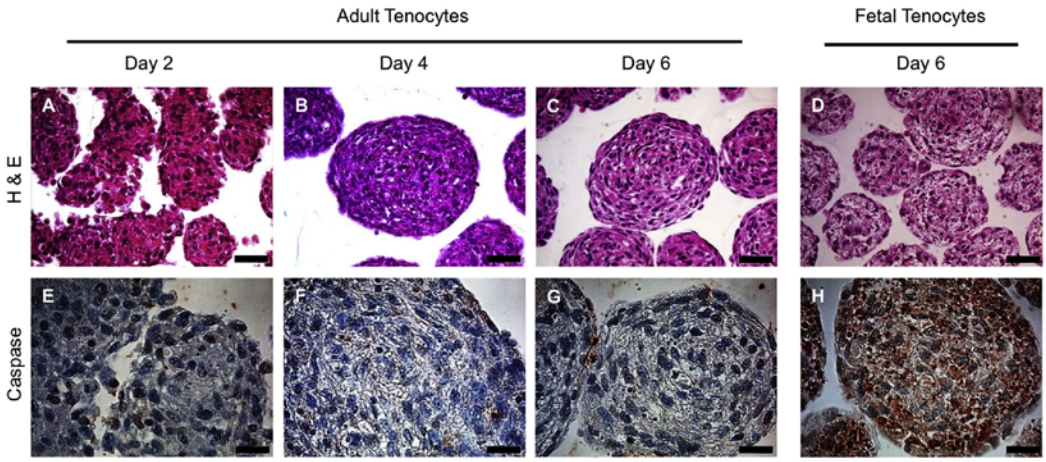

Fig. 2. Representative hematoxylin and eosin stained paraffin wax sections of equine TC-microtissue spheroids cultured for 2 days (A), 4 days (B) and 6 days (C) in GM and equine fetal tenocytes cultured for 6 days (D) in GM. Scale bar = 50 μm. Representative images of active caspase-3 staining (brown) in paraffin wax sections of equine TC-microtissue spheroids cultured for 2 (E), 4 (F) and 6 days (G) in GM. Equine fetal TC-microtissues cultured for 6 days (H) in GM were used as positive controls. Scale bar = 25 μm. (For interpretation of the references to colour in this figure legend, the reader is referred to the web version of this article.)

tenocytes in monolayers. Similarly, TDM-II induced significant increases in *COL3A1*, *SCX* and *TNMD*, whilst significantly reducing the expression of the chondrogenic marker *SOX9*. The chondrogenic marker *COL2A1* was not detected in any of the culture conditions at either the 2 or 6 day time points. Taken together, these results demonstrate the effectiveness of culturing equine tenocytes as hanging drops in the presence of TDM-II for the purpose of maintaining cells in a more tenogenic-like state.

3.3. Tendon-associated protein production by TC-microtissues

Immunohistochemical analysis of TC-microtissue spheroids was undertaken to assess the impact of TDM-II on collagen type I protein expression. A noticeable increase in collagen type I was evident in equine TC-microtissue spheroids cultured in TDM-II for 6 days as compared to those cultured in GM alone (Fig. 6). In both cases, the majority of positive staining was observed at the periphery of the microtissue structures. These observations are in accordance with the differences observed in *COL1A2* gene expression between GM-treated and TDM-II-treated TC-microtissues, and thus supports the use of TDM-II as an efficient means by which to maintain equine tenocytes in 3D cultures. It should be noted that the agarose used to embed the microtissues for the purposes of histological processing also interacted non-specifically with the anti-COL1A antibody at the concentrations tested, thereby generating a diffuse background stain. In an attempt to further confirm the pro-tenogenic effects of the hanging drop culture and TDM-II stimulation, we analysed protein extracts for the presence of tenomodulin using Western blot. Although tenomodulin is predicted to have a molecular weight of 37 kDa, numerous sized bands ranging from 20 to 250 kDa were identified in TC-microtissue protein samples (Supp. Fig. 4). Similarly, numerous different sized protein bands were also detected in protein extracts from native equine tendon, with the most prominent bands being observed at 28, 34, 40, 65 and 250 kDa. Although it remains unclear as to the identity and specificity of these protein products, the 250 kDa protein band was only detected in samples taken from native equine tendon or equine TC-microtissues cultured in TDM-II.

3.4. Equine tenocyte outgrowth from microtissue spheroids

In order to assess the proliferative status of tenocytes cultured as hanging drops in GM or TDM-II, 6-day-old TC-microtissues were transferred to tissue culture plates and visualized by phase contrast microscopy over the course of 3 days (Fig. 7). During the first 24 h of culture, cells were observed to migrate out from the microtissues onto the plastic surface of the tissue culture plate (Fig. 7a and b). Furthermore, cells previously cultured as TC-microtissues in the presence of TDM-II (Fig. 7b) appeared to have a more spindle shaped, tenocyte-like appearance as compared to those cultured in GM alone (Fig. 7a). By day 3, the number of cells populating the tissue culture surface had noticeably increased in both GM- and TDM-II-treated TC-microtissue cultures (Fig. 7c and d). Cells emanating from the TDM-II-treated TC-microtissues continued to demonstrate morphology reminiscent of tenocytes (Fig. 7d) in comparison to the rounded cell appearance of the GM-treated TC-microtissues (Fig. 7c). The ability of tenocytes to migrate out from the microtissue spheroids was further examined using collagen gels as a means by which to simulate a more physiologically relevant 3D environment. Macroscopic observations of TC-microtissue seeded collagen gels revealed noticeable amounts of matrix contraction in gels containing the TDM-II-treated microtissues (Supp. Fig. 5). Gel contraction was already evident after 2 days of TC-microtissue seeding and continued to increase over the next 3 days. By contrast, no such contraction was seen in gels seeded with GM-treated microtissues at any of the time points tested. Similarly to the 2D culture system, migration of tenocytes out from the microtissues was observed for both GM- and TDM-II-treated cells within the first 24 h (Supp. Fig. 6) and continued to increase over the next 4 days in association with a gradual reduction in microtissue structure (Fig. 8). However, in contrast to collagen gels containing GM-treated microtissues, gels seeded with TDM-II-treated microtissues contained numerous, well-orientated cells aligned in the direction of the contracted collagen matrix (Fig. 8b, d and f). Moreover, by day 5 after the initial TC-microtissue seeding, collagen gels containing TDM-II-treated microtissues started to take on a

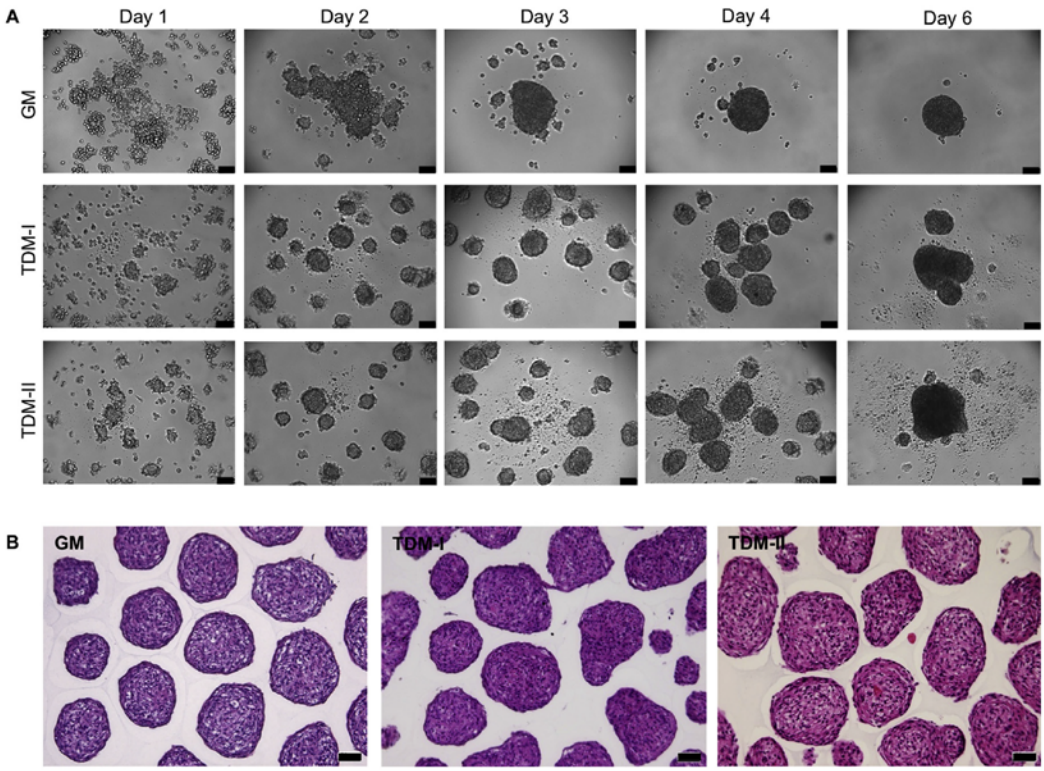

Fig. 3. (A) Representative phase contrast images of microtissue spheroid formation in single hanging drops of tenocyte cultures treated for up to 6 days with either growth medium (GM) alone, tenogenic differentiation medium I (TDM-I) or tenogenic differentiation medium II (TDM-II). Scale bar = 75 μm. (B) Representative images of hematoxylin stained paraffin wax sections of TC-microtissue spheroids at day 6 following treatment with GM, TDM-I or TDM-II. Scale bar = 50 μm.

more native tendon-like appearance, with cells displaying the characteristic spindle-like morphology dispersed throughout the matrix (Fig. 8f) (Supp. Fig. 7).

4. Discussion

Tendons are highly specialized structures composed mainly of collagen type I, whose principal function is to transmit muscular forces to bone and thereby enable stabilization and movement of joints. Furthermore, in horses, specific tendons can function as elastic energy storage structures, allowing for an athletic and energy efficient gait [31]. Repetitive overloading of tendons can result in cumulative micro-damage with degenerative changes of the ECM [32,33], and these alterations are invariably associated with physical disruption of fibres, cross-links and matrix proteins [34], being secondary to impaired tenocyte metabolism possibly also due to hyperthermic insults [35] or hypoxic cell injury [36]. In all cases, the resident cell population of the tendon fails to repair this cumulative micro-damage. As such, efforts are now being made to utilize various cell-based tissue engineering approaches to treat tendon injuries, with an aim to restoring tissue function as well as preventing associated degenerative changes.

As the primary source of collagen production in tendons, tenocytes have long been considered as a potential tissue engineering strategy to facilitate tendon repair and regeneration. Indeed, several studies now exist in which tenocytes have been successfully used for the purpose of augmenting tendon repair in both animal and human subjects [37–40]. However, in order to generate sufficient numbers of tenocytes for use *in vivo*, cells must first be expanded in culture. Although the isolation and expansion of tenocytes is nowadays a relatively standardized procedure, the choice of growth conditions under which tenocytes are cultivated can have a significant impact on their differentiation status and hence their functional capacity to repair tendon tissue. This has been highlighted in several studies in which the expression of tendon-associated markers, including *COL1*, *COL3*, *SCX* and *TNMD*, were shown to be downregulated in tenocytes cultured for extended periods [19,20]. These limitations however, could be overcome to some degree by incorporation of tenocytes into 3D culture systems [25,27,41] or through the addition of specific growth factors [22,24,25]. In the current report, we initially investigated the effectiveness of culturing equine tenocytes as hanging drops as a means by which to generate scaffold-free 3D microtissue spheroids. Tenocytes readily aggregated together and formed well-organized, viable microtissue spheroid structures within 6 days of culture. Furthermore, cells within these late stage

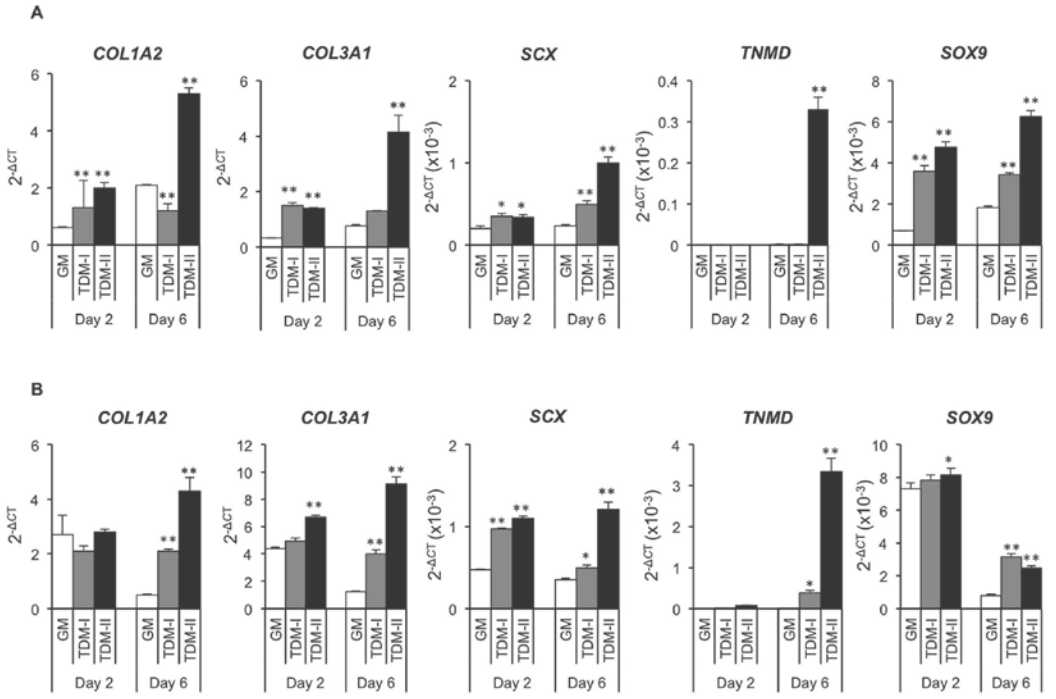

Fig. 4. qRT-PCR analysis of *COL1A2*, *COL3A1*, *SCX*, *TNMD* and *SOX9* in equine tenocytes cultured in 2D monolayers (A) or 3D microtissue spheroids (B) for 2 and 6 days. In each case, gene expression in equine tenocytes cultured in growth medium (GM) alone was compared to cells cultured in either tenogenic differentiation medium I (TDM-I) or tenogenic differentiation medium II (TDM-II) at each of the time points tested. Data was normalized to *GAPDH* and is presented as $2^{-\Delta CT}$. $^{*}p < 0.05$, $^{**}p < 0.01$ as compared to tenocytes cultured in GM. Significance was determined by one-way ANOVA and Tukey's post-hoc test. (±S.D. triplicates).

cultures appeared to have an elongated fibroblast-like morphology and demonstrated a basic cell alignment growth pattern. However, despite tenocyte-derived microtissue spheroids demonstrating early significant increases in tendon-associated markers such as *COL1A2*, *COL3A1* and *SCX* when compared to tenocyte monolayers, they were unable to maintain these elevated levels after prolonged culture times. Interestingly, the pro-chondrogenic marker *SOX9* was significantly reduced in these late-stage 3D cultures as compared to cells grown in monolayers. Moreover, in neither case were tenocytes observed to express *TNMD* or the chondrogenic-associated marker *COL2A1* at any of the time points tested. Taken together, these initial observations suggested that scaffold-free microtissue spheroid cultures may indeed have some immediate beneficial impact on tenocyte differentiation, although lacked the ability to maintain this effect over extended periods in culture.

In order to better optimize the tenogenic status of tenocytes cultured under either 2D or 3D conditions, we next focused our attention on the growth media used in each system. Findings from recent studies have strongly hinted at the use of TGF-β and IGF-1, or combinations thereof, to enhance and possibly even maintain tenocyte differentiation during extended periods of cultivation. Caliari et al. [22] demonstrated that IGF-1 at concentrations ranging from 10 to 200 ng/ml was capable of significantly enhancing *COL1A2*, *COL3A1* and decorin (*DCN*) gene expression in equine tenocytes cultured in collagen scaffolds in the absence of serum for 7 days. By contrast, a study performed by Qiu et al. [24] demonstrated that IGF-I (50 ng/ml) alone was unable to significantly influence *COL1*, *SCX* or *TNMD* expression in human tenocytes. However, incubation of cells with TGF-β3 (10 ng/ml), or TGF-β3 and IGF-1 together, significantly enhanced gene expression above that of control cultures incubated in the presence of serum-supplemented growth medium. In support of this, studies investigating the tenogenic potential of primary canine MSCs revealed that combinations of TGF-β1 and IGF-1 (5 ng/ml of each) were sufficient to induce the expression of *COL1*, *COL3*, *DCN*, *SCX* and *TNMD* after 7 and 14 days in combination with high density 3D culture conditions [26]. Similarly, a more recent report by Barsby et al. [21] has confirmed a synergistic effect between 3D growth environments and the addition of TGF-β3 (20 ng/ml) in the tenogenic differentiation of equine embryonic stem cells (ESCs). Due to its high homology to IGF-1, insulin has also been evaluated for its ability to influence tenogenic differentiation and has proven to be a potent inducer of tenocyte formation in human MSC cultures [42]. Additionally, ascorbic acid has been identified as having a beneficial impact on protein synthesis and cell viability of tendon organ cultures [43]. Therefore, based on these previous findings, we elected to assess the effects of low-serum media containing human TGF-β1 (10 ng/ml) in combination with either human IGF-1 (50 ng/ml) (termed TDM-I), or human insulin and L-ascorbic acid 2-phosphate (termed TDM-II) on tenocyte differentiation in either 2D or 3D culture systems. Treatment of tenocytes in 2D with TDM-I had a moderate effect on most of the genetic markers tested, with the

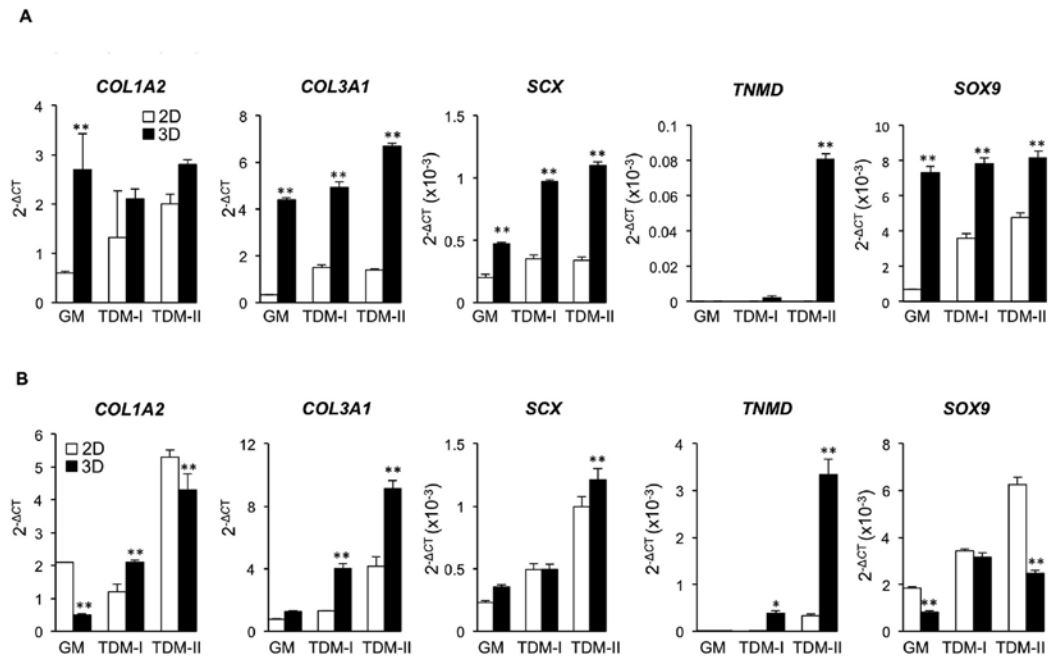

Fig. 5. qRT-PCR analysis of *COL1A2*, *COL3A1*, *SCX*, *TNMD* and *SOX9* in 2D or 3D equine tenocyte cultures at 2 (A) and 6 days (B) after seeding. Comparisons were made between tenocyte monolayers (2D) and microtissue spheroids (3D) when cultured in either growth medium (GM), tenogenic differentiation medium I (TDM-I) or tenogenic differentiation medium II (TDM-II). In each case, gene expression in equine tenocytes cultured in 2D was compared to those cultured in 3D, and data normalized to *GAPDH* and presented as $2^{-\Delta CT}$. $^{*}p < 0.05$, $^{**}p < 0.01$ as compared to tenocytes cultured in 2D monolayers. Significance was determined by one-way ANOVA and Tukey's post-hoc test. (±S.D. triplicates).

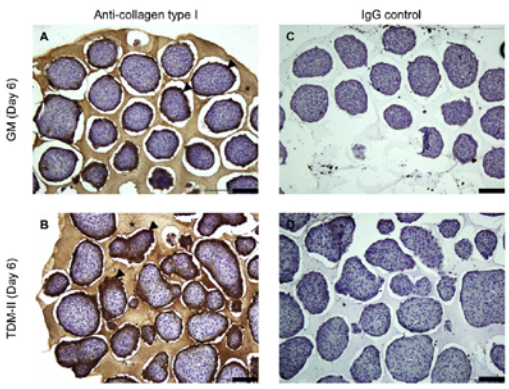

Fig. 6. Representative micrographs of anti-collagen type I stained paraffin wax sections of equine tenocytes cultured in hanging drops for 6 days in either GM (A) or TDM-II (B). Collagen type I was visualized using horseradish peroxidase-diaminodenzidine (dark brown) and sections counterstained with hematoxylin (blue). Examples of positive staining for collagen type I are indicated by arrowheads. (C–D) Representative micrographs of control paraffin wax sections in which the anti-COL1A primary antibody was replaced with normal IgG. *Asterisks*, agarose in which microtissues were embedded. Scale bar = 100 μm. (For interpretation of the references to colour in this figure legend, the reader is referred to the web version of this article.)

majority of genes being significantly increased within the first 2 days of culture as compared to cells cultured in growth medium alone. However, induction of *TNMD* expression was not observed at any time point, and *COL1A2* and *COL3A1* expression levels were reduced by day 6. With regards to 3D cultures, early significant increases in gene expression were limited to *SCX* only, but at later

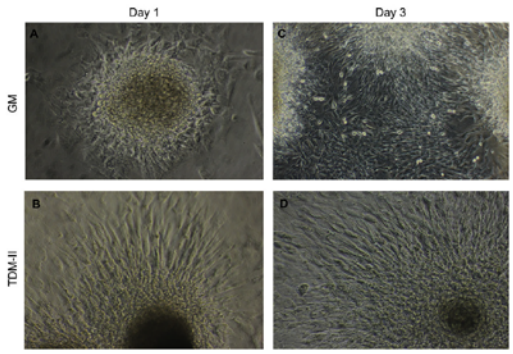

Fig. 7. Phase contrast micrographs demonstrating tenocyte outgrowth from microtissue spheroids under 2D culture conditions. Equine tenocytes were cultured as hanging drops for 6 days in GM or TDM-II and transferred to 48-well plates at 60 spheroids/well for 1 (A, B) and 3 (C, D) days. Magnification = 20×.

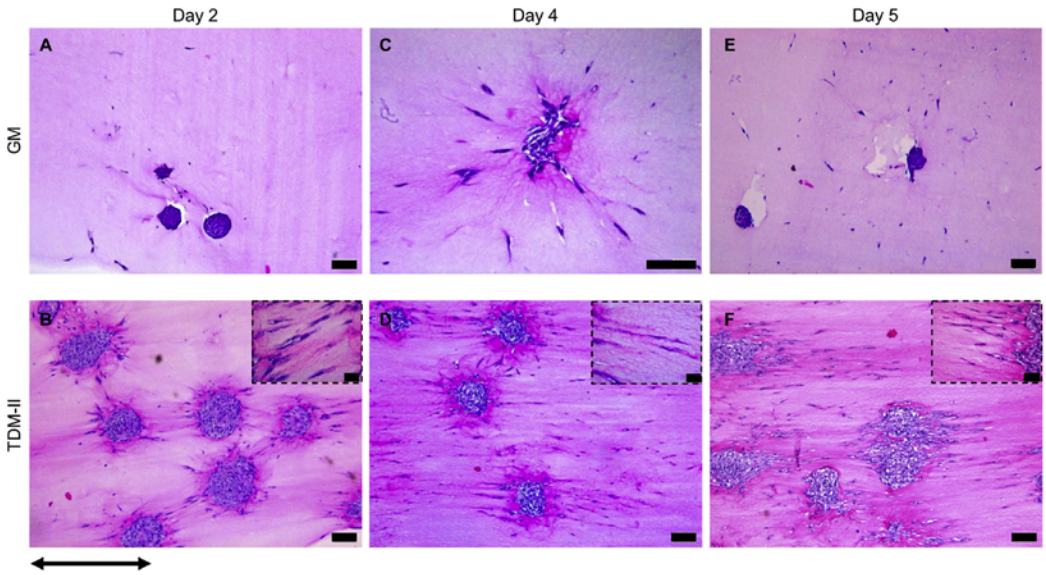

Fig. 8. Outgrowth of equine tenocytes from TC-microtissue and their alignment in static 3D collagen constructs. TC-microtissues were prepared in hanging drops for 6 days in either GM or TDM-II and then embedded in 0.8% collagen matrix. Representative micrographs of hematoxylin and eosin stained paraffin wax sections of gel constructs at 2 (A, B), 4 (C, D) and 5 (E, F) days after TC-microtissue seeding of GM (A, C, E) or TDM-II (B, D, F) treated cultures. Scale bar = 100 μm. *Inset*, scale bar = 20 μm. *Arrow*, orientation of collagen gels based on their positioning in anchored silicon molds.

stages included increases in *COL1A2*, *COL3A1*, *SCX*, *TNMD* and *SOX9*. In comparison to 2D cultures, late stage 3D cultures demonstrated modest benefits in terms of *COL1A2*, *COL3A1* and *TNMD* expression, with similar levels of *SOX9* being observed. These observations therefore go someway to supporting the concept of culturing tenocytes under 3D conditions in the presence of TGF-β and IGF-1 in order to enhance and maintain a tendon like genotype.

With regards to tenogenic gene expression, the most pronounced effects were observed in TDM-II, where IGF-1 had been replaced by insulin and L-ascorbic acid 2-phosphate. Regardless of which system was used, cultivation in TDM-II resulted in marked increases in the expression of all tenogenic gene markers in late stage cultures. Furthermore, in comparison to 2D cultures, TC-microtissue spheroids examined at day 6 demonstrated significantly enhanced expression levels of *COL3A1*, *SCX* and *TNMD*, with a noticeable decrease in the expression of the chondrogenic marker *SOX9*, and a complete absence of *COL2A1*. Moreover, not only were the expression levels of tenogenic markers maintained in this medium, but were also in some cases enhanced at the later stages. Clearly therefore, the combination of TGF-β1, insulin and ascorbic acid appears to represent a novel supplement for the purpose of enhancing and maintaining a tendon-like genotype in 3D tenocyte cultures, without inducing chondrocyte-associated gene expression. It should be noted however, that *SOX9* expression was increased by both TDM-I and TDM-II treatments in 2D and 3D culture systems. The transcription factor SOX9 is recognized as playing a pivotal role in regulating chondrocyte differentiation and as such, is considered to be a reliable marker of chondrogenesis [44]. Therefore, its upregulation in tenocyte cultures in response to TDM-I or TDM-II could imply alterations in tenocyte differentiation towards a more chondrogenic-like state. Certainly, over expression of *SOX9* in cultured tenocytes has been shown to result in decreases in the expression levels of *SCX* and *TNMD* and increases in *COL2A1* [45]. Moreover, forced expression of *SOX9* in chick tendon tissue can lead to ectopic cartilage formation [45]. However, despite our observations that *SOX9* expression levels were significantly elevated in 2D and 3D tenocyte cultures treated with either TDM-I or TDM-II, the expression levels of *SCX* and *TNMD*, where expressed, did not decrease. More importantly, *COL2A1* expression remained below detection levels at all time points, regardless of treatment regime. It therefore seems unlikely that the addition of TDM-I or TDM-II had any profound influence on the chondrogenic status of the equine tenocytes used in the current study. By comparison, tenogenic markers were noticeably absent in 3D cultures treated with TGFβ-1 alone and expression levels of *SOX9* remained significantly elevated, thereby indicating media supplemented solely with TGFβ-1 to be unsuitable for supporting the tenogenic differentiation status of equine tenocytes in 3D microtissue spheroids.

In accordance with these findings, we could demonstrate that collagen type I was also increased at the protein level in TC-microtissue spheroids cultured in the presence of TDM-II. Furthermore, when assessing protein lysates for the presence of TNMD, we detected an additional, high molecular weight protein not observed in TC-microtissue spheroids treated with growth medium alone. It is unclear as to why TNMD was detected in tenocyte cultures treated with growth medium at all, as qRT-PCR analysis failed to detect any *TNMD* mRNA transcript. However, a similar finding was also reported by Barsby et al. [46] in which TNMD protein was observed in TGF-β-treated equine ESC cultures in the absence of any detectable levels of *TNMD* mRNA. The cause for such inconsistencies was accredited to disparities between TNMD protein turnover and mRNA degradation rates. Therefore, it seems plausible that the 250 kDa band observed in the current study represents a high molecular weight variant of TNMD, being

present in native tendon tissue, as well as being induced in TC-microtissue spheroids following stimulation with TDM-II. However, the relevance of this particular protein species with regards to the normal functioning of tendons remains to be determined. In a final series of experiments, we assessed the potential of tenocytes within microtissue spheroids to migrate out from the tissue structures and to re-populate 2D or 3D culture environments. This was based on the assumption that should such tissue constructs be considered as a viable *in vivo* treatment strategy, then the cells contained within the tissue spheroids would be required to grow out and invade the surrounding host tissue in order to mediate their therapeutic effects. Indeed, we could demonstrate that TC-microtissue spheroids treated with TDM-II were capable of growing out from the tissues and could proliferate on a 2D culture surface whilst maintaining a tenocyte-like morphology. Moreover, when transferred to collagen gels, microtissue-derived cells treated with TDM-II also had the capacity to promote contraction of the collagen matrix and were observed to independently align with respect to the orientation of the collagen structure following microtissue outgrowth.

5. Conclusions

Taken together, our findings demonstrate the beneficial effects of culturing tenocytes as gravity-enforced microtissue spheroids and supports the use of low-serum containing growth medium in combination with TGF-β1, insulin and ascorbic acid as an effective means by which to maintain the tenogenic differentiation status of cultured tenocytes. Such a system not only offers the potential for tendon cell and tissue biology to be studied *in vitro* using conditions that more closely simulate the *in vivo* situation, but also raises the interesting possibility of whether this could be directly incorporated into future *in vivo* tissue engineering strategies for the purpose of more effectively treating tendon disorders.

Acknowledgements

This study was funded in part by the Stiftung Forschung für das Pferd. SG and GB were supported by SNSF grants 31003A_134935 and 31003A_156313. AM and NAT were supported by the Uniscientia Foundation. The authors would like to thank Prof. Dr. Brigitte von Rechenberg (Musculoskeletal Research Unit, Equine Department, Vetsuisse-Faculty, University of Zurich) and Dr. Silke Kalchofner-Mark (CABMM, University of Zurich) for their scientific input and support, Prof. Lee Ann Laurent-Applegate (Laboratory of Cellular Therapy, Department of Musculoskeletal Medicine, University Hospital Lausanne) for supplying equine fetal tenocytes and Katalin Zlinszky (Musculoskeletal Research Unit, Equine Department, Vetsuisse-Faculty, University of Zurich) for performing the caspase activity assay.

Appendix A. Supplementary data

Supplementary data related to this article can be found at http://dx.doi.org/10.1016/j.biomaterials.2015.08.013.

References

[1] R.B. Williams, L.S. Harkins, C.J. Hammond, J.L. Wood, Racehorse injuries, clinical problems and fatalities recorded on British racecourses from flat racing and National Hunt racing during 1996, 1997 and 1998, Equine Vet. J. 33 (2001) 478–486.
[2] P.P. Lui, N. Maffulli, C. Rolf, R.K. Smith, What are the validated animal models for tendinopathy? Scand. J. Med. Sci. Sports 21 (2011) 3–17.
[3] D. Gaspar, K. Spanoudes, C. Holladay, A. Pandit, D. Zeugolis, Progress in cell-based therapies for tendon repair, Adv. Drug Deliv. Rev. 84 (2015) 240–256.
[4] D. Deng, W. Wang, B. Wang, P. Zhang, G. Zhou, W.J. Zhang, Y. Cao, W. Liu, Repair of Achilles tendon defect with autologous ASCs engineered tendon in a rabbit model, Biomaterials 35 (2014) 8801–8809.
[5] J. Zhang, B. Li, J.H. Wang, The role of engineered tendon matrix in the stemness of tendon stem cells in vitro and the promotion of tendon-like tissue formation in vivo, Biomaterials 32 (2011) 6972–6981.
[6] J.Y. Lee, Z. Zhou, P.J. Taub, M. Ramcharan, Y. Li, T. Akinbiyi, E.R. Maharam, et al., BMP-12 treatment of adult mesenchymal stem cells in vitro augments tendon-like tissue formation and defect repair in vivo, PLoS One 6 (2011) e17531.
[7] J.L. Chen, Z. Yin, W.L. Shen, X. Chen, B.C. Heng, X.H. Zou, H.W. Ouyang, Efficacy of hESC-MSCs in knitted silk-collagen scaffold for tendon tissue engineering and their roles, Biomaterials 31 (2010) 9438–9451.
[8] R.K. Smith, N.J. Werling, S.G. Dakin, R. Alam, A.E. Goodship, J. Dudhia, Beneficial effects of autologous bone marrow-derived mesenchymal stem cells in naturally occurring tendinopathy, PLoS One 8 (2013) e75697.
[9] J.J. Albano, R.W. Alexander, Autologous fat grafting as a mesenchymal stem cell source and living bioscaffold in a patellar tendon tear, Clin. J. Sport Med. 21 (2011) 359–361.
[10] C.M. McNeilly, A.J. Banes, M. Benjamin, J.R. Ralphs, Tendon cells in vivo form a three dimensional network of cell processes linked by gap junctions, J. Anat. 189 (1996) 593–600.
[11] J. Qi, J.M. Dmochowski, A.N. Banes, M. Tsuzaki, D. Bynum, M. Patterson, A. Creighton, et al., Differential expression and cellular localization of novel isoforms of the tendon biomarker tenomodulin, J. Appl. Physiol. 113 (2012) 861–871.
[12] D. Docheva, E.B. Hunziker, R. Fässler, O. Brandau, Tenomodulin is necessary for tenocyte proliferation and tendon maturation, Mol. Cell Biol. 25 (2005) 699–705.
[13] P. Alberton, S. Dex, C. Popov, C. Shukunami, M. Schieker, D. Docheva, Loss of tenomodulin results in reduced self-renewal and augmented senescence of tendon stem/progenitor cells, Stem Cells Dev. 42 (2015) 597–609.
[14] C. Shukunami, A. Takimoto, M. Oro, Y. Hiraki, Scleraxis positively regulates the expression of tenomodulin, a differentiation marker of tenocytes, Dev. Biol. 298 (2006) 234–247.
[15] R. Schweitzer, E. Zelzer, T. Volk, Connecting muscles to tendons: tendons and musculoskeletal development in flies and vertebrates, Development 137 (2010) 2807–2817.
[16] N.D. Murchison, B.A. Price, D.A. Conner, D.R. Keene, E.N. Olson, C.J. Tabin, R. Schweitzer, Regulation of tendon differentiation by scleraxis distinguishes force-transmitting tendons from muscle-anchoring tendons, Development 134 (2007) 2697–2708.
[17] S.E. Taylor, A. Vaughan-Thomas, D.N. Clements, G. Pinchbeck, L.C. Macrory, R.K. Smith, P.D. Clegg, Gene expression markers of tendon fibroblasts in normal and diseased tissue compared to monolayer and three dimensional culture systems, BMC Musculoskelet. Disord. 10 (2009) 27.
[18] L. Yao, C.S. Bestwick, L.A. Bestwick, Phenotypic drift in human tenocyte culture, Tissue Eng. 12 (2006) 1843–1849.
[19] A.D. Mazzocca, D. Chowaniec, M.B. McCarthy, K. Beitzel, M.P. Cote, W. McKinnon, R. Arciero, In vitro changes in human tenocyte cultures obtained from proximal biceps tendon: multiple passages result in changes in routine cell markers, Knee Surg. Sports Traumatol. Arthrosc. 20 (2012) 1666–1672.
[20] J. Zhu, J. Li, B. Wang, W.J. Zhang, G. Zhou, Y. Cao, W. Liu, The regulation of phenotype of cultured tenocytes by microgrooved surface structure, Biomaterials 31 (2010) 6952–6958.
[21] T. Barsby, E.P. Bavin, D.J. Guest, Three-dimensional culture and transforming growth factor beta3 synergistically promote tenogenic differentiation of equine embryo-derived stem cells, Tissue Eng. Part A 20 (2014) 2604–2613.
[22] S.R. Caliari, B.A. Harley, Composite growth factor supplementation strategies to enhance tenocyte bioactivity in aligned collagen-GAG scaffolds, Tissue Eng. Part A 19 (2013) 1100–1112.
[23] M.A. Costa, C. Wu, B.V. Pham, A.K. Chong, H.M. Pham, J. Chang, Tissue engineering of flexor tendons: optimization of tenocyte proliferation using growth factor supplementation, Tissue Eng. 12 (2006) 1937–1943.
[24] Y. Qiu, X. Wang, Y. Zhang, A.J. Carr, L. Zhu, Z. Xia, A. Sabokbar, Development of a refined tenocyte differentiation culture technique for tendon tissue engineering, Cells Tissues Organs 197 (2013) 27–36.
[25] Y. Qiu, X. Wang, Y. Zhang, A.J. Carr, L. Zhu, Z. Xia, A. Sabokbar, In vitro two-dimensional and three-dimensional tenocyte culture for tendon tissue engineering, J. Tissue Eng. Regen. Med. (2013), http://dx.doi.org/10.1002/term.1791.
[26] P.R. Schneider, C. Buhrmann, A. Mobasheri, U. Matis, M. Shakibaei, Three-dimensional high-density co-culture with primary tenocytes induces tenogenic differentiation in mesenchymal stem cells, J. Orthop. Res. 29 (2011) 1351–1360.
[27] G. Schulze-Tanzil, A. Mobasheri, P.D. Clegg, J. Sendzik, T. John, M. Shakibaei, Cultivation of human tenocytes in high-density culture, Histochem Cell Biol. 122 (2004) 219–228.
[28] J. Braun, A. Hack, M. Weis-Klemm, S. Conrad, S. Treml, K. Kohler, U. Walliser, et al., Evaluation of the osteogenic and chondrogenic differentiation capacities of equine adipose tissue-derived mesenchymal stem cells, Am. J. Vet. Res. 71 (2010) 1228–1236.
[29] A. Mirsaidi, A.N. Tiaden, P.J. Richards, Preparation and osteogenic differentiation of scaffold-free mouse adipose-derived stromal cell microtissue spheroids (ASC-MT), Curr. Protoc. Stem Cell Biol. 27 (2013). Unit 2B.5.

[30] R. Mhanna, E. Öztürk, P. Schlink, M. Zenobi-Wong, Probing the microenvironmental conditions for induction of superficial zone protein expression, Osteoarthr. Cartil. 21 (2013) 1924–1932.
[31] R.K. Smith, Mesenchymal stem cell therapy for equine tendinopathy, Disabil. Rehabil. 30 (2008) 1752–1758.
[32] R. Smith, W. McIlwraith, R. Schweitzer, K. Kadler, J. Cook, B. Caterson, S. Dakin, et al., Advances in the understanding of tendinopathies: a report on the Second Havemeyer Workshop on equine tendon disease, Equine Vet. J. 46 (2014) 4–9.
[33] J.H. Shepherd, G.P. Riley, H.R. Screen, Early stage fatigue damage occurs in bovine tendon fascicles in the absence of changes in mechanics at either the gross or micro-structural level, J. Mech. Behav. Biomed. Mater. 38 (2014) 163–172.
[34] C.S. Avella, R.K.W. Smith, Diagnosis and management of tendon and ligament disorders, in: J.A. Auer, J.A. Stick (Eds.), Equine Surgery, fourth ed., Elsevier Saunders, St. Louis, MO, USA, 2012, pp. 1157–1179.
[35] H.L. Birch, A.M. Wilson, A.E. Goodship, The effect of exercise-induced localised hyperthermia on tendon cell survival, J. Exp. Biol. 200 (1997) 1703–1708.
[36] N.L. Millar, J.H. Reilly, S.C. Kerr, A.L. Campbell, K.J. Little, W.J. Leach, B.P. Rooney, et al., Hypoxia: a critical regulator of early human tendinopathy, Ann. Rheum. Dis. 71 (2012) 302–310.
[37] J.I. Liang, P.C. Lin, M.Y. Chen, T.H. Hsieh, J.J. Chen, M.L. Yeh, The effect of tenocyte/hyaluronic acid therapy on the early recovery of healing Achilles tendon in rats, J. Mater Sci. Mater Med. 25 (2014) 217–227.
[38] A. Wang, W. Breidahl, K.E. Mackie, Z. Lin, A. Qin, J. Chen, M.H. Zheng, Autologous tenocyte injection for the treatment of severe, chronic resistant lateral epicondylitis: a pilot study, Am. J. Sports Med. 41 (2013) 2925–2932.
[39] J. Chen, Q. Yu, B. Wu, Z. Lin, N.J. Pavlos, J. Xu, H. Ouyang, et al., Autologous tenocyte therapy for experimental Achilles tendinopathy in a rabbit model, Tissue Eng. Part A 17 (2011) 2037–2048.
[40] C. Stoll, T. John, C. Conrad, A. Lohan, S. Hondke, W. Ertel, C. Kaps, et al., Healing parameters in a rabbit partial tendon defect following tenocyte/biomaterial implantation, Biomaterials 32 (2011) 4806–4815.
[41] C. Stoll, T. John, M. Endres, C. Rosen, C. Kaps, B. Kohl, M. Sittinger, et al., Extracellular matrix expression of human tenocytes in three-dimensional air-liquid and PLGA cultures compared with tendon tissue: implications for tendon tissue engineering, J. Orthop. Res. 28 (2010) 1170–1177.
[42] A.D. Mazzocca, M.B. McCarthy, D. Chowaniec, M.P. Cote, C.H. Judson, J. Apostolakos, O. Solovyova, et al., Bone marrow-derived mesenchymal stem cells obtained during arthroscopic rotator cuff repair surgery show potential for tendon cell differentiation after treatment with insulin, Arthroscopy 27 (2011) 1459–1471.
[43] J.E. Russell, P.R. Manske, Ascorbic acid requirement for optimal flexor tendon repair in vitro, J. Orthop. Res. 9 (1991) 714–719.
[44] B. de Crombrugghe, V. Lefebvre, R.R. Behringer, W. Bi, S. Murakami, W. Huang, Transcriptional mechanisms of chondrocyte differentiation, Matrix Biol. 19 (2000) 389–394.
[45] A. Takimoto, M. Oro, Y. Hiraki, C. Shukunami, Direct conversion of tenocytes into chondrocytes by Sox9, Exp. Cell Res. 318 (2012) 1492–1507.
[46] T. Barsby, D. Guest, Transforming growth factor beta3 promotes tendon differentiation of equine embryo-derived stem cells, Tissue Eng. Part A 19 (2013) 2156–2165.

2.1.4. Human serine protease HTRA1 positively regulates osteogenesis of human bone marrow-derived mesenchymal stem cells and mineralization of differentiating bone-forming cells through the modulation of extracellular matrix protein.

Authors: Tiaden AN, Breiden M, Mirsaidi A, Weber FA, Bahrenberg G, **Glanz S**, Cinelli P, Ehrmann M, Richards PJ.

Journal: *Stem Cells. 2012;30(10):2271-82. IF:6.523*

Contribution: Assistance in generation of qPCR data and immunoblotting.

STEM CELLS®
TISSUE-SPECIFIC STEM CELLS

Human Serine Protease HTRA1 Positively Regulates Osteogenesis of Human Bone Marrow-Derived Mesenchymal Stem Cells and Mineralization of Differentiating Bone-Forming Cells Through the Modulation of Extracellular Matrix Protein

ANDRÉ N. TIADEN,[a] MAIKE BREIDEN,[b] ALI MIRSAIDI,[a,c] FABIENNE A. WEBER,[d] GREGOR BAHRENBERG,[a,c] STEPHAN GLANZ,[a,c] PAOLO CINELLI,[d] MICHAEL EHRMANN,[b] PETER J. RICHARDS[a,c]

[a]Bone and Stem Cell Research Group, CABMM, Zurich, [c]Zurich Center for Integrative Human Physiology (ZIHP), Zurich, and [d]Institute of Laboratory Animal Science, University of Zurich, Zurich, Switzerland; [b]Centre for Medical Biotechnology, Faculty of Biology and Geography, University Duisburg-Essen, Essen, Germany

Key Words. HTRA1 protein • Mesenchymal stem cell • Differentiation • Bone mineralization

ABSTRACT

Mammalian high-temperature requirement serine protease A1 (HTRA1) is a secreted member of the trypsin family of serine proteases which can degrade a variety of bone matrix proteins and as such has been implicated in musculoskeletal development. In this study, we have investigated the role of HTRA1 in mesenchymal stem cell (MSC) osteogenesis and suggest a potential mechanism through which it controls matrix mineralization by differentiating bone-forming cells. Osteogenic induction resulted in a significant elevation in the expression and secretion of HTRA1 in MSCs isolated from human bone marrow-derived MSCs (hBMSCs), mouse adipose-derived stromal cells (mASCs), and mouse embryonic stem cells. Recombinant HTRA1 enhanced the osteogenesis of hBMSCs as evidenced by significant changes in several osteogenic markers including integrin-binding sialoprotein (*IBSP*), bone morphogenetic protein 5 (*BMP5*), and sclerostin, and promoted matrix mineralization in differentiating bone-forming osteoblasts. These stimulatory effects were not observed with proteolytically inactive HTRA1 and were abolished by small interfering RNA against *HTRA1*. Moreover, loss of HTRA1 function resulted in enhanced adipogenesis of hBMSCs. HTRA1 Immunofluorescence studies showed colocalization of HTRA1 with IBSP protein in osteogenic mASC spheroid cultures and was confirmed as being a newly identified HTRA1 substrate in cell cultures and in proteolytic enzyme assays. A role for HTRA1 in bone regeneration in vivo was also alluded to in bone fracture repair studies where HTRA1 was found localized predominantly to areas of new bone formation in association with IBSP. These data therefore implicate HTRA1 as having a central role in osteogenesis through modification of proteins within the extracellular matrix. STEM CELLS *2012;30:2271–2282*

Disclosure of potential conflicts of interest is found at the end of this article.

INTRODUCTION

Mammalian high-temperature requirement serine protease A1 (HTRA1) belongs to a well-defined group of serine proteases originally identified in bacteria [1, 2]. They share many common features including a highly conserved trypsin-like serine protease domain and at least one Post synaptic density protein, Drosophila disc large tumor suppressor, and Zonula occludens-1 protein domain at the C terminus. To date, four HTRA1 family members have been identified and are termed HTRA1, HTRA2, HTRA3, and HTRA4. HTRA2 is the best characterized of the four and exists as a membrane protein primarily involved in mitochondrial quality control [2, 3]. Both HTRA1 and HTRA2 are primarily regarded as being key regulators of tumor development and subsequent malignancies [4–6], although a growing body of evidence now exists to suggest that HTRA1 may also play a central role in musculoskeletal development and disease through its proteolytic actions on proteins within the extracellular matrix (ECM) [7–10].

The skeletal ECM is a structurally dynamic scaffold that provides a well-organized framework for mineralization and orchestrates many of the cellular processes required for maintaining bone integrity. The bone tissue ECM comprises 70%–90% mineral and 10%–30% protein, the major proportion of which being glycoproteins such as collagen, fibronectin, and noncollagenous small integrin-binding ligand, N-linked

Author contributions: A.N.T.: collection and/or assembly of data, data analysis and interpretation, and manuscript writing; M.B., A.M., F.W., G.B., and S.G.: collection and/or assembly of data; P.C.: data analysis and interpretation; M.E.: data analysis and interpretation and manuscript writing; P.J.R.: conception and design, financial support, collection and/or assembly of data, data analysis and interpretation, and manuscript writing.

Correspondence: Peter J. Richards, Ph.D., CABMM, University of Zurich, Winterthurerstrasse 190, CH-8057 Zürich, Switzerland. Telephone: +41-44-635-3801; Fax: +41-44-635-6840; e-mail: peter.richards@cabmm.uzh.ch Received May 4, 2012; accepted for publication July 21, 2012; first published online in STEM CELLS *EXPRESS* August 3, 2012. 1066-5099/2012/$30.00/0 doi: 10.1002/stem.1190

glycoproteins (SIBLINGs) [11]. A direct interaction between these proteins and bone progenitor cells is essential for the development of a mineralized matrix [12–14]. Furthermore, degradation of specific glycoproteins within the ECM by serine proteases is also thought to play a central role in controlling mineral deposition by osteoblasts [15].

Bone remodeling and regeneration is a strictly regulated process, being reliant on the activities of resident osteoblasts originating from bone marrow-derived mesenchymal stem cells (BMSCs) through the process of osteogenic differentiation [16]. Osteogenesis is governed by a complex series of well-orchestrated events involving numerous different transcription factors, signaling pathways, and growth factors [17, 18]. The potential involvement of HTRA1 in osteogenesis and bone development has already been alluded to in studies examining the expression profile of *HTRA1* in developing mouse embryos and adult mouse bone where it was identified in osteocytes and osteoblasts within the bone matrix [10, 19]. More recently, it was suggested that HTRA1 may actually play a negative role in bone and mineral development through its ability to inhibit osteoblastic differentiation in the mouse 2T3 cell line [20]. However, no studies have yet sought to determine the influence of HTRA1 on the osteogenic differentiation potential of MSCs.

In this study, we examined the effects of recombinant HTRA1 on the osteogenesis of human BMSCs (hBMSCs) and matrix mineralization by differentiating bone-forming cells with an aim to establish a role for HTRA1 in bone formation. Our results demonstrate that HTRA1 is an essential requirement for osteogenesis and that its effects are mediated primarily through its proteolytic actions on ECM proteins.

Materials and Methods

Materials

4-(2-Aminoethyl) benzenesulfonyl fluoride hydrochloride (AEBSF) was from Sigma-Aldrich (Buchs, Switzerland, http://www.sigmaaldrich.com/). Recombinant integrin-binding sialoprotein (IBSP) was purchased from R&D Systems (Abingdon, U.K., http://www.rndsystems.com/). Monoclonal mouse anti-IBSP, C-terminal region (clone ID1.2) and polyclonal donkey anti-collagen type 1 were from LabForce (Nunningen, Switzerland, http://www.labforce.ch/site/site.asp), polyclonal rabbit anti-IBSP, N-terminal region was from Enzo Life Sciences (Lausen, Switzerland, http://www.enzolifesciences.com/), and polyclonal rabbit anti-HTRA1 was generated as previously described [9]. The biotinylated polyclonal swine anti-rabbit IgG was from DAKO (Baar, Switzerland http://www.dako.com/ch/). All anti-IgG horseradish peroxidase (HRP)-conjugated and fluorescence-conjugated secondary antibodies were from Jackson ImmunoResearch (Suffolk, U.K., http://www.jireurope.com/).

Animals

Experiments were performed using 5-month-old senescence-accelerated resistant mice (SAMR1) ($n = 27$) (Harlan, Netherlands, http://www.harlan.com/). All animal research procedures were approved by the Animal Experimentation Committee of the Veterinary Office of the Canton of Zürich, Switzerland (Project License 140/2005 and 151/2010), and followed the guidelines of the Swiss Federal Veterinary Office for the use and care of laboratory animals.

Cell Culture

Mouse adipose-derived stromal cells (mASCs) were isolated from the inguinal fat pads of SAMR1 mice ($n = 4$) and purity confirmed by fluorescence-activated cell sorting (Sca1, 98%; CD29, 100%; CD105, 42%; CD34, 5%; CD45, 0.5%) as previously reported [21]. Mouse embryonic stem cells (mESCs) (E14 129/Ola) are a well-established cell line and were maintained as previously described [22, 23]. hBMSCs were obtained from Lonza (Verviers, Belgium, http://www.lonza.com/) and were confirmed as being positive for CD105, CD166, CD44, and CD26, and negative for CD14, CD34, and CD45 as stated by the manufacturer. Cells were maintained in normal growth medium consisting of Dulbecco's modified Eagle's medium-low glucose (with Glutamax) (Life Technologies, Zug, Switzerland, http://www.lifetechnologies.com/), supplemented with 10% fetal bovine serum (Invitrogen AG), penicillin (50 units/ml), and streptomycin (50 μg/ml) (Life Technologies, Zug, Switzerland, http://www.lifetechnologies.com/). Cells were used between passages 2 and 6 unless otherwise stated. In some cases, hBMSCs undergoing osteogenic differentiation were treated with recombinant active or inactive HTRA1 (5 μg/ml) for up to 18 days. For protease inhibition studies, AEBSF (20 μg/ml) was also included where indicated. For three-dimensional (3D)-spheroids, mASCs were cultured in 25 μl hanging drops in normal growth medium as described above, using Terasaki plates (VWR, Dietikon, Switzerland, https://ch.vwr.com/) at 2,500 cells per drop.

Induction and Analysis of Differentiation

Well-established differentiation protocols were used to induce and analyze either osteogenesis or adipogenesis in mASCs and E14 129/Ola cells [21] and hBMSCs [24]. For differentiation assays, a starting density of 5,000 and 10,000 cells per square centimeter was used for human and mouse cells, respectively. For osteogenic 3D-spheroid preparations, mASCs were predifferentiated in two-dimensional (2D) cultures for 3 days and cultured in hanging drops containing osteogenic culture medium for a further 2, 4, or 6 days, after which time they were harvested and processed for histological analysis using previously described techniques [25]. Mineralization induced by osteogenic differentiation was identified using Alizarin Red S (Sigma-Aldrich, Buchs, Switzerland, http://www.sigmaaldrich.com/). Adipocyte formation was confirmed by positive staining for oil red O (Sigma-Aldrich, Buchs, Switzerland, http://www.sigmaaldrich.com/). Differentiation markers specific to either osteogenesis or adipogenesis were also quantified by reverse-transcription polymerase chain reaction (qRT-PCR) using TaqMan Gene Expression Assays (Life Technologies, Zug, Switzerland, http://www.lifetechnologies.com/) (Supporting Information Table S1). Total RNA was harvested from cells at given time points during differentiation, 0.5 μg total RNA was reverse-transcribed using Superscript II (Life Technologies, Zug, Switzerland, http://www.lifetechnologies.com/), and an equivalent of 10 ng total RNA was applied as cDNA template in the successive qRT-PCR reaction using the StepOnePlus (LifeTechnologies, Zug, Switzerland, http://www.lifetechnologies.com/).

Recombinant HTRA1 Production

Purified recombinant active HTRA1 (HTRA1Δmac) and inactive HTRA1 (HTRA1ΔmacSA) were produced in *Escherichia coli* and purified using metal-affinity chromatography as previously described [26].

SDS-PAGE and Western Blotting

Protein was analyzed by SDS-PAGE using 4%–15% precast Tris-HCl gels (BioRad, Reinach, Switzerland, http://www3.bio-rad.com/) under reducing conditions and electroblotted onto PVDF membranes using the Trans-Blot Turbo blotting system (BioRad, Reinach, Switzerland, http://www3.bio-rad.com/). IBSP was identified using antibodies raised against either the N-terminal (1:800) or C-terminal (1:500) regions of human IBSP and detected using HRP-conjugated secondary antibodies (1:10,000) followed by incubation in SuperSignal West Pico Chemiluminescent Substrate (Thermo Fisher Scientific, Lausanne, Switzerland, http://www.piercenet.com/) and exposure to x-ray film.

Immunofluorescence

Cells in either 2D or 3D cultures were fixed in phosphate buffered saline (PBS) buffered formaldehyde (4%) or ice-cold methanol, blocked with normal goat serum (1:10) and incubated with polyclonal rabbit anti-HTRA1 (1:50), polyclonal donkey anti-collagen type 1 (1:50), or monoclonal mouse anti-IBSP (1:50) in PBS containing 1% bovine serum albumin (BSA) overnight at 4°C. For paraffin wax sections, staining reactions were performed at 37°C for 1 hour. In the case of double immunostaining procedures, samples were incubated with both polyclonal rabbit anti-HTRA1 (1:50) and monoclonal mouse anti-IBSP (1:50) using the conditions described above. Samples were then washed and incubated with either goat anti-rabbit-Cy3 (1:400), goat anti-donkey-Cy3 (1:400), or goat anti-mouse-Cy5 (1:400) for 1 hour and mounted in 4,6-diamidino-2-phenylindole containing mounting solution and images captured using the Leica DMI6000B automated inverted research microscope system (Leica Microsystems, Heerbrugg, Switzerland, http://www.leica-microsystems.com/).

Immunohistochemistry. Dewaxed paraffin sections (8 μm) were rehydrated and blocked with normal swine serum (Dako Baar, Switzerland, http://www.dako.com/ch/) for 30 minutes. Sections were then incubated with polyclonal rabbit anti-HTRA1 (1:50) for 1 hour at 37°C. Sections were then washed in PBS and incubated with biotinylated swine anti-rabbit IgG (1:500) for 1 hour at room temperature followed by washing and a further incubation for 30 minutes with Vectastain (Reactolab, Servion, Switzerland, http://www.vectorlabs.com/). Sections were then developed using 3,3′ diaminobenzidine tetrahydrochloride, counterstained with Harris' Hematoxylin and mounted in dibutylphthalate polystyrene xylene (DPX).

Proteolytic Enzyme Assays

Degradation of IBSP by HTRA1 was determined using methods previously described [9]. Briefly, HTRA1 (45 nM) and IBSP (476 nM) were incubated in 50 mM Tris-HCl, pH 8.5, and 150 mM NaCl for up to 24 hours at 37°C. In some reactions, active HTRA1 was replaced by proteolytically inactive HTRA1. Proteins were separated on a 4%–15% SDS-PAGE gel and analyzed by Western blot as described above. The proteolytic activity of HTRA1 was also investigated in hBMSC cultures using immunofluorescence staining. Cells were incubated in osteogenic induction medium either without or with active or inactive HTRA1 (5 μg/ml), fixed in methanol and IBSP or collagen type 1 detected with specific antibodies using methods as described above.

HTRA1 Enzyme-Linked Immunosorbent Assay

The HTRA1 enzyme-linked immunosorbent assay (ELISA) was performed using HTRA1 specific monoclonal and polyclonal antibodies as previously described [9].

HTRA1 Small Interfering RNA

Specific knockdown of *HTRA1* expression was performed with Silencer Select small interfering RNA (siRNA) oligos (Life Technologies, Zug, Switzerland, http://www.lifetechnologies.com/), according to the manufacturer's protocol. hBMSCs (1×10^5 cells) were transfected with 100 nM *HTRA1*-specific (s11279, s11280) or negative control siRNA (Negative Control-1) using the NEON Transfection System (Life Technologies, Zug, Switzerland, http://www.lifetechnologies.com/). Following transfection, cells were seeded in cell culture plates with fresh growth medium (without antibiotics) and incubated for 24 hours at 37°C, 5% CO_2. Medium was then replaced with either fresh growth medium or differentiation medium and total RNA and supernatants were harvested at selected time points for further analysis.

Fracture Model

A rigidly stabilized, unilateral mid-diaphyseal osteotomy gap was created in the femurs of SAMR1 mice ($n = 5$–6 per time point) using a 0.22 mm gigli saw as previously described [24]. The immunohistochemical and immunofluorescence techniques described above were used to detect both HTRA1 and IBSP protein in decalcified paraffin wax sections (8 μm) from mouse femora at various stages of repair ($n = 3$ per time point).

Statistical Analysis

All statistical analyses were carried out using SPSS18.0 (SPSS Inc., Chicago, IL). Parametric analysis of normally distributed data was performed using the two-tailed unpaired Student's t test for comparison of two groups or one-way analysis of variance followed by Tukey's post hoc test for multiple group comparisons. The sample size used in each study was based upon the observed level of variation between individual experiments and the need for sufficient sample numbers to allow for accurate statistical analyses. In all cases, a p-value of $<.05$ was considered statistically significant, and all data were expressed as mean ± SD.

RESULTS

HTRA1 Production Is Upregulated During Osteogenic Induction of MSCs

Differentiation studies conducted using hBMSCs demonstrated a small but significant increase in the expression of *HTRA1* during the early phases of osteogenic induction with a greater than 1.5-fold ($p < .01$) increase in gene expression being attained by day 14 (Fig. 1A). However, unlike *HTRA1*, expression levels of the closely related HTRA family member, *HTRA3*, decreased during osteogenesis and remained significantly downregulated throughout the course of the study. The early induction of *HTRA1* gene expression was accompanied by significant increases in the expression of the well-known osteogenic markers runt-related transcription factor 2 (*RUNX2*), alkaline phosphatase (*ALP*), *IBSP*, and Collagen type 1A1 (Fig. 1A). The expression level of the late osteogenic marker secreted phosphoprotein 1/osteopontin (*SPP1*) was actually downregulated during early osteogenesis but became significantly increased during the late phase of osteogenesis at day 21, along with noticeable increases in mineralized matrix deposition beginning at day 10 as determined by Alizarin red staining (Fig. 1B). As HTRA1 functions primarily as a secreted protease, we also investigated the effect of osteogenic differentiation on HTRA1 protein secretion from hBMSCs using an HTRA1-specific ELISA and immunofluorescence staining. In accordance with increases in its gene expression, secreted HTRA1 protein levels were also elevated in both the supernatant (Fig. 1C) and in the cell matrices (Fig. 1D) of hBMSC cultures undergoing osteogenic differentiation. Clearly, therefore, induction of osteogenesis in hBMSCs has a major stimulatory effect on HTRA1 production resulting in both enhanced gene expression as well as protein secretion.

In order to investigate whether such effects were limited to adult human stem cells only, we extended these studies to include both mESCs and mASCs. *HtrA1* expression was also significantly upregulated in a time-dependent manner in mESCs (Fig. 2A) and mASCs grown in either 2D- (Fig. 2B) or 3D- (Fig. 2C) culture systems in response to osteogenic stimuli. These increases in *HtrA1* expression were associated with mineralization of differentiating bone-forming cells derived from 2D-culutres of either mESCs

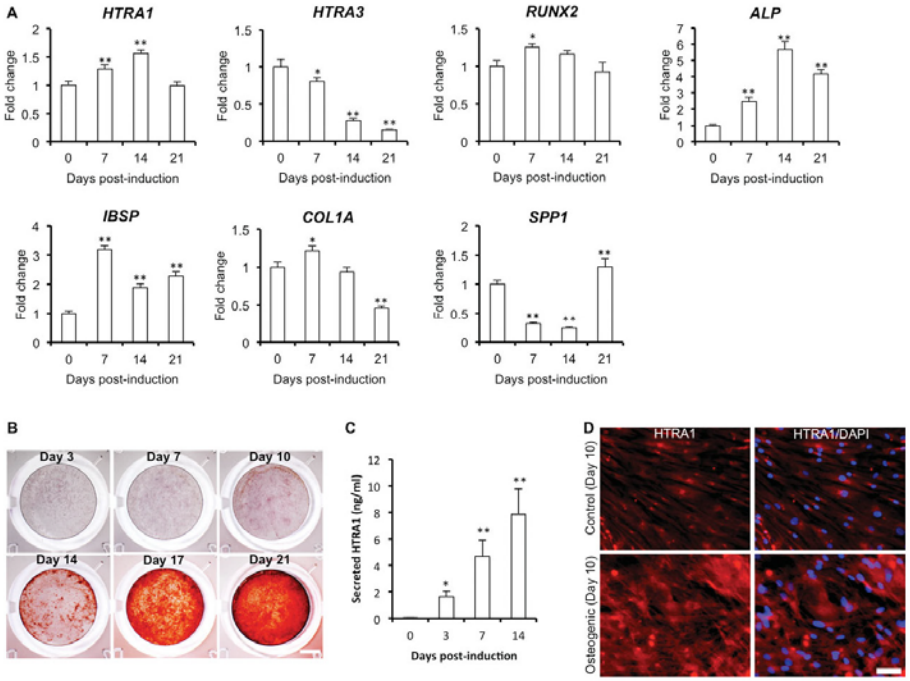

Figure 1. The expression and secretion of HTRA1 is significantly enhanced in human bone marrow-derived MSCs (hBMSCs) undergoing osteogenic differentiation. (**A**): Quantitative polymerase chain reaction analysis of genes regulated during osteogenic differentiation of hBMSCs. Data were normalized to beta glucuronidase and expressed as fold change as compared to noninduced controls at day 0 (value 1) using the comparative C_T method. Data are representative of two independent experiments performed in triplicate ± SD. *, $p < .05$; **, $p < .01$ as determined by one-way analysis of variance (ANOVA). (**B**): Representative images of Alizarin red-stained hBMSC cultures at various time points following osteogenic induction. Scale bar = 2 mm. (**C**): Secretion of HTRA1 by hBMSCs during osteogenic differentiation as determined by HTRA1-specific ELISA ($n = 4$). *, $p < .05$; **, $p < .01$ as determined by one-way ANOVA. (**D**): Representative fluorescence images of anti-HTRA1 (red) and DAPI (blue)-stained hBMSCs undergoing osteogenic differentiation. Scale bar = 25 μm. Abbreviations: ALP, alkaline phosphatase; COL1A, collagen type 1A1; DAPI, 4,6-diamidino-2-phenylindole; HTRA1, high-temperature requirement protease A1; IBSP, integrin-binding sialoprotein; RUNX2, runt-related transcription factor 2; SPP1, secreted phosphoprotein 1.

(Fig. 2D) or mASCs (Fig. 2E) as well as 3D-cultures composed of osteogenic mASCs (Fig. 2F). Furthermore, immunofluorescence staining of paraffin wax sections from mASC 3D-spheroids identified HtrA1 protein in tissues undergoing mineralization, but not in uninduced controls (Fig. 2G), thus giving a first hint as to its role in stem cell osteogenesis.

Silencing of the *HTRA1* Gene Impairs hBMSC Osteogenesis and Enhances Adipogenesis

In order to investigate the role of *HTRA1* gene expression in the regulation of osteogenesis, we next performed loss of function studies by means of RNA interference in hBMSC cultures. The transfection of hBMSCs with siRNA specific for *HTRA1* prior to osteogenic induction resulted in a significant downregulation of *HTRA1* gene expression (Fig. 3A) and HTRA1 protein secretion (Fig. 3B) that was sustained throughout the first 2 weeks of osteogenic differentiation. HTRA1 protein levels both within cells and the ECM were also markedly reduced (Supporting Information Fig. S1). This was accompanied by a noticeable reduction in Alizarin red staining at day 14, indicative of reduced mineral deposition in differentiating bone-forming cells (Fig. 3C). Biochemical analysis using the ALP activity assay revealed that these deficits in mineralization were accompanied by significant reductions in ALP protein activity, which were maintained for up to 14 days (Fig. 3D). Furthermore, *ALP* expression was also significantly downregulated in these cells at an early time point, although expression levels of the osteogenic markers *SPP1* and *RUNX2* were not significantly affected by *HTRA1* silencing (Fig. 3E).

Through the course of our studies, it became apparent that not only was osteogenesis reduced in hBMSCs following *HTRA1* gene silencing but also that the adipogenesis appeared to actually be increased. Evidence of this was first realized in late-stage osteogenic cultures of hBMSC treated with *HTRA1* siRNA, where phase-contrast microscopy revealed more cells containing lipid droplets, reminiscent of mature adipocytes although control siRNA cultures continued to demonstrate matrix mineralization (Fig. 3F). In order to confirm this finding, hBMSCs transfected with

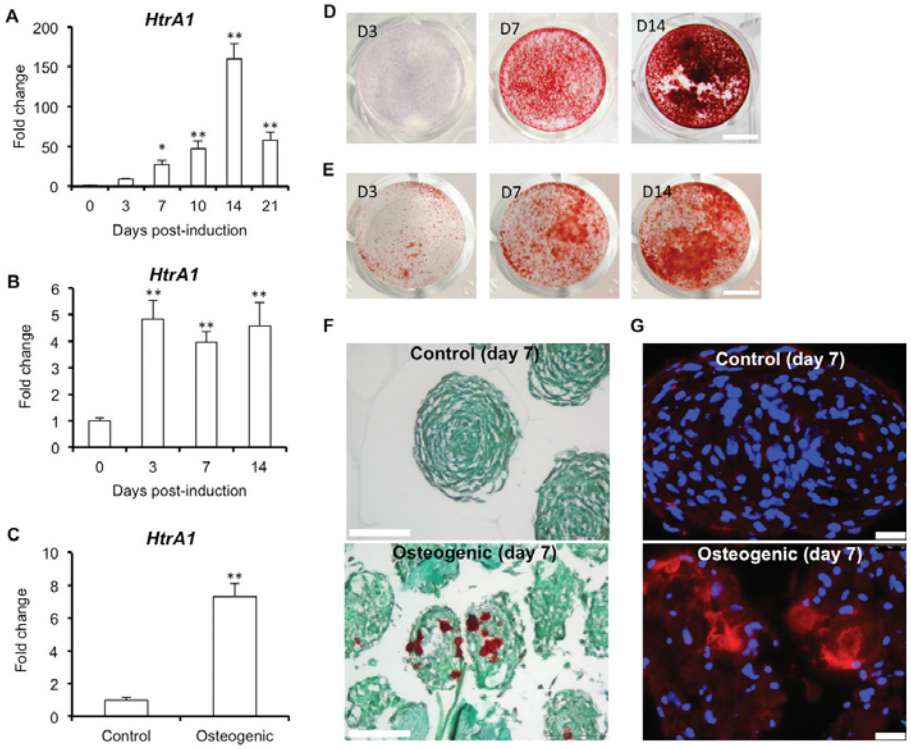

Figure 2. *HtrA1* gene expression is significantly increased in osteogenic mouse embryonic stem cells (mESCs) and mouse adipose-derived stromal cells (mASCs). **(A–C):** *HtrA1* gene expression during osteogenic differentiation of mESCs (A), mASCs (B), and mASC spheroids (day 7) (C) was determined by quantitative polymerase chain reaction and data were normalized to *Mrps12* and expressed as fold change as compared to noninduced controls (Day 0 and control; value 1) using the comparative C_T method. Data are representative of at least two independent experiments performed in triplicate ± SD. *, $p < .05$; **, $p < .01$ as determined by one-way analysis of variance. **(D, E):** Representative images of Alizarin red-stained mESCs (D) and mASCs (E) at various time points following osteogenic induction. Scale bar = 5 mm. **(F):** Representative images of Alizarin red and fast green-stained paraffin wax sections of mASC spheroids incubated without (control) or with osteogenic media (osteogenic) for 7 days. Scale bar = 100 μm. **(G):** Representative immunofluorescence images of HTRA1 (red) and 4,6-diamidino-2-phenylindole (blue) in paraffin wax sections of osteogenic mASC spheroids incubated without (control) or with osteogenic media (osteogenic) for 7 days. Scale bar = 25 μm. Abbreviation: HTRA1, high-temperature requirement protease A1.

either *HTRA1* siRNA or control siRNA were induced to undergo adipogenic differentiation and adipogenic gene expression measured by qRT-PCR (Fig. 3G) and triglyceride accumulation visualized by oil red O staining (Fig. 3H). As anticipated, silencing of the *HTRA1* gene greatly enhanced the number of oil red O-positive cells present with the hBMSC culture and significantly enhanced the expression of specific adipogenic gene markers, peroxisome proliferator-activated receptor gamma 2, and fatty acid binding protein 4, thereby supporting a differential role for HTRA1 in hBMSC lineage commitment.

Recombinant HTRA1 Protein Enhances hBMSC Osteogenesis

As previously mentioned, HTRA1 also exists as a secreted protease and thus may have an extracellular role in the osteogenic differentiation of hBMSCs. We therefore next investigated whether exogenously added recombinant human HTRA1 protein could also influence osteogenic differentiation. hBMSCs undergoing osteogenic differentiation were initially treated every 3 days with either active or inactive HTRA1 for up to 14 days and mineralization determined by Alizarin red staining. Indeed, mineral deposition by differentiating bone-forming cells was greatly enhanced following stimulation with active, but not inactive, HTRA1 (Fig. 4B). Additional studies confirmed that these effects could be reproduced in late-stage (day 10) cultures of osteogenic hBMSCs treated for only 4 days with HTRA1 (Fig. 4C). However, short-term treatment with HTRA1 during the first week of osteogenic differentiation only failed to elicit any noticeable increase in mineralization (Supporting Information Fig. S2), thus implying that the stimulatory actions of HTRA1 were dependent not only on its protease activity but also on the differentiation status of the cells. Further studies using the broad spectrum serine protease inhibitor, AEBSF, confirmed the

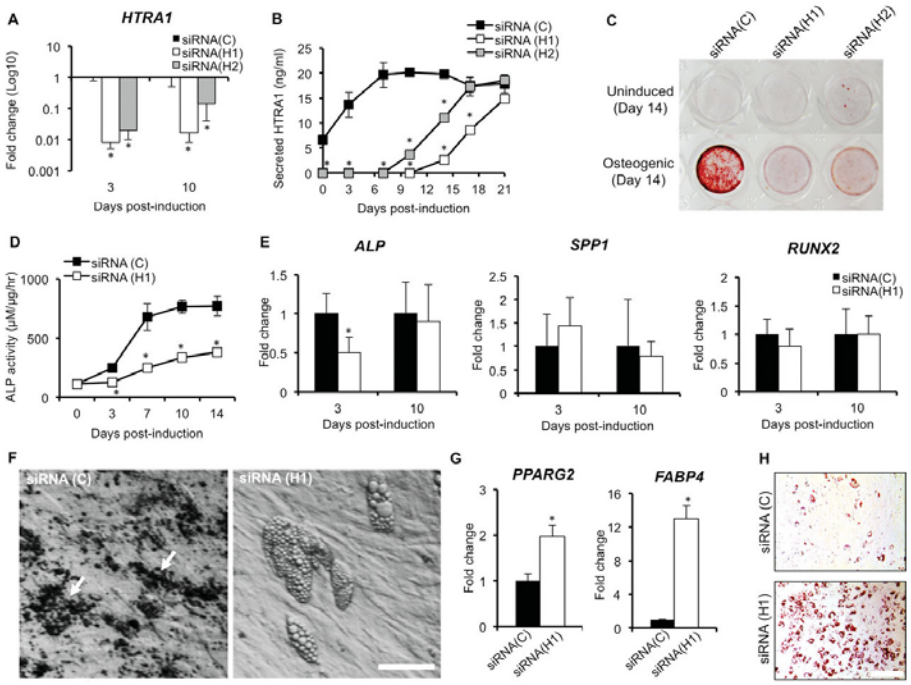

Figure 3. Repression of *HTRA1* gene expression alters lineage commitment of differentiating human bone marrow-derived mesenchymal stem cells (hBMSCs). (**A**): Quantitative polymerase chain reaction analysis of *HTRA1* gene expression in hBMSCs transfected with *HTRA1* siRNAs (siRNA [H1] or [H2]) or control siRNA (siRNA (C)) at 3 and 10 days postosteogenic induction. Data were normalized to beta glucuronidase (*GUSB*) and expressed as fold change (Log10 scale) as compared to cells transfected with control siRNA using the comparative C_T method. *, $p < .01$ as determined by one-way analysis of variance (ANOVA). $n = 3$ separate experiments, ± SD. (**B**): Enzyme-linked immunosorbent assay measurement of secreted HTRA1 from hBMSCs transfected with *HTRA1* siRNAs or control siRNA at various time points postosteogenic induction. *, $p < .01$ as determined by one-way ANOVA. $n = 3$ separate experiments, ± SD. (**C**): Representative images of Alizarin red-stained hBMSCs transfected with *HTRA1* siRNAs or control siRNA at 14 days postosteogenic induction. (**D**): ALP activity in protein lysates from hBMSC transfected with *HTRA1* siRNA or control siRNA at various time points postosteogenic induction. *, $p < .01$ as determined by one-way ANOVA. $n = 3$ separate experiments, ± SD. (**E**): Quantitative polymerase chain reaction analysis of *ALP*, *SPP1*, and *RUNX2* gene expression in hBMSCs transfected with *HTRA1* siRNA or control siRNA at 3 and 10 days postosteogenic induction. Data were normalized to *GUSB* and expressed as fold change as compared to cells transfected with a control siRNA (value 1) using the comparative C_T method. $n = 3$ separate experiments, ± SD. (**F**): Representative phase-contrast micrographs of hBMSCs transfected with control siRNA or *HTRA1* siRNA at 14 days postosteogenic induction. Arrows, mineral deposits. Scale bar = 10 μm. (**G**): Quantitative polymerase chain reaction analysis of *PPARG2* and *FABP4* gene expression in hBMSCs transfected with *HTRA1* siRNA or control siRNA at day 6 postadipogenic induction. Data were normalized to *GUSB* and expressed as fold change as compared to cells transfected with a control siRNA (value 1) using the comparative C_T method. Data are representative of two separate experiments, ± SD. *, $p < .01$ as determined by one-way ANOVA. (**H**): Microscopic images of oil red O-stained hBMSCs transfected with *HTRA1* siRNA or control siRNA at 7 days postadipogenic induction. Scale bar = 20 μm. Images are representative of two separate experiments. Abbreviations: *ALP*, alkaline phosphatase; *FABP4*, fatty acid binding protein 4; HTRA1, high-temperature requirement protease A1; *PPARG2*, peroxisome proliferator-activated receptor gamma 2; *RUNX2*, runt-related transcription factor 2; siRNA, small interfering ribonucleic acid; *SPP1*, secreted phosphoprotein 1.

stimulatory effects of HTRA1 to be dependent on its proteolytic activity (Fig. 4D). Although matrix mineralization was clearly enhanced in differentiating bone-forming cells treated with HTRA1, the expression of several well-known osteogenic markers including *ALP*, *RUNX2*, and *SPP1* remained unaltered at the time point tested (day 10) (Fig. 4E). However, significant increases were observed in the expression levels of *IBSP* and bone morphogenetic protein 5 (*BMP5*). Furthermore, a significant decrease in the expression level of sclerostin (*SOST*) was also observed in cells treated with HTRA1.

IBSP Represents a Novel HTRA1 Substrate During Osteogenic Differentiation of MSCs In Vitro

In this study, we demonstrated that although *IBSP* expression was significantly enhanced in hBMSCs following the addition of HTRA1, IBSP protein was almost completely abolished from the cellular matrix of these cultures, an effect not observed with inactive HTRA1 (Fig. 5A). This was regarded as being specifically due to the HTRA1 protein added due to the fact that collagen Type 1, a proteoglycan not degraded by HTRA1 [20], remained unaffected within the cell matrices

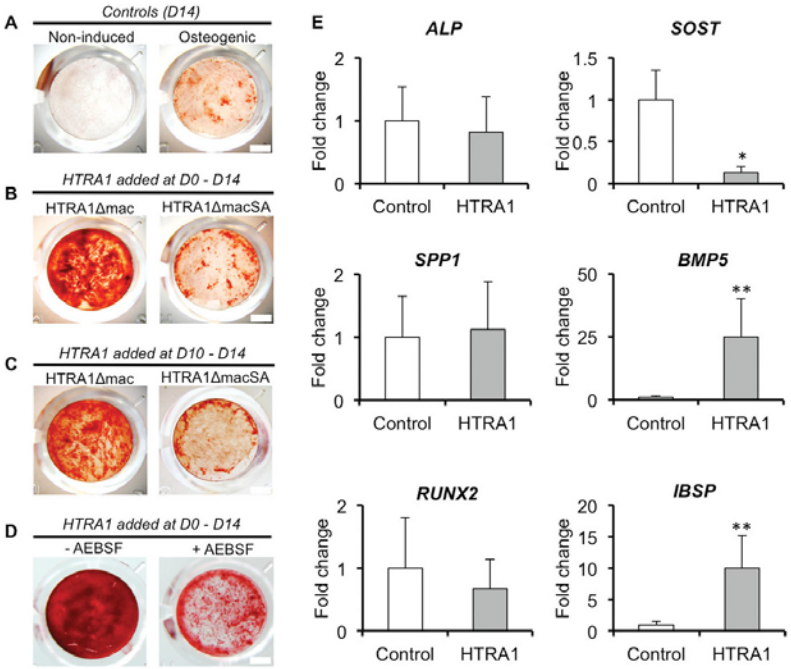

Figure 4. Exogenously added HTRA1 protein enhances human bone marrow-derived mesenchymal stem cell (hBMSC) osteogenic differentiation. **(A–D):** Representative images of Alizarin red-stained day 14 cultures of noninduced hBMSCs (noninduced control) and osteogenic-induced hBMSCs (A), osteogenic-induced hBMSCs previously treated with either proteolytically active (HTRA1Δmac) or inactive (HTRA1ΔmacSA) HTRA1 (5 μg/ml) for 14 days (B) or 4 days (C), and osteogenic-induced hBMSCs previously treated with proteolytically active HTRA1 (5 μg/ml) for 14 days in the presence or absence of AEBSF (20 μg/ml) (D). Data are representative of three independent experiments. Scale bar = 2 mm. **(E):** Quantitative polymerase chain reaction analysis of osteogenic gene expression in hBMSCs treated at day 7 with active HTRA1 (5 μg/ml) and harvested at day 10 postosteogenic induction. Data were normalized to beta glucuronidase and expressed as fold change as compared to untreated cells (value 1) using the comparative C_T method. $n = 3$ separate experiments, ± SD. *, $p < .05$; **, $p < .01$ as determined by Student's t test. Abbreviations: AEBSF, 4-(2-aminoethyl) benzenesulfonyl fluoride hydrochloride; *ALP*, alkaline phosphatase; BMP5, bone morphogenetic protein 5; HTRA1, high-temperature requirement protease A1; IBSP, integrin-binding sialoprotein; RUNX2, runt-related transcription factor 2; SPP1, secreted phosphoprotein 1.

(Supporting Information Fig. S3). The potential for proteolytically active HTRA1 to degrade IBSP was further confirmed by in vitro enzyme assays, where a noticeable reduction in recombinant human IBSP (476 nM) was evident after 8 hours incubation with HTRA1 (45 nM) as determined by Western blot analysis (Fig. 5B). We next used the mASC spheroid culture system to investigate whether endogenous HTRA1 protein could be localized to IBSP directly within differentiating MSCs. Paraffin wax sections of mASCs were stained for HTRA1 and IBSP at various stages of osteogenic differentiation and overlays produced to determine whether HTRA1 could be localized to areas of IBSP protein expression. IBSP was detected within mASC spheroids during the early phase of osteogenesis (day 5), although HTRA1 remained at very low levels and mineral deposition was not detected using Alizarin red staining (Fig. 5C, upper panel and Supporting Information Fig. S4A). By day 9, levels of HTRA1 had greatly increased and it was regularly found colocalized with IBSP in the tissue matrix (Fig. 5C, lower panel). In addition, mineralization of differentiating bone-forming cells within 3D-spheroids was also apparent at this time point as identified by intense Alizarin red staining (Supporting Information Fig. S4B). Sections incubated with isotype-matched IgG antibodies stained negative and served as controls (Supporting Information Fig. S4C).

Localization of HTRA1 and IBSP to Areas of New Bone Formation in Mice

In order to assess the potential involvement of HTRA1 in the reparative process of bone tissue, we used a previously well-established mouse femur osteotomy model (Fig. 6A) [24]. HTRA1 protein was identified in thin paraffin wax bone sections taken from mice at various stages of fracture repair using immunohistochemical staining. At day 7, early osteoid formation was observed within the bone marrow at the osteotomy site and was associated with intense staining for HTRA1 (Fig. 6B). At this time point, HTRA1 was also located within the cells and tissue of the overlying periosteal layer (Supporting Information Fig. S5A). By day 14, the nonmineralized callus had increased greatly in size with numerous HTRA1-positive fibroblast-like cells present throughout the tissue as well as in cells of the newly forming callus (Fig. 6C and Supporting Information Fig. S5B). Large numbers of HTRA1-

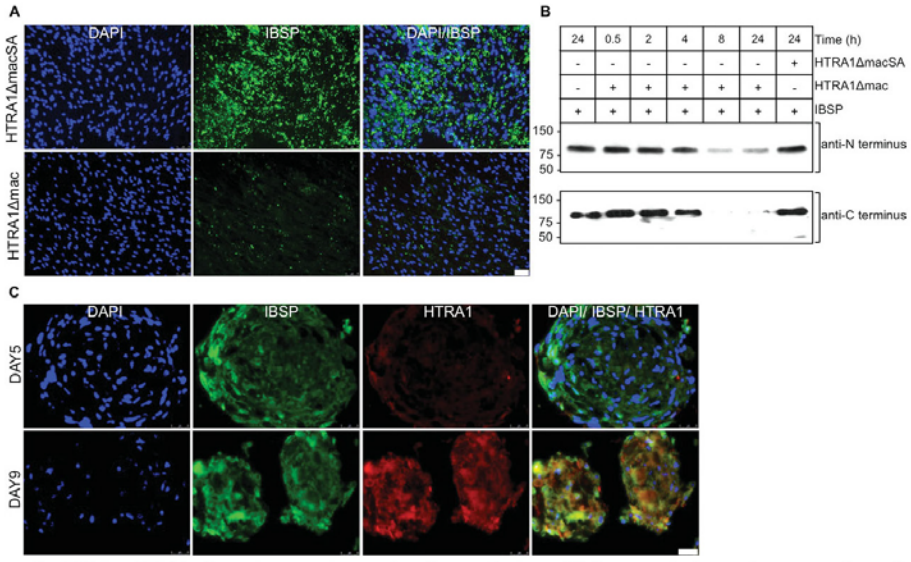

Figure 5. IBSP is an HTRA1 substrate in osteogenic mesenchymal stem cell cultures. (**A**): Representative immunofluorescence micrographs of anti-IBSP (ID1.2) (green) and DAPI (blue)-stained day 14 osteogenic human bone marrow-derived mesenchymal stem cells cultures previously treated for 4 days with 5 μg/ml of either inactive HTRA1 (HTRA1ΔmacSA) or active HTRA1 (HTRA1Δmac). Scale bar = 75 μm. (**B**): Western blot analysis of an in vitro enzyme assay using recombinant human IBSP (476 nM) and HTRA1ΔmacSA (45 nM) or HTRA1Δmac (45 nM), incubated together for up to 24 hours. Equal sample volumes were loaded onto an SDS-PAGE gel and IBSP protein detected using antibodies directed against either the N- or C-terminal regions of human IBSP. (**C**): Representative fluorescence images of anti-IBSP (ID1.2) (green), anti-HTRA1 (red), and DAPI (blue)-stained mouse adipose-derived stromal cell spheroids at 5 and 9 days postosteogenic induction. Scale bar = 25 μm. Data are representative of two independent experiments. Abbreviations: DAPI, 4,6-diamidino-2-phenylindole; HTRA1, high-temperature requirement protease A1; *IBSP*, integrin-binding sialoprotein.

positive chondrocytes were also evident within intact lacunae and represented the early stages of endochondral ossification. By day 28, a substantial proportion of the callus had been replaced by new bone and HTRA1 was now localized to specific areas of active bone formation (Fig. 6D) in association with cuboidal osteoblasts (Supporting Information Fig. S5C). By day 42, the osteotomy gap was almost completely healed (Fig. 6E) and the bone resembled that of a nonoperative control femur (Fig. 6F). In both cases, HTRA1 was almost completely absent, being localized to only a small number of osteocytes within the bone matrix.

Having confirmed that HTRA1 protein was indeed present within actively forming bone tissue, we conducted further investigations to determine whether HTRA1 could also be localized to IBSP within these bone sections, thus providing a potential mode of action for HTRA1 in the context of osteogenesis in vivo. Indeed, colocalization of HTRA1 and IBSP was identified in paraffin wax bone sections from 28-day postoperative mice by double immunofluorescence staining, being confined to areas previously identified as undergoing active regeneration (Fig. 7 and Supporting Information Fig. S6).

Discussion

A complex molecular network of signaling pathways and regulatory factors governs the osteogenesis of multipotent MSCs [17, 18, 27], being reliant on the activation and regulation of a number of key molecular targets including *RUNX2*, *ALP*, *SPP1*, and *IBSP* [28]. Although there have been significant advances in our understanding of the molecular mechanisms involved in controlling osteogenic differentiation, the influence of serine proteases on such processes remains relatively obscure. In this study, we have shown for the first time that the serine protease HTRA1 is a positive regulator of MSC osteogenesis and its presence is required for the efficient mineralization of differentiating bone cells.

The expression of *HTRA1* was upregulated in hBMSCs upon osteogenic induction and was associated with significant increases in the levels of its secreted protein product. Furthermore, HTRA1 production was increased in a time-dependent manner throughout the course of osteogenic differentiation and was closely associated with the appearance of mineralized matrix. Interestingly, expression levels of the closely related HTRA family member, *HTRA3*, were actually downregulated during osteogenesis. This was of particular interest as HTRA1 and HTRA3 are considered to have overlapping functions due to close structural similarities [29]. It may well be therefore that HTRA1 and HTRA3 play differential roles in mediating the osteogenesis of hBMSCs. This pattern of HTRA1 production during osteogenesis of hBMSCs was recapitulated in cultures composed of either mASCs or mESCs, where significant increases in *HtrA1* expression coincided with the appearance of HtrA1 protein and mineralized matrix. Although previous investigations have alluded to the involvement of HTRA1 in mouse osteogenesis [19, 20], our study is the first to report the potential

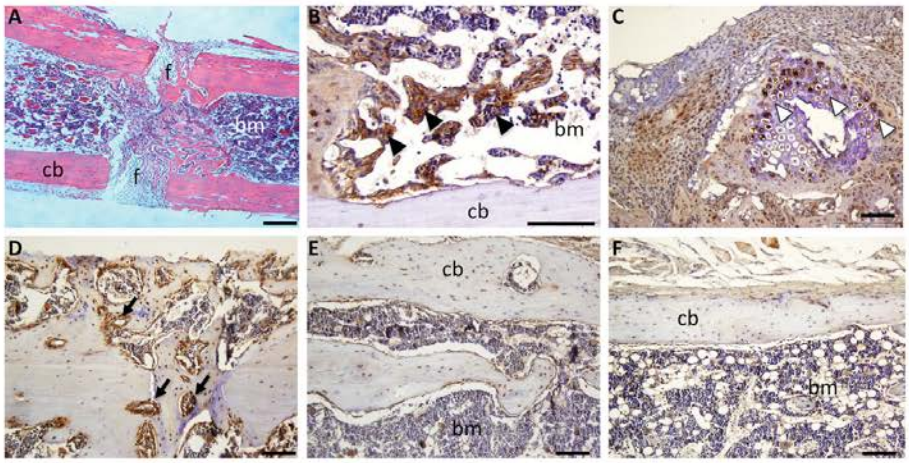

Figure 6. High-temperature requirement protease A1 (HTRA1) protein levels are increased during bone regeneration. (**A**): Representative micrograph of a hematoxylin and eosin-stained paraffin wax section of decalcified mouse femur 7 days following a 0.22 μm osteotomy. Scale bar = 250 μm. **(B–F):** Representative micrographs of anti-HTRA1 (brown)-stained paraffin wax sections of decalcified mouse femora (representative of $n = 3$) at 7 (B), 14 (C), 28 (D), and 42 (E) days following osteotomy. Nonoperative femora served as controls (F). HTRA1 was visualized using horseradish peroxidase-diaminodenzidine and sections counterstained with hematoxylin. HTRA1-positive staining is identified in osteoid (closed arrow heads) at day 7 (B), in chondrocyte lacunae (open arrow heads) and soft tissue, *t*, at day 14 (C), and in sites of active bone regeneration (arrows) at day 28 (D). Scale bar = 100 μm. Abbreviations: bm, bone marrow; cb, cortical bone; f, fracture gap.

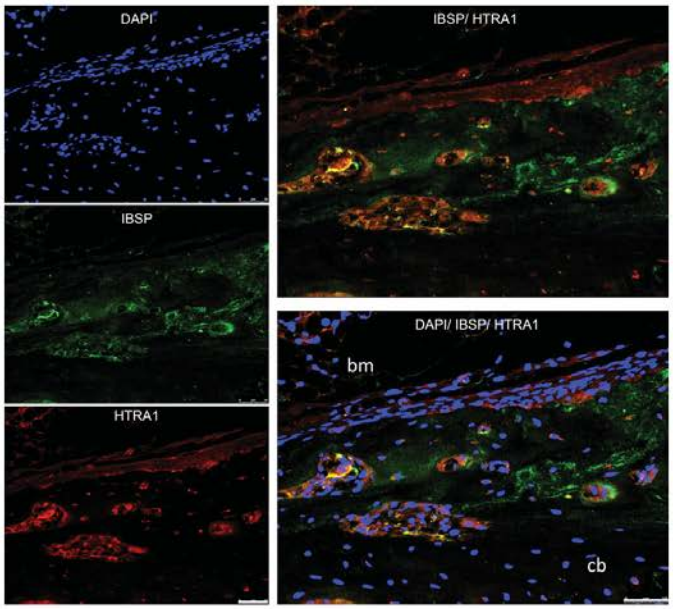

Figure 7. HTRA1 and IBSP colocalize during bone regeneration. Representative immunofluorescence micrographs of paraffin wax sections of decalcified mouse femora at 28 days following osteotomy stained with DAPI (blue), anti-IBSP (ID1.2) (green), and anti-HTRA1 (red). Scale bar = 50 μm. Abbreviations: bm, bone marrow; cb, cortical bone; DAPI, 4,6-diamidino-2-phenylindole; HTRA1, high-temperature requirement protease A1; IBSP, integrin-binding sialoprotein.

role of HTRA1 in human osteogenesis. Based on earlier reports of HTRA1 imparting a negative influence over mineral deposition by murine 2T3 osteoblasts [20], initial expectations were for HTRA1 to inhibit osteogenesis of hBMSCs and thus prevent mineralization of differentiating human bone-forming cells. On the contrary, we found that siRNA-induced loss of HTRA1 function in hBMSCs, effectively suppressed the stimulatory effects of osteogenic culture medium on *ALP* expression and intracellular ALP protein activity by hBMSCs as well as the formation of a mineralized matrix. Although *ALP* expression levels were compromised in cells lacking *HTRA1*, some of the key regulatory factors involved in osteogenesis, including *RUNX2* and *SPP1*, remained intact. It is possible therefore that HTRA1 mediates its effects through specific pathways, independent of these particular elements. In addition to its effects on osteogenesis, *HTRA1* silencing had a profound effect on hBMSC adipogenesis as evidenced by increases in adipogenic gene expression and oil droplet formation. Such observations would suggest that HTRA1 may in fact represent a decisive factor in determining stem cell lineage commitment and that its involvement in stem cell differentiation go somewhat beyond it simply being a mediator of osteoblast formation. Further investigations into the role of HTRA1 in other differentiation pathways, such as chondrogenesis, myogenesis, or even tenogenesis, would therefore represent a logical progression of these studies and may hold particular relevance with regards to the involvement of HTRA1 in musculoskeletal development as has previously been inferred [19].

Based on the fact that HTRA1 is a secreted serine protease, we next directed our attention to the possible influence of HTRA1 on hBMSC osteogenesis by way of its extracellular effects. A specific role for HTRA1 in the osteogenesis of hBMSCs and mineralization of differentiating bone-forming cells was confirmed in studies using both proteolytically active and inactive recombinant forms of human HTRA1 as well the broad spectrum serine protease inhibitor AEBSF. An increase in mineralized matrix formation was observed in cells treated with active HTRA1 only, and was dependent on HTRA1 being present during the initiation phase of mineralization, as short duration treatments prior to the onset of mineralization proved ineffective. This would therefore infer that the stimulatory effects of exogenously added HTRA1 protein on hBMSC osteogenesis and mineralization of differentiating bone-forming cells may be reliant on its ability to regulate factors present within the actively mineralizing ECM. In addition to its ability to affect ECM mineral content, HTRA1 also induced a significant upregulation in the expression of several positive regulators of mineralization, including *BMP5* and *IBSP* [30, 31], although a large proportion of well-known osteogenic genes such as *RUNX2*, *ALP*, and *SPP1* remained unaffected. In addition, the expression level of a potent negative-regulator of mineral formation, *SOST* [32, 33], was markedly downregulated in hBMSCs treated with HTRA1 and may thus represent an additional mechanism by which mineral deposition is enhanced in differentiating bone-forming cells. It is possible, therefore, that the effects of HTRA1 protein on hBMSC mineralization may be mediated indirectly through its ability to modulate the production of both activators and inhibitors of osteogenic differentiation and/or mineralization. These results are in stark contrast to the findings presented in a previous report by Hadfield et al. [20], where HTRA1 was shown to impart a negative influence over mineralized matrix formation by mouse 2T3 osteoblasts. One possible explanation may lie within the fact that 2T3 cells are derived from transgenic mice overexpressing the simian virus 40 (SV40) T antigen and as such are immortalized [34]. The fact that *HTRA1* gene expression is known to be significantly affected in SV40 transformed cells [35] would imply that modifications of the osteogenic status of these cells brought about by changes in HTRA1 expression and activity may not be truly representative of nonimmortalized, primary cells. Further studies aimed at determining the effects of *HtrA1* gene silencing or exogenously added recombinant HTRA1 on primary mASC osteogenesis may help to clarify this point.

Of the osteogenic genes that were regulated by HTRA1, *IBSP* held particular relevance to this study due to the fact that its ability to regulate mineral deposition has previously been reported to be dependent on the actions of serine proteases [15]. Attention was therefore focused on IBSP and its potential involvement in mediating the effects of HTRA1 on both osteogenesis of MSCs and mineralization of differentiating bone-forming cells. IBSP belongs to the family of SIBLING proteins which also includes osteopontin, dentin matrix protein 1, dentin siaolophosphoprotein, and matrix extracellular phosphoglycoprotein [36]. IBSP, along with other SIBLING proteins, is found almost exclusively in bone and dentin and is a major constituent of the mineralizing matrix during new bone formation [37–39]. The primary biological function of IBSP is unclear, although it has been reported to be involved in the initiation of matrix mineralization through the nucleation of hydroxyapatite crystals [40, 41]. Furthermore, it has been proposed that IBSP is required to undergo fragmentation, possibly through the actions of serine proteases, in order to allow for efficient matrix mineralization [15, 42, 43]. In this report, we were able to demonstrate colocalization of HTRA1 and IBSP in osteo-induced mASC spheroid cultures, thus confirming the potential for endogenous HTRA1 to interact with IBSP under osteogenic culture conditions. Additional immunofluorescence analyses of hBMSCs treated with exogenous HTRA1 revealed that this interaction most likely resulted in the digestion and subsequent removal of IBSP protein from the mineralizing matrix. These results would therefore suggest that the stimulatory effects of secreted HTRA1 protein on matrix mineralization in vitro are mediated, at least in part, through its proteolytic actions on IBSP within the ECM. The potential for HTRA1-induced IBSP proteolysis was further confirmed by Western blot analysis where proteolytically active HTRA1 effectively digested recombinant human IBSP protein at equivalent concentrations to those used in the cell culture studies. However, despite us using two different antibodies raised against either the N- or C-terminal regions of IBSP, we were unable to detect any HTRA1 digest fragments. This was somewhat unexpected, as findings from previous studies suggest that IBSP fragmentation plays an important role in its function as an instigator of mineral nodule formation [15]. This is based on the assumption that IBSP facilitates mineralization predominantly through its ability to bind and nucleate hydroxyapatite, although evidence exists to suggest that both intact and fragmented IBSP can also inhibit hydroxyapatite-seeded crystal growth [44]. It is possible therefore that HTRA1 contributes to osteogenesis through the controlled turnover of IBSP within the mineralizing ECM. This is further supported by the observation that *IBSP* gene expression is upregulated by exogenous HTRA1 at the expense of its protein product and may thus constitute a novel feedback mechanism through which HTRA1 regulates matrix mineralization.

The osteogenic differentiation of BMSCs toward mature bone-forming osteoblasts is a critical step in the development and repair of bone tissue. In this study, we used a previously well-established mouse osteotomy model to investigate the expression of HTRA1 protein during bone healing. Immunohistochemical analysis identified high levels of HTRA1 protein within areas of active bone formation at various stages of bone repair although no positive staining was observed in tissue sections from intact bone, thus confirming it to be primarily involved in de novo bone formation. Furthermore, strong positive staining for HTRA1 was also evident in callus tissue

harboring large numbers of chondrocytes and is thus suggestive of its role in both chondrogenesis and endochondral ossification. Such findings could be of significant importance to fracture healing and possibly even cartilage formation, and as such, warrant further investigation. Immunofluorescence analysis of these sections revealed a close association of HTRA1 with IBSP in areas considered to be undergoing active bone regeneration. This lends support to the theory that HTRA1 regulates both osteogenesis of MSCs and mineralization of differentiating bone-forming cells through its interactions with IBSP, although it does not exclude the possibility that HTRA1 mediates its actions through the proteolytic processing of other SIBLING members [45–48].

Summary

The findings from this study therefore implicate HTRA1 as a positive regulator of both osteogenesis of MSCs and mineralization of differentiating bone-forming cells, possibly at the expense of adipogenic differentiation. Based on these properties, HTRA1 may be deemed as a key factor in determining the outcome of diseases such as age-related osteoporosis, where impaired BMSC osteogenesis and upregulated adipogenesis is believed to be a major contributor to the underlying pathology [24, 49].

Acknowledgments

This study was supported in part by the Swiss National Science Foundation Grant 31003A-134935; CABMM Start-up Grant; Forschungskredit of the University of Zurich; Novartis Foundation, formerly Ciba-Geigy-Jubilee-Foundation; and Uniscientia Foundation.

Disclosure of Potential Conflicts of Interest

The authors indicate no potential conflicts of interest.

References

1 Clausen T, Southan C, Ehrmann M. The HtrA family of proteases: Implications for protein composition and cell fate. Mol Cell 2002;10:443–455.
2 Clausen T, Kaiser M, Huber R et al. HTRA proteases: Regulated proteolysis in protein quality control. Nat Rev Mol Cell Biol 2011;12:152–162.
3 Vande Walle L, Lamkanfi M, Vandenabeele P. The mitochondrial serine protease HtrA2/Omi: An overview. Cell Death Diff 2008;15:453–460.
4 Zurawa-Janicka D, Skorko-Glonek J, Lipinska B. HtrA proteins as targets in therapy of cancer and other diseases. Expert Opin Ther Targets 2010;14:665–679.
5 Chien J, Staub J, Hu SI et al. A candidate tumor suppressor HtrA1 is downregulated in ovarian cancer. Oncogene 2004;23:1636–1644.
6 Baldi A, De Luca A, Morini M et al. The HtrA1 serine protease is down-regulated during human melanoma progression and represses growth of metastatic melanoma cells. Oncogene 2002;21:6684–6688.
7 Hu SI, Carozza M, Klein M et al. Human HtrA, an evolutionarily conserved serine protease identified as a differentially expressed gene product in osteoarthritic cartilage. J Biol Chem 1998;273:34406–34412.
8 Wu J, Liu W, Bemis A et al. Comparative proteomic characterization of articular cartilage tissue from normal donors and patients with osteoarthritis. Arthritis Rheum 2007;56:3675–3684.
9 Grau S, Richards PJ, Kerr B et al. The role of human HtrA1 in arthritic disease. J Biol Chem 2006;281:6124–6129.
10 Tsuchiya A, Yano M, Tocharus J et al. Expression of mouse HtrA1 serine protease in normal bone and cartilage and its upregulation in joint cartilage damaged by experimental arthritis. Bone 2005;37:323–336.
11 Zhu W, Robey PG, Boskey AL. The regulatory role of matrix proteins in mineralization of bone. In: Marcus R, Feldman D, Nelson DA et al. Osteoporosis 3rd ed. Elsevier Academic Press, 2007; Chapter 9: 191–240.
12 Kundu AK, Putnam AJ. Vitronectin and collagen I differentially regulate osteogenesis in mesenchymal stem cells. Biochem Biophys Res Commun 2006;347:347–357.
13 Huang CH, Chen MH, Young TH et al. Interactive effects of mechanical stretching and extracellular matrix proteins on initiating osteogenic differentiation of human mesenchymal stem cells. J Cell Biochem 2009;108:1263–1273.
14 Klees RF, Salasznyk RM, Kingsley K et al. Laminin-5 induces osteogenic gene expression in human mesenchymal stem cells through an ERK-dependent pathway. Mol Biol Cell 2005;16:881–890.
15 Huffman NT, Keightley JA, Chaoying C et al. Association of specific proteolytic processing of bone sialoprotein and bone acidic glycoprotein-75 with mineralization within biomineralization foci. J Biol Chem 2007;282:26002–26013.
16 Bruder SP, Fink DJ, Caplan AI. Mesenchymal stem cells in bone development, bone repair, and skeletal regeneration therapy. J Cell Biochem 1994;56:283–294.
17 Marie PJ. Transcription factors controlling osteoblastogenesis. Arch Biochem Biophys 2008;473:98–105.
18 Komori T. Regulation of bone development and maintenance by Runx2. Front Biosci 2008;13:898–903.
19 Oka C, Tsujimoto R, Kajikawa M et al. HtrA1 serine protease inhibits signaling mediated by Tgfbeta family proteins. Development 2004;131:1041–1053.
20 Hadfield KD, Rock CF, Inkson CA et al. HtrA1 inhibits mineral deposition by osteoblasts: Requirement for the protease and PDZ domains. J Biol Chem 2008;283:5928–5938.
21 Mirsaidi A, Kleinhans KN, Rimann M et al. Telomere length, telomerase activity and osteogenic differentiation are maintained in adipose-derived stromal cells from senile osteoporotic SAMP6 mice. J Tissue Eng Regen Med 2012;6:378–390.
22 Casanova EA, Shakhova O, Patel SS et al. Pramel7 mediates LIF/STAT3-dependent self-renewal in embryonic stem cells. Stem Cells 2011;29:474–485.
23 Hooper M, Hardy K, Handyside A et al. HPRT-deficient (Lesch-Nyhan) mouse embryos derived from germline colonization by cultured cells. Nature 1987;326:292–295.
24 Egermann M, Heil P, Tami A et al. Influence of defective bone marrow osteogenesis on fracture repair in an experimental model of senile osteoporosis. J Orthop Res 2010;28:798–804.
25 Kelm JM, Moritz W, Schmidt D et al. In vitro vascularization of human connective microtissues. In: Hauser H, Fussenegger M, eds. Tissue Engineering. Series: Methods in Molecular Medicine. 2nd ed. Humana Press, 2007:162–164.
26 Grau S, Baldi A, Bussani R et al. Implications of the serine protease HtrA1 in amyloid precursor protein processing and Alzheimer's disease. Proc Natl Acad Sci USA 2005;102:6021–6026.
27 Deng ZL, Sharff KA, Tang N et al. Regulation of osteogenic differentiation during skeletal development. Front Biosci 2008;13:2001–2021.
28 Nishimura R, Hata K, Ikeda F et al. Signal transduction and transcriptional regulation during mesenchymal cell differentiation. J Bone Miner Metab 2008;26:203–212.
29 Tocharus J, Tsuchiya A, Kajikawa M et al. Developmentally regulated expression of mouse HtrA3 and its role as an inhibitor of TGF-beta signaling. Dev Growth Differ 2004;46:257–274.
30 Mailhot G, Yang M, Mason-Savas A et al. BMP-5 expression increases during chondrocyte differentiation in vivo and in vitro and promotes proliferation and cartilage matrix synthesis in primary chondrocyte cultures. J Cell Physiol 2008;214:56–64.
31 Gordon JA, Tye CE, Sampaio AV et al. Bone sialoprotein expression enhances osteoblast differentiation and matrix mineralization in vitro. Bone 2007;41:462–473.
32 ten Dijke P, Krause C, de Gorter DJ et al. Osteocyte-derived sclerostin inhibits bone formation: Its role in bone morphogenetic protein and Wnt signaling. J Bone Joint Surg Am 2008;90(suppl 1):31–35.

33 Krause C, Korchynskyi O, de Rooij K et al. Distinct modes of inhibition by sclerostin on bone morphogenetic protein and Wnt signaling pathways. J Biol Chem 2010;285:41614–41626.
34 Ghosh-Choudhury N, Windle JJ, Koop BA et al. Immortalized murine osteoblasts derived from BMP 2-T-antigen expressing transgenic mice. Endocrinology 1996;137:331–339.
35 Zumbrunn J, Trueb B. Primary structure of a putative serine protease specific for IGF-binding proteins. FEBS Lett 1996;398:187–192.
36 Qin C, Baba O, Butler WT. Post-translational modifications of sibling proteins and their roles in osteogenesis and dentinogenesis. Crit Rev Oral Biol Med 2004;15:126–136.
37 Fisher LW, Whitson SW, Avioli LV et al. Matrix sialoprotein of developing bone. J Biol Chem 1983;258:12723–12727.
38 Chen JK, Shapiro HS, Wrana JL et al. Localization of bone sialoprotein (BSP) expression to sites of mineralized tissue formation in fetal rat tissues by in situ hybridization. Matrix 1991;11:133–143.
39 Bianco P, Fisher LW, Young MF et al. Expression of bone sialoprotein (BSP) in developing human tissues. Calcif Tissue Int 1991;49:421–426.
40 Hunter GK, Goldberg HA. Nucleation of hydroxyapatite by bone sialoprotein. Proc Natl Acad Sci USA 1993;90:8562–8565.
41 Tye CE, Rattray KR, Warner KJ et al. Delineation of the hydroxyapatite-nucleating domains of bone sialoprotein. J Biol Chem 2003;278:7949–7955.
42 Kobayashi D, Takita H, Mizuno M et al. Time-dependent expression of bone sialoprotein fragments in osteogenesis induced by bone morphogenetic protein. J Biochem 1996;119:475–481.
43 Gorski JP, Huffman NT, Cui C et al. Potential role of proprotein convertase SKI-1 in the mineralization of primary bone. Cells Tissues Organs 2009;189:25–32.
44 Stubbs JT 3rd, Mintz KP, Eanes ED et al. Characterization of native and recombinant bone sialoprotein: Delineation of the mineral-binding and cell adhesion domains and structural analysis of the RGD domain. J Bone Miner Res 1997;12:1210–1222.
45 Nagata T, Bellows CG, Kasugai S et al. Biosynthesis of bone proteins [SPP-1 (secreted phosphoprotein-1, osteopontin), Bsp (bone sialoprotein) and sparc (osteonectin)] in association with mineralized-tissue formation by fetal-rat calvarial cells in culture. Biochem J 1991;274:513–520.
46 Tsuchiya S, Simmer JP, Hu JC et al. Astacin proteases cleave dentin sialophosphoprotein (DSPP) to generate dentin phosphoprotein (DPP). J Bone Miner Res 2011;26:220–228.
47 Steiglitz BM, Ayala M, Narayanan K et al. Bone morphogenetic protein-1/tolloid-like proteinases process dentin matrix protein-1. J Biol Chem 2004;279:980–986.
48 Guo R, Rowe PS, Liu S et al. Inhibition of MEPE cleavage by Phex. Biochem Biophys Res Commun 2002;297:38–45.
49 Rodriguez JP, Garat S, Gajardo H et al. Abnormal osteogenesis in osteoporotic patients is reflected by altered mesenchymal stem cells dynamics. J Cell Biochem 1999;75:414–423.


See www.StemCells.com for supporting information available online.

2.1.5. Detrimental role for human high temperature requirement serine protease A1 (HTRA1) in the pathogenesis of intervertebral disc (IVD) degeneration.

Authors: Tiaden AN, Klawitter M, Lux V, Mirsaidi A, Bahrenberg G, **Glanz S**, Quero L, Liebscher T, Wuertz K, Ehrmann M, Richards PJ.

Journal: *J Biol Chem. 2012;287(25):21335-45. IF:4.573*

Contribution: Assistance in generation of qPCR data and immunoblotting.

THE JOURNAL OF BIOLOGICAL CHEMISTRY VOL. 287, NO. 25, pp. 21335–21345, June 15, 2012

Detrimental Role for Human High Temperature Requirement Serine Protease A1 (HTRA1) in the Pathogenesis of Intervertebral Disc (IVD) Degeneration*[S]

Received for publication, January 24, 2012, and in revised form, April 30, 2012 Published, JBC Papers in Press, May 3, 2012, DOI 10.1074/jbc.M112.341032

André N. Tiaden[‡1], **Marina Klawitter**[‡§1,2], **Vanda Lux**[¶], **Ali Mirsaidi**[‡‖3], **Gregor Bahrenberg**[‡‖2], **Stephan Glanz**[‡‖2], **Lilian Quero**[§4], **Thomas Liebscher**[**], **Karin Wuertz**[§‖‡‡4], **Michael Ehrmann**[¶], **and Peter J. Richards**[‡‖5]

From the [‡]Bone and Stem Cell Research Group and the [§]Spine Research Group, Center for Applied Biotechnology and Molecular Medicine, University of Zurich, 8057 Zurich, Switzerland, the [¶]Centre for Medical Biotechnology, Faculty of Biology and Geography, University Duisburg-Essen, 45117 Essen, Germany, the [‖]Institute of Physiology and Zurich Center for Integrative Human Physiology (ZIHP), University of Zurich, 8057 Zurich, Switzerland, the [**]Department of Spinal Surgery, SRH Klinikum Karlsbad-Langensteinbach, 76307 Karlsbad, Germany, and the [‡‡]AOSpine Research Network, 8600 Duebendorf, Switzerland

Background: HTRA1 has been associated with intervertebral disc (IVD) degeneration although its role is unknown.
Results: HTRA1 up-regulated matrix metalloproteinase (MMP) production by IVD cells via the generation of fibronectin fragments.
Conclusion: HTRA1 plays a detrimental role in the pathogenesis of IVD degeneration.
Significance: HTRA1 may represent a novel therapeutic target for the treatment of spinal disc degeneration.

Human HTRA1 is a highly conserved secreted serine protease that degrades numerous extracellular matrix proteins. We have previously identified HTRA1 as being up-regulated in osteoarthritic patients and as having the potential to regulate matrix metalloproteinase (MMP) expression in synovial fibroblasts through the generation of fibronectin fragments. In the present report, we have extended these studies and investigated the role of HTRA1 in the pathogenesis of intervertebral disc (IVD) degeneration. *HTRA1* mRNA expression was significantly elevated in degenerated disc tissue and was associated with increased protein levels. However, these increases did not correlate with the appearance of rs11200638 single nucleotide polymorphism in the promoter region of the *HTRA1* gene, as has previously been suggested. Recombinant HTRA1 induced MMP production in IVD cell cultures through a mechanism critically dependent on MEK but independent of IL-1β signaling. The use of a catalytically inactive mutant confirmed these effects to be primarily due to HTRA1 serine protease activity. HTRA1-induced fibronectin proteolysis resulted in the generation of various sized fragments, which when added to IVD cells in culture, caused a significant increase in MMP expression. Furthermore, one of these fragments was identified as being the amino-terminal fibrin- and heparin-binding domain and was also found to be increased within HTRA1-treated IVD cell cultures as well as in disc tissue from patients with IVD degeneration. Our results therefore support a scenario in which HTRA1 promotes IVD degeneration through the proteolytic cleavage of fibronectin and subsequent activation of resident disc cells.

Degeneration of the intervertebral disc (IVD)[6] is now regarded as one of the major causes of lower back pain, which is a highly prevalent, debilitating, and costly disorder (1, 2). The pathogenesis of degeneration is a highly complex and poorly understood process with many different genetic, biological, and mechanical influences playing key roles in the breakdown of extracellular matrix (ECM) components (3). The predominant means by which ECM is degraded is thought to be due to the proteolytic actions of matrix metalloproteinases (MMPs) and aggrecanases (ADAMTS). A number of MMPs, including MMP-1, -3, -7, -9, and -13, as well as ADAMTS-4, have been shown to increase in the IVD during disc degeneration and are responsible for the breakdown of several matrix components, the most notable being aggrecan and collagen (4–7). Both MMPs and their inhibitors (TIMP-1, -2, and -3) have been localized to the resident chondrocyte-like cells of the nucleus pulposus and inner fibrosus compartments of the IVD (4), thus implicating these cells in disease pathogenesis. The secretion of MMPs by human IVD cells is mediated in part through the stimulatory effects of various pro-inflammatory cytokines, the most prominent of which is IL-1β (8). In addition, fibronectin peptide fragments of the ECM have also been shown to induce MMP production by IVD cells (9) and are potent instigators of experimental disc degeneration (10). Moreover, fibronectin fragments have been shown to accumulate in the IVD during

* This work was supported by a grant from the Center for Applied Biotechnology and Molecular Medicine Start-up Grant/Mäxi Foundation.
[S] This article contains supplemental Table 1 and Figs. 1–4.
[1] Both authors contributed equally to this work.
[2] Supported by grants from the Swiss National Science Foundation.
[3] Supported by grants from the Stiftung Osteoporose Schweiz and Forschungskredit UZH, University of Zurich.
[4] Supported by grants from AOSpine. We thank Dr. Jurgen Klasen (University Hospital Balgrist, University of Zurich, Zurich, Switzerland) for providing fresh human disc biopsies used for all cell culture experiments.
[5] To whom correspondence should be addressed: Center for Applied Biotechnology and Molecular Medicine, University of Zürich, Winterthurerstrasse 190, Zürich 8057, Switzerland. Tel.: 41-44-635-3801; Fax: 41-44-635-6840; E-mail: peter.richards@cabmm.uzh.ch.

[6] The abbreviations used are: IVD, intervertebral disc; ECM, extracellular matrix; SNP, single nucleotide polymorphism; MMP, matrix metalloproteinase; IL-1RA, IL-1 receptor antagonist; ANOVA, analysis of variance; qRT-PCR, quantitative RT-PCR.

degeneration (11), although the proteases responsible for their formation remain elusive.

Human HTRA1 (high temperature requirement serine protease A1) belongs to a well defined family of serine proteases originally identified in bacteria (12). Although primarily regarded as a key regulator of tumor development and subsequent malignancies (13–15), a growing body of evidence now exists to suggest that HTRA1 may also play a central role in determining the outcome of various musculoskeletal disease pathologies, including Duchenne muscular dystrophy (16), osteoarthritis (17–19), and rheumatoid arthritis (19, 20). It has recently been shown in a Japanese population study that a single nucleotide polymorphism (SNP) located within the HTRA1 promoter is associated with spinal disc degeneration, where increases in spinal disc narrowing were observed in patients without the G allele (AA) as compared with those bearing at least one G allele (GG + GA) (21). It would therefore appear that HTRA1 may also play a role in disc pathology, although its influence on disease and its mechanism of action have not yet been elucidated.

Observations from our own studies examining the role of HTRA1 in osteoarthritis imply that HTRA1 may actually have a detrimental effect on the pathogenesis of musculoskeletal disease. Elevated levels of HTRA1 protein were measured in the synovial fluid from osteoarthritic patients, and primary synovial fibroblasts isolated from diseased patients were identified as being a major source of HTRA1 (19). The addition of proteolytically active HTRA1 to fibroblast cultures resulted in marked up-regulation of various MMPs, including MMP-1 and MMP-3, both of which have been implicated in cartilage and joint destruction in arthritic patients. Further experiments confirmed that the stimulatory effects of HTRA1 on MMP expression were protease-dependent and were related to the formation of fibronectin fragments due to extracellular degradation. Such observations are therefore strongly suggestive of a central role for HTRA1 in joint degeneration through its proteolytic actions on ECM components and thus may also be indicative of its role in other disease pathologies, such as disc degeneration.

In the current study, we used IVD tissue and cell samples from surgical patients in order to further investigate the potential involvement of HTRA1 in IVD degeneration. Our findings implicate HTRA1 as a key factor in the underlying pathology associated with IVD degeneration. HTRA1 may therefore represent a novel target for the development of more effective therapeutic strategies to treat this debilitating condition.

EXPERIMENTAL PROCEDURES

Materials—Human fibronectin and rabbit IgG were purchased from R & D Systems (Abingdon, UK). IL-1 receptor antagonist (IL-1RA) was obtained from Abcam (Cambridge, UK), and MEK1/2 inhibitors PD98059 and U0126 were from Sigma-Aldrich (Buchs, Switzerland). Monoclonal antibodies against the fibronectin carboxyl-terminal heparin-binding domain (Mab1935) and the amino-terminal fibrin- and heparin-binding domain (Mab1936) were from Chemicon International. A polyclonal anti-HTRA1 antibody was generated as described previously (19). All anti-IgG horseradish peroxidase (HRP)-conjugated, fluorescence-conjugated secondary antibodies and normal serum were from Jackson ImmunoResearch (Suffolk, UK). DAPI was purchased from Sigma-Aldrich. Collagenase NB4 was purchased from Serva/Promega (Duebendorf, Switzerland), and dispase II was from Roche Applied Science (Rotkreuz, Switzerland).

Tissue Harvesting—IVD tissue and/or blood was obtained from a total of 39 patients undergoing spinal surgery for symptomatic degenerative disc disease, disc herniation, or spinal trauma following informed consent in accordance with the local ethical guidelines (carried out at the SRH Clinic Karlsbad-Langensteinbach, Karlsbad, Germany). The degree of IVD degeneration in patients was assessed prior to surgical intervention by magnetic resonance imaging (MRI) using a four-level grading system based on Pfirrmann's classification of disc degeneration (22). Degeneration grades were assigned as follows: grade 1, non-degenerated (normal disc height); grade 2, mild degeneration (slight decrease in disc height); grade 3, moderate degeneration (moderate decrease in disc height); grade 4, severe degeneration (collapsed disc space).

Isolation and Culture of IVD Cells—Human IVD cells were isolated from the discs of a total of 14 patients undergoing spinal surgery for disc herniation (carried out at Balgrist University Hospital, Zürich, Switzerland) as described previously (23). Briefly, IVD tissue was enzymatically digested (0.2% collagenase NB4, 0.3% dispase II) for 4–8 h, and cells were thereafter cultured in growth medium consisting of DMEM/F-12 supplemented with 10% FCS, penicillin (50 units/ml), streptomycin (50 μg/ml), and amphotericin B (25 μg/ml) and incubated at 37 °C with 5% CO_2 and used at passages 2–3.

Recombinant Human HTRA1—Purified recombinant His-tagged HTRA1 in which the amino-terminal mac25 homology domain was absent (termed HTRA1Δmac) was produced in *Escherichia coli* and purified using Ni^{2+}-NTA chromatography as described previously (19, 24). The enzymatically inactive mutated form of HTRA1Δmac, termed HTRA1ΔmacSA, was generated through conversion of residue serine 328 to alanine by mutagenesis.

Stimulation of IVD Cells with Recombinant HTRA1—IVD cells were cultured in 6-well plates at 3.5×10^5 cells/well and serum starved for 2 h prior to stimulation. Cells were incubated in medium alone or in medium supplemented with either HTRA1Δmac (5 μg/ml) or HTRA1ΔmacSA (5 μg/ml) for up to 24 h. Concentrations used were based on previous observations using human synovial fibroblasts (19). After this time, RNA and culture supernatants were harvested for further analysis. In the case of inhibition studies, IVD cells were preincubated with either PD98059 (10 μM), U0126 (10 μM), or IL-1RA (250 ng/ml) for 2 h prior to stimulation.

Quantitative RT-PCR (qRT-PCR)—Total RNA was isolated from either intact IVD tissue or cells and purified using TRIzol reagent (Invitrogen AG, Basel, Switzerland) according to the manufacturer's instructions. RNA (0.5 μg) was reverse transcribed to cDNA using Superscript II (Invitrogen AG) and random hexanucleotide primers (Promega AG, Dübendorf, Switzerland). Quantification of mRNA expression was performed with TaqMan Gene Expression Assays (Applied Biosystems, Rotkreuz, Switzerland) (supplemental Table 1) using the StepOnePlus real-time PCR system (Applied Biosystems), and

values were normalized to *GAPDH* mRNA levels and presented as -fold change according to the $2^{-\Delta\Delta}C_T$ method. In cases where individual patients ($n = 36$) were compared for expression levels of *HTRA1* and *FN* mRNA in IVD tissue, data were normalized to *TBP* and presented as $2^{-\Delta}C_T$. Each 10-μl reaction consisted of 1× TaqMan fast universal PCR master mix (Applied Biosystems), 1× TaqMan gene expression assay, and 10 ng of cDNA (based upon initial RNA concentrations). All reactions were performed in triplicate in fast optical 96-well reaction plates (Applied Biosystems) at 95 °C for 20 s and 40 cycles of 95 °C for 1 s and 60 °C for 20 s.

SNP Analysis—A total of 35 patients were genotyped using a TaqMan SNP genotyping assay specific for the SNP, rs11200638, according to the manufacturer's instructions (Applied Biosystems). Patients were grouped according to their individual genotypes, and association studies were performed in order to determine the influence of the rs11200638 (A) risk allele on susceptibility to IVD degeneration. The influence of rs11200638 on *HTRA1* expression in IVD tissue was also assessed in patients from whom both RNA and DNA samples were obtained ($n = 32$).

Western Blot Analysis of Patient IVD Tissue—Patient IVD samples ($n = 12$) were selected based on degeneration grade. Protein was extracted using CelLytic M (Sigma-Aldrich) containing a protease inhibitor mixture (Sigma-Aldrich), and protein amounts were determined initially by a Bio-Rad protein assay (Bio-Rad, Reinach, Switzerland). Protein samples were boiled for 5 min in loading buffer (50 mM Tris-HCl, pH 6.8, 2% SDS, 10% glycerol, 100 mM DTT, 0.002% bromphenol blue), and equal amounts of protein were loaded onto 12% SDS-polyacrylamide gels. Further corrections to the loading volumes were made following densitometric analysis of Coomassie Blue-stained gels, thus allowing for accurate comparisons to be made between individual patient samples. Protein was then electroblotted onto PVDF membranes using the Trans-Blot Turbo blotting system (Bio-Rad) and incubated in 5% skim milk, 50 mM Tris-HCl, pH 7.6, 150 mM NaCl, 0.1% Tween 20 (TBST) for 1 h at room temperature. Membranes were then incubated for 1 h at room temperature with either rabbit anti-human HTRA1 (1:2000) or mouse anti-fibronectin amino-terminal fibrin- and heparin-binding domain (Mab1936) (1 μg/ml). After washing in TBST three times for 5 min each, membranes were incubated with a HRP-conjugated anti-mouse or anti-rabbit IgG (1:10,000) for 1 h at room temperature. Following a further washing step, peroxidase activity was detected using SuperSignal West Pico Chemiluminescent Substrate (Thermo Scientific, Lausanne, Switzerland).

Immunofluorescence Microscopy—Unfixed frozen IVD tissue sections were air-dried for 20 min, blocked with normal goat serum (1:10), and incubated with polyclonal anti-HTRA1 (1:50) or control rabbit IgG (2 μg/ml) in phosphate-buffered saline (PBS), pH 7.3, 1% BSA for 16 h at 4 °C. Tissue samples containing HTRA1 were then identified using goat anti-rabbit-Cy3 (1:400). Sections were mounted in Mowiol/DABCO (1,4-diazabicyclo[2.2.2]octane) (Sigma-Aldrich) containing DAPI (0.5 g/ml), and images were captured using the Leica DMI6000B automated inverted research microscope system (Leica Microsystems).

Quantification of Secreted MMP-3—MMP-3 protein levels in culture supernatants were determined using an MMP-3-specific ELISA kit according to the manufacturer's instructions (R & D Systems).

Proteolytic Enzyme Assays—Degradation of fibronectin by HTRA1Δmac was determined using methods described previously (19). Briefly, HTRA1Δmac and recombinant human fibronectin, in an equimolar ratio, were incubated together in Tris-buffered saline (TBS), pH 8.5, for 16 h at 37 °C. In some reactions, HTRA1Δmac was replaced by proteolytically inactive HTRA1ΔmacSA. Fibronectin, HTRA1Δmac, and HTRA1ΔmacSA were also incubated separately under the same conditions and served as controls. In order to assess whether HTRA1Δmac could also generate fibronectin fragments in IVD cell cultures, supernatants (20 ml) were harvested from cells treated with HTRA1Δmac (5 μg/ml) or HTRA1ΔmacSA (5 μg/ml) for 24 h and concentrated using Amicon Ultra-15, 10,000 molecular weight cut-off filter units (Millipore). Fibronectin fragments were analyzed on 4–15% Mini-PROTEAN TGX Precast gels (Bio-Rad) by Coomassie Blue staining and immunoblotting using either mouse anti-fibronectin carboxyl-terminal heparin-binding domain (Mab1935) (1 μg/ml) or mouse-anti-fibronectin amino-terminal fibrin- and heparin-binding domain (Mab1936) (1 μg/ml) as described above. The EnzCheck elastase kit (Molecular Probes, Basel, Switzerland) was used to confirm the proteolytic activity of recombinant HTRA1 proteins according to the manufacturer's protocol.

Effect of Fibronectin Fragments on MMP Expression—Equimolar concentrations of fibronectin (20 μg) and HTRA1Δmac (5 μg) were incubated under the conditions described above. Control reactions were also performed and included TBS, pH 8.5, alone or in combination with either fibronectin or HTRA1Δmac. Samples were then diluted into equilibration buffer containing TBS, pH 7.6, with 20 mM imidazole and incubated with 50 μl of pre-equilibrated HisPur Ni^{2+}-NTA resin (Qiagen, Hombrechtikon, Switzerland) in spin columns (Thermo Scientific) for 1 h at 4 °C. Columns were then centrifuged for 5 min at 1600 rpm, and the affinity column flow-through fraction was collected, dialyzed in TBS for 4 h at 4 °C using Slide-A-Lyzer MINI dialysis devices (3500 molecular weight cut-off) (Thermo Scientific), and then incubated with IVD cells for up to 24 h, after which time MMP expression was evaluated by qRT-PCR.

Statistical Analysis—All statistical analyses were carried out using SPSS19.0 (SPSS Inc., Chicago, IL). Parametric analysis of normally distributed data were performed using the two-tailed unpaired Student's t test or one-way analysis of variance (ANOVA) followed by Tukey's post hoc tests for multiple-group comparisons. Pearson's correlation coefficient was used to evaluate the relationship between the expression levels of selected genes in patient tissue samples. The χ^2 test was used to compare allele frequencies in patients with or without IVD degeneration (1 degree of freedom). In all cases, a p value of <0.05 was considered statistically significant.

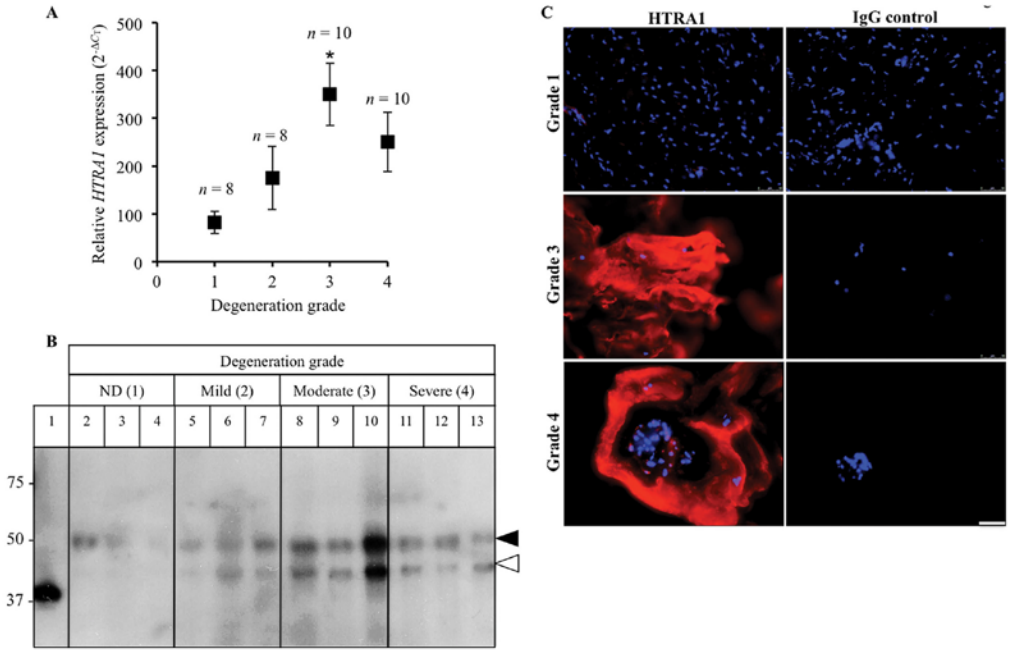

FIGURE 1. **Detection of HTRA1 in human IVD tissue.** *A*, *HTRA1* mRNA levels in intact IVD tissue samples from patients ($n = 36$) with varying degrees of IVD degeneration were determined by qRT-PCR and presented as $2^{-\Delta}C_T$. *, $p < 0.05$, as determined by one-way ANOVA *Error bars*, S.E. *B*, protein extracts from patient IVD tissues ($n = 12$) were loaded onto a 12% SDS-polyacrylamide gel, and immunoblotting was performed using a polyclonal antibody specific for HTRA1. *Lane 1*, *HTRA1Δmac* (4 ng); *lanes 2–4*, non-degenerated (*ND*) discs; *lanes 5–7*, mildly degenerated discs; *lanes 8–10*, moderately degenerated discs; *lanes 11–13*, severely degenerated discs. *Closed arrowhead*, 50-kDa HTRA1; *open arrowhead*, 42-kDa HTRA1. *C*, representative images of HTRA1 protein within frozen IVD tissue sections as identified by immunofluorescence staining. HTRA1 was detected using a Cy3-labeled secondary antibody (*red*), and nuclei were labeled with DAPI (*blue*). The specificity of staining was confirmed through the use of a nonspecific rabbit IgG control (*IgG*). Grade 1 represents a normal, non-degenerated IVD, whereas grades 3 and 4 signify moderate and severe degeneration, respectively. *Scale bar*, 50 μm.

RESULTS

We have previously demonstrated that HTRA1 plays a central role in the regulation of MMP expression in synovial fibroblasts from arthritic patients and that its stimulatory effects may be linked to the generation of fibronectin fragments (19). In the present report, we further investigated this property of HTRA1 in IVD cell cultures and aimed to establish its potential role in IVD degeneration.

Identification of HTRA1 in Patient Tissue—HTRA1 mRNA levels within IVD tissue samples from patients with varying degrees of disc degeneration were normalized to *TBP* and presented as $2^{-\Delta}C_T$. Expression levels significantly correlated ($r = 0.375$; $p = 0.024$) with patient degeneration grade and were found to be markedly increased in patients with severity scores of 3 (4-fold; $p = 0.015$) and 4 (3-fold; $p = 0.2$) as compared with control patients (Fig. 1*A*). Western blot analysis of IVD protein samples using a polyclonal antibody against HTRA1 identified two main species of HTRA1 protein migrating at ~50 kDa (*closed arrowhead*) and ~42 kDa (*open arrowhead*), which most likely represented the full-length and processed forms of HTRA1, respectively (Fig. 1*B* and supplemental Fig. 1) (25). The 50-kDa HTRA1 was found at varying levels in the majority samples tested, whereas the 42-kDa form of HTRA1 was identified in degenerated IVD protein samples only and was noticeably increased in the more severely affected discs. HTRA1 protein was also identified within both the cells and ECM of frozen IVD tissue sections, as determined by immunofluorescence staining, and levels were found to be increased in the more severely affected patients as compared with the control trauma patients (Fig. 1*C*).

Analysis of Patient rs11200638 SNP Genotype—In light of the recent evidence linking the rs11200638 SNP (G>A) in the *HTRA1* gene promoter and spinal disc degeneration in Japanese women (21), we investigated whether the rs11200638 risk allele frequency between patient groups used in the current study was associated with susceptibility to IVD degeneration. DNA from a total of 35 patients was subjected to SNP genotyping using the TaqMan SNP genotyping assay specific for rs11200638 SNP. Contrary to previous expectations, we were unable to demonstrate any significant differences in SNP allele frequencies between control patients without disc degeneration (25%) and patients with degeneration grades of 2 (14.3%; $p = 0.4$), 3 (15%; $p = 0.37$), or 4 (15%; $p = 0.37$) (Table 1). We also performed a comparative analysis of *HTRA1* expression levels in IVD tissue from 32 patients of known genotype. However, no significant associations could be made between

TABLE 1
rs11200638 SNP Genotyping of European patients with and without IVD degeneration

Genotype	Degeneration grade				*n*	Relative *HTRA1* expression[a]	*p* value[b]
	1 (*n* = 8)	2 (*n* = 7)	3 (*n* = 10)	4 (*n* = 10)			
GG	5	5	7	7	23	204.1 ± 35.6	
GA	2	2	3	3	8	307 ± 87.3	0.20
AA	1	0	0	0	1	14.9	
GA + AA	3	2	3	3	9	274.5 ± 83.5	0.37
G allele	12	12	17	17			
A allele[c]	4 (25%)	2 (14.3%) $p = 0.4^d$	3 (15%) $p = 0.37^d$	3 (15%) $p = 0.37^d$			

[a] Comparisons were made between *HTRA1* expression levels ± S.E. in IVD tissue and genotype frequency in patients where both RNA and DNA samples were available (*n* = 32).
[b] Student's *t* test was used to compare *HTRA1* expression levels between patients carrying the risk allele (GA/AA) and those homozygous for the wild type allele (GG).
[c] Percentages refer to risk allele (A) frequency.
[d] The χ^2 test was used to evaluate the significance of differences in risk allele (A) frequency between patients with IVD degeneration (grades 2–4) and control patients without IVD degeneration (grade 1) (*n* = 35).

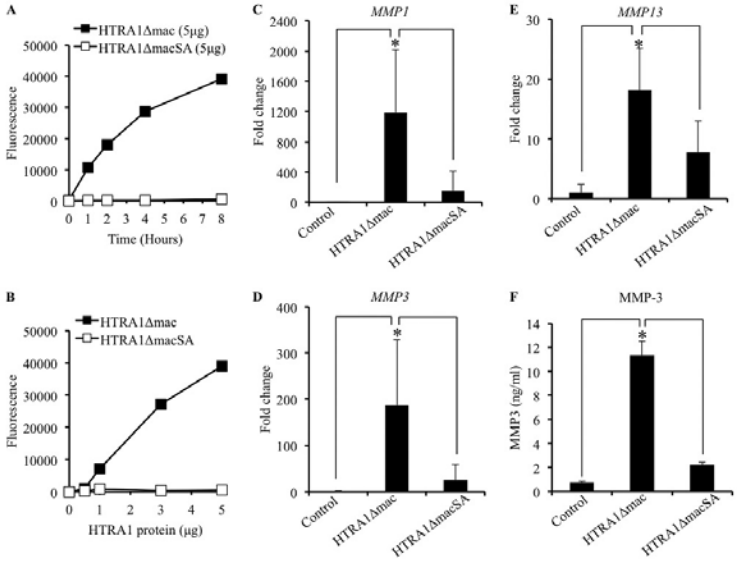

FIGURE 2. **Regulation of MMP expression in IVD cells by recombinant HTRA1.** *A* and *B*, recombinant HTRA1 proteolytic activity was determined using soluble bovine BODIPY FL-labeled DQ-elastin (100 μg/ml) as a substrate. Digestion of the DQ-elastin yielded fluorescent fragments detectable at 530 nm by a fluorescence microplate reader. The amount of DQ-elastin digestion was measured at selected time points (0, 1, 2, 4, and 8 h) using a defined amount of HTRA1 (5 μg) (*A*) or was determined after incubation for 8 h with varying amounts of HTRA1 (0, 0.5, 1, 3, and 5 μg) (*B*). *C–E*, the effects of recombinant HTRA1 (5 μg/ml) on MMP expression levels in IVD cells after a 24-h incubation period were determined by qRT-PCR, and the -fold change as compared with untreated controls was determined using the $2^{-\Delta\Delta C_T}$ method (*n* = 4–6 patients). *F*, a specific MMP-3 ELISA was used to investigate the effects of recombinant HTRA1 on MMP protein secretion in supernatants obtained from IVD cells. Shown are results of triplicate determinations ± S.D. (*error bars*). *, $p < 0.01$, as determined by one-way ANOVA.

HTRA1 expression levels and the rs11200638 genotype (Table 1).

Effect of Recombinant HTRA1 on MMP Production by IVD Cells—In order to investigate how HTRA1 may contribute to IVD degeneration, we generated both proteolytically active and inactive recombinant forms of HTRA1 lacking the amino-terminal mac25 homology domain as described previously (19). The protease activity of the active protein, termed HTRA1Δmac, was confirmed by its ability to cleave purified bovine elastin and was dependent on both incubation time (Fig. 2*A*) and protein amount (Fig. 2*B*). No such activity was observed with the proteolytically inactive form of HTRA1 (HTRA1ΔmacSA) in which serine 328, part of the serine protease catalytic triad domain, had been substituted for alanine. The effects of these recombinant proteins on MMP production by cultured IVD cells were then investigated. Cells were incubated for up to 24 h with either HTRA1Δmac (5 μg/ml) or HTRA1ΔmacSA (5 μg/ml), and the -fold change in mRNA expression levels of *MMP1*, *MMP3*, and *MMP13* was determined by qRT-PCR. HTRA1Δmac induced a significant increase in the expression levels of MMPs tested as compared with untreated cells and cells treated with the proteolytically inactive HTRA1ΔmacSA (Fig. 2, *C–E*). In addition, HTRA1Δmac also enhanced the expression of *ADAMTS4* (aggrecanase-1), although no increase was observed in *MMP2* (gelatinase A) expression, and *ACAN* (aggrecan) expression was actually reduced (supplemental Fig. 2). MMP expression was also up-regulated in HTRA1ΔmacSA-treated cells,

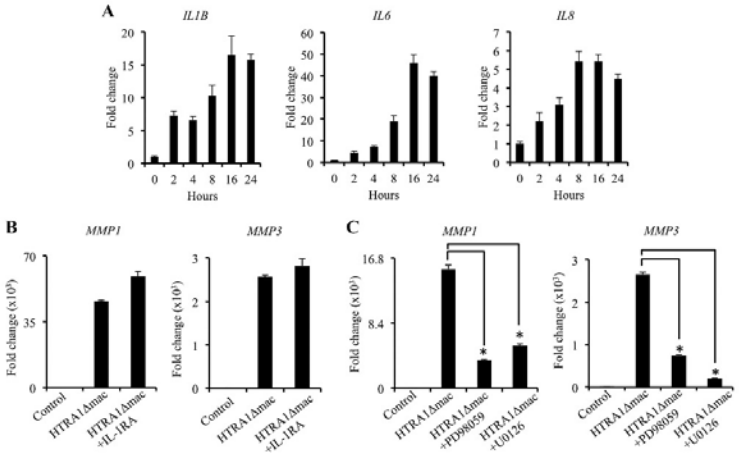

FIGURE 3. **Down-regulation of HTRA1-induced MMP expression in IVD cells by MEK inhibition.** *A*, *IL1B*, *IL6*, and *IL8* mRNA expression levels were measured in IVD cell cultures by qRT-PCR in response to HTRA1Δmac (5 μg/ml) stimulation over the course of 24 h, and the -fold change as compared with untreated cells was determined using the $2^{-\Delta\Delta}C_T$ method. *B*, the influence of IL-1β inhibition on HTRA1-induced *MMP1* and *MMP3* expression by IVD cells was evaluated by qRT-PCR after a 24-h incubation with HTRA1Δmac (5 μg/ml) in combination with the IL-1RA (250 ng/ml), and the -fold change as compared with untreated controls was determined using the $2^{-\Delta\Delta}C_T$ method. *C*, the effects of MEK inhibitors PD98059 (10 μM) and U0126 (10 μM) on HTRA1-induced *MMP1* and *MMP3* expression by IVD cells were evaluated by qRT-PCR after a 24-h incubation, and the -fold change as compared with untreated controls was determined using the $2^{-\Delta\Delta}C_T$ method. In each case, data are representative of at least two separate experiments performed using IVD cells isolated from a total of $n = 5$ patients. Shown are results of triplicate determinations ± S.D. (*error bars*). *, $p < 0.01$, as determined by one-way ANOVA.

although expression levels were over 3–7-fold less than those observed in cells incubated with HTRA1Δmac and were not deemed statistically significant as compared with untreated control cells (*MMP1*, $p = 0.19$; *MMP3*, $p = 0.41$; *MMP13*, $p = 0.41$). Clearly, therefore, HTRA1-induced MMP expression in IVD cells is primarily a protease-dependent phenomenon, although it would appear that other routes of activation may also exist. In addition to its stimulatory effects on MMP mRNA expression, HTRA1Δmac also enhanced MMP protein production, as evidenced by results obtained from the MMP-3 ELISA (Fig. 2*F*). Low levels of secreted MMP-3 were detected in the supernatants of untreated cells (0.76 ng/ml ± 0.04) but became significantly elevated following stimulation with HTRA1Δmac (11.33 ng/ml ± 0.68; $p < 0.001$). As with our previous findings, these stimulatory effects of HTRA1 were significantly diminished following inactivation of its protease activity, although levels remained elevated as compared with untreated cells (2.23 ± 0.13 ng/ml; $p = 0.089$).

Influence of MEK and IL-1β Inhibition on HTRA1-induced MMP Production—Of the known instigators of MMP expression by IVD cells, IL-1β is considered to be the most potent and, as such, is centrally involved in both IVD cell activation and IVD degeneration (8). Furthermore, IL-1β has previously been shown to play a central role in mediating MMP production by fibronectin fragments in cultures of bovine articular cartilage (26). We therefore investigated if the expression of IL-1β, along with several other cytokines, including IL-6 and IL-8, was up-regulated in IVD cells by HTRA1Δmac and whether this had any influence on the induction of MMP expression by HTRA1Δmac. Indeed, expression levels of the cytokines tested were up-regulated in IVD cells stimulated with HTRA1Δmac (5 μg/ml) in a time-dependent manner (Fig. 3*A*). However, additional studies focusing on the inhibition of IL-1β signaling using the IL-1RA (250 ng/ml) failed to demonstrate any significant alterations in the ability of HTRA1 to induce MMP expression in IVD cells (Fig. 3*B* and supplemental Fig. 3). This would suggest that HTRA1 does not mediate its stimulatory effects through IL-1β production, although we cannot exclude the possibility that other cytokines may be involved.

We have previously demonstrated that MMP expression by human synovial fibroblasts is up-regulated in response to HTRA1 stimulation and that this was at least partly dependent on the generation of fibronectin fragments (19). Furthermore, fibronectin fragments were recently confirmed as being potent inducers of MMP expression in IVD cells, mediating their effects through activation of the MEK pathway (27). We therefore investigated whether inhibition of MEK could influence the actions of HTRA1 on IVD MMP expression. Indeed, inclusion of either of the specific MEK inhibitors PD98059 (10 μM) or U0126 (10 μM) 2 h prior to treatment with HTRA1Δmac (5 μg/ml) significantly abrogated its stimulatory effects on the expression of *MMP1* and *MMP3* (Fig. 3*C*), thereby supporting the theory that fibronectin fragments may represent one possible route through which HTRA1 mediates its stimulatory effects on IVD cells.

Effect of Fibronectin Fragments on MMP Expression by IVD Cells—Based on the above results, we further investigated the potential involvement of fibronectin fragments in mediating the actions of HTRA1 on IVD cells. We observed a noticeable increase in the level of a 27–29-kDa fibronectin fragment containing the amino-terminal fibrin- and heparin-binding domain in the supernatants from IVD cell cultures previously treated with HTRA1Δmac (5 μg/ml) as compared with cells incubated in medium alone or with the inactive

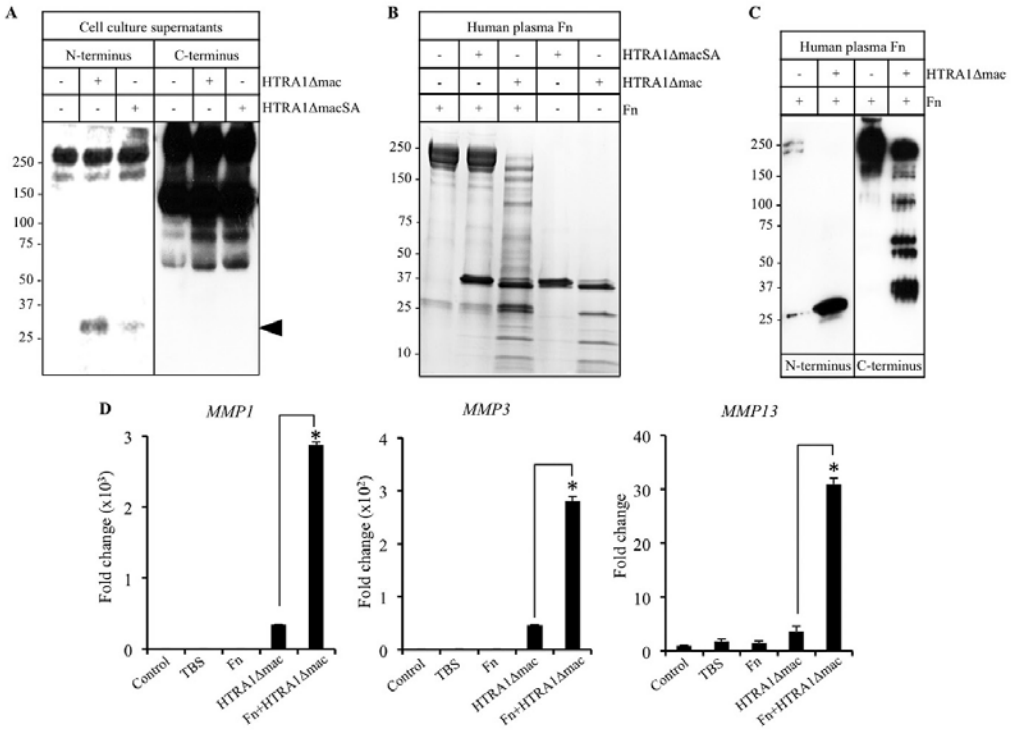

FIGURE 4. **Stimulation of IVD cells with HTRA1-generated fibronectin fragments.** *A*, concentrated protein supernatants (15 μg) from IVD cells treated for 24 h without or with HTRA1Δmac (5 μg/ml) or HTRA1ΔmacSA (5 μg/ml) were subjected to immunoblotting using antibody Mab1935 specific for the fibronectin carboxyl-terminal heparin-binding domain (*C terminus*) or Mab1936 specific for the fibronectin amino-terminal fibrin- and heparin-binding domain (*N terminus*). Fibronectin fragments containing the amino-terminal fibrin- and heparin-binding domain are identified by the *closed arrowhead*. *B*, purified human plasma-derived fibronectin (*Fn*) was incubated with HTRA1Δmac or HTRA1ΔmacSA at equimolar concentrations in TBS, pH 8.5, for 16 h at 37 °C, and samples were loaded onto a 4–15% gradient gel and stained with Coomassie Blue. Fibronectin and recombinant HTRA1 alone were also loaded and served as controls. *C*, an equimolar concentration of human plasma-derived fibronectin and HTRA1Δmac were incubated for 16 h, and fibronectin fragments were visualized by Western blot analysis using the antibodies described in *A*. *D*, equimolar concentrations of fibronectin (20 μg) and HTRA1Δmac (5 μg) were incubated for 16 h, and fibronectin fragments were purified by affinity chromatography. IVD cells were incubated with purified HTRA1-digested fibronectin (*Fn+HTRA1Δmac*) for 24 h, and expression levels of *MMP1*, *MMP3*, and *MMP13* mRNA were determined by qRT-PCR and the -fold change as compared with untreated controls was determined using the $2^{-\Delta\Delta}C_T$ method. Additional cultures were incubated with either affinity-purified Tris-buffered saline, pH 7.6 (*TBS*), fibronectin (*Fn*), or HTRA1 (*HTRA1Δmac*) or left untreated (*Control*). Data are representative of two separate experiments performed using IVD cells from two patients. Shown are results of triplicate determinations ± S.D. *, $p < 0.01$, as determined by one-way ANOVA.

HTRA1ΔmacSA (5 μg/ml) (Fig. 4*A* and supplemental Fig. 4*A*). Interestingly, increases in fibronectin fragments containing the carboxyl-terminal heparin-binding domain were evident in both HTRA1Δmac- and HTRA1ΔmacSA-treated cell cultures as compared with untreated controls. Further analyses confirmed that HTRA1Δmac, but not HTRA1ΔmacSA, could digest equimolar concentrations of human plasma-derived fibronectin after a 16-h incubation period, resulting in various sized fragments being generated, as determined by SDS-PAGE (Fig. 4*B*). The appearance of HTRA1Δmac as several bands is due to its autoproteolytic activity, as described previously (19), an effect not observed with HTRA1ΔmacSA. Western blot analysis of the products generated from HTRA1Δmac-induced fibronectin proteolysis revealed the presence of numerous fragments containing the carboxyl-terminal heparin-binding domain as well as the 27–29-kDa fragment containing the amino-terminal fibrin- and heparin-binding domain previously identified in the supernatants from HTRA1Δmac-treated IVD cells (Fig. 4*C*). We next investigated whether the fibronectin fragments generated by HTRA1 were also capable of activating IVD cells. Following an overnight incubation of human plasma-derived fibronectin with HTRA1Δmac (equimolar concentration), digested and undigested fibronectin was purified by affinity chromatography using Ni^{2+}-NTA to remove the majority of His-tagged HTRA1Δmac (supplemental Fig. 4*B*) and then incubated for up to 24 h with IVD cells. The expression levels of *MMP1*, *MMP3*, and *MMP13* (Fig. 4*D*) were all significantly increased in IVD cells incubated with the purified mixture of fibronectin fragments. By comparison, MMP expression in control cultures stimulated with the affinity column flow-through fraction from HTRA1Δmac samples in the absence of fibronectin was 6–9-fold less ($p < 0.01$), thus confirming that fibronectin fragments were the predominant cause of IVD cell activation.

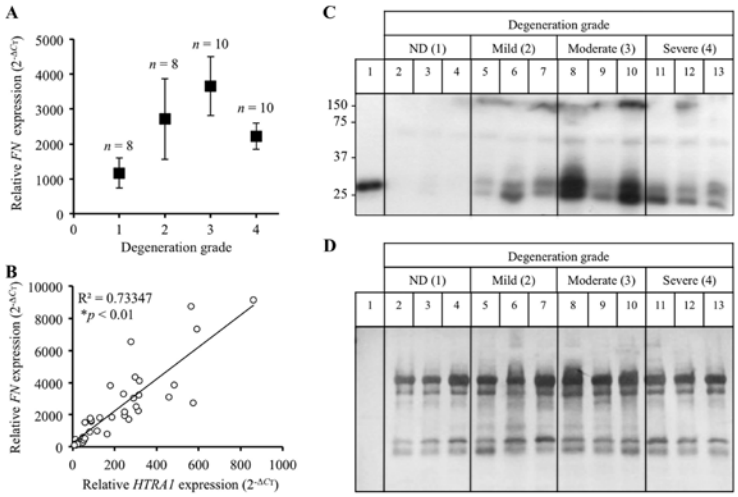

FIGURE 5. **Detection of fibronectin fragments in degenerated IVD tissue.** *A*, fibronectin (*FN*) mRNA levels in intact IVD tissue samples from patients ($n = 36$) with varying degrees of IVD degeneration were determined by qRT-PCR and presented as $2^{-\Delta}C_T \pm$ S.E. (*error bars*). *B*, correlation study between *FN* and *HTRA1* mRNA levels ($2^{-\Delta}C_T$) in patient IVD tissue samples ($n = 36$). R^2, square of correlation coefficient; $p < 0.01$ as determined from Pearson's correlation coefficient. *C*, protein extracts from patient IVD tissues ($n = 12$) were loaded onto a 12% SDS-polyacrylamide gel, and immunoblotting was performed using a monoclonal antibody (Mab1936) specific for the amino-terminal fibrin- and heparin-binding domain. *D*, the PVDF membrane used in *C* was stained with Coomassie Blue in order to confirm equal protein loading. *Lane 1*, HTRA1-digested human plasma-derived fibronectin; *lanes 2–4*, non-degenerated (*ND*) discs; *lanes 5–7*, mildly degenerated discs; *lanes 8–10*, moderately degenerated discs; *lanes 11–13*, severely degenerated discs.

Association of Fibronectin Fragments with Disc Degeneration—Both fibronectin and fibronectin fragments are known to increase with increasing disc degeneration and are thus considered to be an integral part of the underlying pathology (11). In the present study, fibronectin mRNA levels within IVD tissue samples from patients with varying degrees of disc degeneration were normalized to *TBP* and presented as $2^{-\Delta}C_T$. Fibronectin expression levels within patient disc tissue samples were indeed elevated in response to increases in degeneration grade (Fig. 5*A*) and correlated significantly with *HTRA1* mRNA expression levels ($r = 0.856$; $p < 0.01$) (Fig. 5*B*). Furthermore, Western blot analysis of IVD protein samples revealed an increase in fibronectin fragments containing the amino-terminal fibrin- and heparin-binding domain (Fig. 5*C*) in degenerated discs. Moreover, the majority of amino-terminal fragments identified were found to be of a similar size (27–29 kDa) to the fragment identified within samples of HTRA1-digested human fibronectin (*lane 1*). Membranes were counterstained with Coomassie Blue to confirm equal protein loading (Fig. 5*D*).

DISCUSSION

In the current study, we have identified HTRA1 mRNA and protein in the IVDs of human subjects and demonstrated an association between expression levels and severity of IVD degeneration. HTRA1 has previously been linked with disc degeneration following the association of a single nucleotide polymorphism, rs11200638, in the *HTRA1* gene and loss of disc height in postmenopausal Japanese women (21). In the present study, we were unable to show any significant association between the frequency of the risk allele (A) of SNP rs11200638 and IVD degeneration in a small European surgical patient population ($n = 35$). Furthermore, we found no evidence to suggest that the A allele of SNP rs11200638 has any significant influence on *HTRA1* expression levels in IVD tissue. This is supported by findings from studies investigating the role of HTRA1 in age-related macular degeneration, where, although closely associated with disease risk, rs11200638 alone was unable to significantly alter *HTRA1* expression (28, 29). It was subsequently reported that the additional disruption of the adjacent gene, *LOC387715*, was necessary in order for rs11200638 to have a positive influence on *HTRA1* expression (28).

We have previously shown that HTRA1 has the potential to stimulate MMP production by human synovial fibroblasts, thus implicating it in the pathogenesis of arthritis (19). As in the joints of arthritic patients, MMPs play a central role in orchestrating ECM breakdown in discs of patients with IVD degeneration (4–7). Therefore, we next investigated whether HTRA1 could also influence MMP production in human IVD cells. Consistent with our earlier findings with human synovial fibroblasts, recombinant HTRA1 was able to induce the expression of *MMP1*, *MMP3*, and *MMP13* mRNA, as well as MMP-3 protein, in short term IVD cell cultures. In addition, we also observed a significant increase in *ADAMTS4* expression in IVD cells stimulated with HTRA1. As with MMP-1, -3, and -13, ADAMTS-4 is also up-regulated in degenerated discs (4) and may therefore represent an additional route through which HTRA1 could influence ECM breakdown. These stimulatory effects were found to be primarily reliant on HTRA1 protease activity as evidenced by the fact that the proteolytically inactive form of HTRA1 (HTRA1ΔmacSA) was unable to significantly enhance MMP production. Neverthe-

less, increases in MMP production were apparent in cultures treated with HTRA1ΔmacSA and may be indicative of an additional, and as yet unidentified, protease-independent mechanism through which HTRA1 mediates its stimulatory effects. It is possible that further studies utilizing other mutant forms of HTRA1 may further assist in trying to decipher the exact cause of these stimulatory effects.

Degradation of the ECM within degenerated IVDs can give rise to fibronectin fragments of various sizes, which themselves are capable of activating resident disc cells to produce matrix-degrading proteases in a MEK-dependent manner (9, 27). Furthermore, the stimulatory properties of certain fibronectin fragment species on cellular MMP production are known to be mediated through the actions of IL-1β (26). In the current report, we demonstrated that the stimulatory effects of HTRA1 on MMP production by IVD cells were indeed MEK-dependent. Moreover, despite the fact HTRA1 induced the expression of *IL1B*, along with several other cytokines, inhibition of IL-1β signaling through the use of the IL-1RA failed to have any significant impact on HTRA1-induced MMP expression in IVD cells. On closer examination, it was revealed that IVD cell cultures and purified human plasma-derived fibronectin incubated with HTRA1Δmac both consisted of increased levels of a fibronectin fragment containing the 27–29-kDa amino-terminal fibrin- and heparin-binding domain. Furthermore, MMP expression was enhanced in IVD cells following stimulation with the proteolytic products of HTRA1-digested human plasma-derived fibronectin. Considering this, together with the additional observation that HTRA1-induced MMP expression was also dependent on MEK activity, we conclude that the stimulatory effects of HTRA1 on MMP production by IVD cells are mediated, at least in part, through the generation of fibronectin fragments. Interestingly, increases in fibronectin fragments containing the carboxyl-terminal heparin-binding domain, were also evident in the culture supernatants of cells treated with the HTRA1ΔmacSA. The fact that HTRA1ΔmacSA was proteolytically inactive and only able to generate fibronectin fragments in the presence of cells would suggest that these effects were most likely mediated through the stimulated secretion of other active proteases. This may therefore offer some explanation as to why MMP production by IVD cells was enhanced with HTRA1ΔmacSA, although the mechanism of action still remains to be determined. Furthermore, the observation that levels of the 27–29-kDa fibronectin fragment containing the amino-terminal fibrin- and heparin-binding domain were elevated predominantly in cell cultures treated with HTRA1Δmac would further imply that these fragment species are of particular relevance with regard to IVD cell activation.

Increased production of fibronectin by resident IVD cells has been observed within degenerated disc tissue samples and is considered to be central to the ongoing reparative and remodeling processes associated with IVD degeneration (30, 31). In the present study, we observed a marked increase in fibronectin expression in IVD tissue from patients with moderate to severe disc degeneration, which correlated significantly with changes in *HTRA1* expression levels. At present, it is not known whether fibronectin and HTRA1 share common regulatory pathways,

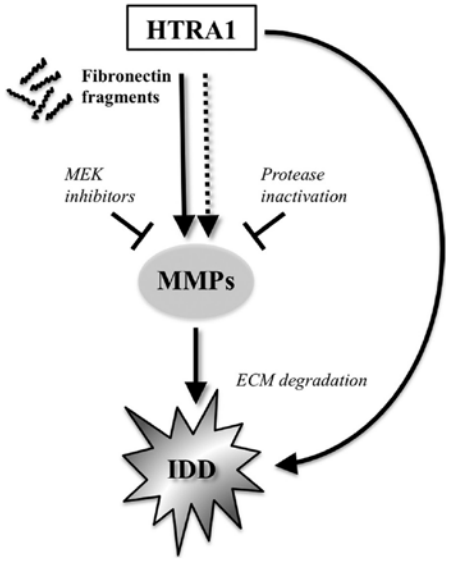

FIGURE 6. **A theoretical model for the role of HTRA1 in IVD degeneration.** Based on our findings, we propose that HTRA1 accumulates in IVD tissue undergoing degeneration and stimulates MMP production by resident cells in a predominantly protease-dependent manner, via activation of the MEK pathway. Furthermore, we suggest that the stimulatory effects of HTRA1 on IVD cells are mediated indirectly through its ability to generate fibronectin fragments, although other routes of cellular activation cannot be ruled out. *IDD*, intervertebral disc degeneration.

although it would appear that both of their expression patterns are dependent on factors intrinsic to the degenerative process. Given the fact that HTRA1-generated fibronectin fragments serve as potent inducers of MMP production, overexpression of fibronectin and *HTRA1* within IVDs is likely to have a significant influence on the development of disc degeneration. This is supported by our finding that small molecular mass fragments (27–29 kDa) containing the amino-terminal fibrin- and heparin-binding domain of fibronectin could also be identified within degenerated disc samples. The involvement of such fragments in disc degeneration has already been alluded to in a recent report by Anderson *et al.* (32), where a single fibronectin fragment with an estimated size of 25 kDa was detected in degenerated discs by immunoblotting with the same monoclonal antibody as used in the current study. It is possible, therefore, that HTRA1 protease activity may in fact be one of the main causative agents responsible for generating such fibronectin fragments within degenerated discs.

Taken together, these findings led us to propose a working model for the biological role of HTRA1 in IVD degeneration (Fig. 6). In addition to its already well characterized ability to directly degrade ECM proteins known to be present within IVDs (19, 20, 33–35), HTRA1 may also further modulate ECM breakdown indirectly through fibronectin fragment production and subsequent up-regulation of MMPs by resident disc cells. Clearly, further investigations are required in order to identify which particular fragments are responsible for the activation of

IVD cells *in vitro* and to clarify the involvement of fibronectin fragments in IVD degeneration. Furthermore, additional studies are needed to fully evaluate the potential stimulatory effects of other soluble mediators (*e.g.* cytokines) released by IVD cells following incubation with HTRA1. Moreover, examination of the possible interplay between inflammatory mediators and fibronectin fragments in the regulation of Toll-like receptor signaling pathways in IVD cells may also lend further insight into how HTRA1 contributes to the catabolic response in IVD degeneration (36). These results therefore encourage the design of specific HTRA1 inhibitors for the treatment of patients with disc degeneration, an endeavor that will no doubt be facilitated by information gleaned from the recently solved crystal structure of HTRA1 (37).

REFERENCES

1. Peterson, C. K., Bolton, J. E., and Wood, A. R. (2000) A cross-sectional study correlating lumbar spine degeneration with disability and pain. *Spine* **25,** 218–223
2. Luoma, K., Riihimäki, H., Luukkonen, R., Raininko, R., Viikari-Juntura, E., and Lamminen A. (2000) Low back pain in relation to lumbar disc degeneration. *Spine* **25,** 487–492
3. Freemont, A. J., Watkins, A., Le Maitre, C., Jeziorska, M., and Hoyland, J. A. (2002) Current understanding of cellular and molecular events in intervertebral disc degeneration. Implications for therapy. *J. Pathol.* **196,** 374–379
4. Le Maitre, C. L., Freemont, A. J., and Hoyland, J. A. (2004) Localization of degradative enzymes and their inhibitors in the degenerate human intervertebral disc. *J. Pathol.* **204,** 47–54
5. Le Maitre, C. L., Freemont, A. J., and Hoyland, J. A. (2006) Human disc degeneration is associated with increased MMP 7 expression. *Biotech. Histochem.* **81,** 125–131
6. Roberts, S., Caterson, B., Menage, J., Evans, E. H., Jaffray, D. C., and Eisenstein, S. M. (2000) Matrix metalloproteinases and aggrecanase. Their role in disorders of the human intervertebral disc. *Spine* **25,** 3005–3013
7. Bachmeier, B. E., Nerlich, A., Mittermaier, N., Weiler, C., Lumenta, C., Wuertz, K., and Boos, N. (2009) Matrix metalloproteinase expression levels suggest distinct enzyme roles during lumbar disc herniation and degeneration. *Eur. Spine J.* **18,** 1573–1586
8. Millward-Sadler, S. J., Costello, P. W., Freemont, A. J., and Hoyland, J. A. (2009) Regulation of catabolic gene expression in normal and degenerate human intervertebral disc cells. Implications for the pathogenesis of intervertebral disc degeneration. *Arthritis Res. Ther.* **11,** R65
9. Anderson, D. G., Li, X., and Balian, G. (2005) A fibronectin fragment alters the metabolism by rabbit intervertebral disc cells *in vitro*. *Spine* **30,** 1242–1246
10. Greg Anderson, D., Li, X., Tannoury, T., Beck, G., and Balian, G. (2003) A fibronectin fragment stimulates intervertebral disc degeneration *in vivo*. *Spine* **28,** 2338–2345
11. Oegema, T. R., Jr., Johnson, S. L., Aguiar, D. J., and Ogilvie, J. W. (2000) Fibronectin and its fragments increase with degeneration in the human intervertebral disc. *Spine* **25,** 2742–2747
12. Clausen, T., Kaiser, M., Huber, R., and Ehrmann, M. (2011) HTRA proteases. Regulated proteolysis in protein quality control. *Nat. Rev. Mol. Cell Biol.* **12,** 152–162
13. Shridhar, V., Sen, A., Chien, J., Staub, J., Avula, R., Kovats, S., Lee, J., Lillie, J., and Smith, D. I. (2002) Identification of underexpressed genes in early and late stage primary ovarian tumors by suppression subtraction hybridization. *Cancer Res.* **62,** 262–270
14. Chien, J., Staub, J., Hu, S. I., Erickson-Johnson, M. R., Couch, F. J., Smith, D. I., Crowl, R. M., Kaufmann, S. H., and Shridhar, V. (2004) A candidate tumor suppressor HtrA1 is down-regulated in ovarian cancer. *Oncogene* **23,** 1636–1644
15. Baldi, A., De Luca, A., Morini, M., Battista, T., Felsani, A., Baldi, F., Catricalà, C., Amantea, A., Noonan, D. M., Albini, A., Natali, P. G., Lombardi, D., and Paggi, M. G. (2002) The HtrA1 serine protease is down-regulated during human melanoma progression and represses growth of metastatic melanoma cells. *Oncogene* **21,** 6684–6688
16. Bakay, M., Zhao, P., Chen, J., and Hoffman, E. P. (2002) A Web-accessible complete transcriptome of normal human and DMD muscle. *Neuromuscul. Disord.* **12,** S125–S141
17. Hu, S. I., Carozza, M., Klein, M., Nantermet, P., Luk, D., and Crowl, R. M. (1998) Human HtrA, an evolutionarily conserved serine protease identified as a differentially expressed gene product in osteoarthritic cartilage. *J. Biol. Chem.* **273,** 34406–34412
18. Wu, J., Liu, W., Bemis, A., Wang, E., Qiu, Y., Morris, E. A., Flannery, C. R., and Yang, Z. (2007) Comparative proteomic characterization of articular cartilage tissue from normal donors and patients with osteoarthritis. *Arthritis Rheum.* **56,** 3675–3684
19. Grau, S., Richards, P. J., Kerr, B., Hughes, C., Caterson, B., Williams, A. S., Junker, U., Jones, S. A., Clausen, T., and Ehrmann, M. (2006) The role of human HtrA1 in arthritic disease. *J. Biol. Chem.* **281,** 6124–6129
20. Tsuchiya, A., Yano, M., Tocharus, J., Kojima, H., Fukumoto, M., Kawaichi, M., and Oka, C. (2005) Expression of mouse HtrA1 serine protease in normal bone and cartilage and its up-regulation in joint cartilage damaged by experimental arthritis. *Bone* **37,** 323–336
21. Urano, T., Narusawa, K., Kobayashi, S., Shiraki, M., Horie-Inoue, K., Sasaki, N., Hosoi, T., Ouchi, Y., Nakamura, T., and Inoue, S. (2010) Association of HTRA1 promoter polymorphism with spinal disc degeneration in Japanese women. *J. Bone Miner. Metab.* **28,** 220–226
22. Pfirrmann, C. W., Metzdorf, A., Zanetti, M., Hodler, J., and Boos, N. (2001) Magnetic resonance classification of lumbar intervertebral disc degeneration. *Spine* **26,** 1873–1878
23. Wuertz, K., Urban, J. P., Klasen, J., Ignatius, A., Wilke, H. J., Claes, L., and Neidlinger-Wilke, C. (2007) Influence of extracellular osmolarity and mechanical stimulation on gene expression of intervertebral disc cells. *J. Orthop. Res.* **25,** 1513–1522
24. Grau, S., Baldi, A., Bussani, R., Tian, X., Stefanescu, R., Przybylski, M., Richards, P., Jones, S. A., Shridhar, V., Clausen, T., and Ehrmann, M. (2005) Implications of the serine protease HtrA1 in amyloid precursor protein processing. *Proc. Natl. Acad. Sci. U.S.A.* **102,** 6021–6026
25. Nie, G., Li, Y., and Salamonsen, L. A. (2005) Serine protease HtrA1 is developmentally regulated in trophoblast and uterine decidual cells during placental formation in the mouse. *Dev. Dyn.* **233,** 1102–1109
26. Yasuda, T., and Poole, A. R. (2002) A fibronectin fragment induces type II collagen degradation by collagenase through an interleukin-1-mediated pathway. *Arthritis Rheum.* **46,** 138–148
27. Xia, M., and Zhu, Y. (2011) Fibronectin fragment activation of ERK increasing integrin α and β subunit expression to degenerate nucleus pulposus cells. *J. Orthop. Res.* **29,** 556–561
28. Yang, Z., Tong, Z., Chen, Y., Zeng, J., Lu, F., Sun, X., Zhao, C., Wang, K., Davey, L., Chen, H., London, N., Muramatsu, D., Salasar, F., Carmona, R., Kasuga, D., Wang, X., Bedell, M., Dixie, M., Zhao, P., Yang, R., Gibbs, D., Liu, X., Li, Y., Li, C., Li, Y., Campochiaro, B., Constantine, R., Zack, D. J., Campochiaro, P., Fu, Y., Li, D. Y., Katsanis, N., and Zhang, K. (2010) Genetic and functional dissection of HTRA1 and LOC387715 in age-related macular degeneration. *PLoS Genet.* **6,** e1000836
29. Kanda, A., Chen, W., Othman, M., Branham, K. E., Brooks, M., Khanna, R., He, S., Lyons, R., Abecasis, G. R., and Swaroop, A. (2007) A variant of mitochondrial protein LOC387715/ARMS2, not HTRA1, is strongly associated with age-related macular degeneration. *Proc. Natl. Acad. Sci. U.S.A.* **104,** 16227–16232
30. Nerlich, A. G., Bachmeier, B. E., and Boos, N. (2005) Expression of fibronectin and TGF-β1 mRNA and protein suggest altered regulation of extracellular matrix in degenerated disc tissue. *Eur. Spine J.* **14,** 17–26
31. Gruber, H. E., Hoelscher, G. L., Ingram, J. A., Bethea, S., Zinchenko, N., and Hanley, E. N. Jr. (2011) Variations in aggrecan localization and gene expression patterns characterize increasing stages of human intervertebral disk degeneration. *Exp. Mol. Pathol.* **91,** 534–539
32. Anderson, D. G., Markova, D., Adams, S. L., Pacifici, M., An, H. S., and Zhang, Y. (2010) Fibronectin splicing variants in human intervertebral disc and association with disc degeneration. *Spine* **35,** 1581–1588
33. Tocharus, J., Tsuchiya, A., Kajikawa, M., Ueta, Y., Oka, C., and Kawaichi,

M. (2004) Developmentally regulated expression of mouse HtrA3 and its role as an inhibitor of TGF-β signaling. *Dev. Growth Differ.* **46,** 257–274
34. Hadfield, K. D., Rock, C. F., Inkson, C. A., Dallas, S. L., Sudre, L., Wallis, G. A., Boot-Handford, R. P., and Canfield, A. E. (2008) HtrA1 inhibits mineral deposition by osteoblasts. Requirement for the protease and PDZ domains. *J. Biol. Chem.* **283,** 5928–5938
35. Chamberland, A., Wang, E., Jones, A. R., Collins-Racie, L. A., LaVallie, E. R., Huang, Y., Liu, L., Morris, E. A., Flannery, C. R., and Yang, Z. (2009) Identification of a novel HtrA1-susceptible cleavage site in human aggrecan. Evidence for the involvement of HtrA1 in aggrecan proteolysis *in vivo*. *J. Biol. Chem.* **284,** 27352–27359
36. Su, S. L., Tsai, C. D., Lee, C. H., Salter, D. M., and Lee, H. S. (2005) Expression and regulation of Toll-like receptor 2 by IL-1β and fibronectin fragments in human articular chondrocytes. *Osteoarthr. Cartil.* **13,** 879–886
37. Truebestein, L., Tennstaedt, A., Mönig, T., Krojer, T., Canellas, F., Kaiser, M., Clausen, T., and Ehrmann, M. (2011) Substrate-induced remodeling of the active site regulates human HTRA1 activity. *Nat. Struct. Mol. Biol.* **18,** 386–388

Molecular Bases of Disease:

Detrimental Role for Human High Temperature Requirement Serine Protease A1 (HTRA1) in the Pathogenesis of Intervertebral Disc (IVD) Degeneration

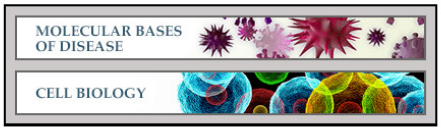

André N. Tiaden, Marina Klawitter, Vanda Lux, Ali Mirsaidi, Gregor Bahrenberg, Stephan Glanz, Lilian Quero, Thomas Liebscher, Karin Wuertz, Michael Ehrmann and Peter J. Richards

J. Biol. Chem. 2012, 287:21335-21345.
doi: 10.1074/jbc.M112.341032 originally published online May 3, 2012

---

3. Unpublished Data

3.1. ATRA-mediated induction of *mHtrA1* expression

The osteogenic medium (OM) used to induce mASC osteogenesis was composed of αMEM, 10% FCS, ascorbic acid, β-glycerophosphate, and ATRA. Upon addition of OM, expression of *mHtrA1* mRNA was significantly up-regulated within the first 24 h (Fig. 6A) and was found to be completely reliant on the presence of ATRA (Fig. 6B). This was further confirmed in studies in which knockdown of retinoic acid receptor expression (Fig. 7A) could significantly impair the ability of OM to induce *HtrA1* expression in mASCs (Fig. 7B). These initial studies therefore led us to conclude that HtrA1 production was most likely regulated at the transcriptional level in mASCs by ATRA.

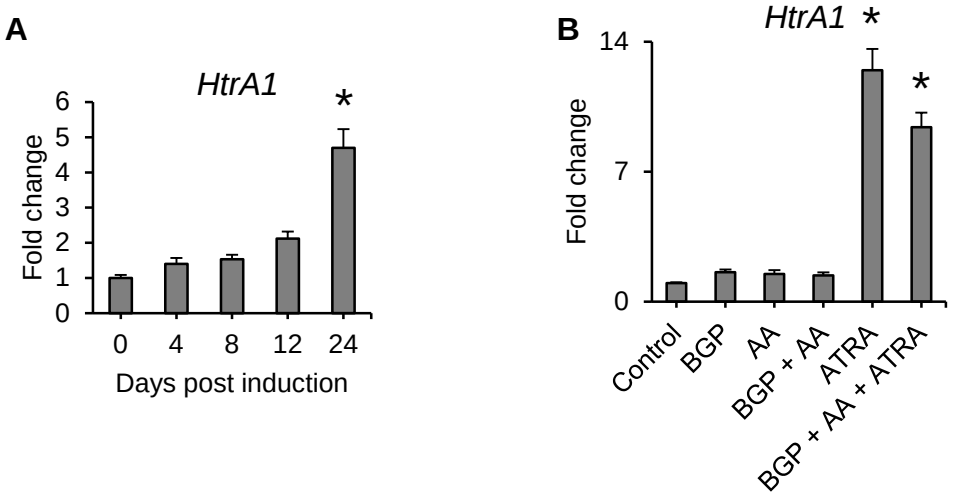

Figure 6. (A) mASCs were induced to undergo osteogenesis with osteogenic medium (OM) containing ascorbic acid, β-glycerophosphate, and ATRA for up to 24 h. At selected time points, RNA was isolated and *HtrA1* gene expression determined by RT-qPCR. **(B)** mASCs were induced to undergo osteogenesis with osteogenic medium (OM) containing ascorbic acid (AA), β-glycerophosphate (BGP), and ATRA, or variations thereof. After 24 h, RNA was isolated and *HtrA1* gene expression determined by RT-qPCR. In each case, the fold change in *HtrA1* gene expression was compared to non-induced controls using the $2^{-\Delta\Delta CT}$ method. * $p < 0.01$ as determined using one-way ANOVA.

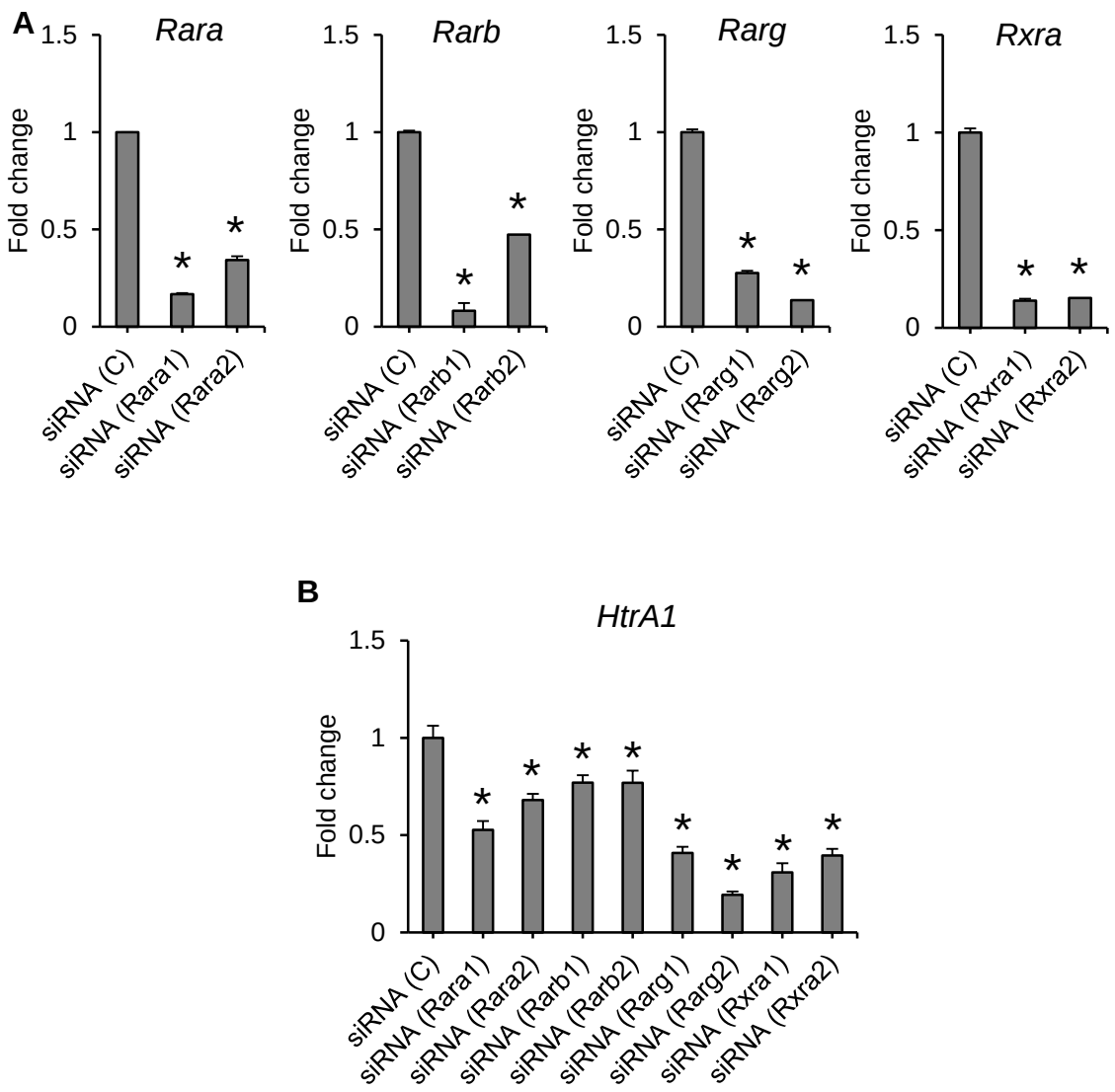

Figure 7. (A) siRNA-mediated knockdown of retinoic acid receptors (Rar) alpha (*Rara*), beta (*Rarb*) and gamma (*Rarg*), and retinoid X receptor alpha (*Rxra*) in mASCs as determined by RT-qPCR. Two different siRNAs (1 and 2) were used to target each receptor gene. **(B)** Influence of siRNA-mediated *Rar* and *Rxr* gene silencing on ATRA-induced HtrA1 expression in mASCs after 24 h as determined by RT-qPCR. In each case, gene expression was compared to mASCs treated with scrambled siRNA controls (siRNA(C)) using the $2^{-\Delta\Delta CT}$ method. * $p < 0.01$ as determined using one-way ANOVA.

3.2. Transcriptional regulation of *mHtrA1*

Further studies conducted using the RNA polymerase II (POLII) inhibitors Actinomycin D and α-Amanitin confirmed that the observed increase in *HtrA1* expression in mASCs in response to ATRA was primarily regulated at the transcriptional level (Fig. 8)

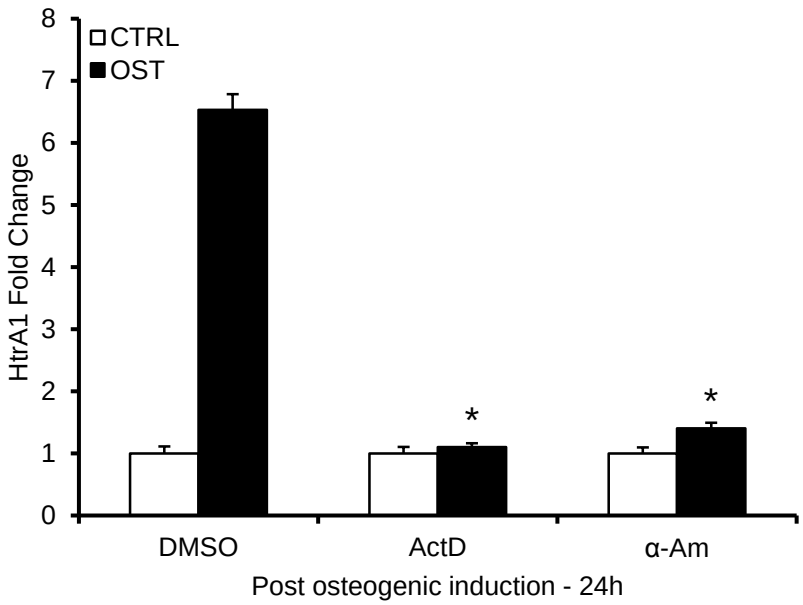

Figure 8. Osteogenic induction of mASCs while inhibiting POLII using the well-known POLII inhibitors Actinomycin D (ActD) and α-Amanitin (α-Am) completely abolishes *mHtrA1* transcriptional upregulation. Data were normalized to ribosomal protein S12 (*Rps12*) transcripts and expressed as fold change in comparison to cells treated with DMSO only using the comparative C_T method. Representative graphs of at least three independent experiments are shown. CTRL, uninduced controls; OST, osteogenic induced. * $p<0.001$ as compared to DMSO-treated osteogenic cells using Student's t-test.

When inhibiting POLII by using the well-accepted inhibitors such as Actinomycin D and α-Amanitin, the increase in *mHtrA1* mRNA expression upon OM treatment was completely abolished (Fig. 8), concluding that *mHtrA1* expression is regulated at the transcriptional level. Consequently, as a next step we tried to identify involved effectors in a knock-down screen targeting well known transcription factors (TFs) and co-activators associated with osteogenesis.

3.2.1. Analysis of *mHtrA1* gene regulation through siRNA-mediated knockdown of osteogenic-related TFs in mASCs

Successful transduction of the signal from extracellular space through the cytoplasm to the nucleus finally results in binding of an effector to the target promoter and thereby either regulating transcription of the target gene directly or subsequently recruiting co-activators or co-repressors. To identify potential candidates involved in transcriptional regulation of *mHtrA1* gene expression, siRNA mediated knock-down of several osteogenic TFs was carried out in osteogenic-induced mASCs (Fig. 9). To ensure reliability, each individual knock-down was performed using at least two different oligos for the same target. Consequently, only those showing convergent reduction of osteogenic induced *mHtrA1* expression amongst oligos were considered for further investigation, such as nuclear factor I/A (siRNA_Nfia1/2), nuclear transcription factor Y subunit alpha (siRNA_NYA1/2), CAMP responsive element binding protein 1 (siRNA_Creb1_1/2/3), activating transcription factor 1 (siRNA_Atf1_1/2/3), activating transcription factor 2 (siRNA_Atf2_1/2/3) and transcriptional coactivator p300 (siRNA_p300_1/2). Subsequently a deletion analysis of the *mHtrA1* promoter activity in a luciferase assay was carried out to narrow down the areas of interest potentially harbouring the respective transcription factor binding sites.

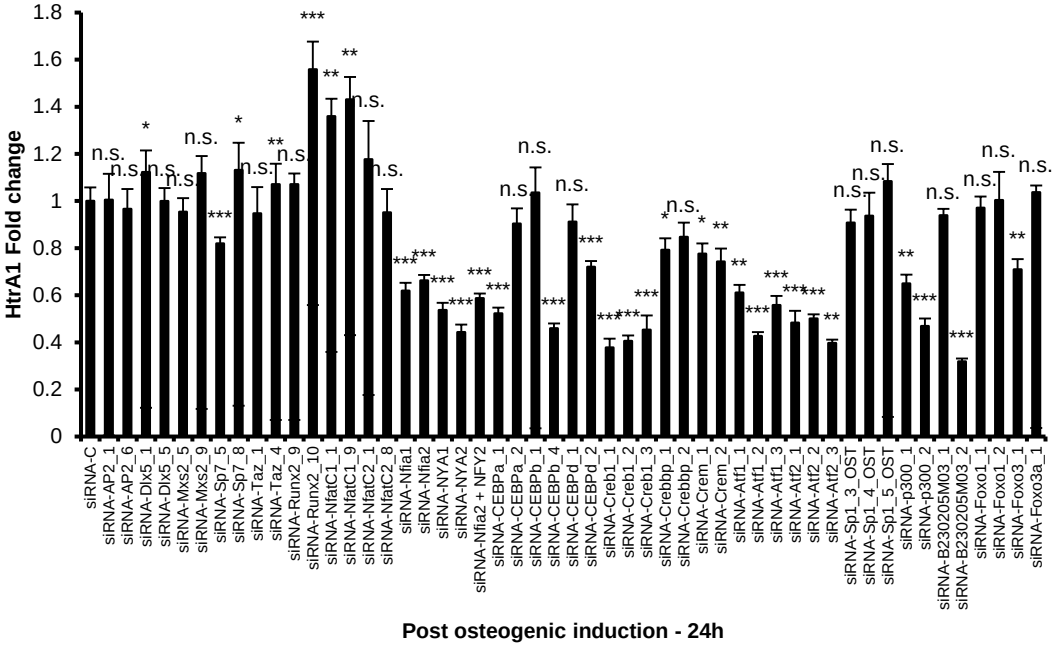

Figure 9. Quantitative polymerase chain reaction analysis of *mHtrA1* gene expression in mASCs transfected with various siRNA oligos using the NEON electroporation method and analysed 24h post osteogenic induction. siRNA-C = scrambled control, siRNA-AP2 = Activating Protein 2, siRNA-Dlx5 = Distal-less homeobox 5, siRNA-Mxs2 = Homeobox transcription factor muscle segment homeobox 2, siRNA-Sp7 = Transcription factor osterix, siRNA-Taz = transcriptional coactivator with PDZ-binding motif, siRNA-Runx2 = runt-related transcription factor 2, siRNA-NfatC = nuclear factor of activated T cells, siRNA-Nfia = nuclear factor I/A, siRNA-NYA = nuclear transcription factor Y subunit alpha, siRNA-CEBP = CCAAT-enhancer-binding proteins, siRNA-Creb = CAMP responsive element binding protein, siRNA-Crebbp = Creb binding protein, siRNA-Crem = cAMP response element modulator, siRNA-Atf = activating transcription factor, siRNA-SP1 = specificity protein 1, siRNA-p300 = transcriptional coactivator p300, siRNA-B230205M03 = cAMP responsive element binding protein-like 2, siRNA-Foxo = orkhead box protein O1. Considering only convergent effects with at least two siRNA oligos, repression of nuclear factor I/A (siRNA_Nfia1/2), nuclear transcription factor Y subunit alpha (siRNA_NYA1/2), CAMP responsive element binding protein 1 (siRNA_Creb1_1/2/3), activating transcription factor 1 (siRNA_Atf1_1/2/3), activating transcription factor 2 (siRNA_Atf2_1/2/3) and transcriptional coactivator p300 (siRNA_p300_1/2), significantly impaired osteogenesis induced upregulation of *mHtrA1* gene expression. Data were normalized to transcriptional levels of ribosomal protein S12 (*Rps12*) and expressed as fold change in comparison to cells transfected with a non-target control siRNA-C using the comparative C_T method. Representative graphs of at least three independent experiments are shown. Significances were calculated using the Student's t-test and are referring to control oligo siRNA-C versus target oligos, * $p<0.05$, ** $p<0.01$, *** $p<0.001$. N.s., not significant.

3.2.2.Analysis of *mHtrA1* promoter

In order to further determine which specific TF binding sites within the *mHtrA1* promoter were responsible for its upregulation in response to osteogenic medium, luciferase deletion constructs covering different parts of the *mHtrA1* promoter ranging

from -10000bp to +400bp relative to the ATG start site were generated, and their activity measured as depicted in Fig. 10.

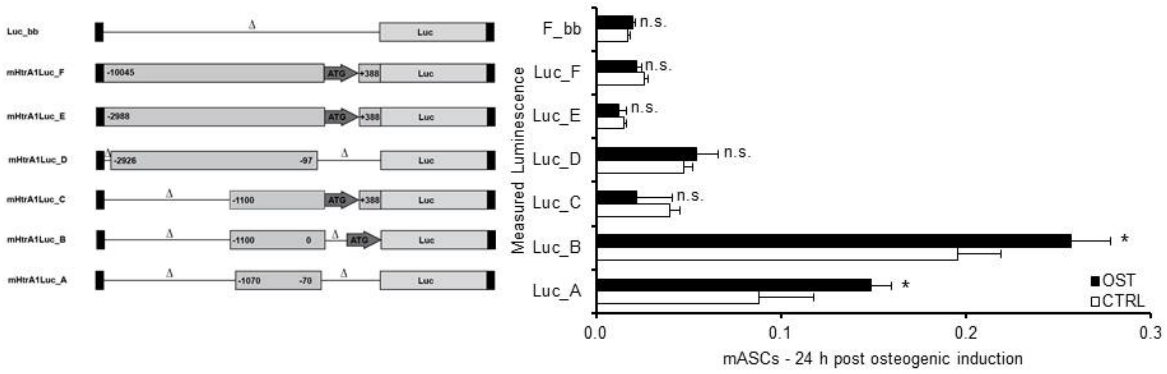

Figure 10. Deletion analysis of *mHtrA1* promoter activity. Left panel : Truncated *mHtrA1* promoter luciferase reporter constructs were generated to determine the minimal promoter region required for *mHtrA1* promoter activity Right panel : Data representation of the truncated *mHtrA1* luciferase reporter assay. Expression of Firefly Luciferase was normalized to SV40 driven Renilla Luciferase expression. Representative graphs of at least three independent experiments are shown. CTRL, uninduced controls; OST, osteogenic induced. * $p<0.05$ as compared to uninduced controls (CTRL) using Student's t-test. N.s., not significant.

Amongst all constructs, regardless of length, there was a noticeable lack of responsiveness upon osteogenic stimulation. Nonetheless, the shortest constructs mHtrA1Luc_A and mHtrA1Luc_B, showed a noticeable increase in basal promoter activity as compared to all other constructs, and demonstrated minor, but significant increase under OST conditions as compared to CTRL conditions. Hence, the area from -1100pb downstream, as covered by the mHTRA1Luc_B construct was considered a candidate for further investigation to identify potential TF binding sites responsible for *mHtrA1* promoter activity. As shown in Fig. 11, all putative transcription factor binding sites of interest are covered in the deletion constructs as used in Fig. 10, such as Retinoic Acid response element DR5 (RARE DR5) (Fig. 11 – line 01), specificity protein 1 (Sp1) (Fig. 11 – line 10), cAMP responsive element binding protein (CREB), activating transcription factor (ATF) (Fig. 11 – line 11) and nuclear transcription factor Y (NYA) (Fig. 11 – line 11). Importantly, no putative site TATA box was identified within the *mHtrA1* promoter.

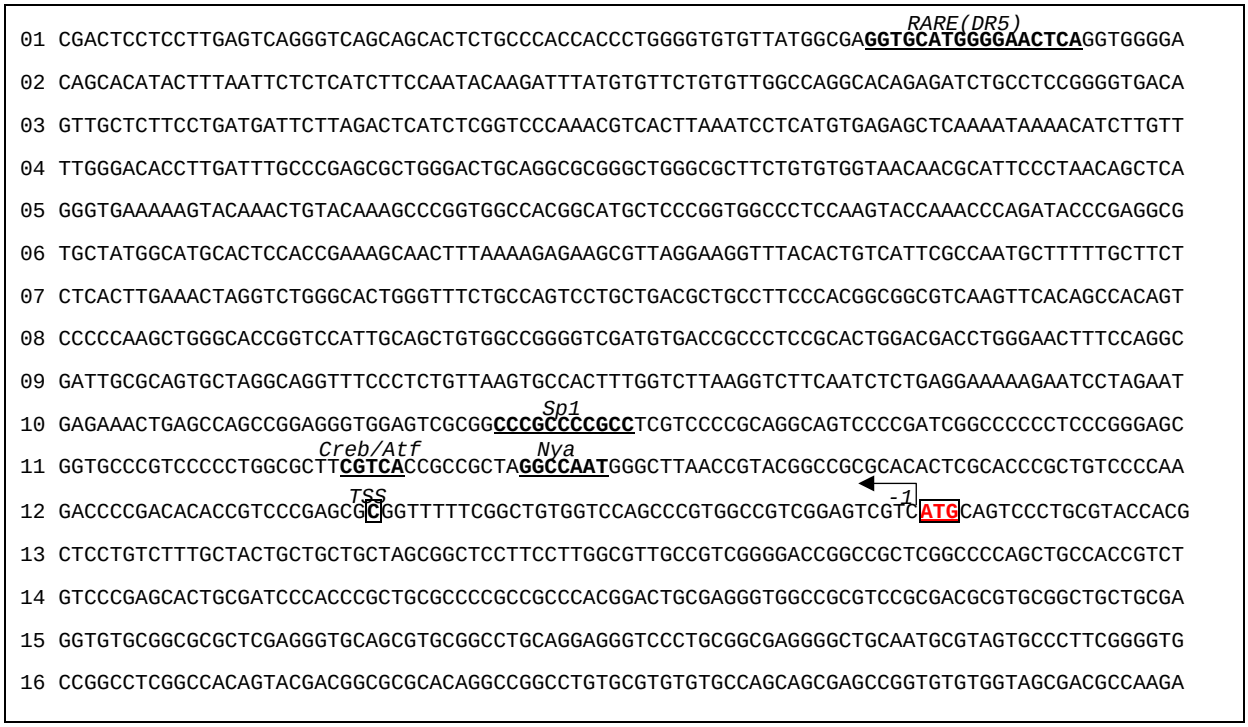

Figure 11. DNA sequence showing transcription factor binding sites of interest upstream of the transcription start site (TSS). Potential Retinoic Acid Response Element DR5 (RARE DR5) (line 01), specificity protein 1 (Sp1) (line 10), CAMP Responsive Element Binding Protein (CREB), Activating Transcription Factor (ATF) (line11), Nuclear Transcription Factor Y (NYA) (line11).

The previously mentioned mHtrA1Luc_B construct demonstrated the highest promoter activity and was therefore selected as a starting point to generate further deletion constructs to locate the responsive sites within the promoter. Due to higher transfection efficiency, further assays were carried out in the multipotent stromal cell (MSC) cell line C3H10T1/2. Initial observations confirmed that this cell line was also responsive to ATRA mediated *HtrA1* upregulation (Fig. 12, left panel). To verify basic functionality of the assay, a RARE Reporter Assay Kit (Qiagen) was used. This showed the expected increase in luciferase expression upon stimulation with ATRA-containing osteogenic media due to its multiple consecutive RAREs (Fig. 12, right panel).

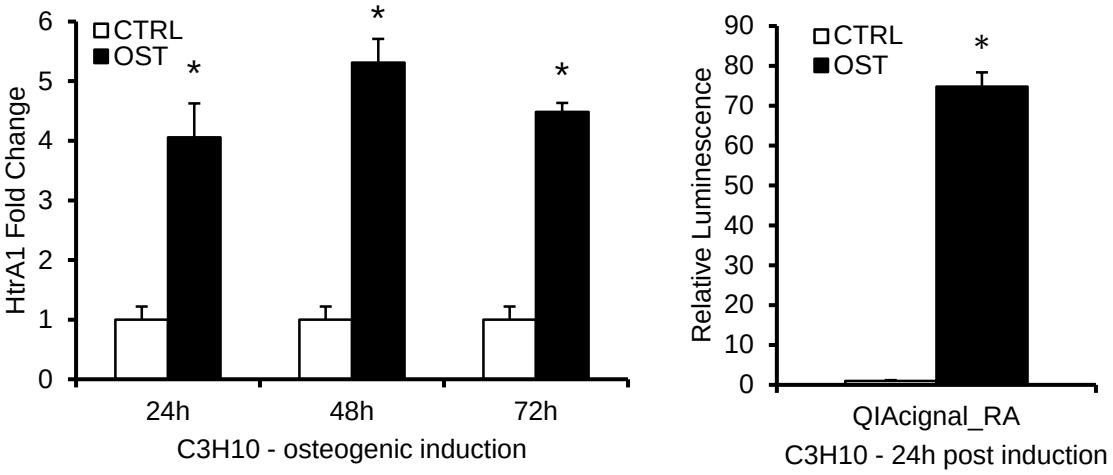

Figure 12. Left panel: Time course showing upregulation of *mHtrA1* gene expression in MSC C3H10T1/2 cell line upon stimulation with osteogenic medium (OST) as compared to uninduced controls (CTRL). Right panel: Quantification of luminescence in OST-stimulated C3H10T1/2 cells using the RARE Reporter Assay kit. CTRL, uninduced controls; OST, osteogenic induced. * $p<0.001$ as compared to uninduced controls (CTRL) using Student's t-test.

In order to investigate further potential transcription factor binding sites involved in *mHtrA1* promoter activity, several versions of the mHtrA1Luc_B were generated (Fig. 13).

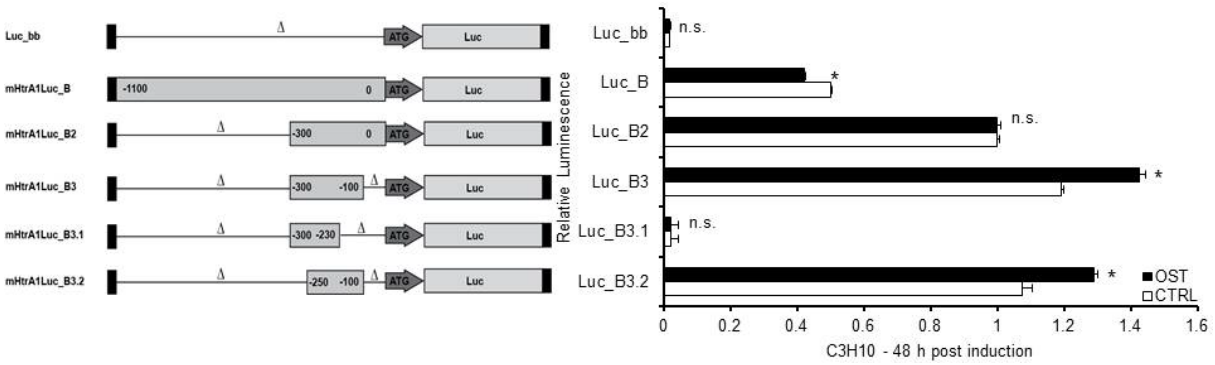

Figure 13. Deletion analysis of *mHtrA1* promoter activity focusing on various putative transcription factor binding sites, carried out in C3H10T1/2 cell line and measured at 48h post osteogenic induction. Left panel: Based on the previously designed mHtrA1Luc_B construct, further truncated *mHtrA1* promoter luciferase reporter constructs were generated to determine the contribution of individual transcription factor binding sites to *mHtrA1* promoter activity. Right: Data representation of the

truncated *mHtrA1* luciferase reporter assay. Representative graphs of at least three independent experiments are shown. Expression of Firefly Luciferase was normalized to SV40 driven Renilla Luciferase expression. Representative graphs of at least three independent experiments are shown. CTRL, uninduced controls; OST, osteogenic induced. * $p<0.05$ as compared to uninduced controls (CTRL) using Student's t-test. N.s., not significant.

All truncated luciferase reporter constructs of this assay are based on the previously identified mHtrA1Luc_B that showed the highest *mHtrA1* promoter activity. Despite differences in basal activity, only negligible differences could be observed between OST and CTRL conditions. The mHtrA1Luc_B contained all potential transcription factor binding sites as depicted above and additionally included two potential RAREs at -1169bp and -972bp relative to ATG. The mHtrA1Luc_B2 reporter construct consisted of the first 300bps upstream of start site in *mHtrA1* promoter region only, and carried all putative transcription factor binding sites of interest, with the exception of the potential RAREs. Interestingly, despite being much shorter in length and lacking the potential RAREs, the mHtrA1Luc_B2 construct showed a higher promoter activity than its precursor construct, the mHtrA1Luc_B. Furthermore, no reductions in Luciferase activity were observed following the removal of an additional 100bps (mHtrA1Luc_B2). Finally the mHtrA1Luc_B3 truncated luciferase reporter was split up into two new constructs to investigate the possible contribution of each region to *mHtrA1* promoter activity. Accordingly, mHtrA1Luc_B3.1 excludes the NYA and putative TFAP2alpha binding sites. Although only minimal differences in Luciferase activity could be observed between uninduced and osteogenic induced cells, the results did indicate that region -250 to -100 of the *mHtrA1* promoter maybe important for basal *mHtrA1* promoter activity.

After extensive and unsuccessful attemts to identify the upstream part of the promoter responsible for upregulation of *mHtrA1* gene expression upon osteogenic treatment, the possibility of involvement of downstream elements such as inhibitory STAT sites located within the first intron, as well as unknown negative regulatory elements further downstream of the start site were considered (Fig. 14).


RARE(DR5)
01 CGACTCCTCCTTGAGTCAGGGTCAGCAGCACTCTGCCCACCACCCTGGGGTGTGTTATGGCGAGGTGCATGGGGAACTCAGGTGGGGA
02 CAGCACATACTTTAATTCTCTCATCTTCCAATACAAGATTTATGTGTTCTGTGTTGGCCAGGCACAGAGATCTGCCTCCGGGGTGACA
03 GTTGCTCTTCCTGATGATTCTTAGACTCATCTCGGTCCCAAACGTCACTTAAATCCTCATGTGAGAGCTCAAAATAAAACATCTTGTT
04 TTGGGACACCTTGATTTGCCCGAGCGCTGGGACTGCAGGCGCGGGCTGGGCGCTTCTGTGTGGTAACAACGCATTCCCTAACAGCTCA
05 GGGTGAAAAAGTACAAACTGTACAAAGCCCGGTGGCCACGGCATGCTCCCGGTGGCCCTCCAAGTACCAAACCCAGATACCCGAGGCG
06 TGCTATGGCATGCACTCCACCGAAAGCAACTTTAAAAGAGAAGCGTTAGGAAGGTTTACACTGTCATTCGCCAATGCTTTTTGCTTCT
07 CTCACTTGAAACTAGGTCTGGGCACTGGGTTTCTGCCAGTCCTGCTGACGCTGCCTTCCCACGGCGGCGTCAAGTTCACAGCCACAGT
08 CCCCCAAGCTGGGCACCGGTCCATTGCAGCTGTGGCCGGGGTCGATGTGACCGCCCTCCGCACTGGACGACCTGGGAACTTTCCAGGC
09 GATTGCGCAGTGCTAGGCAGGTTTCCCTCTGTTAAGTGCCACTTTGGTCTTAAGGTCTTCAATCTCTGAGGAAAAAGAATCCTAGAAT
Sp1
10 GAGAAACTGAGCCAGCCGGAGGGTGGAGTCGCGGCCCGCCCCGCCTCGTCCCCGCAGGCAGTCCCCGATCGGCCCCCCTCCCGGGAGC
Creb/Atf
Nya
11 GGTGCCCGTCCCCCTGGCGCTTCGTCACCGCCGCTAGGCCAATGGGCTTAACCGTACGGCCGCGCACACTCGCACCCGCTGTCCCCAA
TSS
-1
12 GACCCCGACACACCGTCCCGAGCGCGGTTTTTCGGCTGTGGTCCAGCCCGTGGCCGTCGGAGTCGTCATGCAGTCCCTGCGTACCACG
13 CTCCTGTCTTTGCTACTGCTGCTGCTAGCGGCTCCTTCCTTGGCGTTGCCGTCGGGGACCGGCCGCTCGGCCCCAGCTGCCACCGTCT
14 GTCCCGAGCACTGCGATCCCACCCGCTGCGCCCCGCCGCCCACGGACTGCGAGGGTGGCCGCGTCCGCGACGCGTGCGGCTGCTGCGA
15 GGTGTGCGGCGCGCTCGAGGGTGCAGCGTGCGGCCTGCAGGAGGGTCCCTGCGGCGAGGGGCTGCAATGCGTAGTGCCCTTCGGGGTG
16 CCGGCCTCGGCCACAGTACGACGGCGCGCACAGGCCGGCCTGTGCGTGTGTGCCAGCAGCGAGCCGGTGTGTGGTAGCGACGCCAAGA
17 CCTACACCAACCTGTGCCAGCTGCGCGCCGCCAGCCGCCGCTCCGAGAAGCTTCGCCAGCCGCCGGTCATCGTCCTGCAGCGCGGCGC
1st Intron
18 CTGCGGCCAAGGTACCCGCCCCGCCCTGCGCTGCACTCCTGGGTGGCTCCCCACTCTCGCCAACTCAGCCCGACCAGTCAGGACCGTC
19 GGGAGGGGATGCGGAGGTGCAGAGAAGCACTGCGGGGTGTTCTAGGCATCCAGTTAGTGGGAGAGAGAGACGATGGGGCTCGGGGTAG
STAT
20 CTGTGTTTCAAAGGCTCCCTCCGGCCCTATTTCTGCGCCAAGCATCGGGTCGTTTCGAGAAACGCCAAGCAGGTGCTTTGCGCGCTTT
21 GGTCCAGCACCCCCTGGCCGGGGTGACTAGGCATCGCGCTGGGGAAAGCCGCGTATCATACCAGGGATCTTGGCAATGTTGAGATACA
STAT
22 TGGCTTTGGGATCGCAAGAACTCTTGTCGCCTTCCCTTCCTTCTCCCTTTCTGCTGAGTCCTCTCTTCTTGGAACTATCTAAGCAGTG
STAT
23 TTTTTCTTATAGAACCTCTTCGTGAAAACTTTCACTTTGGGGAGAGGGAACATCTCTGCTCAACTCAGCAAGCATTTTTCTCACCCCG
24 CCTCCTAAGCAGAAAACGATTTAGTAACTCCGGCCCTCTTCCTCCATTGATTTAAATCAACTTTACAAAAACGCCCACGATTTGGTCC
25 TTTTTTGGTCCTTTGGTCCTTTTGCCTGAGTTCAACCAGGTAGTGGACCGTGAAATTTGAGGTAGAGGAGGGGCCCACTGGGGATGAA
26 GAAAAAAATGCACCCTCTACCCTCTCTCTCCTTGTGGGACCTTTCTGTACCCACAAGAGCTGGACGTGGTGGTGGCGACAGGGTAAAG
STAT
27 GGGCTTGGAGAACTGCCCAGCTCCCTGCAGGACCTTCCAGAGAAAAGCTTCGGTTAAATCCAGAGATACCCTGTGGAAAAACAGTAAA
28 TTCATACTGGCCACTACAGCGCTGTGGGGACCAGCCAGCTGGGCTCCAGTACATTTGGCTTCAGCTACAGGGCTCCTGCCCAAACCTA
29 GCACCTCCCTCCCCTCCGCCCCCCCACCCCCCATGTGGTGGGGAGGACAGGAAAGCACGGGAGAGGGAAAGAGAGATTGAGCTAGATT
30 TTTCTTTATAGGAATATGGTCGCCTATGACCACTTTGAATTTGGCAAAACTTTACTCGAATGCACAGGAAAGTACTCCAGGTGGTGTA
31 GGAAGAGGTGGGCTGGTGTTTATATTCTTACCACAGGAGCACAGGACTGGACCTCAGTCCCAGGAAACTCAGCCTCCATAGAGAGAAG
32 AAAAGGGTTTTTGTTTGTTTGTTTGTTTGTTTGTTTGTTTTCAGAGAGGACTGATCCCGGGGTCCCTACCTACTAAGTCCCAGC
33 CCATGTGACAAGTGAGTTATCCTGTGACTCTATTTGGTCTCCTAGACCCGGGAGGAGGAAGCTCCTGGCCTCGTCTTTGTCTTAGATG
34 AGGTGGAACTGGGGATGAATAACTTGTCCAAGGTCACTCAGCTGGAACCTGAATGCTGGCAAACTCAGAACAGGCCAGAGCTAGACCT
35 CAAGGCTATGGGAAATGGGCTTCCAGGGGGCTGGACCAGCCAACTCACCTTGGGGAGAGGTAGAGAACTATGTAGCTCCTGAGTGGAT
36 ACTTTGAGGTGGAGAATAGATTGGTGTTAGTTAGTTAGTTAGTTAGTTAGTTAGACAGACACGGGCAGAAGTGACCCACAGTGG
STAT
37 TGGCTCAGAGTCCCCTGGGGAGGAAGTAGTGTGTCACACGTGCAGATATCCTTGAGTAGTTCTTGAATAGGCTCTGTTCAGAGGAGGG
STAT
38 CTGGCGTAGAACTAGCCTAGAGGGGGAGGGCAGAAGGTAGGAATCTGGGCTACTTTCACCAGAATCTGAGTGTGCACAGGTGACATTT
39 TTTTTTTTTTTAAAAAGCACATTTTGGTGGGAAACCAGGTAGCTGTCACTCTTTGTAGTCTTGCTGCACAAGGCCAGGAGTTACAGAC
40 ATCAGCAGAGGCCAAATACTTGGCTGGTTGAGTTGTATTGGGGAGACAGGTCCTTTGTTGGCCAGCAGGGCCCCAGTGGCCCCTAAGT
41 GTGGAGACAGCCACAGATGAAGCATAGAGCTGGTGGTAGCCATCTCCCCTCCTTTTGTAAATATCTGTTGCTCTGTATCACGTCTGAC
42 ATGTGTGCCTGGTACTTAGGGACAGCTAGTTACGTGGGAGGATGGATAGAAAGACAGGAGATACTTGGCGTACACAGCCGACCCTCAG
43 CCTGGCTTCGCCCTGACTCTCCATCTGAGGCTGTCTTAAGGTCCCAGGAGCAGAGTCTGTGAGTCAGTGAGCTGCTTTCATTCAGTCC
44 CTTTCTGGCCCCCGCTTTTAGCAGCTGGTGTCCAGGGACAGCTAGTGTACTTGATGTCACCCTTGAGTAAGGAGAACTGGCTGCCTGC

Figure 14. DNA sequence showing potential TF binding sites of interest upstream and downstream of the transcription start site (TSS) extending into the first intron. Retinoic Acid Response Element DR5 (RARE DR5) (line 01), specificity protein 1 (Sp1) (line 10), CAMP Responsive Element Binding Protein (CREB), Activating Transcription Factor (ATF) (line11), Nuclear Transcription Factor Y (NYA) (line 11),

Signal Transducer and Activator of Transcription (STAT) (lines 20, 22, 23, 27, 37, 38), RAR-related orphan receptor beta (ROR-β) (lines 70, 71).

This was tested through the generation of the three luciferase reporter constructs mHtrA1Luc_LLI, mHtrA1Luc_LLII and mHtrA1Luc_LLIII covering large downstream parts of the promoter as shown in Fig. 15. To minimize interference of dual ATG sites, from the *mHtrA1* promoter as well as from the luciferase gene, the *mHtrA1* ATG of all three luciferase constructs was mutated to AAA using site directed mutagenesis.

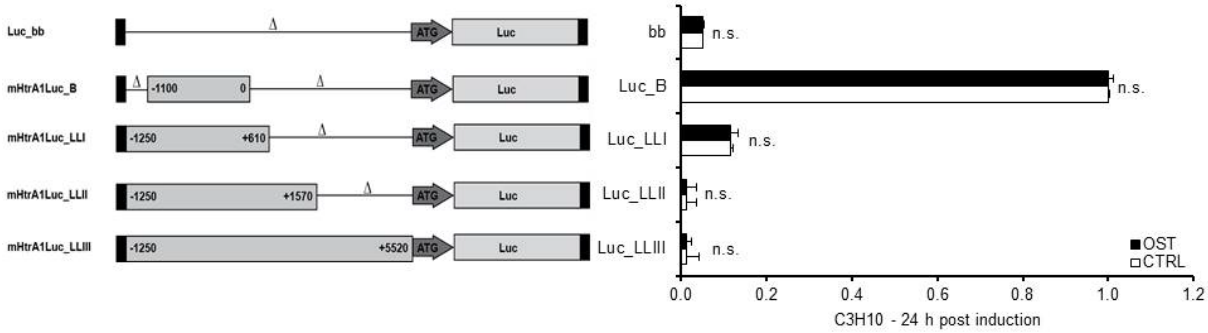

Figure 15. Deletion analysis of *mHtrA1* promoter activity focusing on downstream elements, along with part of the first intron of the *mHtrA1* gene. Assay carried out in C3H10T1/2 mouse fibroblasts and measured at 24h post osteogenic induction (OST). Left: Based on the previously used mHtrA1Luc_B construct, additional *mHtrA1* promoter luciferase reporter constructs were generated to determine the contribution of downstream elements on *mHtrA1* promoter activity. Right: Data representation of the *mHtrA1* luciferase reporter assay. Expression of Firefly Luciferase was normalized to SV40 driven Renilla expression. Representative graphs of at least three independent experiments are shown. CTRL, uninduced controls; OST, osteogenic induced. Not significant (n.s.) as compared to uninduced controls (CTRL) using Student's t-test.

Despite the additional upstream and downstream elements contained in mHtrA1Luc_LLI construct as compared to the mHtrA1Luc_B construct, no significant differences were observed between uninduced and osteogenic induced cells. However, basal Luciferase activity was noticeably reduced. Similarly, the mHtrA1Luc_LLII, which is based on mHtrA1Luc_LLI but with the inclusion of an additional 960bps extending into the 1st intron also failed to show any responsiveness

to osteogenic induction. Extending even further downstream, the mHtrA1Luc_LLIII luciferase reporter construct, which is based on mHtrA1Luc_LLII reaches as far as +5500bp to include potential cis negative regulatory elements, but despite differences in basal promoter activity levels, this construct also failed to show any responsiveness to osteogenic induction. Hence, it seems plausible therefore that either ATRA-mediated *mHtrA1* expression is not regulated at the transcriptional level or that the Luciferase assay approach is simply not a suitable to investigate this. Notably, to exclude the possibility of interference of naturally occurring low levels of ATRA within FSC, charcoal stripped FCS was used as well as Phenol red free media as this pH indicator is known to be a weak estrogen mimic that binds to and activates steroid hormone receptors, which could then subsequently interfere with the RARs.

In order to try and further identify other potential candidates involved in transcriptional regulation of ATRA-mediated *mHtrA1* expression, we concentrated our efforts on investigating the role of various components of the ATRA signaling cascade using the siRNA approach. We targeted key components of the bone morphogenetic protein (BMP) and AMP-activated protein kinase (AMPK) signaling pathways, which are known to be responsible for transduction of ATRA signaling during osteogenic induction. Subsequently, the impact on *mHtrA1* expression under osteogenic conditions was determined as depicted in Fig. 16. Knock-down of BMP signaling components, the small mothers against decapentaplegic (SMADs), does not seem to have a major impact on *mHtrA1* gene expression (siRNA-SMAD_5_1/4, siRNA-SMAD_1_1/2, siRNA-SMAD_9_1/4). However, repression of AMPK related signaling components did indeed reduce *mHtrA1* gene expression, as observed when knocking down AMPK alpha 1 and AMPK alpha 2 catalytic subunits (siRNA-Prkaa_1_1/2/3, Prkaa_2_1/2/3 and siRNA-AMPK_α-1_1/2) or its upstream effector Liver kinase B1 (Lkb1) (siRNA-Stk11_1/2), suggesting it`s potential role in regulating *mHtrA1* mRNA expression.

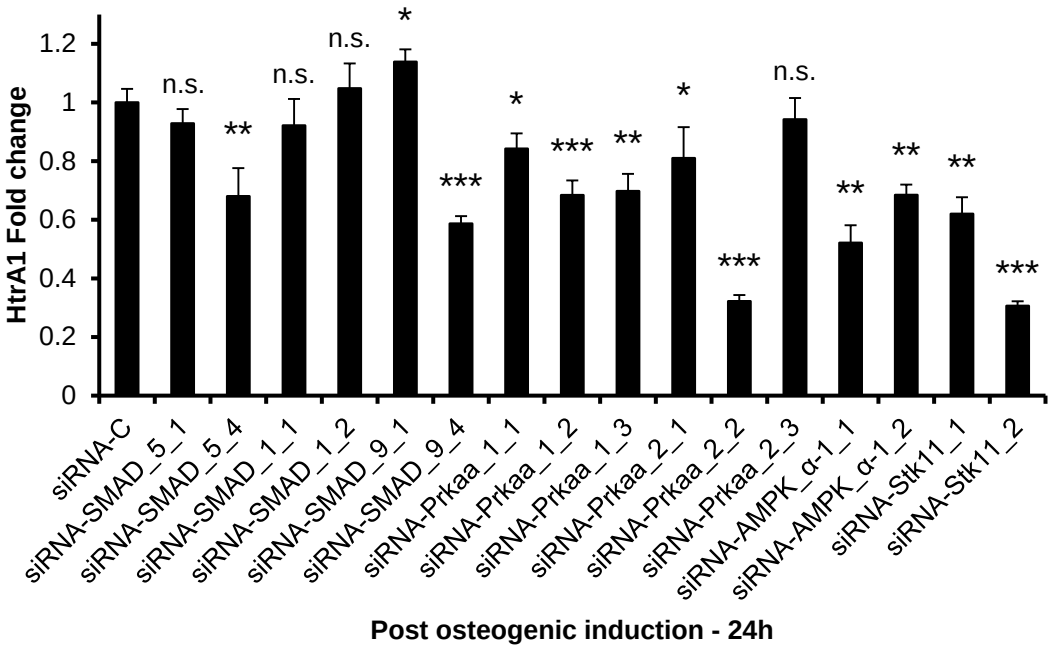

Figure 16. siRNA mediated knock-down of key BMP and AMPK signaling pathway components associated with osteogenic differentiation in osteogenic mASCs. Quantitative polymerase chain reaction analysis of *mHtrA1* gene expression in mASCs transfected with indicated siRNA oligos using the NEON electroporation method and analysed 24h post osteogenic induction. Data were normalized to expression levels of ribosomal protein S12 (*Rps12*) and expressed as fold change in comparison to cells transfected with a non-target control siRNA-C using the comparative C_T method. Small mothers against decapentaplegic (SMADs) (siRNA-SMAD_5_1/4, siRNA-SMAD_1_1/2, siRNA-SMAD_9_1/4), AMPK alpha 1 and AMPK alpha 2 catalytical subunits (siRNA-Prkaa_1_1/2/3, Prkaa_2_1/2/3 and siRNA-AMPK_α-1_1/2), Liver kinase B1 (Lkb1) (siRNA-Stk11_1/2). Significances were calculated using the Student's t-test and are referring to control oligo siRNA-C versus target oligos, * $p<0.05$, ** $p<0.01$, *** $p<0.001$. N.s., not significant.

The major signaling pathways regulated by ATRA are through alterations in protein kinase activity, including mitogen-activated protein kinases (MAPKs) and AMP-activated protein kinase (AMPK). In line with our findings of AMPK affecting *mHtrA1* expression, AMPK production and activation levels in mASCs were increased by 24 h in response to osteogenic induction, suggesting its possible involvement in ATRA-mediated regulation of osteogenesis. Assuming AMPK is a major player within the signaling cascade regulating expression of *mHtrA1*, selectively targeting it with a specific activator, would therefore be expected to increase *mHtrA1* expression. As

shown in Fig. 17, mASCs were treated with the selective AMPK activator Metformin and subsequently the impact on *mHtrA1* expression was measured.

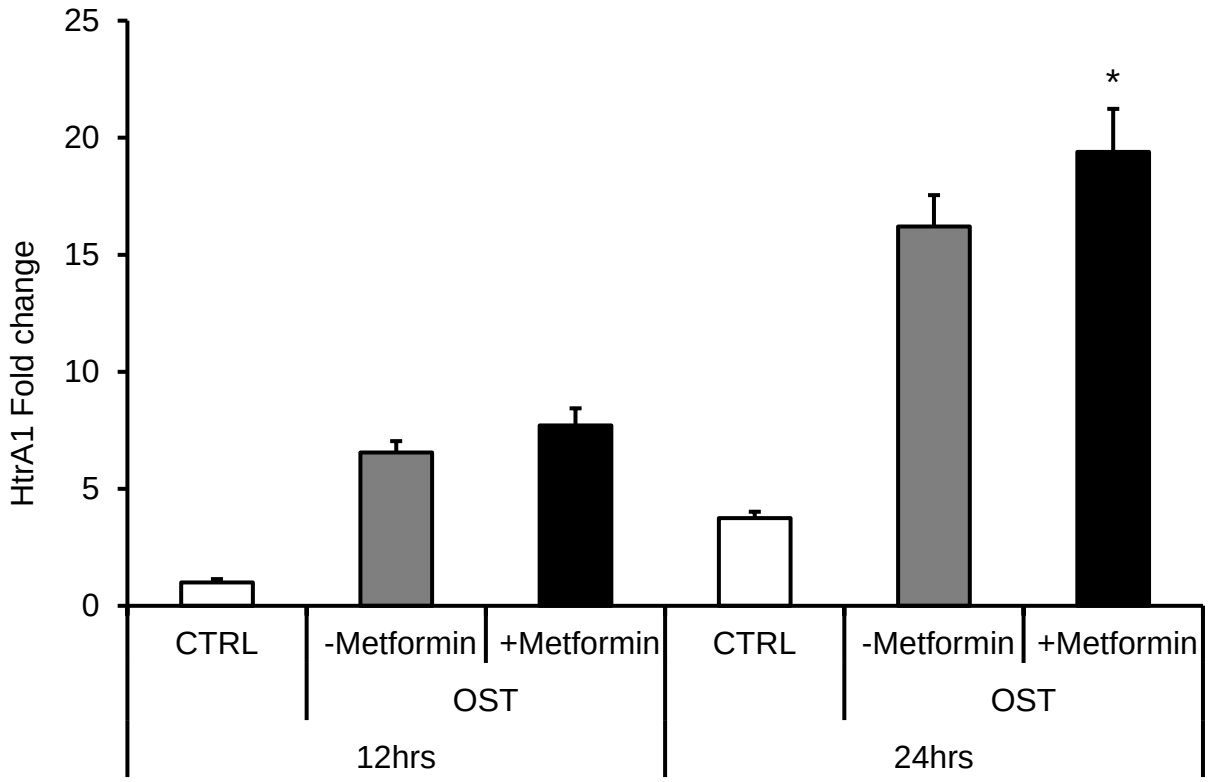

Figure 17. Quantitative polymerase chain reaction analysis of *mHtrA1* gene expression in mASCs pre-treated for 2h with 1mM of the selective AMPK activator Metformin and throughout the whole osteogenic time course. Expression was analysed 24h post-osteogenic induction (OST). Data were normalized to expression levels of ribosomal protein S12 (*Rps12*) and expressed as fold change in comparison to OST cells without inhibitor using the comparative C_T method. Representative graphs of at least three independent experiments are shown. *$p < 0.05$ as compared to –Metformin at day 24 as determined by one-way ANOVA.

Treatment with Metformin had no effect on early *mHtrA1* expression levels, although a small but significant ($p = 0.01$) increase was observed after 24h. Attempts to investigate this further using the selective AMPK inhibitor Dorsomorphin were complicated by high levels of cell death, even at low doses. Therefore, on the minimal effects observed with Metformin, we considered the involvement of AMPK in mediating the effects of ATRA on *mHtrA1* expression to be minimal.

3.2.3.Post-transcriptional regulation of *HtrA1*

Due to the lack of findings in identifying transcriptional regulators of *HtrA1* or components within their upstream network governing their action, we also considered posttranscriptional regulation of *mHtrA1* gene expression through micro RNAs (miRNAs) as a possible scenario. A previous study investigating the role of HtrA1 in the regulation of radial glia cell proliferation has already identified miR-30e and miR-181d as being important regulators of *HtrA1* expression [1]. Two approaches were chosen. Firstly, we investigated the action of predicted miRs, namely members of the miR-30 family, on *mHtrA1* gene expression. Secondly, we investigated the potential repressive effects of the *mHtrA1* 3' UTR in a Luciferase assay.

As a control for functionality of the assay, the well-known tumour suppressor miRNA let-7c which represses expression of the High-mobility group AT-hook 2 (*Hmga2*) oncogene, was inhibited in mASCs using its specific miRNA inhibitor miR-Let7c. Successful transfection of the miR-Let7c was therefore expected to interfere with miRNA let-7c mediated suppression resulting in the up-regulation of *Hmga2* gene expression. This was indeed the case as shown in Fig. 18.

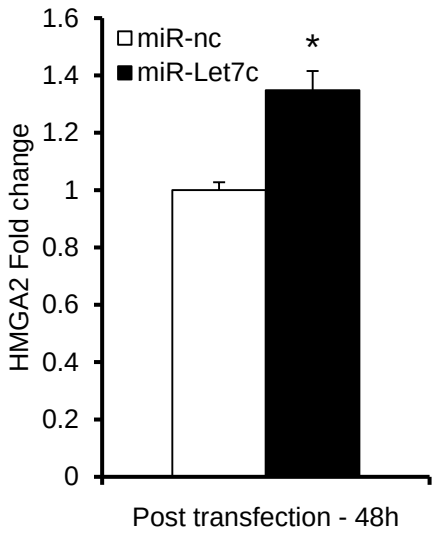

Figure 18. Up-regulation of *Hmga2* oncogene expression in mASCs upon successful transfection of miRNA let-7c inhibitor miR-Let7c using the siRNAmax lipofection method. Quantitative polymerase chain reaction analysis of *Hmga2* gene expression analysed 48h post transfection. Data were normalized to ribosomal protein S12

(*Rps12*) expression levels and expressed as fold change in comparison to cells transfected with a non-target control miR-nc using the comparative C_T method. Representative graphs of at least three independent experiments are shown. Significances were calculated using the Student's t-test and are referring to control oligo miR-nc versus target oligo miR-Let7c, * $p<0.01$.

Based on their previously reported role in regulating HtrA1 gene expression, as well as their involvement in MSC osteogenesis, we predicted the two miRNAs miR-30a and miR-30b as potential post-transcriptional regulators of *mHtrA1* gene expression in osteogenic mASCs. As determined by using a negative control miR oligo (miR-nc) the optimal concentration with the least side effects on *mHtrA1* gene expression was shown to be 50 nM (Fig. 19 – left panel). However, the predicted miRNA inhibitors of *HtrA1* miR-30a and miR-30b did not result in any significant increase of *mHtrA1* gene expression, regardless of concentration, indicating that they are either not targeting the regulatory miRNA or *mHtrA1* is not post-transcriptionally regulated by miRNA under these conditions (Fig. 19 – right panel).

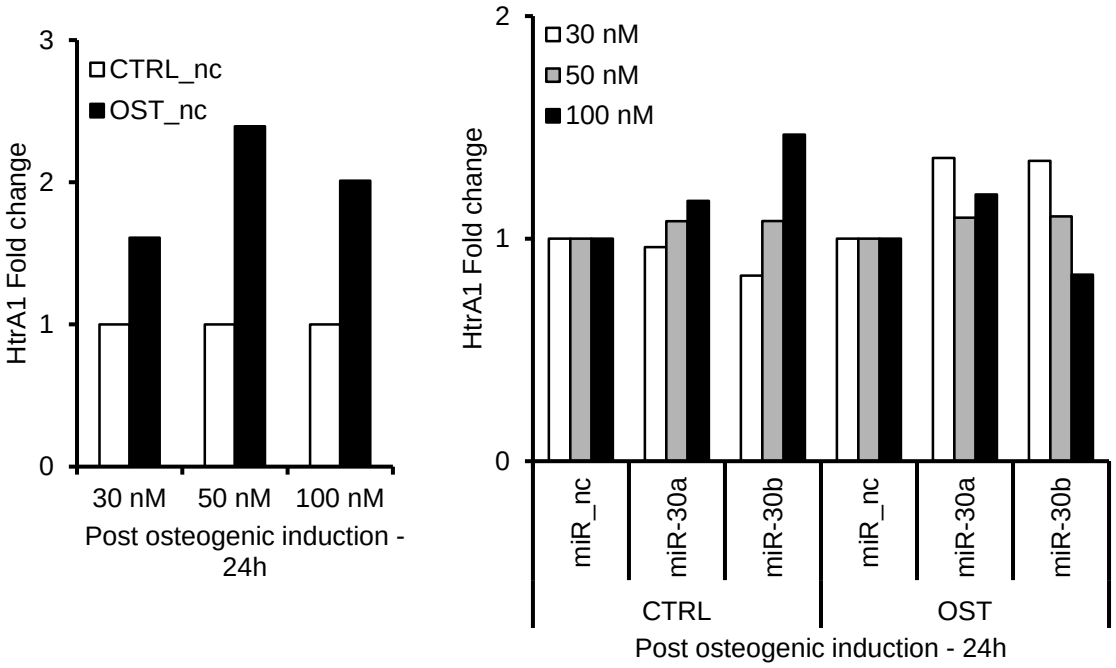

Figure 19. Determination of optimal miR oligo concentration in mASCs (left panel). Effect of miR-30a and miR-30b on *mHtrA1* gene expression under normal (CTRL) and osteogenic conditions (OST). Quantitative polymerase chain reaction analysis of

mHtrA1 gene expression in mASCs transfected with miRNA control and target oligos using the RNAiMAX method and analysed 24h post osteogenic induction. Data were normalized to expression levels of ribosomal protein S12 (*Rps12*) and expressed as fold change in comparison to cells transfected with a non-target control miR-nc using the comparative C_T method. Representative graphs of two independent experiments are shown.

Equivalent to their effect on *mHtrA1* gene expression, miR-30a and miR-30b also failed to have any impact on the mineralization capacity of transfected mASCs (Fig. 20).

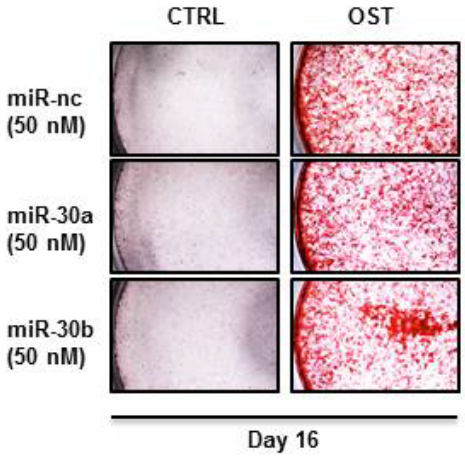

Figure 20. Representative images of Alizarin red-stained mASC cultures transfected with miR oligos miR-nc, miR-30a and miR-30b as indicated under control (CTRL) and osteogenic (OST) conditions.

Taken together, these results suggested that it was unlikely that *mHtrA1* gene expression was being regulated by these particular miRNAs. Therefore, we decided to additionally look at the contribution of potential miRNAs on a less specific level. Here we utilized the mHtrA1 3' UTR as a potential binding site for inhibitory miRNAs by incorporating it into a constitutively active luciferase construct with the intention of inhibiting basal Luciferase activity (Fig. 21).

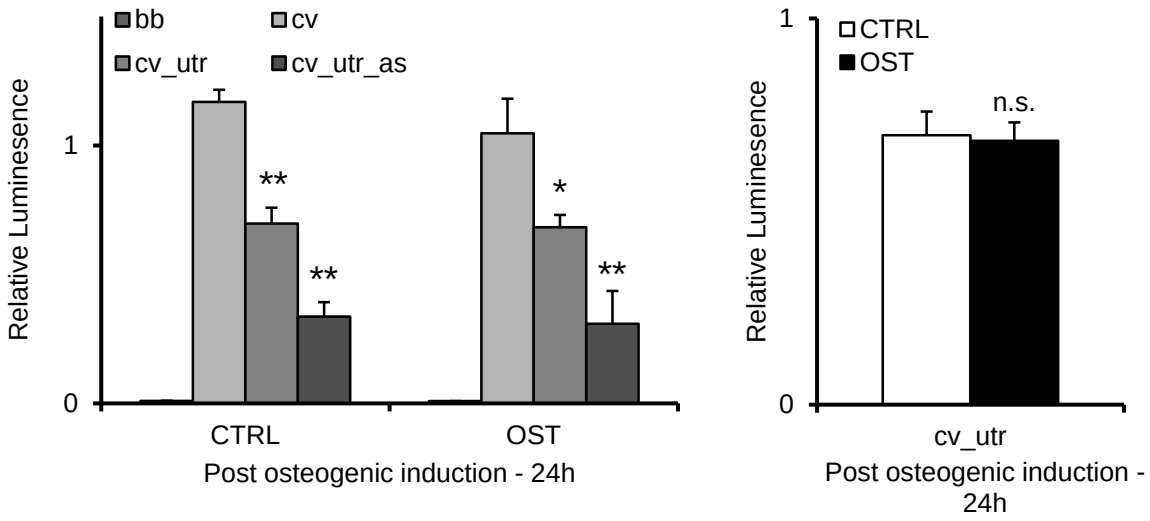

Figure 21. Luciferase assay of *mHtrA1* 3' UTR tagged constitutively active luciferase reporter vector in sense (cv_utr) and antisense orientation (cv_utr_as) in comparison to non-tagged control vector (cv), under normal (CTRL) and osteogenic (OST) conditions (left panel). Direct comparison of *mHtrA1* 3' UTR tagged vector only under both conditions (right panel). Assay carried out in mASCs and measured at 24h post osteogenic induction. Expression of Firefly Luciferase was normalized to SV40 driven Renilla expression. Representative graphs of at least three independent experiments are shown .Significances were calculated using the Student's t-test and are referring to left panel: untagged control vector (cv) versus *mHtrA1* 3' UTR sense tagged (cv_utr) and *mHtrA1* 3' UTR antisense tagged (cv_utr_as), right panel: *mHtrA1* 3' UTR sense tagged (cv_utr) normal conditions CTRL versus osteogenic conditions OST, * $p<0.05$, ** $p<0.01$. N.s., not significant.

As depicted in Fig. 21 (left panel), the *mHtrA1* 3' UTR tagged control vector (cv_utr) shows a significant reduction in luciferase activity under control conditions as expected. However, this effect could not be reverted under osteogenic conditions (for direct comparison see Fig. 21 – right panel), indicating that a post-transcriptional regulation of *mHtrA1* by miRNAs is a very unlikely scenario. Also a control vector tagged with the *mHtrA1* 3' UTR in antisense orientation (cv_utr_as) shows the opposite effect and is even further reduced instead of being equivalent to the non-tagged control vector (cv). Therefore we were unsuccessful in confirming the contribution of miRNAs to the regulation of *mHtrA1* expression under these conditions.

In order to exclude the idea of *mHtrA1* expression being regulated by miRNAs under osteogenic conditions, we additionally targeted the mRNA degrading RISC complex and examined *mHtrA1* expression. As regulation of gene expression by miRNAs presumes a constitutively active promoter, and the RISC complex is responsible for degrading microRNA, inhibition of the RISC complex should then under non-osteogenic conditions result in the same upregulation of *mHtrA1* gene expression as seen under osteogenic conditions. Therefore we used the two well-known RISC inhibitors Aurintricarboxylic acid (ATA) and Suramin hexasodium salt (each at 25µM) which both inhibit miRNA loading to Ago2 of the RISC complex as well as de novo RISC assembly. As seen in Fig. 22, inhibition of mRNA degrading RISC complex does not affect *mHtrA1* gene expression, confirming that miRNAs and therefore the scenario of regulation of *mHtrA1* gene on a post-transcriptional level can be excluded.

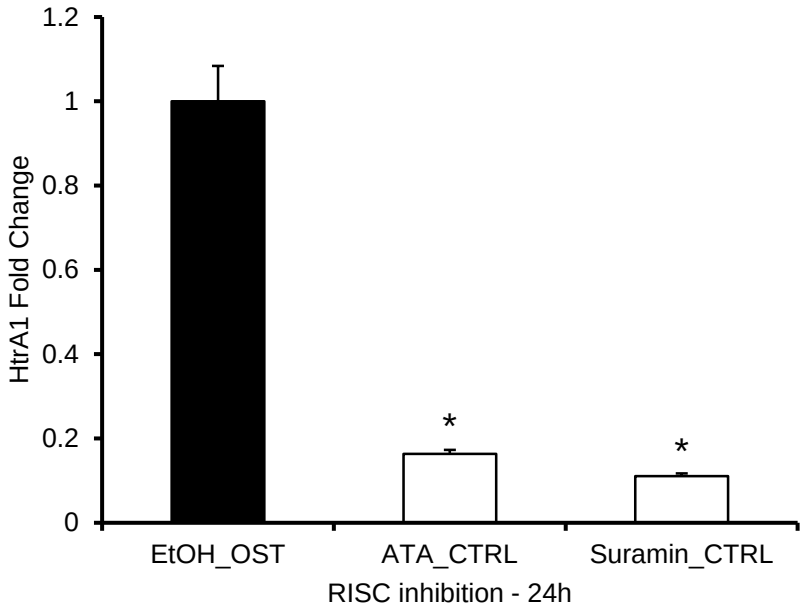

Figure 22. Effect of inhibition of the RISC complex using Aurintricarboxylic acid (ATA) and Suramin hexasodium salt on expression of *mHtrA1*. Quantitative polymerase chain reaction analysis of *mHtrA1* gene expression in mASCs treated with RISC inhibitors both at 25µM final concentrations and analysed 24h post osteogenic induction. Cells were treated 2h pre-osteogenic induction and throughout the whole assay. Data were normalized to expression of ribosomal protein S12 (*Rps12*) and expressed as fold change in comparison to cells treated with the solvent ethanol only using the comparative C_T method. Representative graphs of at least

three independent experiments are shown. Significances were calculated using the Student's t-test and are referring to EtOH_OST versus ATA_CTRL and Suramin_CTRL, * p<0.001.

3.2.4.Regulators of basal *mHtrA1* promoter activity

Although we were unable to identify transcriptional regulators of ATRA-mediated *mHtrA1* expression, basal promoter activity was affected using truncated luciferase reporter constructs and therefore in the next step we tried to identify the regulators of basal *mHtrA1* expression based on the putative transcription factor binding sites as depicted in Fig. 11.

3.2.4.1. NYA binding site

We initially investigated the Nuclear Transcription Factor Y, Alpha (NYA) predicted binding site located at -118bp relative to ATG (Fig. 11 – line 11). NYA is a highly conserved trimeric transcription factor known to bind to the highly conserved sequence motif 5'-CCAAT-3' and thereby facilitating transcriptional activation [464-468]. Knock-down of NYA using two different siRNA oligos significantly reduced *mHtrA1* expression in osteogenic mASCs (Fig. 23).

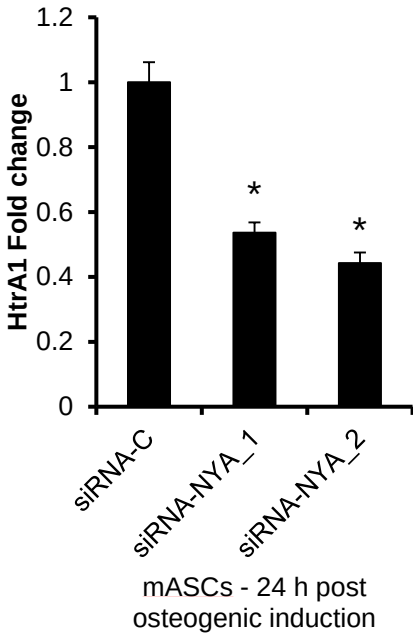

Figure 23. Effect of siRNA mediated knock-down of NYA (siRNA-NYA_1/2) on *mHtrA1* expression in osteogenic mASCs. Quantitative polymerase chain reaction analysis of *mHtrA1* gene expression in mASCs transfected with corresponding siRNA oligos using the NEON electroporation method and analysed 24h post osteogenic induction. Data were normalized to expression levels of ribosomal protein S12 (*Rps12*) and expressed as fold change in comparison to cells transfected with a non-target control siRNA-C using the comparative C_T method. Representative graphs of at least three independent experiments are shown. Significances were calculated using the Student's t-test and are referring to control oligo siRNA-C versus target oligos siRNA-NYA_1 and siRNA-NYA_2, * $p<0.001$.

In the next step, we attempted to confirm the binding of NYA to sequences within the *mHtrA1* promoter using the electrophoretic mobility shift assay (EMSA). Here, nuclear lysates from osteogenic mASCs were incubated with radio-labelled oligonucleotides containing either NYA consensus sequences or NYA predicated sequences contained within the *mHtrA1* promoter (Fig. 24).

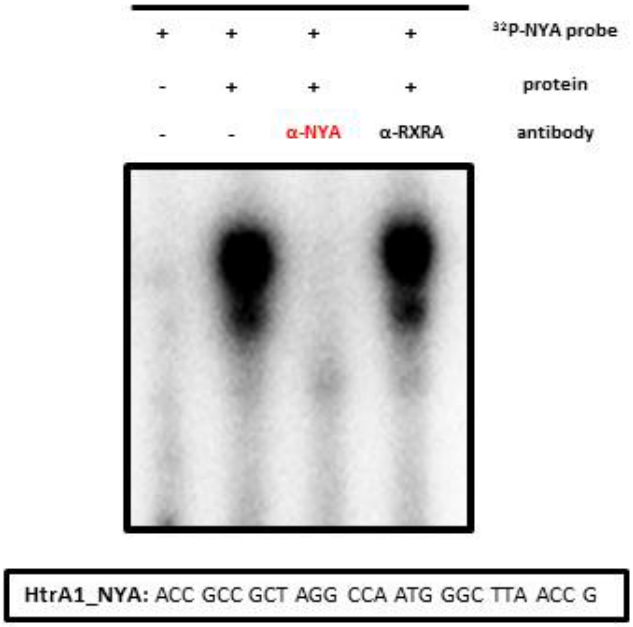

Figure 24. EMSA super-shift assay of the predicted NYA site within the upstream part of the *mHtrA1* promoter. Gel shift assays were performed exactly as described in [469]. Nuclear extracts of mASCs were harvested 24h post osteogenic induction and 4µg of protein incubated with 2µg of antibody for 1h at ambient temperature followed by addition of 1.75pmol ^{32}P labelled double stranded oligo (^{32}P-NYA) and another hour of incubation at room temperature.

An obvious shift was observed using the HtrA1_NYA oligo which was super-shifted using an α-NYA antibody but not α-RXRA antibody, thereby confirming the binding specificity. Therefore, NYA may be involved in regulation of *mHtrA1* promoter activity and represents a potential target for further modifications of *mHtrA1* transcriptional regulation.

3.2.4.2. Creb/Atf binding site

Here, the putative cAMP response element binding protein (CREB) / Activating transcription factors (ATF) site located at -134bp relative to ATG (Fig. 11 – line 11) was investigated. CREB binds to the cAMP response element (CRE) with the highly conserved sequence motif 5'-TGACGTCA-3'. The CREB [470-474] / ATF [475-479] transcription factors are considered to be the major targets of AMPK signaling, which in turn is known to be involved in osteogenesis, and therefore are of particular interest. Initial experiments confirmed that the siRNA mediated knock-down of *Creb*

resulted in a significant reduction in *mHtrA1* expression in osteogenic mASCs (Fig. 25).

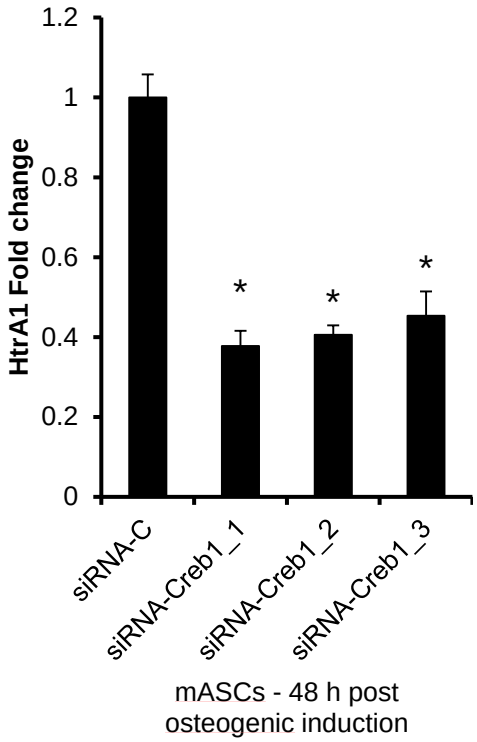

Figure 25. Effect of siRNA mediated knock-down of cAMP responsive element binding protein 1 (siRNA_Creb1_1/2/3) on *mHtrA1* gene expression levels in osteogenic mASCs. Quantitative polymerase chain reaction analysis of *mHtrA1* gene expression in mASCs transfected with corresponding siRNA oligos using the NEON electroporation method and analysed 24h post osteogenic induction. Data were normalized to expression levels of ribosomal protein S12 (*Rps12*) and expressed as fold change in comparison to cells transfected with a non-target control siRNA-C using the comparative C_T method. Representative graphs of at least three independent experiments are shown. Significances were calculated using the Student's t-test and are referring to control oligo siRNA-C versus target oligos, * $p<0.001$.

In the next step, we attempted to confirm the binding of CREB to sequences within the *mHtrA1* promoter using the electrophoretic mobility shift assay (EMSA). Here, nuclear lysates from osteogenic mASCs were incubated with radio-labelled oligonucleotides containing either CREB consensus sequences or CREB predicated sequences contained within the *mHtrA1* promoter (Fig. 26). EMSA competition

assays using a non-radiolabeled consensus control oligo (CTRL) or a mutated oligo (HtrA1_CREB_mut) were used to test specificity of the reaction. Initial observations confirmed that a consensus CREB oligo (CTRL) could produce a shift. Similarly, the CREB site located at -134bp relative to ATG in the *mHtrA1* promoter (HtrA1_CREB) also produced a shift and was abolished by using the mutant oligo HtrA1_CREB_mut. Furthermore, the shift observed using the consensus control oligo (CTRL) was markedly reduced by 100-fold excess of unlabelled HtrA1_CREB. Therefore, CREB/ATF may be involved in regulation of *mHtrA1* promoter activity and represents a potential target for further modifications of *mHtrA1* transcriptional regulation.

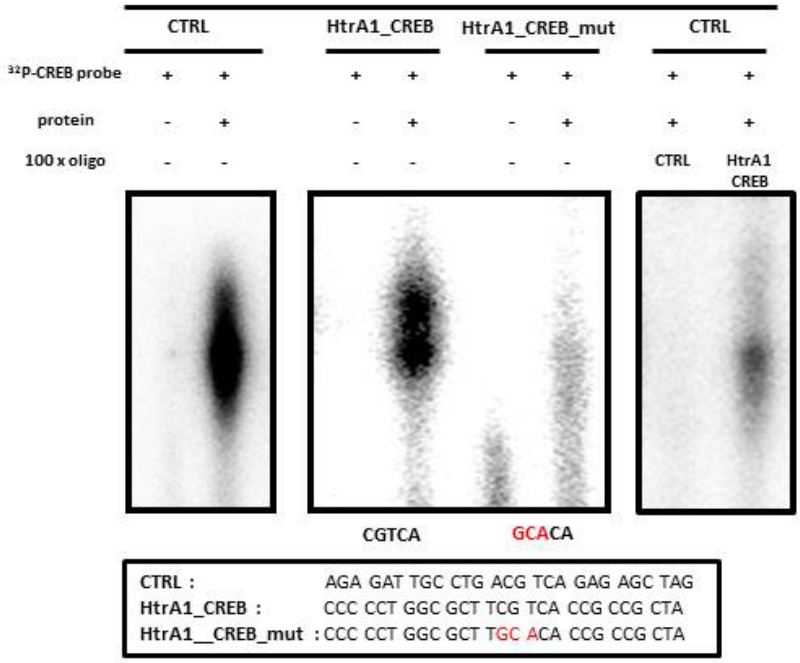

Figure 26. EMSA assay of the potential CREB/ATF site within the upstream part of the *mHtrA1* promoter. Gel shift assays were performed exactly as described in [469]. Nuclear extracts of mASCs were harvested 24h post osteogenic induction and 4µg of protein incubated with 100 fold excess of the indicated unlabelled oligo (100 x oligo) for 1h at ambient temperature followed by addition of 1.75pmol ^{32}P labelled double stranded oligo (^{32}P-CREB probe) and another hour of incubation at room temperature.

3.2.4.3. Sp1 binding site

Located at -211bp upstream relative to ATG within the *mHtrA1* promoter (Figure 11 – line 10) is a potential binding site for the specificity protein 1 (SP1) transcription factor, which can act either as transcriptional activator or repressor by binding to GC-rich motifs and thereby regulating expression of target genes [480-484]. In order to investigate its potential involvement in regulating *mHtrA1* expression, we first tested the impact of siRNA mediated knock-down of *Sp1* on *mHtrA1* gene expression. In the knock-down approach three different oligos were used to target SP1 (siRNA-Sp1_3/4/5) (Fig. 27). The knock-down of *Sp1* did not affect the transcriptional regulation of *mHtrA1* under osteogenic conditions.

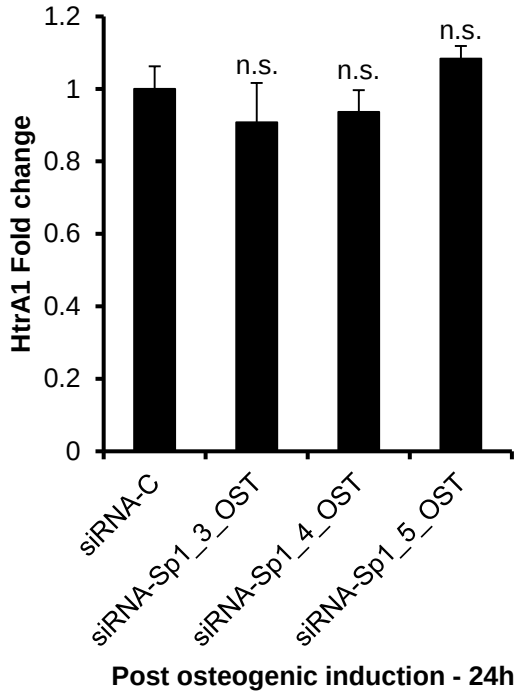

Figure 27. siRNA mediated knock-down screen in mASCs of Sp1 (siRNA-Sp1_3/4/5) showing the impact by reduction of *mHtrA1* gene expression levels under osteogenic conditions. Quantitative polymerase chain reaction analysis of *mHtrA1* gene expression in mASCs transfected with corresponding siRNA oligos using the NEON electroporation method and analysed 24h post osteogenic induction. Data were normalized to expression levels of ribosomal protein S12 (*Rps12*) and expressed as fold change in comparison to cells transfected with a non-target control siRNA-C

using the comparative C_T method. Representative graphs of at least three independent experiments are shown. Significances were calculated using the Student's t-test and are referring to control oligo siRNA-C versus target oligos. N.s., not significant.

Further analysis was carried out using EMSA. Here, a consensus SP1 control oligo (CTRL), target oligo (SP1_HtrA1) and mutated oligo (SP1_HtrA1_mut) were used along with a specific α-SP1 antibody for super-shift assays. Initial experiments confirmed that the consensus SP1 control oligo (CTRL) produced a shift when incubated with mASC nuclear extract and could be significantly shifted using an α-SP1 antibody (Fig. 28). Although the SP1_HTRA1 oligo was capable of producing an obvious shift, it was unfortunately unspecific as this was also observed with the mutated SP1 oligo (SP1_HtrA1_mut) and could be super-shifted with a non-specific antibody. It was therefore deemed unlikely that Sp1 plays a role in regulating basal *mHTRA1* expression.

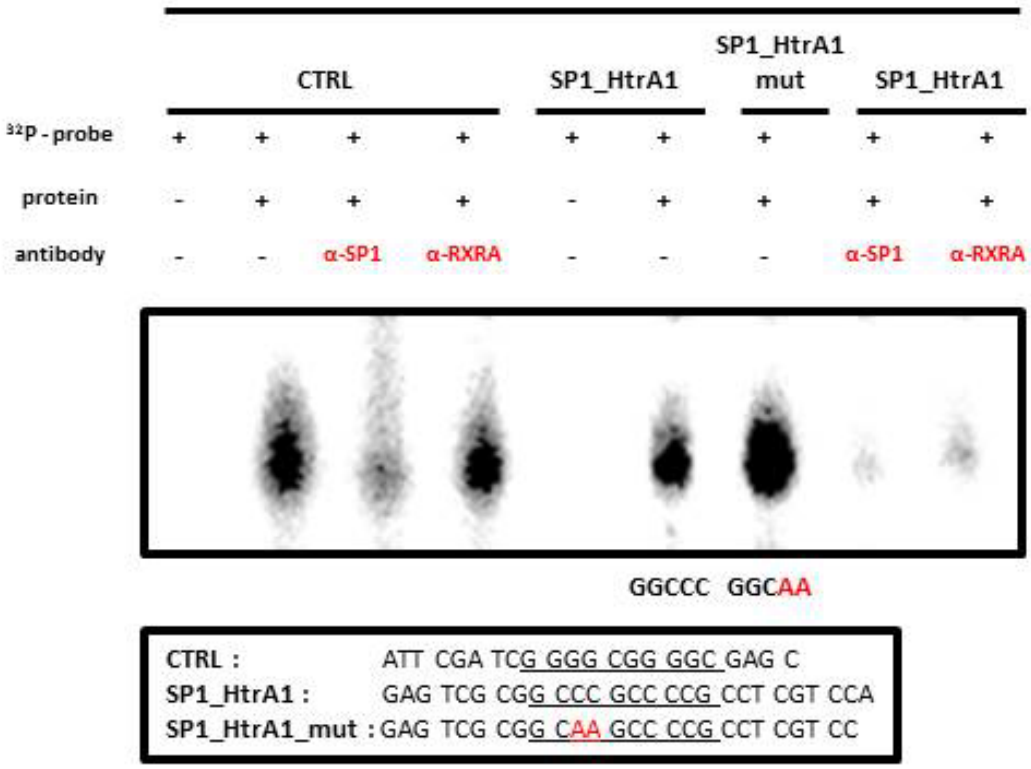

Figure 28. EMSA super-shift assay of the putative SP1 site within the upstream part of the *mHtrA1* promoter. Gel shift assay was performed exactly as described in [469]. Nuclear extracts of mASCs were harvested 24h post osteogenic induction and 4µg of

protein incubated with 2µg of antibody for 1h at ambient temperature followed by addition of 1.75pmol ^{32}P labelled double stranded oligo and another hour of incubation at room temperature. A consensus control oligo (CTRL), target oligo (SP1_HtrA1) and mutated oligo (SP1_HtrA1_mut) were used.

Therefore, our inability to identify a reliable mechanism with which to explain the ATRA-mediated upregulation of *mHtrA1* led us to undertake a different approach to investigating HtrA1's role in mASC osteogenesis as detailed in the manuscript currently in preparation for submission to *Journal of Biological Chemistry*, which accompanies this Thesis.

4. General discussion and future perspectives

Efficient osteogenic induction of mouse adipose-derived stromal cells (mASCs) is reliant on the actions of all-*trans* retinoic acid (ATRA), the carboxylic acid form of vitamin A [263, 368, 372, 485-488]. This is in contrast to mouse and human bone marrow stromal cells (BMSCs), where dexamethasone is primarily used to instigate osteogenesis through upregulation of four and a half LIM domains 2 (FHL2) and activation of Wnt/β catenin signaling [489]. ATRA's ability to influence osteoblast differentiation has been observed in several different cell systems and is considered to be largely dependent on the concentration of ATRA used. Whilst ATRA acts to enhance osteogenesis at micro molar concentrations [263, 368, 372, 485-488, 490, 491], at nano molar concentrations, it has been shown to inhibit both osteoblast gene expression and mineralization [427, 429, 431]. The concentration of ATRA used to stimulate mASC osteogenesis *in vitro* is generally within the range of 1 to 5 μM, where it acts to enhance the expression of several osteogenic markers including alkaline phosphatase (*Alpl*) and osteopontin (*Spp1*) and induce mineralization of mASC-derived osteoblasts [263, 487]. In addition, ATRA's ability to direct mASCs along the osteoblast lineage *in vitro* has also be exploited for the purpose of enhancing mASC-induced new bone formation *in vivo*. Priming of mASCs with ATRA prior to their implantation into mouse calvarial defects resulted in accelerated bone regeneration as compared to mice treated with unstimulated mASCs [343]. However, the mechanisms through which ATRA instigates its osteogenic effects in these cells remain unclear. Findings from studies investigating the combined effects of ATRA and bone morphogenetic protein (BMP)-2 on mASC osteogenesis suggested that ATRA's primary function was to regulate BMP signaling through enhanced BMP receptor (BMPR) expression [368]. However, ATRA also has the ability to induce osteogenic differentiation of mASCs in the absence of exogenous BMP-2 [263, 372, 485-488]. Therefore, it's likely that in addition to BMP signaling, ATRA targets other pathways critically involved in regulating mASC osteogenesis.

We have previously identified high temperature requirement protease A1 (HtrA1) as a novel mediator of human BMSC (hBMSC) differentiation, where it acts to enhance osteogenesis and subsequent mineralization by differentiating bone-forming cells [372]. Furthermore, *HtrA1* expression is upregulated in mASCs in response to ATRA-containing osteogenic induction medium [372]. HtrA1 is a member of the HtrA family

of serine proteases and has been linked to various biological processes by virtue of its ability to interact with numerous intracellular and extracellular substrates [376]. Tuberous sclerosis complex 2 (TSC2) was the first cytoplasmic HtrA1 substrate to be identified, and its degradation by HtrA1 was shown to result in activation of the mammalian target of rapamycin (mTOR) pathway as confirmed by alterations in the phosphorylation of downstream targets eukaryotic initiation factor 4E binding protein 1 (4E-BP1) and p70 ribosomal protein S6 kinase (p70S6K) [400]. This bears particular significance with regards to mASC osteogenesis based on the fact that mTOR signaling plays a positive role in the osteogenic induction of several cell types including BMSCs [209, 217, 218]. However, no studies have yet sort to investigate its involvement in mediating the osteoinductive effects of ATRA on mASCs, or whether HtrA1's ability to influence mTOR signaling plays a role in determining mASC osteogenic potential.

mASCs represent a readily available source of osteoprogenitor cells, which unlike mBMSCs, have the advantage of being able to sustain a high level of osteogenic differentiation potential with age and under conditions of low bone quality [263, 357, 492-494]. Subsequently, mASCs are fast becoming the preferred choice for stem cell-based approaches in bone tissue engineering [495, 496]. Certainly, results from our previous studies have confirmed that mASCs harvested from SAMP6 mice, a model for senile osteoporosis, have the capability of increasing bone quality when re-injected back into SAMP6 tibia [486]. However, despite their widespread usage, the underlying mechanisms through which mASC osteogenic differentiation is controlled remain incompletely understood. In the current report, we identify the serine protease HtrA1 as being a positive regulator of ATRA-induced mASC osteogenesis and mASC-derived osteoblast mineralization. Furthermore, we provide evidence, which supports p70S6K as playing a role in mediating the pro-osteogenic effects of HtrA1 in mASCs in response to ATRA.

We have previously identified *HtrA1* expression being upregulated in mASCs in response to ATRA-containing osteogenic medium [372]. Accordingly, as one of the first steps we aimed to identify the regulators of *HtrA1* expression in a forward approach by implementing luciferase reporter assays, siRNA mediated knock-down screens and EMSA assays. As shown in chapter 3.1 Figure 6, within 24 hours the expression of *HtrA1* increases in response to osteogenic medium containing ATRA but not without ATRA. Assuming ATRA to be the critical component in regulation of

HtrA1 expression and subsequent successful osteoblastogenesis, loss-of-function of the corresponding RARs should result in reduced *HtrA1* production. Indeed, as depicted in chapter 3.1 Figure 7, the siRNA mediated knock-down of all four RARs significantly impaired ATRA-induced *HtrA1* expression. Therefore, the production of HtrA1 is most likely regulated through the RARs on the transcriptional level. Nonetheless, to exclude the scenario of a post-transcriptional regulation through miRNAs we conducted further studies using the well-known POLII inhibitors Actinomycin D and α-Amanitin. Thereby we could confirm that the observed increase in *HtrA1* expression in mASCs in response to ATRA was primarily regulated at the transcriptional level, as the POLII inhibitors completely abolished *HtrA1* transcriptional upregulation upon osteogenic stimulation (Chapter 3.2, Figure 8). Based on this, as well as on our investigations of putative *HtrA1* regulatory miRNAs (Chapter 3.2.3, Figure 18-20) and the HtrA1 3' UTR (Chapter 3.2.3, Figure 21-22), we could rule out the scenario of posttranscriptional regulation and focused our attention entirely on the *HtrA1* promoter and its potential regulation by ATRA. Therefore we generated deletion constructs ranging from -10000 bp up to +5000 bp relative to the TSS to narrow down the ATRA responsive part of the promoter (Chapter 3.2.2, Figures 10,13,15). Despite numerous cloning efforts we remained unsuccessful in identifying a region of the promoter considered crucial for the upregulation of *HtrA1* in response to ATRA. Nevertheless, the possibility of very distant positive or negative regulatory elements not covered within the investigated 15000 bp could not be excluded and should be considered when conducting further studies. Due to limitations in transfection efficiency in mASCs, experiments were also performed using the multipotent cell line C3H10T1/2. These cells were confirmed as being easily transfected and responsive to ATRA, as identified through the use of control studies utilizing expression plasmids containing multiple RAREs. However, we were still unable to demonstrate responsiveness of the *HtrA1* promoter to ATRA. It is well known that the cellular response to ATRA varies greatly and is highly dependent on the cell type, as exemplified by its non-genomic effects of activating kinase-signaling cascades. For example, as reviewed in [441], in fibroblasts, mouse embryo carcinoma cells, mammary breast tumour cells and leukaemia cells [497-500], ATRA is known to activate the p38 mitogen-activated protein kinase (p38MAPK) whereas in neuronal cells, Sertoli cells and embryonic stem cells, ATRA instead activates the p42/p44 extracellular signal-regulated kinase (Erk) or classical

MAPKs [501-507]. Erk could then activate downstream kinases such as MSK1 or ribosomal protein S6 kinase. Furthermore, in the non-genomic responses to ATRA, the RARs are not limited to the nucleus but are also found in lipid rafts [500], on the cell membrane [506] or even as RARG associated with the sarcome kinase [502]. Additionally, triggering histone modifications is another non-genomic effect of ATRA to be considered, as upon recruitment to RAREs harbouring target promoters, MSK1 phosphorylates histones H3 [497], thereby contributing to transcription in a non-genomic way through chromatin remodelling [497, 508, 509]. Expanding beyond chromatin remodelling, ATRA activated p38MAPK phosphorylates corepressors and coactivators thereby modulating their interaction with the RARs as exemplified through the ATRA triggered phosphorylation of SMRT leading to its release from the retinoic acid receptors, thereby disrupting the organisation of the corepressor complex and subsequently attracting coactivators [510, 511]. Alternatively, ATRA leads to phosphorylation and thereby marks SRC-3 for ubiquitination and subsequent degradation through the proteasome [512], which is thought to be another non-genomic mechanism of transcriptional control by triggering degradation of coregulators. Another scenario of non-genomic regulation through ATRA is the phosphorylation and activation of factors involved in the regulation of primary targets, which then in turn regulate subsequent targets in a secondary response thereby broadening the spectrum of ATRAs biological activity. For example, in ATRA-treated P19 cells, the activated Erks phosphorylate the testicular nuclear receptor 2 (TR2), which then becomes a repressor of the Oct4 gene and can facilitate cellular differentiation [501]. Similarly, ATRA activates JAKs which then phosphorylate the transcription factor STAT5 leading to its nuclear translocation and subsequent expression of target genes such as SOCS3 and PPARγ resulting in inhibition of insulin signaling and lipid accumulation [513-515].

Therefore, ATRA's mode of action as well as the location of its cognate receptors, may vary greatly depending on the cell type. In consideration of this and the fact that there are no putative RAREs within the investigated promoter region of HtrA1, it might well be that the upregulation of *HtrA1* is a secondary response upon ATRA treatment [446], through transcription factors harbouring a RARE which are activated in the primary response, or that ATRA mediates this effect via non-genomic pathways, as discussed above [497-507, 516, 517]. To further investigate these scenarios, it may be useful for upcoming studies to implement techniques such as

chromatin immunoprecipitation sequencing (ChIP-Seq) for RXRA to screen for promoters of promising transcription factor candidates and follow those up using siRNA mediated knock-down screens. Additionally, RNA sequencing would give a much broader overview of the changes in transcriptome upon ATRA treatment and allow for the identification of new transcription factors targets.

Despite producing negligible differences in Luciferase activity between uninduced and osteogenic induced cells transfected with numerous different deletion constructs of the *HtrA1* promoter, the results did indicate that region -250 to -100 of the *HtrA1* promoter may be important for basal *HtrA1* promoter activity (Chapter 3.2.2, Figure 13). Furthermore, in loss-of-function studies as well as in an EMSA super-shift and EMSA competition assays, we could confirm NYA (Chapter 3.2.4.1, Figure 23 and Figure 24) and CREB/ATF (Chapter 3.2.4.2, Figure 25 and Figure 26) as being essential for the basal regulation of the mouse *HtrA1* promoter. In future approaches, the identified transcription factors NYA and CREB/ATF may serve as valuable starting points in a backward approach to further elucidate details of the upstream networks governing the expression of *HtrA1*.

Mammalian HtrA1 was originally identified by Zumbrunn and Trueb [381] and has since been implicated in numerous biological processes and diseases [376, 406]. HtrA1 is classified as a secreted serine protease and as such, its influence over cellular processes is largely thought to be due to its extracellular actions [372, 403, 407]. However, it is also equally likely that HtrA1 instigates many of its effects intracellularly. Indeed, HtrA1 has been shown to interact with and functionally regulate several intracellular substrates including X-linked inhibitor of apoptosis protein (XIAP) [518], tubulin [395], proTGFβ1 [519], tau [389] and TSC2 [400]. In the context of the present study, HtrA1's regulatory influence over TSC2 activity holds particular relevance given the importance of mTOR signaling in stem cell multipotency [209, 217, 218].

The mTOR protein makes up the catalytic subunit of two separate complexes, namely mTOR complex 1 (mTORC1) and mTOR complex 2 (mTORC2) [518]. mTORC1 functions to control cell growth and protein synthesis through phosphorylation of 4E-BP1 and p70S6K, and has been implicated in osteoblast differentiation [209, 520-522]. mTORC1 is negatively regulated by the GTPase-activating protein (GAP) TSC1/2 complex and as such, relies on the actions of Akt for its activation through phosphorylation of TSC2 [523]. Although several studies have

demonstrated activation of the Akt/mTOR signaling pathway in response to ATRA [524-526], no investigations have yet been undertaken to examine Akt/mTOR activation in ATRA-stimulated mASCs or to evaluate its consequences for their commitment towards osteoblasts. Our findings have confirmed that increases in mTOR phosphorylation levels, Akt and p70S6K, but not 4E-BP1, are rapidly activated in mASCs undergoing ATRA-mediated osteogenic differentiation. Similar rapid increases in several other kinase cascades have previously been demonstrated in various cell systems in response to ATRA [462, 498, 499, 506]. Such effects are considered to be independent of the classical genomic effects of ATRA, and are instead regulated through atypical, non-genomic events possibly through interactions with membrane-associated RARs [503].

Rapamycin treatment completely inhibited the ability of ATRA to upregulate p70S6K phosphorylation in these cells. It would therefore appear that ATRA-mediated p70S6K activation in mASCs is rapamycin sensitive and as such, reliant on mTOR signaling. Furthermore, ATRA-mediated p70S6K activation in mASCs might additionally be reliant upon increases in mTOR activity through the phosphorylation of sites other than Ser2448. Certainly, mTOR has been reported to have several potential phosphorylation sites whose functions remain largely undefined [441]. The ability of HtrA1 to influence the mTOR signaling pathway in osteogenic induced mASCs was made evident by the fact that phosphorylation levels of p70S6K were noticeably reduced in ATRA-stimulated HtrA1-deficient mASCs. However, in contrast to cells treated with rapamycin, ATRA-dependent p70S6K phosphorylation was not completely abolished in HtrA1-deficient cells. It therefore appears that ATRA stimulates p70S6K activation in mASCs in a rapamycin-sensitive and HtrA1-dependent manner, although HtrA1's specific mode of action over mTOR activation remains to be elucidated. The activation of p70S6K is considered to be of paramount importance in determining mASC adipocyte lineage commitment [527], though its functional role in mASC osteogenesis has not yet been established. Our findings from studies using the mTOR inhibitor rapamycin, along with siRNA-dependent inhibition of *Rps6kb1* gene expression, confirmed that the mTOR/p70S6K signaling pathway was indeed an essential requirement for efficient mASC osteogenesis and mASC-derived osteoblast mineralization. As far as we are aware, this is the first report to demonstrate such a role for mTOR/p70S6K in ATRA-mediated mASC osteogenesis. Therefore, these studies identified both HtrA1 and mTOR/p70S6K as

being important regulators of ATRA-mediated mASC osteogenesis. However, it was still unclear as to whether HtrA1's ability to regulate p70S6K phosphorylation in response to ATRA was directly related to its pro-osteogenic effects. We therefore performed a study in which we introduced plasmids encoding DNA for either active or inactive mutants of p70S6K into HtrA1-deficient mASCs in an attempt to rescue osteoblastogenesis. Indeed, our results revealed that the mineralizing capacity of HtrA1-deficient mASC-derived osteoblasts could be fully restored when cells were engineered to overexpress the constitutively active p70S6K mutant. These findings therefore confirm that HtrA1's pro-osteogenic effects in mASCs are related to its ability to regulate p70S6K activation. However, it remains unclear as to how HtrA1 may function to elicit such a response in mASCs, especially since it has not yet been determined through which route HtrA1 instigates its action on p70S6K. We would anticipate that if HtrA1 were acting to regulate p70S6K activity through its interaction with TSC2 [400], then reductions in phosphorylation of mTOR on Ser2448 would be evident [528]. However, as no such reductions were observed, the involvement of additional mTOR phosphorylation sites or alternative signaling pathways may need to be considered. The suggestion that the TSC-complex may in fact regulate p70S6K independently of mTOR [529], might offer some explanation as to why loss-of-function of HtrA1 reduced p70S6K phosphorylation with only modest changes in phospho-mTOR levels. Alternatively, HtrA1 may act to regulate p70S6K phosphorylation through mTOR, but in a TSC2-independent manner. Certainly, mTOR is not solely reliant on TSC2 inhibition for its activation as confirmed by studies in which Akt was shown to activate mTOR by relieving the inhibitory effects of proline-rich Akt/PKB substrate 40 kDa (PRAS40) on mTORC1 [530], and more recently, through its ability to promote mTORC1 phosphorylation at Ser1415 via the actions of IkB kinase alpha (IKKα) [531]. Further studies are therefore required in order to ascertain the involvement of TSC2 and mTOR in mediating the effects of HtrA1 on p70S6K phosphorylation in osteogenic mASCs.

The next logical step to validate the physiological relevance of these findings will be to test the proposed mechanism *in vivo*. In this context, performing studies using an HtrA1 knock-out mouse model and the well-established SAMP6 mouse model would be of particular interest. Assuming the loss-of-function of HtrA1 does impair bone quality in the knock-out mouse model and no redundant compensatory mechanisms exist by other members of the HtrA family, it would be interesting to restore the

putative detrimental effect of HtrA1 loss by targeting p70S6K through activation of TOR signaling. Alternatively, it would be interesting to test whether low peak bone mass could be avoided or even better bone mineralization restored by a diet rich in ATRA, in comparison to a control group fed a diet rich in the biologically inactive form 9,13dcRA [532]. Nonetheless, Vitamin A or “fat soluble A” [422] is an “accessory fat soluble food factor” [421], that is essential for survival [423] and no diet can be depleted entirely of it. Consequently, a certain amount of Vitamin A taken up by diet will inevitably always be metabolized to ATRA and therefore may compensate for the lack of biologically active ATRA. In another approach, mASCs transiently overexpressing HtrA1 could be injected into osteoporotic bone to restore BMD. Another aspect to consider is to what extent other members of the HtrA family may compensate for the loss of HtrA1. Intracellular HtrA2 for example is a stress-activated protease [533] that is localized in the mitochondrial intermembrane space and is released to the cytosol in response to apoptotic stimuli [534]. HtrA3, initially identified as pregnancy-related serine protease (PRSP) [396] shares a relatively high homology to HtrA1 (56% of the amino acids) [535, 536]. However, no biochemical characterisation has been published so far for HtrA4, which also shares a high degree of structural and domain homology with HtrA1 [373, 396].

As ASCs are an easily accessible source of multipotent stromal cells in comparison to their BMSC counterparts, and are easily modified and undergo robust osteogenic differentiation [263, 357, 537]], which makes them a valuable tool for bone tissue engineering [344, 538-542]. Interestingly, it has been shown that the supernatant from cultures of osteoporotic human patient-derived ASCs are able to exert a pro-osteogenic effect on human osteoporotic patient-derived BMSCs *in vitro* [486]. Although these findings suggest an ASC-derived soluble factor(s) is responsible for mediating these pro-osteogenic effects, its identity still remains elusive. It would therefore be interesting to examine further whether HtrA1 may play a role in regulating this effect. However, to do so would require a specific HtrA1 inhibitor, which so far does not exist. Furthermore, the role of HtrA1 in bone formation still remains controversial. It has been suggested that it acts as an inhibitor of matrix mineralization by preventing BMP-2 induced mineral deposition in 2T3 osteoblasts and that loss-of-function of HtrA1 actually results in their enhanced mineralization [408]. HtrA1 has also been shown to antagonize TGF-β signaling by cleaving type II and type III TGF-β receptors (TβRII and TβRIII) and that HtrA1 deficiencies

consequently enhance bone formation in mice as shown by a marked increase in trabecular bone mass [543]. HtrA1's ability to regulate TGF-β signaling extends to the cytoplasm as it has further been shown to reduce the amount of mature extracellular TGF-β1 by degrading pro-TGF-β within the ER and targeting it to the ER-associated degradation (ERAD) system [519]. Controversially, it has been reported that loss-of-function of HtrA1 impairs TGF-β signaling by decreasing the bioavailability of mature TGF-β due to reduced liberation of TGF-β from ECM associated latent TGF-β binding protein 1 (LTBP) [544].

In summary, we have identified p70S6K as an important regulator of mASC osteogenesis, being activated in response to ATRA via pathways involving mTOR and HtrA1 (Chapter 2.1.1, Fig. 7). As such, it is proposed that HtrA1 represents a newly identified positive regulator of ATRA-mediated mASC osteogenesis and mASC-derived osteoblast mineralization.

5. References

1. Evans, M., *Discovering pluripotency: 30 years of mouse embryonic stem cells.* Nat Rev Mol Cell Biol, 2011. **12**(10): p. 680-6.
2. Stevens, L.C. and C.C. Little, *Spontaneous Testicular Teratomas in an Inbred Strain of Mice.* Proc Natl Acad Sci U S A, 1954. **40**(11): p. 1080-7.
3. Pierce, G.B., *Teratocarcinoma: model for a developmental concept of cancer.* Curr Top Dev Biol, 1967. **2**: p. 223-46.
4. Stevens, L.C., *The biology of teratomas.* Adv Morphog, 1967. **6**: p. 1-31.
5. Evans, M.J., *The isolation and properties of a clonal tissue culture strain of pluripotent mouse teratoma cells.* J Embryol Exp Morphol, 1972. **28**(1): p. 163-76.
6. Martin, G.R. and M.J. Evans, *The morphology and growth of a pluripotent teratocarcinoma cell line and its derivatives in tissue culture.* Cell, 1974. **2**(3): p. 163-72.
7. Martin, W.R., et al., *The metabolism of thioinosinic acid by 6-mercaptopurine sensitive and resistant leukemic leukocytes.* Proc Soc Exp Biol Med, 1972. **140**(2): p. 423-8.
8. Evans, M.J., *Germ Cell Tumours (eds Anderson, C. J., Jones, W. G. & Milford-Ward, A.).* Taylor and Francis, London, 1981.
9. Papaioannou, V.E., et al., *Fate of teratocarcinoma cells injected into early mouse embryos.* Nature, 1975. **258**(5530): p. 70-73.
10. Bradley, A., et al., *Formation of germ-line chimaeras from embryo-derived teratocarcinoma cell lines.* Nature, 1984. **309**(5965): p. 255-6.
11. Evans, M.J., et al., *The ability of EK cells to form chimeras after selection of clones in G418 and some observations on the integration of retroviral vector proviral DNA into EK cells.* Cold Spring Harb Symp Quant Biol, 1985. **50**: p. 685-9.
12. Kuehn, M.R., et al., *A potential animal model for Lesch-Nyhan syndrome through introduction of HPRT mutations into mice.* Nature, 1987. **326**(6110): p. 295-8.
13. Robertson, E., et al., *Germ-line transmission of genes introduced into cultured pluripotential cells by retroviral vector.* Nature, 1986. **323**(6087): p. 445-8.
14. Jopling, C., S. Boue, and J.C. Izpisua Belmonte, *Dedifferentiation, transdifferentiation and reprogramming: three routes to regeneration.* Nat Rev Mol Cell Biol, 2011. **12**(2): p. 79-89.
15. Poss, K.D., L.G. Wilson, and M.T. Keating, *Heart regeneration in zebrafish.* Science, 2002. **298**(5601): p. 2188-90.
16. Jopling, C., et al., *Zebrafish heart regeneration occurs by cardiomyocyte dedifferentiation and proliferation.* Nature, 2010. **464**(7288): p. 606-9.
17. Raya, A., et al., *Activation of Notch signaling pathway precedes heart regeneration in zebrafish.* Proc Natl Acad Sci U S A, 2003. **100 Suppl 1**: p. 11889-95.
18. Kikuchi, K., et al., *Primary contribution to zebrafish heart regeneration by gata4(+) cardiomyocytes.* Nature, 2010. **464**(7288): p. 601-5.
19. Burkhart, D.L. and J. Sage, *Cellular mechanisms of tumour suppression by the retinoblastoma gene.* Nat Rev Cancer, 2008. **8**(9): p. 671-82.
20. Tanaka, E.M., et al., *Newt myotubes reenter the cell cycle by phosphorylation of the retinoblastoma protein.* J Cell Biol, 1997. **136**(1): p. 155-65.
21. Camarda, G., et al., *A pRb-independent mechanism preserves the postmitotic state in terminally differentiated skeletal muscle cells.* J Cell Biol, 2004. **167**(3): p. 417-23.

22. McGann, C.J., S.J. Odelberg, and M.T. Keating, *Mammalian myotube dedifferentiation induced by newt regeneration extract.* Proc Natl Acad Sci U S A, 2001. **98**(24): p. 13699-704.
23. Sherr, C.J., et al., *p53-Dependent and -independent functions of the Arf tumor suppressor.* Cold Spring Harb Symp Quant Biol, 2005. **70**: p. 129-37.
24. Pajcini, K.V., et al., *Transient inactivation of Rb and ARF yields regenerative cells from postmitotic mammalian muscle.* Cell Stem Cell, 2010. **7**(2): p. 198-213.
25. Lee, J., et al., *Activation of p38 MAPK induces cell cycle arrest via inhibition of Raf/ERK pathway during muscle differentiation.* Biochem Biophys Res Commun, 2002. **298**(5): p. 765-71.
26. Rumyantsev, P.P., *Interrelations of the proliferation and differentiation processes during cardiact myogenesis and regeneration.* Int Rev Cytol, 1977. **51**: p. 186-273.
27. Engel, F.B., et al., *p38 MAP kinase inhibition enables proliferation of adult mammalian cardiomyocytes.* Genes Dev, 2005. **19**(10): p. 1175-87.
28. Meyer, D. and C. Birchmeier, *Multiple essential functions of neuregulin in development.* Nature, 1995. **378**(6555): p. 386-90.
29. Gassmann, M., et al., *Aberrant neural and cardiac development in mice lacking the ErbB4 neuregulin receptor.* Nature, 1995. **378**(6555): p. 390-4.
30. Lee, K.F., et al., *Requirement for neuregulin receptor erbB2 in neural and cardiac development.* Nature, 1995. **378**(6555): p. 394-8.
31. Vierbuchen, T., et al., *Direct conversion of fibroblasts to functional neurons by defined factors.* Nature, 2010. **463**(7284): p. 1035-41.
32. Ieda, M., et al., *Direct reprogramming of fibroblasts into functional cardiomyocytes by defined factors.* Cell, 2010. **142**(3): p. 375-86.
33. Jayawardena, T.M., et al., *MicroRNA-mediated in vitro and in vivo direct reprogramming of cardiac fibroblasts to cardiomyocytes.* Circ Res, 2012. **110**(11): p. 1465-73.
34. Liao, H.T. and C.T. Chen, *Osteogenic potential: Comparison between bone marrow and adipose-derived mesenchymal stem cells.* World J Stem Cells, 2014. **6**(3): p. 288-95.
35. Zuk, P.A., et al., *Multilineage cells from human adipose tissue: implications for cell-based therapies.* Tissue Eng, 2001. **7**(2): p. 211-28.
36. Guenther, M.G., et al., *Chromatin structure and gene expression programs of human embryonic and induced pluripotent stem cells.* Cell Stem Cell, 2010. **7**(2): p. 249-57.
37. Newman, A.M. and J.B. Cooper, *Lab-specific gene expression signatures in pluripotent stem cells.* Cell Stem Cell, 2010. **7**(2): p. 258-62.
38. Bock, C., et al., *Reference Maps of human ES and iPS cell variation enable high-throughput characterization of pluripotent cell lines.* Cell, 2011. **144**(3): p. 439-52.
39. Takahashi, K. and S. Yamanaka, *Induction of pluripotent stem cells from mouse embryonic and adult fibroblast cultures by defined factors.* Cell, 2006. **126**(4): p. 663-76.
40. Yamanaka, S. and H.M. Blau, *Nuclear reprogramming to a pluripotent state by three approaches.* Nature, 2010. **465**(7299): p. 704-12.
41. Jaenisch, R. and R. Young, *Stem cells, the molecular circuitry of pluripotency and nuclear reprogramming.* Cell, 2008. **132**(4): p. 567-82.
42. Niwa, H., *How is pluripotency determined and maintained?* Development, 2007. **134**(4): p. 635-46.
43. Loh, Y.H., et al., *The Oct4 and Nanog transcription network regulates pluripotency in mouse embryonic stem cells.* Nat Genet, 2006. **38**(4): p. 431-40.

44. Kuroda, T., et al., *Octamer and Sox elements are required for transcriptional cis regulation of Nanog gene expression.* Mol Cell Biol, 2005. **25**(6): p. 2475-85.
45. van den Berg, D.L., et al., *An Oct4-centered protein interaction network in embryonic stem cells.* Cell Stem Cell, 2010. **6**(4): p. 369-81.
46. Pardo, M., et al., *An expanded Oct4 interaction network: implications for stem cell biology, development, and disease.* Cell Stem Cell, 2010. **6**(4): p. 382-95.
47. Hansson, J., et al., *Highly coordinated proteome dynamics during reprogramming of somatic cells to pluripotency.* Cell Rep, 2012. **2**(6): p. 1579-92.
48. Polo, J.M., et al., *A molecular roadmap of reprogramming somatic cells into iPS cells.* Cell, 2012. **151**(7): p. 1617-32.
49. Kouzarides, T., *Histone methylation in transcriptional control.* Curr Opin Genet Dev, 2002. **12**(2): p. 198-209.
50. Martin, C. and Y. Zhang, *The diverse functions of histone lysine methylation.* Nat Rev Mol Cell Biol, 2005. **6**(11): p. 838-49.
51. Peterson, C.L. and M.A. Laniel, *Histones and histone modifications.* Curr Biol, 2004. **14**(14): p. R546-51.
52. Yang, P., et al., *RCOR2 is a subunit of the LSD1 complex that regulates ESC property and substitutes for SOX2 in reprogramming somatic cells to pluripotency.* Stem Cells, 2011. **29**(5): p. 791-801.
53. Gao, Y., et al., *Replacement of Oct4 by Tet1 during iPSC induction reveals an important role of DNA methylation and hydroxymethylation in reprogramming.* Cell Stem Cell, 2013. **12**(4): p. 453-69.
54. Shinagawa, T., et al., *Histone variants enriched in oocytes enhance reprogramming to induced pluripotent stem cells.* Cell Stem Cell, 2014. **14**(2): p. 217-27.
55. Onder, T.T., et al., *Chromatin-modifying enzymes as modulators of reprogramming.* Nature, 2012. **483**(7391): p. 598-602.
56. Miyoshi, N., et al., *Reprogramming of mouse and human cells to pluripotency using mature microRNAs.* Cell Stem Cell, 2011. **8**(6): p. 633-8.
57. Anokye-Danso, F., et al., *Highly efficient miRNA-mediated reprogramming of mouse and human somatic cells to pluripotency.* Cell Stem Cell, 2011. **8**(4): p. 376-88.
58. Leitch, H.G., et al., *Naive pluripotency is associated with global DNA hypomethylation.* Nat Struct Mol Biol, 2013. **20**(3): p. 311-6.
59. Ying, Q.L., et al., *The ground state of embryonic stem cell self-renewal.* Nature, 2008. **453**(7194): p. 519-23.
60. Martello, G., et al., *Esrrb is a pivotal target of the Gsk3/Tcf3 axis regulating embryonic stem cell self-renewal.* Cell Stem Cell, 2012. **11**(4): p. 491-504.
61. Yamaji, M., et al., *PRDM14 ensures naive pluripotency through dual regulation of signaling and epigenetic pathways in mouse embryonic stem cells.* Cell Stem Cell, 2013. **12**(3): p. 368-82.
62. Mikkelsen, T.S., et al., *Dissecting direct reprogramming through integrative genomic analysis.* Nature, 2008. **454**(7200): p. 49-55.
63. Huangfu, D., et al., *Induction of pluripotent stem cells by defined factors is greatly improved by small-molecule compounds.* Nat Biotechnol, 2008. **26**(7): p. 795-7.
64. Huangfu, D., et al., *Induction of pluripotent stem cells from primary human fibroblasts with only Oct4 and Sox2.* Nat Biotechnol, 2008. **26**(11): p. 1269-75.
65. Esteban, M.A., et al., *Vitamin C enhances the generation of mouse and human induced pluripotent stem cells.* Cell Stem Cell, 2010. **6**(1): p. 71-9.
66. Wang, T., et al., *The histone demethylases Jhdm1a/1b enhance somatic cell reprogramming in a vitamin-C-dependent manner.* Cell Stem Cell, 2011. **9**(6): p. 575-87.

67. Zhu, S., et al., *Reprogramming of human primary somatic cells by OCT4 and chemical compounds.* Cell Stem Cell, 2010. **7**(6): p. 651-5.
68. Hou, P., et al., *Pluripotent stem cells induced from mouse somatic cells by small-molecule compounds.* Science, 2013. **341**(6146): p. 651-4.
69. Theunissen, T.W. and R. Jaenisch, *Molecular control of induced pluripotency.* Cell Stem Cell, 2014. **14**(6): p. 720-34.
70. Hsu, Y.C. and E. Fuchs, *A family business: stem cell progeny join the niche to regulate homeostasis.* Nat Rev Mol Cell Biol, 2012. **13**(2): p. 103-14.
71. Gros, J., et al., *A common somitic origin for embryonic muscle progenitors and satellite cells.* Nature, 2005. **435**(7044): p. 954-8.
72. Collins, C.A., et al., *Stem cell function, self-renewal, and behavioral heterogeneity of cells from the adult muscle satellite cell niche.* Cell, 2005. **122**(2): p. 289-301.
73. Doetsch, F., et al., *Subventricular zone astrocytes are neural stem cells in the adult mammalian brain.* Cell, 1999. **97**(6): p. 703-16.
74. Zhang, C.L., et al., *A role for adult TLX-positive neural stem cells in learning and behaviour.* Nature, 2008. **451**(7181): p. 1004-7.
75. Morris, R.J. and C.S. Potten, *Highly persistent label-retaining cells in the hair follicles of mice and their fate following induction of anagen.* J Invest Dermatol, 1999. **112**(4): p. 470-5.
76. Cotsarelis, G., T.T. Sun, and R.M. Lavker, *Label-retaining cells reside in the bulge area of pilosebaceous unit: implications for follicular stem cells, hair cycle, and skin carcinogenesis.* Cell, 1990. **61**(7): p. 1329-37.
77. Tumbar, T., et al., *Defining the epithelial stem cell niche in skin.* Science, 2004. **303**(5656): p. 359-63.
78. Fuchs, E., *The tortoise and the hair: slow-cycling cells in the stem cell race.* Cell, 2009. **137**(5): p. 811-9.
79. Villeda, S.A., et al., *The ageing systemic milieu negatively regulates neurogenesis and cognitive function.* Nature, 2011. **477**(7362): p. 90-4.
80. Li, L. and H. Clevers, *Coexistence of quiescent and active adult stem cells in mammals.* Science, 2010. **327**(5965): p. 542-5.
81. Dexter, T.M., T.D. Allen, and L.G. Lajtha, *Conditions controlling the proliferation of haemopoietic stem cells in vitro.* J Cell Physiol, 1977. **91**(3): p. 335-44.
82. Lord, B.I., N.G. Testa, and J.H. Hendry, *The relative spatial distributions of CFUs and CFUc in the normal mouse femur.* Blood, 1975. **46**(1): p. 65-72.
83. Schofield, R., *The relationship between the spleen colony-forming cell and the haemopoietic stem cell.* Blood Cells, 1978. **4**(1-2): p. 7-25.
84. Zipori, D., *Biology of Stem Cells and the Molecular Basis of the Stem State.* Humana Press, 2009.
85. Wang, X., et al., *Characterization of mesenchymal stem cells isolated from mouse fetal bone marrow.* Stem Cells, 2006. **24**(3): p. 482-93.
86. Short, B., et al., *Mesenchymal stem cells.* Arch Med Res, 2003. **34**(6): p. 565-71.
87. Muguruma, Y., et al., *Reconstitution of the functional human hematopoietic microenvironment derived from human mesenchymal stem cells in the murine bone marrow compartment.* Blood, 2006. **107**(5): p. 1878-87.
88. Colfen, H., *Biomineralization: A crystal-clear view.* Nat Mater, 2010. **9**(12): p. 960-1.
89. Taichman, R.S., *Blood and bone: two tissues whose fates are intertwined to create the hematopoietic stem-cell niche.* Blood, 2005. **105**(7): p. 2631-9.
90. Moore, K.A., *Recent advances in defining the hematopoietic stem cell niche.* Curr Opin Hematol, 2004. **11**(2): p. 107-11.

91. Taichman, R.S., M.J. Reilly, and S.G. Emerson, *Human osteoblasts support human hematopoietic progenitor cells in vitro bone marrow cultures.* Blood, 1996. **87**(2): p. 518-24.
92. Taichman, R., et al., *Hepatocyte growth factor is secreted by osteoblasts and cooperatively permits the survival of haematopoietic progenitors.* Br J Haematol, 2001. **112**(2): p. 438-48.
93. Zhang, J., et al., *Identification of the haematopoietic stem cell niche and control of the niche size.* Nature, 2003. **425**(6960): p. 836-41.
94. Calvi, L.M., et al., *Osteoblastic cells regulate the haematopoietic stem cell niche.* Nature, 2003. **425**(6960): p. 841-6.
95. Visnjic, D., et al., *Conditional ablation of the osteoblast lineage in Col2.3deltatk transgenic mice.* J Bone Miner Res, 2001. **16**(12): p. 2222-31.
96. Visnjic, D., et al., *Hematopoiesis is severely altered in mice with an induced osteoblast deficiency.* Blood, 2004. **103**(9): p. 3258-64.
97. Miyamoto, K., et al., *Osteoclasts are dispensable for hematopoietic stem cell maintenance and mobilization.* J Exp Med, 2011. **208**(11): p. 2175-81.
98. Raaijmakers, M.H., et al., *Bone progenitor dysfunction induces myelodysplasia and secondary leukaemia.* Nature, 2010. **464**(7290): p. 852-7.
99. Kunisaki, Y., et al., *Arteriolar niches maintain haematopoietic stem cell quiescence.* Nature, 2013. **502**(7473): p. 637-43.
100. Ivanovska, I.L., et al., *Stem cell mechanobiology: diverse lessons from bone marrow.* Trends Cell Biol, 2015.
101. Engler, A.J., et al., *Matrix elasticity directs stem cell lineage specification.* Cell, 2006. **126**(4): p. 677-89.
102. Kilian, K.A., et al., *Geometric cues for directing the differentiation of mesenchymal stem cells.* Proc Natl Acad Sci U S A, 2010. **107**(11): p. 4872-7.
103. Fu, J., et al., *Mechanical regulation of cell function with geometrically modulated elastomeric substrates.* Nat Methods, 2010. **7**(9): p. 733-6.
104. Raab, M., et al., *Crawling from soft to stiff matrix polarizes the cytoskeleton and phosphoregulates myosin-II heavy chain.* J Cell Biol, 2012. **199**(4): p. 669-83.
105. Tse, J.R. and A.J. Engler, *Stiffness gradients mimicking in vivo tissue variation regulate mesenchymal stem cell fate.* PLoS One, 2011. **6**(1): p. e15978.
106. Isenberg, B.C., et al., *Vascular smooth muscle cell durotaxis depends on substrate stiffness gradient strength.* Biophys J, 2009. **97**(5): p. 1313-22.
107. Pittenger, M.F., et al., *Multilineage potential of adult human mesenchymal stem cells.* Science, 1999. **284**(5411): p. 143-7.
108. Dominici, M., et al., *Minimal criteria for defining multipotent mesenchymal stromal cells. The International Society for Cellular Therapy position statement.* Cytotherapy, 2006. **8**(4): p. 315-7.
109. Keating, A., *Mesenchymal stromal cells: new directions.* Cell Stem Cell, 2012. **10**(6): p. 709-16.
110. Zuk, P.A., et al., *Human adipose tissue is a source of multipotent stem cells.* Mol Biol Cell, 2002. **13**(12): p. 4279-95.
111. In 't Anker, P.S., et al., *Isolation of mesenchymal stem cells of fetal or maternal origin from human placenta.* Stem Cells, 2004. **22**(7): p. 1338-45.
112. Shih, D.T., et al., *Isolation and characterization of neurogenic mesenchymal stem cells in human scalp tissue.* Stem Cells, 2005. **23**(7): p. 1012-20.
113. Erices, A., P. Conget, and J.J. Minguell, *Mesenchymal progenitor cells in human umbilical cord blood.* Br J Haematol, 2000. **109**(1): p. 235-42.

114. Sarugaser, R., et al., *Human umbilical cord perivascular (HUCPV) cells: a source of mesenchymal progenitors.* Stem Cells, 2005. **23**(2): p. 220-9.
115. Wang, H.S., et al., *Mesenchymal stem cells in the Wharton's jelly of the human umbilical cord.* Stem Cells, 2004. **22**(7): p. 1330-7.
116. Gronthos, S., et al., *Postnatal human dental pulp stem cells (DPSCs) in vitro and in vivo.* Proc Natl Acad Sci U S A, 2000. **97**(25): p. 13625-30.
117. Nadri, S. and M. Soleimani, *Comparative analysis of mesenchymal stromal cells from murine bone marrow and amniotic fluid.* Cytotherapy, 2007. **9**(8): p. 729-37.
118. De Bari, C., et al., *Multipotent mesenchymal stem cells from adult human synovial membrane.* Arthritis Rheum, 2001. **44**(8): p. 1928-42.
119. Patki, S., et al., *Human breast milk is a rich source of multipotent mesenchymal stem cells.* Hum Cell, 2010. **23**(2): p. 35-40.
120. da Silva Meirelles, L., P.C. Chagastelles, and N.B. Nardi, *Mesenchymal stem cells reside in virtually all post-natal organs and tissues.* J Cell Sci, 2006. **119**(Pt 11): p. 2204-13.
121. Panepucci, R.A., et al., *Comparison of gene expression of umbilical cord vein and bone marrow-derived mesenchymal stem cells.* Stem Cells, 2004. **22**(7): p. 1263-78.
122. Lee, R.H., et al., *Characterization and expression analysis of mesenchymal stem cells from human bone marrow and adipose tissue.* Cell Physiol Biochem, 2004. **14**(4-6): p. 311-24.
123. Kaltz, N., et al., *Novel markers of mesenchymal stem cells defined by genome-wide gene expression analysis of stromal cells from different sources.* Exp Cell Res, 2010. **316**(16): p. 2609-17.
124. Nauta, A.J. and W.E. Fibbe, *Immunomodulatory properties of mesenchymal stromal cells.* Blood, 2007. **110**(10): p. 3499-506.
125. Tolar, J., et al., *Concise review: hitting the right spot with mesenchymal stromal cells.* Stem Cells, 2010. **28**(8): p. 1446-55.
126. Chen, P.M., et al., *Immunomodulatory properties of human adult and fetal multipotent mesenchymal stem cells.* J Biomed Sci, 2011. **18**: p. 49.
127. Le Blanc, K. and O. Ringden, *Immunomodulation by mesenchymal stem cells and clinical experience.* J Intern Med, 2007. **262**(5): p. 509-25.
128. Uccelli, A., L. Moretta, and V. Pistoia, *Mesenchymal stem cells in health and disease.* Nat Rev Immunol, 2008. **8**(9): p. 726-36.
129. Yang, S.H., et al., *Soluble mediators from mesenchymal stem cells suppress T cell proliferation by inducing IL-10.* Exp Mol Med, 2009. **41**(5): p. 315-24.
130. Choi, H., et al., *Anti-inflammatory protein TSG-6 secreted by activated MSCs attenuates zymosan-induced mouse peritonitis by decreasing TLR2/NF-kappaB signaling in resident macrophages.* Blood, 2011. **118**(2): p. 330-8.
131. Jones, S., et al., *The antiproliferative effect of mesenchymal stem cells is a fundamental property shared by all stromal cells.* J Immunol, 2007. **179**(5): p. 2824-31.
132. Salem, H.K. and C. Thiemermann, *Mesenchymal stromal cells: current understanding and clinical status.* Stem Cells, 2010. **28**(3): p. 585-96.
133. Ranganath, S.H., et al., *Harnessing the mesenchymal stem cell secretome for the treatment of cardiovascular disease.* Cell Stem Cell, 2012. **10**(3): p. 244-58.
134. Horwitz, E.M., et al., *Isolated allogeneic bone marrow-derived mesenchymal cells engraft and stimulate growth in children with osteogenesis imperfecta: Implications for cell therapy of bone.* Proc Natl Acad Sci U S A, 2002. **99**(13): p. 8932-7.

135. Horwitz, E.M., et al., *Transplantability and therapeutic effects of bone marrow-derived mesenchymal cells in children with osteogenesis imperfecta.* Nat Med, 1999. **5**(3): p. 309-13.
136. Gerstenfeld L, E.C., Kakar S, Jacobsen KA, Einhorn TA., *Osteogenic growth factors and cytokines and their role in bone repair engineering of functional skeletal tissues.* Topics Bone Biol, 2007.
137. Li, X. and X. Cao, *BMP signaling and skeletogenesis.* Ann N Y Acad Sci, 2006. **1068**: p. 26-40.
138. Shimizu, T., et al., *Notch signaling pathway enhances bone morphogenetic protein 2 (BMP2) responsiveness of Msx2 gene to induce osteogenic differentiation and mineralization of vascular smooth muscle cells.* J Biol Chem, 2011. **286**(21): p. 19138-48.
139. Md Shaifur Rahman, N.A., Hossen Mohammad Jamil, Rajat Suvra Banik & Sikder M Asaduzzaman, *TGF-β/BMP signaling and other molecular events: regulation of osteoblastogenesis and bone formation.* Bone Res, 2015.
140. Liu, J., et al., *Bmi1 regulates mitochondrial function and the DNA damage response pathway.* Nature, 2009. **459**(7245): p. 387-92.
141. Caetano-Lopes, J., H. Canhao, and J.E. Fonseca, *Osteoblasts and bone formation.* Acta Reumatol Port, 2007. **32**(2): p. 103-10.
142. Abzhanov, A., et al., *Regulation of skeletogenic differentiation in cranial dermal bone.* Development, 2007. **134**(17): p. 3133-44.
143. Raggatt, L.J. and N.C. Partridge, *Cellular and molecular mechanisms of bone remodeling.* J Biol Chem, 2010. **285**(33): p. 25103-8.
144. Kronenberg, H.M., *Developmental regulation of the growth plate.* Nature, 2003. **423**(6937): p. 332-6.
145. Compston, J.E., *Bone marrow and bone: a functional unit.* J Endocrinol, 2002. **173**(3): p. 387-94.
146. Hardouin, P., V. Pansini, and B. Cortet, *Bone marrow fat.* Joint Bone Spine, 2014. **81**(4): p. 313-9.
147. Cawthorn, W.P., et al., *Bone marrow adipose tissue is an endocrine organ that contributes to increased circulating adiponectin during caloric restriction.* Cell Metab, 2014. **20**(2): p. 368-75.
148. Brennan, B.M. and S.M. Shalet, *Endocrine late effects after bone marrow transplant.* Br J Haematol, 2002. **118**(1): p. 58-66.
149. Fazzalari, N.L., *Bone remodeling: A review of the bone microenvironment perspective for fragility fracture (osteoporosis) of the hip.* Semin Cell Dev Biol, 2008. **19**(5): p. 467-72.
150. Neve, A., A. Corrado, and F.P. Cantatore, *Osteoblast physiology in normal and pathological conditions.* Cell Tissue Res, 2011. **343**(2): p. 289-302.
151. Vaananen, H.K., et al., *The cell biology of osteoclast function.* J Cell Sci, 2000. **113 (Pt 3)**: p. 377-81.
152. Ochiai-Shino, H., et al., *A novel strategy for enrichment and isolation of osteoprogenitor cells from induced pluripotent stem cells based on surface marker combination.* PLoS One, 2014. **9**(6): p. e99534.
153. Karppanen, H., *Minerals and blood pressure.* Ann Med, 1991. **23**(3): p. 299-305.
154. Staudinger, K.C. and V.S. Roth, *Occupational lead poisoning.* Am Fam Physician, 1998. **57**(4): p. 719-26, 731-2.
155. Bergwitz, C. and H. Juppner, *Regulation of phosphate homeostasis by PTH, vitamin D, and FGF23.* Annu Rev Med, 2010. **61**: p. 91-104.

156. Manolagas, S.C., *Role of cytokines in bone resorption.* Bone, 1995. **17**(2 Suppl): p. 63S-67S.
157. Simonet, W.S., et al., *Osteoprotegerin: a novel secreted protein involved in the regulation of bone density.* Cell, 1997. **89**(2): p. 309-19.
158. Khosla, S., *Minireview: the OPG/RANKL/RANK system.* Endocrinology, 2001. **142**(12): p. 5050-5.
159. Poole, K.E. and J. Reeve, *Parathyroid hormone - a bone anabolic and catabolic agent.* Curr Opin Pharmacol, 2005. **5**(6): p. 612-7.
160. Vaananen, H.K. and P.L. Harkonen, *Estrogen and bone metabolism.* Maturitas, 1996. **23 Suppl**: p. S65-9.
161. Riggs, B.L., *The mechanisms of estrogen regulation of bone resorption.* J Clin Invest, 2000. **106**(10): p. 1203-4.
162. Antebi, B., G. Pelled, and D. Gazit, *Stem cell therapy for osteoporosis.* Curr Osteoporos Rep, 2014. **12**(1): p. 41-7.
163. Feng, X. and J.M. McDonald, *Disorders of bone remodeling.* Annu Rev Pathol, 2011. **6**: p. 121-45.
164. Haden, S.T., et al., *The effects of age and gender on parathyroid hormone dynamics.* Clin Endocrinol (Oxf), 2000. **52**(3): p. 329-38.
165. Rodriguez, J.P., et al., *Mesenchymal stem cells from osteoporotic patients produce a type I collagen-deficient extracellular matrix favoring adipogenic differentiation.* J Cell Biochem, 2000. **79**(4): p. 557-65.
166. Lane, N.E., *Epidemiology, etiology, and diagnosis of osteoporosis.* American journal of obstetrics and gynecology, 2006. **194**(2 Suppl): p. S3-11.
167. Moyer, V.A. and U.S.P.S.T. Force*, *Vitamin D and calcium supplementation to prevent fractures in adults: U.S. Preventive Services Task Force recommendation statement.* Ann Intern Med, 2013. **158**(9): p. 691-6.
168. Rosen, C.J., *Clinical practice. Postmenopausal osteoporosis.* N Engl J Med, 2005. **353**(6): p. 595-603.
169. Beederman M, L.J., Nan G, *BMP signaling in mesenchymal stem cell differentiation and bone formation.* j biomed sci, 2013.
170. Zhang, Y., et al., *Mechanisms underlying the osteo- and adipo-differentiation of human mesenchymal stem cells.* ScientificWorldJournal, 2012. **2012**: p. 793823.
171. Das, S., R.S. Samant, and L.A. Shevde, *The hedgehog pathway conditions the bone microenvironment for osteolytic metastasis of breast cancer.* Int J Breast Cancer, 2012. **2012**: p. 298623.
172. Fuller, K., et al., *Cathepsin K inhibitors prevent matrix-derived growth factor degradation by human osteoclasts.* Bone, 2008. **42**(1): p. 200-11.
173. Hughes, F.J., et al., *Effects of growth factors and cytokines on osteoblast differentiation.* Periodontol 2000, 2006. **41**: p. 48-72.
174. Carreira, A.C., et al., *Bone morphogenetic proteins: facts, challenges, and future perspectives.* J Dent Res, 2014. **93**(4): p. 335-45.
175. Lechleider, R.J., et al., *Targeted mutagenesis of Smad1 reveals an essential role in chorioallantoic fusion.* Dev Biol, 2001. **240**(1): p. 157-67.
176. Zhao, G.Q., *Consequences of knocking out BMP signaling in the mouse.* Genesis, 2003. **35**(1): p. 43-56.
177. Urist, M.R., *Bone morphogenetic protein: the molecularization of skeletal system development.* J Bone Miner Res, 1997. **12**(3): p. 343-6.
178. Guo, L., R.C. Zhao, and Y. Wu, *The role of microRNAs in self-renewal and differentiation of mesenchymal stem cells.* Exp Hematol, 2011. **39**(6): p. 608-16.

179. Bessa, P.C., M. Casal, and R.L. Reis, *Bone morphogenetic proteins in tissue engineering: the road from laboratory to clinic, part II (BMP delivery).* J Tissue Eng Regen Med, 2008. **2**(2-3): p. 81-96.
180. Kim, J.H., et al., *Wnt signaling in bone formation and its therapeutic potential for bone diseases.* Ther Adv Musculoskelet Dis, 2013. **5**(1): p. 13-31.
181. Issack, P.S., D.L. Helfet, and J.M. Lane, *Role of Wnt signaling in bone remodeling and repair.* HSS J, 2008. **4**(1): p. 66-70.
182. Terada K, M.S., Katase N, Nishimatsu S, Nohno T., *Interaction of Wnt Signaling with BMP/Smad Signaling during the Transition from Cell Proliferation to Myogenic Differentiation in Mouse Myoblast-Derived Cells.* int j cell biol, 2013.
183. Horikiri, Y., et al., *Sonic hedgehog regulates osteoblast function by focal adhesion kinase signaling in the process of fracture healing.* PLoS One, 2013. **8**(10): p. e76785.
184. Reichert, J.C., et al., *Synergistic effect of Indian hedgehog and bone morphogenetic protein-2 gene transfer to increase the osteogenic potential of human mesenchymal stem cells.* Stem Cell Res Ther, 2013. **4**(5): p. 105.
185. Xiang, X., et al., *mTOR and the differentiation of mesenchymal stem cells.* Acta Biochim Biophys Sin (Shanghai), 2011. **43**(7): p. 501-10.
186. Wu, J.W., et al., *Crystal structure of a phosphorylated Smad2. Recognition of phosphoserine by the MH2 domain and insights on Smad function in TGF-beta signaling.* Mol Cell, 2001. **8**(6): p. 1277-89.
187. Makkar, P., et al., *Modeling and analysis of MH1 domain of Smads and their interaction with promoter DNA sequence motif.* J Mol Graph Model, 2009. **27**(7): p. 803-12.
188. Moustakas, A. and C.H. Heldin, *The regulation of TGFbeta signal transduction.* Development, 2009. **136**(22): p. 3699-714.
189. ten Dijke, P., K. Miyazono, and C.H. Heldin, *Signaling inputs converge on nuclear effectors in TGF-beta signaling.* Trends Biochem Sci, 2000. **25**(2): p. 64-70.
190. Kusanagi, K., et al., *Characterization of a bone morphogenetic protein-responsive Smad-binding element.* Mol Biol Cell, 2000. **11**(2): p. 555-65.
191. Liu, F., et al., *A human Mad protein acting as a BMP-regulated transcriptional activator.* Nature, 1996. **381**(6583): p. 620-3.
192. Zhao, M., et al., *The zinc finger transcription factor Gli2 mediates bone morphogenetic protein 2 expression in osteoblasts in response to hedgehog signaling.* Mol Cell Biol, 2006. **26**(16): p. 6197-208.
193. Kretzschmar, M., et al., *A mechanism of repression of TGFbeta/ Smad signaling by oncogenic Ras.* Genes Dev, 1999. **13**(7): p. 804-16.
194. Sapkota, G., et al., *Balancing BMP signaling through integrated inputs into the Smad1 linker.* Mol Cell, 2007. **25**(3): p. 441-54.
195. Lamouille, S., et al., *TGF-beta-induced activation of mTOR complex 2 drives epithelial-mesenchymal transition and cell invasion.* J Cell Sci, 2012. **125**(Pt 5): p. 1259-73.
196. Song, K., et al., *Novel roles of Akt and mTOR in suppressing TGF-beta/ALK5-mediated Smad3 activation.* EMBO J, 2006. **25**(1): p. 58-69.
197. Fingar, D.C., et al., *Mammalian cell size is controlled by mTOR and its downstream targets S6K1 and 4EBP1/eIF4E.* Genes Dev, 2002. **16**(12): p. 1472-87.
198. Feng, Z., et al., *The coordinate regulation of the p53 and mTOR pathways in cells.* Proc Natl Acad Sci U S A, 2005. **102**(23): p. 8204-9.
199. Brunn, G.J., et al., *Phosphorylation of the translational repressor PHAS-I by the mammalian target of rapamycin.* Science, 1997. **277**(5322): p. 99-101.

200. Burnett, P.E., et al., *RAFT1 phosphorylation of the translational regulators p70 S6 kinase and 4E-BP1.* Proc Natl Acad Sci U S A, 1998. **95**(4): p. 1432-7.
201. Kim, D.H., et al., *mTOR interacts with raptor to form a nutrient-sensitive complex that signals to the cell growth machinery.* Cell, 2002. **110**(2): p. 163-75.
202. Kim, D.H., et al., *GbetaL, a positive regulator of the rapamycin-sensitive pathway required for the nutrient-sensitive interaction between raptor and mTOR.* Mol Cell, 2003. **11**(4): p. 895-904.
203. Astrinidis, A. and E.P. Henske, *Tuberous sclerosis complex: linking growth and energy signaling pathways with human disease.* Oncogene, 2005. **24**(50): p. 7475-81.
204. Jozwiak, J., *Hamartin and tuberin: working together for tumour suppression.* Int J Cancer, 2006. **118**(1): p. 1-5.
205. Manning, B.D. and L.C. Cantley, *Rheb fills a GAP between TSC and TOR.* Trends Biochem Sci, 2003. **28**(11): p. 573-6.
206. Aspuria, P.J. and F. Tamanoi, *The Rheb family of GTP-binding proteins.* Cell Signal, 2004. **16**(10): p. 1105-12.
207. Brown, E.J., et al., *Control of p70 s6 kinase by kinase activity of FRAP in vivo.* Nature, 1995. **377**(6548): p. 441-6.
208. Lee, K.W., et al., *Rapamycin promotes the osteoblastic differentiation of human embryonic stem cells by blocking the mTOR pathway and stimulating the BMP/Smad pathway.* Stem Cells Dev, 2010. **19**(4): p. 557-68.
209. Singha, U.K., et al., *Rapamycin inhibits osteoblast proliferation and differentiation in MC3T3-E1 cells and primary mouse bone marrow stromal cells.* J Cell Biochem, 2008. **103**(2): p. 434-46.
210. Minamitani, C., et al., *p70 S6 kinase limits tumor necrosis factor-alpha-induced interleukin-6 synthesis in osteoblast-like cells.* Mol Cell Endocrinol, 2010. **315**(1-2): p. 195-200.
211. Takai, S., et al., *P70 S6 kinase negatively regulates fibroblast growth factor 2-stimulated interleukin-6 synthesis in osteoblasts: function at a point downstream from protein kinase C.* J Endocrinol, 2008. **197**(1): p. 131-7.
212. Takai, S., et al., *Limitation by p70 S6 kinase of platelet-derived growth factor-BB-induced interleukin 6 synthesis in osteoblast-like MC3T3-E1 cells.* Metabolism, 2007. **56**(4): p. 476-83.
213. Kozawa, O., H. Matsuno, and T. Uematsu, *Involvement of p70 S6 kinase in bone morphogenetic protein signaling: vascular endothelial growth factor synthesis by bone morphogenetic protein-4 in osteoblasts.* J Cell Biochem, 2001. **81**(3): p. 430-6.
214. Takai, S., et al., *Negative regulation by p70 S6 kinase of FGF-2-stimulated VEGF release through stress-activated protein kinase/c-Jun N-terminal kinase in osteoblasts.* J Bone Miner Res, 2007. **22**(3): p. 337-46.
215. Mori, K., et al., *Conditioned media from mouse osteosarcoma cells promote MC3T3-E1 cell proliferation using JAKs and PI3-K/Akt signal crosstalk.* Cancer Sci, 2008. **99**(11): p. 2170-6.
216. Tseng, W.P., et al., *Hypoxia induces BMP-2 expression via ILK, Akt, mTOR, and HIF-1 pathways in osteoblasts.* J Cell Physiol, 2010. **223**(3): p. 810-8.
217. Isomoto, S., et al., *Rapamycin as an inhibitor of osteogenic differentiation in bone marrow-derived mesenchymal stem cells.* J Orthop Sci, 2007. **12**(1): p. 83-8.
218. Shoba, L.N. and J.C. Lee, *Inhibition of phosphatidylinositol 3-kinase and p70S6 kinase blocks osteogenic protein-1 induction of alkaline phosphatase activity in fetal rat calvaria cells.* J Cell Biochem, 2003. **88**(6): p. 1247-55.

219. Ogawa, T., et al., *Osteoblastic differentiation is enhanced by rapamycin in rat osteoblast-like osteosarcoma (ROS 17/2.8) cells.* Biochem Biophys Res Commun, 1998. **249**(1): p. 226-30.
220. James, A.W., *Reviewof Signaling Pathways Governing MSC Osteogenic and Adipogenic Differentiation.* Scientifica (Cairo), 2013.
221. Krishnan, V., H.U. Bryant, and O.A. Macdougald, *Regulation of bone mass by Wnt signaling.* J Clin Invest, 2006. **116**(5): p. 1202-9.
222. Cadigan, K.M. and Y.I. Liu, *Wnt signaling: complexity at the surface.* J Cell Sci, 2006. **119**(Pt 3): p. 395-402.
223. Komiya, Y. and R. Habas, *Wnt signal transduction pathways.* Organogenesis, 2008. **4**(2): p. 68-75.
224. Papathanasiou, I., K.N. Malizos, and A. Tsezou, *Bone morphogenetic protein-2-induced Wnt/beta-catenin signaling pathway activation through enhanced low-density-lipoprotein receptor-related protein 5 catabolic activity contributes to hypertrophy in osteoarthritic chondrocytes.* Arthritis Res Ther, 2012. **14**(2): p. R82.
225. Lamplot, J.D., et al., *BMP9 signaling in stem cell differentiation and osteogenesis.* Am J Stem Cells, 2013. **2**(1): p. 1-21.
226. McCarthy, T.L. and M. Centrella, *Novel links among Wnt and TGF-beta signaling and Runx2.* Mol Endocrinol, 2010. **24**(3): p. 587-97.
227. Hill, T.P., et al., *Canonical Wnt/beta-catenin signaling prevents osteoblasts from differentiating into chondrocytes.* Dev Cell, 2005. **8**(5): p. 727-38.
228. Bennett, C.N., et al., *Regulation of osteoblastogenesis and bone mass by Wnt10b.* Proc Natl Acad Sci U S A, 2005. **102**(9): p. 3324-9.
229. Urs, S., et al., *Sprouty1 is a critical regulatory switch of mesenchymal stem cell lineage allocation.* FASEB J, 2010. **24**(9): p. 3264-73.
230. Jaiswal, R.K., et al., *Adult human mesenchymal stem cell differentiation to the osteogenic or adipogenic lineage is regulated by mitogen-activated protein kinase.* J Biol Chem, 2000. **275**(13): p. 9645-52.
231. Isenmann, S., et al., *TWIST family of basic helix-loop-helix transcription factors mediate human mesenchymal stem cell growth and commitment.* Stem Cells, 2009. **27**(10): p. 2457-68.
232. Quach, J.M., et al., *Zinc finger protein 467 is a novel regulator of osteoblast and adipocyte commitment.* J Biol Chem, 2011. **286**(6): p. 4186-98.
233. Calo, E., et al., *Rb regulates fate choice and lineage commitment in vivo.* Nature, 2010. **466**(7310): p. 1110-4.
234. Lian, J.B., et al., *MicroRNA control of bone formation and homeostasis.* Nat Rev Endocrinol, 2012. **8**(4): p. 212-27.
235. Huang, G., et al., *miR-20a encoded by the miR-17-92 cluster increases the metastatic potential of osteosarcoma cells by regulating Fas expression.* Cancer Res, 2012. **72**(4): p. 908-16.
236. Tome, M., et al., *miR-335 orchestrates cell proliferation, migration and differentiation in human mesenchymal stem cells.* Cell Death Differ, 2011. **18**(6): p. 985-95.
237. Yin, Q., et al., *MicroRNA miR-155 inhibits bone morphogenetic protein (BMP) signaling and BMP-mediated Epstein-Barr virus reactivation.* J Virol, 2010. **84**(13): p. 6318-27.
238. Engin, F. and B. Lee, *NOTCHing the bone: insights into multi-functionality.* Bone, 2010. **46**(2): p. 274-80.

239. Ramasamy, S.K., et al., *Endothelial Notch activity promotes angiogenesis and osteogenesis in bone.* Nature, 2014. **507**(7492): p. 376-80.
240. Mariani, E., L. Pulsatelli, and A. Facchini, *Signaling pathways in cartilage repair.* Int J Mol Sci, 2014. **15**(5): p. 8667-98.
241. Eliseev, R.A., et al., *Smad7 mediates inhibition of Saos2 osteosarcoma cell differentiation by NFkappaB.* Exp Cell Res, 2006. **312**(1): p. 40-50.
242. Verma, S., et al., *Adipocytic proportion of bone marrow is inversely related to bone formation in osteoporosis.* J Clin Pathol, 2002. **55**(9): p. 693-8.
243. Liu, Y., et al., *All-trans retinoic acid modulates bone morphogenic protein 9-induced osteogenesis and adipogenesis of preadipocytes through BMP/Smad and Wnt/beta-catenin signaling pathways.* Int J Biochem Cell Biol, 2014. **47**: p. 47-56.
244. Park, S.R., R.O. Oreffo, and J.T. Triffitt, *Interconversion potential of cloned human marrow adipocytes in vitro.* Bone, 1999. **24**(6): p. 549-54.
245. Takahashi, T., *Overexpression of Runx2 and MKP-1 stimulates transdifferentiation of 3T3-L1 preadipocytes into bone-forming osteoblasts in vitro.* Calcif Tissue Int, 2011. **88**(4): p. 336-47.
246. Zuo, C., et al., *Osteoblastogenesis regulation signals in bone remodeling.* Osteoporos Int, 2012. **23**(6): p. 1653-63.
247. Sapir-Koren, R. and G. Livshits, *Osteocyte control of bone remodeling: is sclerostin a key molecular coordinator of the balanced bone resorption-formation cycles?* Osteoporos Int, 2014. **25**(12): p. 2685-700.
248. Hendrickx, G., E. Boudin, and W. Van Hul, *A look behind the scenes: the risk and pathogenesis of primary osteoporosis.* Nat Rev Rheumatol, 2015.
249. Bouxsein, M.L. and D. Karasik, *Bone geometry and skeletal fragility.* Curr Osteoporos Rep, 2006. **4**(2): p. 49-56.
250. Lopez-Otin, C., et al., *The hallmarks of aging.* Cell, 2013. **153**(6): p. 1194-217.
251. Matsushita, M., et al., *Age-related changes in bone mass in the senescence-accelerated mouse (SAM). SAM-R/3 and SAM-P/6 as new murine models for senile osteoporosis.* Am J Pathol, 1986. **125**(2): p. 276-83.
252. Tanisawa, K., et al., *Exome sequencing of senescence-accelerated mice (SAM) reveals deleterious mutations in degenerative disease-causing genes.* BMC Genomics, 2013. **14**: p. 248.
253. Lewis, D.B., et al., *Osteoporosis induced in mice by overproduction of interleukin 4.* Proc Natl Acad Sci U S A, 1993. **90**(24): p. 11618-22.
254. Egermann, M., et al., *Influence of defective bone marrow osteogenesis on fracture repair in an experimental model of senile osteoporosis.* J Orthop Res, 2010. **28**(6): p. 798-804.
255. Jilka, R.L., et al., *Linkage of decreased bone mass with impaired osteoblastogenesis in a murine model of accelerated senescence.* J Clin Invest, 1996. **97**(7): p. 1732-40.
256. Kuro-o, M., et al., *Mutation of the mouse klotho gene leads to a syndrome resembling ageing.* Nature, 1997. **390**(6655): p. 45-51.
257. Ohnishi, M. and M.S. Razzaque, *Dietary and genetic evidence for phosphate toxicity accelerating mammalian aging.* FASEB J, 2010. **24**(9): p. 3562-71.
258. Kawaguchi, H., et al., *Independent impairment of osteoblast and osteoclast differentiation in klotho mouse exhibiting low-turnover osteopenia.* J Clin Invest, 1999. **104**(3): p. 229-37.
259. Li, Y., et al., *FGF23 affects the lineage fate determination of mesenchymal stem cells.* Calcif Tissue Int, 2013. **93**(6): p. 556-64.
260. Haussler, M.R., et al., *The role of vitamin D in the FGF23, klotho, and phosphate bone-kidney endocrine axis.* Rev Endocr Metab Disord, 2012. **13**(1): p. 57-69.

261. Saeed, H., et al., *Telomerase-deficient mice exhibit bone loss owing to defects in osteoblasts and increased osteoclastogenesis by inflammatory microenvironment.* J Bone Miner Res, 2011. **26**(7): p. 1494-505.
262. Brennan, T.A., et al., *Mouse models of telomere dysfunction phenocopy skeletal changes found in human age-related osteoporosis.* Dis Model Mech, 2014. **7**(5): p. 583-92.
263. Mirsaidi, A., et al., *Telomere length, telomerase activity and osteogenic differentiation are maintained in adipose-derived stromal cells from senile osteoporotic SAMP6 mice.* J Tissue Eng Regen Med, 2012. **6**(5): p. 378-90.
264. Chang, S., et al., *Essential role of limiting telomeres in the pathogenesis of Werner syndrome.* Nat Genet, 2004. **36**(8): p. 877-82.
265. de Boer, J., et al., *Premature aging in mice deficient in DNA repair and transcription.* Science, 2002. **296**(5571): p. 1276-9.
266. Diderich, K.E., et al., *Bone fragility and decline in stem cells in prematurely aging DNA repair deficient trichothiodystrophy mice.* Age (Dordr), 2012. **34**(4): p. 845-61.
267. Chen, Q., et al., *DNA damage drives accelerated bone aging via an NF-kappaB-dependent mechanism.* J Bone Miner Res, 2013. **28**(5): p. 1214-28.
268. Wang, L., et al., *Cdc42 GTPase-activating protein deficiency promotes genomic instability and premature aging-like phenotypes.* Proc Natl Acad Sci U S A, 2007. **104**(4): p. 1248-53.
269. Osorio, F.G., et al., *Splicing-directed therapy in a new mouse model of human accelerated aging.* Sci Transl Med, 2011. **3**(106): p. 106ra107.
270. Liu, B., et al., *Resveratrol rescues SIRT1-dependent adult stem cell decline and alleviates progeroid features in laminopathy-based progeria.* Cell Metab, 2012. **16**(6): p. 738-50.
271. Tyner, S.D., et al., *p53 mutant mice that display early ageing-associated phenotypes.* Nature, 2002. **415**(6867): p. 45-53.
272. Koczor, C.A., et al., *Mitochondrial matrix P53 sensitizes cells to oxidative stress.* Mitochondrion, 2013. **13**(4): p. 277-81.
273. Almeida, M., *Aging mechanisms in bone.* Bonekey Rep, 2012. **1**.
274. Manolagas, S.C., *From estrogen-centric to aging and oxidative stress: a revised perspective of the pathogenesis of osteoporosis.* Endocr Rev, 2010. **31**(3): p. 266-300.
275. Smietana, M.J., et al., *Reactive oxygen species on bone mineral density and mechanics in Cu,Zn superoxide dismutase (Sod1) knockout mice.* Biochem Biophys Res Commun, 2010. **403**(1): p. 149-53.
276. Nojiri, H., et al., *Cytoplasmic superoxide causes bone fragility owing to low-turnover osteoporosis and impaired collagen cross-linking.* J Bone Miner Res, 2011. **26**(11): p. 2682-94.
277. Ambrogini, E., et al., *FoxO-mediated defense against oxidative stress in osteoblasts is indispensable for skeletal homeostasis in mice.* Cell Metab, 2010. **11**(2): p. 136-46.
278. Essers, M.A., et al., *Functional interaction between beta-catenin and FOXO in oxidative stress signaling.* Science, 2005. **308**(5725): p. 1181-4.
279. Almeida, M., et al., *Oxidative stress antagonizes Wnt signaling in osteoblast precursors by diverting beta-catenin from T cell factor- to forkhead box O-mediated transcription.* J Biol Chem, 2007. **282**(37): p. 27298-305.
280. Almeida, M., *Unraveling the role of FoxOs in bone--insights from mouse models.* Bone, 2011. **49**(3): p. 319-27.

281. R., H., *The significance of DNA methylation in cellular aging.* Molecular Biology of Aging, 1985.
282. Fairweather, D.S., M. Fox, and G.P. Margison, *The in vitro lifespan of MRC-5 cells is shortened by 5-azacytidine-induced demethylation.* Exp Cell Res, 1987. **168**(1): p. 153-9.
283. Sun, L.Q., et al., *Growth retardation and premature aging phenotypes in mice with disruption of the SNF2-like gene, PASG.* Genes Dev, 2004. **18**(9): p. 1035-46.
284. Van Vlasselaer, P., et al., *Characterization and purification of osteogenic cells from murine bone marrow by two-color cell sorting using anti-Sca-1 monoclonal antibody and wheat germ agglutinin.* Blood, 1994. **84**(3): p. 753-63.
285. Bonyadi, M., et al., *Mesenchymal progenitor self-renewal deficiency leads to age-dependent osteoporosis in Sca-1/Ly-6A null mice.* Proc Natl Acad Sci U S A, 2003. **100**(10): p. 5840-5.
286. Jilka, R.L.e.a., *Dysfunctional osteocytes increase RANKL and promote cortical pore formation in their vicinity: a mechanistic explanation for the development of cortical porosity with age.* J Bone Miner Res, 2012. **27**.
287. Jilka, R.L., et al., *Dysapoptosis of osteoblasts and osteocytes increases cancellous bone formation but exaggerates cortical porosity with age.* J Bone Miner Res, 2014. **29**(1): p. 103-17.
288. Tomkinson, A., et al., *The death of osteocytes via apoptosis accompanies estrogen withdrawal in human bone.* J Clin Endocrinol Metab, 1997. **82**(9): p. 3128-35.
289. Tomkinson, A., et al., *The role of estrogen in the control of rat osteocyte apoptosis.* J Bone Miner Res, 1998. **13**(8): p. 1243-50.
290. Almeida, M., et al., *Skeletal involution by age-associated oxidative stress and its acceleration by loss of sex steroids.* J Biol Chem, 2007. **282**(37): p. 27285-97.
291. Seeman, E., *Periosteal bone formation--a neglected determinant of bone strength.* N Engl J Med, 2003. **349**(4): p. 320-3.
292. Seeman, E., *Pathogenesis of bone fragility in women and men.* Lancet, 2002. **359**(9320): p. 1841-50.
293. Zebaze, R.M., et al., *Intracortical remodelling and porosity in the distal radius and post-mortem femurs of women: a cross-sectional study.* Lancet, 2010. **375**(9727): p. 1729-36.
294. Syed, F.A., et al., *Effects of chronic estrogen treatment on modulating age-related bone loss in female mice.* J Bone Miner Res, 2010. **25**(11): p. 2438-46.
295. Shahnazari, M., et al., *Bone turnover markers in peripheral blood and marrow plasma reflect trabecular bone loss but not endocortical expansion in aging mice.* Bone, 2012. **50**(3): p. 628-37.
296. Manolagas, S.C., C.A. O'Brien, and M. Almeida, *The role of estrogen and androgen receptors in bone health and disease.* Nat Rev Endocrinol, 2013. **9**(12): p. 699-712.
297. Eisman, J.A. and R. Bouillon, *Vitamin D: direct effects of vitamin D metabolites on bone: lessons from genetically modified mice.* Bonekey Rep, 2014. **3**: p. 499.
298. Christodoulou, S., et al., *Vitamin D and bone disease.* Biomed Res Int, 2013. **2013**: p. 396541.
299. Bonjour, J.P., et al., *Dairy in adulthood: from foods to nutrient interactions on bone and skeletal muscle health.* J Am Coll Nutr, 2013. **32**(4): p. 251-63.
300. Heaney, R.P. and D.K. Layman, *Amount and type of protein influences bone health.* Am J Clin Nutr, 2008. **87**(5): p. 1567S-1570S.
301. Sebastian, A., *Dietary protein content and the diet's net acid load: opposing effects on bone health.* Am J Clin Nutr, 2005. **82**(5): p. 921-2.

302. Shen, C.L., et al., *Fruits and dietary phytochemicals in bone protection.* Nutr Res, 2012. **32**(12): p. 897-910.
303. Rajendran, P., et al., *Antioxidants and human diseases.* Clin Chim Acta, 2014. **436**: p. 332-47.
304. Leeuwenburgh, C. and J.W. Heinecke, *Oxidative stress and antioxidants in exercise.* Curr Med Chem, 2001. **8**(7): p. 829-38.
305. Ozcivici, E., et al., *Mechanical signals as anabolic agents in bone.* Nat Rev Rheumatol, 2010. **6**(1): p. 50-9.
306. Semenov, M., K. Tamai, and X. He, *SOST is a ligand for LRP5/LRP6 and a Wnt signaling inhibitor.* J Biol Chem, 2005. **280**(29): p. 26770-5.
307. Li, X., et al., *Sclerostin binds to LRP5/6 and antagonizes canonical Wnt signaling.* J Biol Chem, 2005. **280**(20): p. 19883-7.
308. Balemans, W., et al., *Identification of a 52 kb deletion downstream of the SOST gene in patients with van Buchem disease.* J Med Genet, 2002. **39**(2): p. 91-7.
309. Balemans, W., et al., *Increased bone density in sclerosteosis is due to the deficiency of a novel secreted protein (SOST).* Hum Mol Genet, 2001. **10**(5): p. 537-43.
310. Rochefort, G.Y., S. Pallu, and C.L. Benhamou, *Osteocyte: the unrecognized side of bone tissue.* Osteoporos Int, 2010. **21**(9): p. 1457-69.
311. Boudin, E., et al., *The role of extracellular modulators of canonical Wnt signaling in bone metabolism and diseases.* Semin Arthritis Rheum, 2013. **43**(2): p. 220-40.
312. Wang, Y., et al., *Wnt and the Wnt signaling pathway in bone development and disease.* Front Biosci (Landmark Ed), 2014. **19**: p. 379-407.
313. Ronis, M.J., K. Mercer, and J.R. Chen, *Effects of nutrition and alcohol consumption on bone loss.* Curr Osteoporos Rep, 2011. **9**(2): p. 53-9.
314. Chen, J.R., et al., *Protective effects of estradiol on ethanol-induced bone loss involve inhibition of reactive oxygen species generation in osteoblasts and downstream activation of the extracellular signal-regulated kinase/signal transducer and activator of transcription 3/receptor activator of nuclear factor-kappaB ligand signaling cascade.* J Pharmacol Exp Ther, 2008. **324**(1): p. 50-9.
315. Chen, J.R., et al., *A role for ethanol-induced oxidative stress in controlling lineage commitment of mesenchymal stromal cells through inhibition of Wnt/beta-catenin signaling.* J Bone Miner Res, 2010. **25**(5): p. 1117-27.
316. Maurel, D.B., et al., *Alcohol and bone: review of dose effects and mechanisms.* Osteoporos Int, 2012. **23**(1): p. 1-16.
317. Kanis, J.A., et al., *Smoking and fracture risk: a meta-analysis.* Osteoporos Int, 2005. **16**(2): p. 155-62.
318. Ward, K.D. and R.C. Klesges, *A meta-analysis of the effects of cigarette smoking on bone mineral density.* Calcif Tissue Int, 2001. **68**(5): p. 259-70.
319. Yoon, V., N.M. Maalouf, and K. Sakhaee, *The effects of smoking on bone metabolism.* Osteoporos Int, 2012. **23**(8): p. 2081-92.
320. Herzog, *Verlangerung osteotomie unter Verwendung des Perkutan gezielt verriegelten Markangels.* Unfallheilkunde, 1951. **42:26**.
321. Connolly, J.F., *Injectable bone marrow preparations to stimulate osteogenic repair.* Clin Orthop Relat Res, 1995(313): p. 8-18.
322. Grayson, W.L., et al., *Stromal cells and stem cells in clinical bone regeneration.* Nat Rev Endocrinol, 2015. **11**(3): p. 140-50.
323. Neovius, E. and T. Engstrand, *Craniofacial reconstruction with bone and biomaterials: review over the last 11 years.* J Plast Reconstr Aesthet Surg, 2010. **63**(10): p. 1615-23.

324. Casser-Bette, M., et al., *Bone formation by osteoblast-like cells in a three-dimensional cell culture.* Calcif Tissue Int, 1990. **46**(1): p. 46-56.
325. Halvorsen, Y.D., et al., *Extracellular matrix mineralization and osteoblast gene expression by human adipose tissue-derived stromal cells.* Tissue Eng, 2001. **7**(6): p. 729-41.
326. Levi, B., et al., *Differences in osteogenic differentiation of adipose-derived stromal cells from murine, canine, and human sources in vitro and in vivo.* Plast Reconstr Surg, 2011. **128**(2): p. 373-86.
327. Justesen, J., et al., *Subcutaneous adipocytes can differentiate into bone-forming cells in vitro and in vivo.* Tissue Eng, 2004. **10**(3-4): p. 381-91.
328. Sandor, G.K., et al., *Adipose stem cells used to reconstruct 13 cases with cranio-maxillofacial hard-tissue defects.* Stem Cells Transl Med, 2014. **3**(4): p. 530-40.
329. Hicok, K.C., et al., *Human adipose-derived adult stem cells produce osteoid in vivo.* Tissue Eng, 2004. **10**(3-4): p. 371-80.
330. Mesimaki, K., et al., *Novel maxillary reconstruction with ectopic bone formation by GMP adipose stem cells.* Int J Oral Maxillofac Surg, 2009. **38**(3): p. 201-9.
331. Wolff, J., et al., *GMP-level adipose stem cells combined with computer-aided manufacturing to reconstruct mandibular ameloblastoma resection defects: Experience with three cases.* Ann Maxillofac Surg, 2013. **3**(2): p. 114-25.
332. Dupont, K.M., et al., *Human stem cell delivery for treatment of large segmental bone defects.* Proc Natl Acad Sci U S A, 2010. **107**(8): p. 3305-10.
333. Rehman, J., et al., *Secretion of angiogenic and antiapoptotic factors by human adipose stromal cells.* Circulation, 2004. **109**(10): p. 1292-8.
334. Traktuev, D.O., et al., *A population of multipotent CD34-positive adipose stromal cells share pericyte and mesenchymal surface markers, reside in a periendothelial location, and stabilize endothelial networks.* Circ Res, 2008. **102**(1): p. 77-85.
335. Miyazaki, M., et al., *Comparison of human mesenchymal stem cells derived from adipose tissue and bone marrow for ex vivo gene therapy in rat spinal fusion model.* Spine (Phila Pa 1976), 2008. **33**(8): p. 863-9.
336. Warnke, P.H., et al., *Growth and transplantation of a custom vascularised bone graft in a man.* Lancet, 2004. **364**(9436): p. 766-70.
337. Sandor, G.K., et al., *Adipose stem cell tissue-engineered construct used to treat large anterior mandibular defect: a case report and review of the clinical application of good manufacturing practice-level adipose stem cells for bone regeneration.* J Oral Maxillofac Surg, 2013. **71**(5): p. 938-50.
338. Lendeckel, S., et al., *Autologous stem cells (adipose) and fibrin glue used to treat widespread traumatic calvarial defects: case report.* J Craniomaxillofac Surg, 2004. **32**(6): p. 370-3.
339. Quarto, R., et al., *Repair of large bone defects with the use of autologous bone marrow stromal cells.* N Engl J Med, 2001. **344**(5): p. 385-6.
340. Marcacci, M., et al., *Stem cells associated with macroporous bioceramics for long bone repair: 6- to 7-year outcome of a pilot clinical study.* Tissue Eng, 2007. **13**(5): p. 947-55.
341. Kawate, K., et al., *Tissue-engineered approach for the treatment of steroid-induced osteonecrosis of the femoral head: transplantation of autologous mesenchymal stem cells cultured with beta-tricalcium phosphate ceramics and free vascularized fibula.* Artif Organs, 2006. **30**(12): p. 960-2.
342. Muschler, G.F., et al., *Selective retention of bone marrow-derived cells to enhance spinal fusion.* Clin Orthop Relat Res, 2005(432): p. 242-51.

343. Cowan, C.M., et al., *Bone morphogenetic protein 2 and retinoic acid accelerate in vivo bone formation, osteoclast recruitment, and bone turnover.* Tissue Eng, 2005. **11**(3-4): p. 645-58.
344. Yoon, E., et al., *In vivo osteogenic potential of human adipose-derived stem cells/poly lactide-co-glycolic acid constructs for bone regeneration in a rat critical-sized calvarial defect model.* Tissue Eng, 2007. **13**(3): p. 619-27.
345. Lee, S.J., et al., *Enhancement of bone regeneration by gene delivery of BMP2/Runx2 bicistronic vector into adipose-derived stromal cells.* Biomaterials, 2010. **31**(21): p. 5652-9.
346. Brian E. Grottkau, Y.L., *Osteogenesis of Adipose-Derived Stem Cells.* bone res, 2013.
347. Vats, A., et al., *Stem cells: sources and applications.* Clin Otolaryngol Allied Sci, 2002. **27**(4): p. 227-32.
348. Le Blanc, K. and M. Pittenger, *Mesenchymal stem cells: progress toward promise.* Cytotherapy, 2005. **7**(1): p. 36-45.
349. Schaffler, A. and C. Buchler, *Concise review: adipose tissue-derived stromal cells--basic and clinical implications for novel cell-based therapies.* Stem Cells, 2007. **25**(4): p. 818-27.
350. Palou, M., et al., *Gene expression patterns in visceral and subcutaneous adipose depots in rats are linked to their morphologic features.* Cell Physiol Biochem, 2009. **24**(5-6): p. 547-56.
351. Ahn, H.H., et al., *In vivo osteogenic differentiation of human adipose-derived stem cells in an injectable in situ-forming gel scaffold.* Tissue Eng Part A, 2009. **15**(7): p. 1821-32.
352. Aust, L., et al., *Yield of human adipose-derived adult stem cells from liposuction aspirates.* Cytotherapy, 2004. **6**(1): p. 7-14.
353. Zhu, Y., et al., *Adipose-derived stem cell: a better stem cell than BMSC.* Cell Biochem Funct, 2008. **26**(6): p. 664-75.
354. Kern, S., et al., *Comparative analysis of mesenchymal stem cells from bone marrow, umbilical cord blood, or adipose tissue.* Stem Cells, 2006. **24**(5): p. 1294-301.
355. Izadpanah, R., et al., *Biologic properties of mesenchymal stem cells derived from bone marrow and adipose tissue.* J Cell Biochem, 2006. **99**(5): p. 1285-97.
356. Wu, W., L. Niklason, and D.M. Steinbacher, *The effect of age on human adipose-derived stem cells.* Plast Reconstr Surg, 2013. **131**(1): p. 27-37.
357. Shi, Y.Y., et al., *The osteogenic potential of adipose-derived mesenchymal cells is maintained with aging.* Plast Reconstr Surg, 2005. **116**(6): p. 1686-96.
358. Chen, H.T., et al., *Proliferation and differentiation potential of human adipose-derived mesenchymal stem cells isolated from elderly patients with osteoporotic fractures.* J Cell Mol Med, 2012. **16**(3): p. 582-93.
359. Helvering, L.M., et al., *Regulation of the promoters for the human bone morphogenetic protein 2 and 4 genes.* Gene, 2000. **256**(1-2): p. 123-38.
360. Cho, H.H., et al., *NF-kappaB activation stimulates osteogenic differentiation of mesenchymal stem cells derived from human adipose tissue by increasing TAZ expression.* J Cell Physiol, 2010. **223**(1): p. 168-77.
361. Cho, H.H., et al., *Induction of osteogenic differentiation of human mesenchymal stem cells by histone deacetylase inhibitors.* J Cell Biochem, 2005. **96**(3): p. 533-42.
362. Sumanasinghe, R.D., J.A. Osborne, and E.G. Loboa, *Mesenchymal stem cell-seeded collagen matrices for bone repair: effects of cyclic tensile strain, cell density, and media conditions on matrix contraction in vitro.* J Biomed Mater Res A, 2009. **88**(3): p. 778-86.

363. Hammerick, K.E., et al., *Pulsed direct current electric fields enhance osteogenesis in adipose-derived stromal cells.* Tissue Eng Part A, 2010. **16**(3): p. 917-31.
364. McCullen, S.D., et al., *Application of low-frequency alternating current electric fields via interdigitated electrodes: effects on cellular viability, cytoplasmic calcium, and osteogenic differentiation of human adipose-derived stem cells.* Tissue Eng Part C Methods, 2010. **16**(6): p. 1377-86.
365. Ogston, N., et al., *Dexamethasone and retinoic acid differentially regulate growth and differentiation in an immortalised human clonal bone marrow stromal cell line with osteoblastic characteristics.* Steroids, 2002. **67**(11): p. 895-906.
366. Yun, Z., et al., *Inhibition of PPAR gamma 2 gene expression by the HIF-1-regulated gene DEC1/Stra13: a mechanism for regulation of adipogenesis by hypoxia.* Dev Cell, 2002. **2**(3): p. 331-41.
367. Schwarz, E.J., et al., *Retinoic acid blocks adipogenesis by inhibiting C/EBPbeta-mediated transcription.* Mol Cell Biol, 1997. **17**(3): p. 1552-61.
368. Wan, D.C., et al., *Osteogenic differentiation of mouse adipose-derived adult stromal cells requires retinoic acid and bone morphogenetic protein receptor type IB signaling.* Proc Natl Acad Sci U S A, 2006. **103**(33): p. 12335-40.
369. Skillington, J., L. Choy, and R. Derynck, *Bone morphogenetic protein and retinoic acid signaling cooperate to induce osteoblast differentiation of preadipocytes.* J Cell Biol, 2002. **159**(1): p. 135-46.
370. Chen, D., et al., *Differential roles for bone morphogenetic protein (BMP) receptor type IB and IA in differentiation and specification of mesenchymal precursor cells to osteoblast and adipocyte lineages.* J Cell Biol, 1998. **142**(1): p. 295-305.
371. Orimo, H. and T. Shimada, *Regulation of the human tissue-nonspecific alkaline phosphatase gene expression by all-trans-retinoic acid in SaOS-2 osteosarcoma cell line.* Bone, 2005. **36**(5): p. 866-76.
372. Tiaden, A.N., et al., *Human serine protease HTRA1 positively regulates osteogenesis of human bone marrow-derived mesenchymal stem cells and mineralization of differentiating bone-forming cells through the modulation of extracellular matrix protein.* Stem Cells, 2012. **30**(10): p. 2271-82.
373. Clausen, T., C. Southan, and M. Ehrmann, *The HtrA family of proteases: implications for protein composition and cell fate.* Mol Cell, 2002. **10**(3): p. 443-55.
374. Lipinska, B., S. Sharma, and C. Georgopoulos, *Sequence analysis and regulation of the htrA gene of Escherichia coli: a sigma 32-independent mechanism of heat-inducible transcription.* Nucleic Acids Res, 1988. **16**(21): p. 10053-67.
375. Strauch, K.L. and J. Beckwith, *An Escherichia coli mutation preventing degradation of abnormal periplasmic proteins.* Proc Natl Acad Sci U S A, 1988. **85**(5): p. 1576-80.
376. Clausen, T., et al., *HTRA proteases: regulated proteolysis in protein quality control.* Nat Rev Mol Cell Biol, 2011. **12**(3): p. 152-62.
377. Vande Walle, L., M. Lamkanfi, and P. Vandenabeele, *The mitochondrial serine protease HtrA2/Omi: an overview.* Cell Death Differ, 2008. **15**(3): p. 453-60.
378. Zurawa-Janicka, D., J. Skorko-Glonek, and B. Lipinska, *HtrA proteins as targets in therapy of cancer and other diseases.* Expert Opin Ther Targets, 2010. **14**(7): p. 665-79.
379. Chien, J., et al., *A candidate tumor suppressor HtrA1 is downregulated in ovarian cancer.* Oncogene, 2004. **23**(8): p. 1636-44.
380. Baldi, A., et al., *The HtrA1 serine protease is down-regulated during human melanoma progression and represses growth of metastatic melanoma cells.* Oncogene, 2002. **21**(43): p. 6684-8.

381. Zumbrunn, J. and B. Trueb, *Primary structure of a putative serine protease specific for IGF-binding proteins.* FEBS Lett, 1996. **398**(2-3): p. 187-92.
382. Spiess, C., A. Beil, and M. Ehrmann, *A temperature-dependent switch from chaperone to protease in a widely conserved heat shock protein.* Cell, 1999. **97**(3): p. 339-47.
383. Krojer, T., et al., *Structural basis for the regulated protease and chaperone function of DegP.* Nature, 2008. **453**(7197): p. 885-90.
384. Wilken, C., et al., *Crystal structure of the DegS stress sensor: How a PDZ domain recognizes misfolded protein and activates a protease.* Cell, 2004. **117**(4): p. 483-94.
385. Li, W., et al., *Structural insights into the pro-apoptotic function of mitochondrial serine protease HtrA2/Omi.* Nat Struct Biol, 2002. **9**(6): p. 436-41.
386. Truebestein, L., et al., *Substrate-induced remodeling of the active site regulates human HTRA1 activity.* Nat Struct Mol Biol, 2011. **18**(3): p. 386-8.
387. Sheng, M. and C. Sala, *PDZ domains and the organization of supramolecular complexes.* Annu Rev Neurosci, 2001. **24**: p. 1-29.
388. Hou, J., D.R. Clemmons, and S. Smeekens, *Expression and characterization of a serine protease that preferentially cleaves insulin-like growth factor binding protein-5.* J Cell Biochem, 2005. **94**(3): p. 470-84.
389. Tennstaedt, A., et al., *Human high temperature requirement serine protease A1 (HTRA1) degrades tau protein aggregates.* J Biol Chem, 2012. **287**(25): p. 20931-41.
390. Schlott, B., et al., *Interaction of Kazal-type inhibitor domains with serine proteinases: biochemical and structural studies.* J Mol Biol, 2002. **318**(2): p. 533-46.
391. Rawlings, N.D., D.P. Tolle, and A.J. Barrett, *Evolutionary families of peptidase inhibitors.* Biochem J, 2004. **378**(Pt 3): p. 705-16.
392. Spiess, C., et al., *Biochemical characterization and mass spectrometric disulfide bond mapping of periplasmic alpha-amylase MalS of Escherichia coli.* J Biol Chem, 1997. **272**(35): p. 22125-33.
393. Shen, Q.T., et al., *Bowl-shaped oligomeric structures on membranes as DegP's new functional forms in protein quality control.* Proc Natl Acad Sci U S A, 2009. **106**(12): p. 4858-63.
394. Jones, C.H., et al., *Escherichia coli DegP protease cleaves between paired hydrophobic residues in a natural substrate: the PapA pilin.* J Bacteriol, 2002. **184**(20): p. 5762-71.
395. Chien, J., et al., *Serine protease HtrA1 associates with microtubules and inhibits cell migration.* Mol Cell Biol, 2009. **29**(15): p. 4177-87.
396. Chien, J., et al., *HtrA serine proteases as potential therapeutic targets in cancer.* Curr Cancer Drug Targets, 2009. **9**(4): p. 451-68.
397. Chien, J., et al., *Serine protease HtrA1 modulates chemotherapy-induced cytotoxicity.* J Clin Invest, 2006. **116**(7): p. 1994-2004.
398. Launay, S., et al., *HtrA1-dependent proteolysis of TGF-beta controls both neuronal maturation and developmental survival.* Cell Death Differ, 2008. **15**(9): p. 1408-16.
399. Oka, C., et al., *HtrA1 serine protease inhibits signaling mediated by Tgfbeta family proteins.* Development, 2004. **131**(5): p. 1041-53.
400. Campioni, M., et al., *The serine protease HtrA1 specifically interacts and degrades the tuberous sclerosis complex 2 protein.* Mol Cancer Res, 2010. **8**(9): p. 1248-60.

401. An, E., et al., *Identification of novel substrates for the serine protease HTRA1 in the human RPE secretome.* Invest Ophthalmol Vis Sci, 2010. **51**(7): p. 3379-86.
402. Tsuchiya, A., et al., *Expression of mouse HtrA1 serine protease in normal bone and cartilage and its upregulation in joint cartilage damaged by experimental arthritis.* Bone, 2005. **37**(3): p. 323-36.
403. Grau, S., et al., *The role of human HtrA1 in arthritic disease.* J Biol Chem, 2006. **281**(10): p. 6124-9.
404. Hu, S.I., et al., *Human HtrA, an evolutionarily conserved serine protease identified as a differentially expressed gene product in osteoarthritic cartilage.* J Biol Chem, 1998. **273**(51): p. 34406-12.
405. Wu, J., et al., *Comparative proteomic characterization of articular cartilage tissue from normal donors and patients with osteoarthritis.* Arthritis Rheum, 2007. **56**(11): p. 3675-84.
406. Tiaden, A.N. and P.J. Richards, *The emerging roles of HTRA1 in musculoskeletal disease.* Am J Pathol, 2013. **182**(5): p. 1482-8.
407. Tiaden, A.N., et al., *Detrimental role for human high temperature requirement serine protease A1 (HTRA1) in the pathogenesis of intervertebral disc (IVD) degeneration.* J Biol Chem, 2012. **287**(25): p. 21335-45.
408. Hadfield, K.D., et al., *HtrA1 inhibits mineral deposition by osteoblasts: requirement for the protease and PDZ domains.* J Biol Chem, 2008. **283**(9): p. 5928-38.
409. Chamberland, A., et al., *Identification of a novel HtrA1-susceptible cleavage site in human aggrecan: evidence for the involvement of HtrA1 in aggrecan proteolysis in vivo.* J Biol Chem, 2009. **284**(40): p. 27352-9.
410. Bottini, N. and G.S. Firestein, *Duality of fibroblast-like synoviocytes in RA: passive responders and imprinted aggressors.* Nat Rev Rheumatol, 2013. **9**(1): p. 24-33.
411. Burrage, P.S., K.S. Mix, and C.E. Brinckerhoff, *Matrix metalloproteinases: role in arthritis.* Front Biosci, 2006. **11**: p. 529-43.
412. Homandberg, G.A., *Potential regulation of cartilage metabolism in osteoarthritis by fibronectin fragments.* Front Biosci, 1999. **4**: p. D713-30.
413. Stanton, H., L. Ung, and A.J. Fosang, *The 45 kDa collagen-binding fragment of fibronectin induces matrix metalloproteinase-13 synthesis by chondrocytes and aggrecan degradation by aggrecanases.* Biochem J, 2002. **364**(Pt 1): p. 181-90.
414. Le Maitre, C.L., A.J. Freemont, and J.A. Hoyland, *Localization of degradative enzymes and their inhibitors in the degenerate human intervertebral disc.* J Pathol, 2004. **204**(1): p. 47-54.
415. Adams, M.A. and P.J. Roughley, *What is intervertebral disc degeneration, and what causes it?* Spine (Phila Pa 1976), 2006. **31**(18): p. 2151-61.
416. Katz, J.N. and M.B. Harris, *Clinical practice. Lumbar spinal stenosis.* N Engl J Med, 2008. **358**(8): p. 818-25.
417. Kuemmerle, J.F. and H. Zhou, *Insulin-like growth factor-binding protein-5 (IGFBP-5) stimulates growth and IGF-I secretion in human intestinal smooth muscle by Ras-dependent activation of p38 MAP kinase and Erk1/2 pathways.* J Biol Chem, 2002. **277**(23): p. 20563-71.
418. Bakay, M., et al., *A web-accessible complete transcriptome of normal human and DMD muscle.* Neuromuscul Disord, 2002. **12 Suppl 1**: p. S125-41.
419. Nowak, K.J. and K.E. Davies, *Duchenne muscular dystrophy and dystrophin: pathogenesis and opportunities for treatment.* EMBO Rep, 2004. **5**(9): p. 872-6.
420. FG, H., *The analyst and the medical man.* Analyst, 1906. **31:385-404**.
421. Hopkins, F.G., *Feeding experiments illustrating the importance of accessory factors in normal dietaries.* J Physiol, 1912. **44**(5-6): p. 425-60.

422. McCollum EV, S.N., Parsons HT., *A biological analysis of pellagra-producingdiets:V.Thenatureofthedietarydeficienciesofadietderivedfrom peas, wheat flour, and cottonseed oil.* J Biol Chem, 1918. **33:411-23**.
423. Drummond, J.C., *The Nomenclature of the so-called Accessory Food Factors (Vitamins).* Biochem J, 1920. **14**(5): p. 660.
424. Strauss, M.B. and S. Maddock, *The Relation of Increased Intra-abdominal Pressure to the Liver Lesions of Eclampsia.* Am J Pathol, 1934. **10**(6): p. 821-5.
425. Michaelsson, K., et al., *Serum retinol levels and the risk of fracture.* N Engl J Med, 2003. **348**(4): p. 287-94.
426. Feskanich, D., et al., *Vitamin A intake and hip fractures among postmenopausal women.* JAMA, 2002. **287**(1): p. 47-54.
427. Ohishi, K., et al., *Physiological concentrations of retinoic acid suppress the osteoblastic differentiation of fetal rat calvaria cells in vitro.* Eur J Endocrinol, 1995. **133**(3): p. 335-41.
428. Nuka, S., et al., *All-trans retinoic acid inhibits dexamethasone-induced ALP activity and mineralization in human osteoblastic cell line SV HFO.* Cell Struct Funct, 1997. **22**(1): p. 27-32.
429. Lind, T., et al., *Vitamin a is a negative regulator of osteoblast mineralization.* PLoS One, 2013. **8**(12): p. e82388.
430. Kneissel, M., et al., *Retinoid-induced bone thinning is caused by subperiosteal osteoclast activity in adult rodents.* Bone, 2005. **36**(2): p. 202-14.
431. Iba, K., et al., *Phase-independent inhibition by retinoic acid of mineralization correlated with loss of tetranectin expression in a human osteoblastic cell line.* Cell Struct Funct, 2001. **26**(4): p. 227-33.
432. Henning, P., H.H. Conaway, and U.H. Lerner, *Retinoid receptors in bone and their role in bone remodeling.* Front Endocrinol (Lausanne), 2015. **6**: p. 31.
433. D'Ambrosio, D.N., R.D. Clugston, and W.S. Blaner, *Vitamin A metabolism: an update.* Nutrients, 2011. **3**(1): p. 63-103.
434. Ross, A.C. and R. Zolfaghari, *Cytochrome P450s in the regulation of cellular retinoic acid metabolism.* Annu Rev Nutr, 2011. **31**: p. 65-87.
435. White, J.A., et al., *Identification of the retinoic acid-inducible all-trans-retinoic acid 4-hydroxylase.* J Biol Chem, 1996. **271**(47): p. 29922-7.
436. White, J.A., et al., *cDNA cloning of human retinoic acid-metabolizing enzyme (hP450RAI) identifies a novel family of cytochromes P450.* J Biol Chem, 1997. **272**(30): p. 18538-41.
437. Fujii, H., et al., *Metabolic inactivation of retinoic acid by a novel P450 differentially expressed in developing mouse embryos.* EMBO J, 1997. **16**(14): p. 4163-73.
438. Abu-Abed, S., et al., *The retinoic acid-metabolizing enzyme, CYP26A1, is essential for normal hindbrain patterning, vertebral identity, and development of posterior structures.* Genes Dev, 2001. **15**(2): p. 226-40.
439. Niederreither, K., et al., *Genetic evidence that oxidative derivatives of retinoic acid are not involved in retinoid signaling during mouse development.* Nat Genet, 2002. **31**(1): p. 84-8.
440. Bastien, J. and C. Rochette-Egly, *Nuclear retinoid receptors and the transcription of retinoid-target genes.* Gene, 2004. **328**: p. 1-16.
441. Al Tanoury, Z., A. Piskunov, and C. Rochette-Egly, *Vitamin A and retinoid signaling: genomic and nongenomic effects.* J Lipid Res, 2013. **54**(7): p. 1761-75.
442. Krust, A., et al., *A third human retinoic acid receptor, hRAR-gamma.* Proc Natl Acad Sci U S A, 1989. **86**(14): p. 5310-4.

443. Mic, F.A., et al., *Retinoid activation of retinoic acid receptor but not retinoid X receptor is sufficient to rescue lethal defect in retinoic acid synthesis.* Proc Natl Acad Sci U S A, 2003. **100**(12): p. 7135-40.
444. Langston, A.W. and L.J. Gudas, *Identification of a retinoic acid responsive enhancer 3' of the murine homeobox gene Hox-1.6.* Mech Dev, 1992. **38**(3): p. 217-27.
445. LaRosa, G.J. and L.J. Gudas, *An early effect of retinoic acid: cloning of an mRNA (Era-1) exhibiting rapid and protein synthesis-independent induction during teratocarcinoma stem cell differentiation.* Proc Natl Acad Sci U S A, 1988. **85**(2): p. 329-33.
446. Gudas, L.J. and J.A. Wagner, *Retinoids regulate stem cell differentiation.* J Cell Physiol, 2011. **226**(2): p. 322-30.
447. Chen, J.D., K. Umesono, and R.M. Evans, *SMRT isoforms mediate repression and anti-repression of nuclear receptor heterodimers.* Proc Natl Acad Sci U S A, 1996. **93**(15): p. 7567-71.
448. Nagy, L., et al., *Nuclear receptor repression mediated by a complex containing SMRT, mSin3A, and histone deacetylase.* Cell, 1997. **89**(3): p. 373-80.
449. Akamatsu, W., et al., *Suppression of Oct4 by germ cell nuclear factor restricts pluripotency and promotes neural stem cell development in the early neural lineage.* J Neurosci, 2009. **29**(7): p. 2113-24.
450. Gu, P., et al., *Orphan nuclear receptor GCNF is required for the repression of pluripotency genes during retinoic acid-induced embryonic stem cell differentiation.* Mol Cell Biol, 2005. **25**(19): p. 8507-19.
451. Wolf, G., *Retinoic acid as cause of cell proliferation or cell growth inhibition depending on activation of one of two different nuclear receptors.* Nutr Rev, 2008. **66**(1): p. 55-9.
452. Schug, T.T., et al., *Opposing effects of retinoic acid on cell growth result from alternate activation of two different nuclear receptors.* Cell, 2007. **129**(4): p. 723-33.
453. Berry, D.C. and N. Noy, *Is PPARbeta/delta a Retinoid Receptor?* PPAR Res, 2007. **2007**: p. 73256.
454. Ziouzenkova, O. and J. Plutzky, *Retinoid metabolism and nuclear receptor responses: New insights into coordinated regulation of the PPAR-RXR complex.* FEBS Lett, 2008. **582**(1): p. 32-8.
455. Stehlin-Gaon, C., et al., *All-trans retinoic acid is a ligand for the orphan nuclear receptor ROR beta.* Nat Struct Biol, 2003. **10**(10): p. 820-5.
456. Jetten, A.M., *Retinoid-related orphan receptors (RORs): critical roles in development, immunity, circadian rhythm, and cellular metabolism.* Nucl Recept Signal, 2009. **7**: p. e003.
457. Giguere, V., et al., *Isoform-specific amino-terminal domains dictate DNA-binding properties of ROR alpha, a novel family of orphan hormone nuclear receptors.* Genes Dev, 1994. **8**(5): p. 538-53.
458. Giguere, V., L.D. McBroom, and G. Flock, *Determinants of target gene specificity for ROR alpha 1: monomeric DNA binding by an orphan nuclear receptor.* Mol Cell Biol, 1995. **15**(5): p. 2517-26.
459. Canon, E., et al., *Rapid effects of retinoic acid on CREB and ERK phosphorylation in neuronal cells.* Mol Biol Cell, 2004. **15**(12): p. 5583-92.
460. Poon, M.M. and L. Chen, *Retinoic acid-gated sequence-specific translational control by RARalpha.* Proc Natl Acad Sci U S A, 2008. **105**(51): p. 20303-8.

461. Chen, N., B. Onisko, and J.L. Napoli, *The nuclear transcription factor RARalpha associates with neuronal RNA granules and suppresses translation.* J Biol Chem, 2008. **283**(30): p. 20841-7.
462. Chen, N. and J.L. Napoli, *All-trans-retinoic acid stimulates translation and induces spine formation in hippocampal neurons through a membrane-associated RARalpha.* FASEB J, 2008. **22**(1): p. 236-45.
463. Duester, G., *Retinoic acid synthesis and signaling during early organogenesis.* Cell, 2008. **134**(6): p. 921-31.
464. Yamada, K., et al., *Analysis of zinc-fingers and homeoboxes (ZHX)-1-interacting proteins: molecular cloning and characterization of a member of the ZHX family, ZHX3.* Biochem J, 2003. **373**(Pt 1): p. 167-78.
465. Lim, K. and H.I. Chang, *O-GlcNAcylation of Sp1 interrupts Sp1 interaction with NF-Y.* Biochem Biophys Res Commun, 2009. **382**(3): p. 593-7.
466. Lee, M.R., et al., *Transcription factors NF-YA regulate the induction of human OGG1 following DNA-alkylating agent methylmethane sulfonate (MMS) treatment.* J Biol Chem, 2004. **279**(11): p. 9857-66.
467. Li, X.Y., et al., *Evolutionary variation of the CCAAT-binding transcription factor NF-Y.* Nucleic Acids Res, 1992. **20**(5): p. 1087-91.
468. Ge, Y., et al., *Synergistic regulation of human cystathionine-beta-synthase-1b promoter by transcription factors NF-YA isoforms and Sp1.* Biochim Biophys Acta, 2002. **1579**(2-3): p. 73-80.
469. Promega, *Technical Bulletin - Gel Shift Assay System : Instructions for use of products E3050 and E3300.* 2011.
470. Perlis, R.H., et al., *Clinical and genetic dissection of anger expression and CREB1 polymorphisms in major depressive disorder.* Biol Psychiatry, 2007. **62**(5): p. 536-40.
471. Du, K. and M. Montminy, *CREB is a regulatory target for the protein kinase Akt/PKB.* J Biol Chem, 1998. **273**(49): p. 32377-9.
472. Comerford, K.M., et al., *Small ubiquitin-related modifier-1 modification mediates resolution of CREB-dependent responses to hypoxia.* Proc Natl Acad Sci U S A, 2003. **100**(3): p. 986-91.
473. Screaton, R.A., et al., *The CREB coactivator TORC2 functions as a calcium- and cAMP-sensitive coincidence detector.* Cell, 2004. **119**(1): p. 61-74.
474. David, S. and R.G. Kalb, *Serum/glucocorticoid-inducible kinase can phosphorylate the cyclic AMP response element binding protein, CREB.* FEBS Lett, 2005. **579**(6): p. 1534-8.
475. Rehfuss, R.P., et al., *The cAMP-regulated enhancer-binding protein ATF-1 activates transcription in response to cAMP-dependent protein kinase A.* J Biol Chem, 1991. **266**(28): p. 18431-4.
476. Yoshimura, T., J. Fujisawa, and M. Yoshida, *Multiple cDNA clones encoding nuclear proteins that bind to the tax-dependent enhancer of HTLV-1: all contain a leucine zipper structure and basic amino acid domain.* EMBO J, 1990. **9**(8): p. 2537-42.
477. Zucman, J., et al., *EWS and ATF-1 gene fusion induced by t(12;22) translocation in malignant melanoma of soft parts.* Nat Genet, 1993. **4**(4): p. 341-5.
478. Hallor, K.H., et al., *Fusion of the EWSR1 and ATF1 genes without expression of the MITF-M transcript in angiomatoid fibrous histiocytoma.* Genes Chromosomes Cancer, 2005. **44**(1): p. 97-102.
479. Iwasaki, K., K. Hailemariam, and Y. Tsuji, *PIAS3 interacts with ATF1 and regulates the human ferritin H gene through an antioxidant-responsive element.* J Biol Chem, 2007. **282**(31): p. 22335-43.

480. Szpirer, J., et al., *The Sp1 transcription factor gene (SP1) and the 1,25-dihydroxyvitamin D3 receptor gene (VDR) are colocalized on human chromosome arm 12q and rat chromosome 7.* Genomics, 1991. **11**(1): p. 168-73.
481. Parks, C.L. and T. Shenk, *The serotonin 1a receptor gene contains a TATA-less promoter that responds to MAZ and Sp1.* J Biol Chem, 1996. **271**(8): p. 4417-30.
482. Narayan, V.A., R.W. Kriwacki, and J.P. Caradonna, *Structures of zinc finger domains from transcription factor Sp1. Insights into sequence-specific protein-DNA recognition.* J Biol Chem, 1997. **272**(12): p. 7801-9.
483. Zhang, Y., M. Liao, and M.L. Dufau, *Phosphatidylinositol 3-kinase/protein kinase Czeta-induced phosphorylation of Sp1 and p107 repressor release have a critical role in histone deacetylase inhibitor-mediated derepression [corrected] of transcription of the luteinizing hormone receptor gene.* Mol Cell Biol, 2006. **26**(18): p. 6748-61.
484. Olofsson, B.A., et al., *Phosphorylation of Sp1 in response to DNA damage by ataxia telangiectasia-mutated kinase.* Mol Cancer Res, 2007. **5**(12): p. 1319-30.
485. Wan, D.C., et al., *Refining retinoic acid stimulation for osteogenic differentiation of murine adipose-derived adult stromal cells.* Tissue Eng, 2007. **13**(7): p. 1623-31.
486. Mirsaidi, A., et al., *Therapeutic potential of adipose-derived stromal cells in age-related osteoporosis.* Biomaterials, 2014. **35**(26): p. 7326-35.
487. Malladi, P., et al., *Functions of vitamin D, retinoic acid, and dexamethasone in mouse adipose-derived mesenchymal cells.* Tissue Eng, 2006. **12**(7): p. 2031-40.
488. Mirsaidi, A., A.N. Tiaden, and P.J. Richards, *Preparation and osteogenic differentiation of scaffold-free mouse adipose-derived stromal cell microtissue spheroids (ASC-MT).* Curr Protoc Stem Cell Biol, 2013. **27**: p. Unit 2B 5.
489. Hamidouche, Z., et al., *FHL2 mediates dexamethasone-induced mesenchymal cell differentiation into osteoblasts by activating Wnt/beta-catenin signaling-dependent Runx2 expression.* FASEB J, 2008. **22**(11): p. 3813-22.
490. Hisada, K., et al., *Retinoic acid regulates commitment of undifferentiated mesenchymal stem cells into osteoblasts and adipocytes.* J Bone Miner Metab, 2013. **31**(1): p. 53-63.
491. Song, H.M., et al., *High-dose retinoic acid modulates rat calvarial osteoblast biology.* J Cell Physiol, 2005. **202**(1): p. 255-62.
492. Schipper, B.M., et al., *Regional anatomic and age effects on cell function of human adipose-derived stem cells.* Ann Plast Surg, 2008. **60**(5): p. 538-44.
493. Zhu, M., et al., *The effect of age on osteogenic, adipogenic and proliferative potential of female adipose-derived stem cells.* J Tissue Eng Regen Med, 2009. **3**(4): p. 290-301.
494. Porter, R.S. and J.R. DiPalma, *Coronary artery thrombolysis: comparison of approved agents.* Am Fam Physician, 1991. **44**(2): p. 591-8.
495. Liu, H.Y., et al., *The effect of diminished osteogenic signals on reduced osteoporosis recovery in aged mice and the potential therapeutic use of adipose-derived stem cells.* Biomaterials, 2012. **33**(26): p. 6105-12.
496. You, L., et al., *Suppression of zinc finger protein 467 alleviates osteoporosis through promoting differentiation of adipose derived stem cells to osteoblasts.* J Transl Med, 2012. **10**: p. 11.
497. Bruck, N., et al., *A coordinated phosphorylation cascade initiated by p38MAPK/MSK1 directs RARalpha to target promoters.* EMBO J, 2009. **28**(1): p. 34-47.

498. Gianni, M., et al., *Phosphorylation by p38MAPK and recruitment of SUG-1 are required for RA-induced RAR gamma degradation and transactivation.* EMBO J, 2002. **21**(14): p. 3760-9.
499. Alsayed, Y., et al., *Activation of Rac1 and the p38 mitogen-activated protein kinase pathway in response to all-trans-retinoic acid.* J Biol Chem, 2001. **276**(6): p. 4012-9.
500. Piskunov, A. and C. Rochette-Egly, *A retinoic acid receptor RARalpha pool present in membrane lipid rafts forms complexes with G protein alphaQ to activate p38MAPK.* Oncogene, 2012. **31**(28): p. 3333-45.
501. Gupta, P., et al., *Retinoic acid-stimulated sequential phosphorylation, PML recruitment, and SUMOylation of nuclear receptor TR2 to suppress Oct4 expression.* Proc Natl Acad Sci U S A, 2008. **105**(32): p. 11424-9.
502. Dey, N., et al., *CSK controls retinoic acid receptor (RAR) signaling: a RAR-c-SRC signaling axis is required for neuritogenic differentiation.* Mol Cell Biol, 2007. **27**(11): p. 4179-97.
503. Bost, F., et al., *Retinoic acid activation of the ERK pathway is required for embryonic stem cell commitment into the adipocyte lineage.* Biochem J, 2002. **361**(Pt 3): p. 621-7.
504. Stavridis, M.P., B.J. Collins, and K.G. Storey, *Retinoic acid orchestrates fibroblast growth factor signaling to drive embryonic stem cell differentiation.* Development, 2010. **137**(6): p. 881-90.
505. Cheung, Y.T., et al., *Effects of all-trans-retinoic acid on human SH-SY5Y neuroblastoma as in vitro model in neurotoxicity research.* Neurotoxicology, 2009. **30**(1): p. 127-35.
506. Masia, S., et al., *Rapid, nongenomic actions of retinoic acid on phosphatidylinositol-3-kinase signaling pathway mediated by the retinoic acid receptor.* Mol Endocrinol, 2007. **21**(10): p. 2391-402.
507. Pellegrini, M., et al., *ATRA and KL promote differentiation toward the meiotic program of male germ cells.* Cell Cycle, 2008. **7**(24): p. 3878-88.
508. Vicent, G.P., et al., *Induction of progesterone target genes requires activation of Erk and Msk kinases and phosphorylation of histone H3.* Mol Cell, 2006. **24**(3): p. 367-81.
509. Vicent, G.P., et al., *Two chromatin remodeling activities cooperate during activation of hormone responsive promoters.* PLoS Genet, 2009. **5**(7): p. e1000567.
510. Varlakhanova, N., J.B. Hahm, and M.L. Privalsky, *Regulation of SMRT corepressor dimerization and composition by MAP kinase phosphorylation.* Mol Cell Endocrinol, 2011. **332**(1-2): p. 180-8.
511. Jonas, B.A., et al., *Response of SMRT (silencing mediator of retinoic acid and thyroid hormone receptor) and N-CoR (nuclear receptor corepressor) corepressors to mitogen-activated protein kinase kinase kinase cascades is determined by alternative mRNA splicing.* Mol Endocrinol, 2007. **21**(8): p. 1924-39.
512. Ferry, C., et al., *Cullin 3 mediates SRC-3 ubiquitination and degradation to control the retinoic acid response.* Proc Natl Acad Sci U S A, 2011. **108**(51): p. 20603-8.
513. Berry, D.C., et al., *Cross talk between signaling and vitamin A transport by the retinol-binding protein receptor STRA6.* Mol Cell Biol, 2012. **32**(15): p. 3164-75.
514. Berry, D.C. and N. Noy, *Signaling by vitamin A and retinol-binding protein in regulation of insulin responses and lipid homeostasis.* Biochim Biophys Acta, 2012. **1821**(1): p. 168-76.

515. Berry, D.C., et al., *Signaling by vitamin A and retinol-binding protein regulates gene expression to inhibit insulin responses.* Proc Natl Acad Sci U S A, 2011. **108**(11): p. 4340-5.
516. Pan, J., et al., *Activation of Rac1 by phosphatidylinositol 3-kinase in vivo: role in activation of mitogen-activated protein kinase (MAPK) pathways and retinoic acid-induced neuronal differentiation of SH-SY5Y cells.* J Neurochem, 2005. **93**(3): p. 571-83.
517. Losel, R. and M. Wehling, *Nongenomic actions of steroid hormones.* Nat Rev Mol Cell Biol, 2003. **4**(1): p. 46-56.
518. He, X., et al., *HtrA1 sensitizes ovarian cancer cells to cisplatin-induced cytotoxicity by targeting XIAP for degradation.* Int J Cancer, 2012. **130**(5): p. 1029-35.
519. Shiga, A., et al., *Cerebral small-vessel disease protein HTRA1 controls the amount of TGF-beta1 via cleavage of proTGF-beta1.* Hum Mol Genet, 2011. **20**(9): p. 1800-10.
520. Zoncu, R., A. Efeyan, and D.M. Sabatini, *mTOR: from growth signal integration to cancer, diabetes and ageing.* Nat Rev Mol Cell Biol, 2011. **12**(1): p. 21-35.
521. Kim, J., et al., *Erythropoietin mediated bone formation is regulated by mTOR signaling.* J Cell Biochem, 2012. **113**(1): p. 220-8.
522. Kim, J.K., et al., *mTor plays an important role in odontoblast differentiation.* J Endod, 2011. **37**(8): p. 1081-5.
523. Tang, C.H., et al., *Ultrasound induces hypoxia-inducible factor-1 activation and inducible nitric-oxide synthase expression through the integrin/integrin-linked kinase/Akt/mammalian target of rapamycin pathway in osteoblasts.* J Biol Chem, 2007. **282**(35): p. 25406-15.
524. Lal, L., et al., *Activation of the p70 S6 kinase by all-trans-retinoic acid in acute promyelocytic leukemia cells.* Blood, 2005. **105**(4): p. 1669-77.
525. Tee, A.R., et al., *Tuberous sclerosis complex gene products, Tuberin and Hamartin, control mTOR signaling by acting as a GTPase-activating protein complex toward Rheb.* Curr Biol, 2003. **13**(15): p. 1259-68.
526. Busada, J.T., et al., *Retinoic acid regulates Kit translation during spermatogonial differentiation in the mouse.* Dev Biol, 2015. **397**(1): p. 140-9.
527. Ekim, B., et al., *mTOR kinase domain phosphorylation promotes mTORC1 signaling, cell growth, and cell cycle progression.* Mol Cell Biol, 2011. **31**(14): p. 2787-801.
528. Carnevalli, L.S., et al., *S6K1 plays a critical role in early adipocyte differentiation.* Dev Cell, 2010. **18**(5): p. 763-74.
529. Inoki, K., et al., *Rheb GTPase is a direct target of TSC2 GAP activity and regulates mTOR signaling.* Genes Dev, 2003. **17**(15): p. 1829-34.
530. Jaeschke, A., et al., *Tuberous sclerosis complex tumor suppressor-mediated S6 kinase inhibition by phosphatidylinositide-3-OH kinase is mTOR independent.* J Cell Biol, 2002. **159**(2): p. 217-24.
531. Vander Haar, E., et al., *Insulin signaling to mTOR mediated by the Akt/PKB substrate PRAS40.* Nat Cell Biol, 2007. **9**(3): p. 316-23.
532. Chen, W.C., et al., *Biological effects and metabolism of 9-cis-retinoic acid and its metabolite 9,13-di-cis-retinoic acid in HaCaT keratinocytes in vitro: comparison with all-trans-retinoic acid.* Arch Dermatol Res, 2000. **292**(12): p. 612-20.
533. Gray, C.W., et al., *Characterization of human HtrA2, a novel serine protease involved in the mammalian cellular stress response.* Eur J Biochem, 2000. **267**(18): p. 5699-710.
534. Suzuki, Y., et al., *A serine protease, HtrA2, is released from the mitochondria and interacts with XIAP, inducing cell death.* Mol Cell, 2001. **8**(3): p. 613-21.

535. Nie, G.Y., et al., *Identification and cloning of two isoforms of human high-temperature requirement factor A3 (HtrA3), characterization of its genomic structure and comparison of its tissue distribution with HtrA1 and HtrA2.* Biochem J, 2003. **371**(Pt 1): p. 39-48.
536. Nie, G.Y., et al., *A novel serine protease of the mammalian HtrA family is up-regulated in mouse uterus coinciding with placentation.* Mol Hum Reprod, 2003. **9**(5): p. 279-90.
537. Khan, W.S., et al., *The epitope characterisation and the osteogenic differentiation potential of human fat pad-derived stem cells is maintained with ageing in later life.* Injury, 2009. **40**(2): p. 150-7.
538. Helder, M.N., et al., *Stem cells from adipose tissue allow challenging new concepts for regenerative medicine.* Tissue Eng, 2007. **13**(8): p. 1799-808.
539. Dudas, J.R., et al., *The osteogenic potential of adipose-derived stem cells for the repair of rabbit calvarial defects.* Ann Plast Surg, 2006. **56**(5): p. 543-8.
540. Li, H., et al., *Bone regeneration by implantation of adipose-derived stromal cells expressing BMP-2.* Biochem Biophys Res Commun, 2007. **356**(4): p. 836-42.
541. Liu, Y., et al., *Injectable tissue-engineered bone composed of human adipose-derived stromal cells and platelet-rich plasma.* Biomaterials, 2008. **29**(23): p. 3338-45.
542. Zhou, Y., et al., *The role of simvastatin in the osteogenesis of injectable tissue-engineered bone based on human adipose-derived stromal cells and platelet-rich plasma.* Biomaterials, 2010. **31**(20): p. 5325-35.
543. Graham, J.R., et al., *Serine protease HTRA1 antagonizes transforming growth factor-beta signaling by cleaving its receptors and loss of HTRA1 in vivo enhances bone formation.* PLoS One, 2013. **8**(9): p. e74094.
544. Beaufort, N., et al., *Cerebral small vessel disease-related protease HtrA1 processes latent TGF-beta binding protein 1 and facilitates TGF-beta signaling.* Proc Natl Acad Sci U S A, 2014. **111**(46): p. 16496-501.

6. Curriculum vitae

EDUCATION

- DOCTORAL THESIS - PhD. | 2011 - 2015
  UZH / ETH - Life Science Zurich Graduate School - Molecular Medicine
  Transcription factor targeted stem cell based therapy for osteoporosis
- MINI MBA | 2010
  Danube University Krems
  Translation of Life Science into Business
- MASTER THESIS - Mag. | 2009 - 2011
  University of Vienna
  Establishment of method for isolation of RNA binding proteins *in vivo*
- MASTER STUDIES | 2004 - 2009
  University of Vienna
  Genetics and Microbiology - Focus : Molecular patholgy / Biotechnology

LANGUAGES

- ENGLISH
- GERMAN
- ITALIAN
- FRENCH

WORK EXPERIENCE

- SPORT CONSULTING | 2014 - PRESENT
  Ultrasport : Guide and support athletes from various backgrounds to exceed their limitations beyond what is considered humanly possible.
- SKIPPER | 2004 - 2009
  Sailing : Leading leisure blue water sailing to team building events, when big waves, stress and anxiety are the most efficient teachers.
- VARIOUS | 2004 - 2009
  Student occupations : Broad variation of part-time jobs to finance my studies, from project supervision over photography to airport catering.
- MILITARY | 2003 - 2004
  Mission : Honoured truck driver on two turns of Austrian frontier protection for retrieving refugees, facing the brutal arbitrariness of human misery.

GLANZ Stephan

Scientist / Ultra-Athlete

QUITTING

...is not an option : Sports as school of life - countless competitions including shattering defeats and sweet victories have taught me that quitting is never an option, but discipline, focus and determination are the virtues leading to success. Needless to say how helpful this experience is during the highs and especially inevitable lows of everyday business life.

PROFESSIONAL SKILLS

80% FLEXIBILITY	98% RELIANCE
97% RESILIENCE	100% LEADERSHIP
100% TEAM WORK	90% NETWORKING

N. GLANZ Stephan
T. +41 (0) 76436 4477
B. 10th of Feb. 1984
M. stephan.glanz@gmail.com
N. AUSTRIAN - Vienna / Swiss : B-Permit
A. Mutschellenstrasse 163, 8038 Zurich

ACHIEVMENTS

- **TRIATHLON | 2008 - 2012**
  IRONMAN Racing Series : Numerous top 3 rankings and in 2012 listed amongst top 15 within the IRONMAN Racing Series Europe.
- **ULTRACYCLING | 2012 - PRESENT**
  Race Around Austria : First place and record after 2200km non-stop cycling and successful finish of multiple international competitions.
- **SAILING | 2003 - PRESENT**
  Regatta : Pro big-crew skipper and trainer with top rankings in international comeptitions such as Rolex Cup, BMW Cup, RPC.

THE REFERENCES

PD Peter J. **Richards** / CABMM

...he is clearly very enthusiastic about his work and has a natural desire to undertake difficult challenges and overcome them.

+41 (0)44 635 3800 peter.richards@cabmm.uzh.ch PI

Prof. Christine **Hohenadl** / Croma Pharma

... a very motivated, dedicated and highly responsible young scientist with a quick intellectual grasp and strong communication skills.

+43 (0)680 127 8892 christine.hohenadl@croma.at CTO

Prof. Walter **Günzburg** / Austrianova

...actively seeks constructive criticism of his work and is receptive to new ideas.

+65 6779 3867 gunzburg@sgaustria.com Chairman and CTO

GLANZ Stephan

Scientist / Ultra-Athlete

IMPOSSIBLE

...is nothing : Forcing your body far beyond the limits, under maximum tension, the opponents in the back pushing you to make a mistake, communicating and keeping the team calm, always focused on the aim. Since more than ten years I am successfully leading and participating with my teams in numerous international ultrasport competitions. Under maximal mental stress, physical exhaustion, efficiently working on minimal space, will necessarily shape you to improve team-work and leadership skills, or you lose. We won!

PERSONAL SKILLS

80% CREATIVITY	100% DISCIPLINE
100% DETERMINATION	97% INTEGRITY
75% PATIENCE	100% ENDURANCE

7. Acknowledgements

I want to thank a few very special individuals who affected me the one way or another during the last 1500 days of my PhD project.

First of all a big thank you to my PhD committee members Prof. Dr. Ernst Hafen, Prof. Dr. Michael Hottiger and Prof. Dr. Michael Ehrmann for their valuable input and time to make the project succeed. A very special thanks to my supervisor PD. Dr. Peter Richards who apparently never sleeps and comes up with new ideas, action plans and solutions around the clock. Although everything developed pretty much the opposite as expected, the same way we learned things we never expected.

Further thanks, not less important, goes to: Nicki for pretending to be our postdoc lab dad, Ali for not killing us all and doing with me the “last experiment” since two years, Gladys for the psychological support by means of sauccisson and vervein, Cristina the Puerto Rican princess for providing us life long valentines day / secret Santa nightmares, and of course : Gregor, my cell mate! Not to forget : Eva for mental support and amazing Klosters weekends, Nataša and Sarma, Anneli and countless Ultra-Frisbee injuries, Friedrich and BVB, Flo and Michelle.

Last but not least, there`s supporting family too, without whom I could not have achieved where I am today, sport wise as well as PhD wise: Thanks to Silvia and Gisa for Hollersaft and thanks to my mother Anneliese for the regular Viennese food supply packages without which I would have starved to death here in Switzerland. A big thank you to my brother Philipp for not being such an academic nerd as I am and showing me how to use a screwdriver in real life. Finally, a big thank you to my father Ernst for insane sailing action. To be continued!